PB98-109002

INVESTIGATION OF SEISMIC RESPONSE OF BUILDING WITH LINEAR AND NONLINEAR FLUID VISCOUS DAMPERS

21 MAY 97

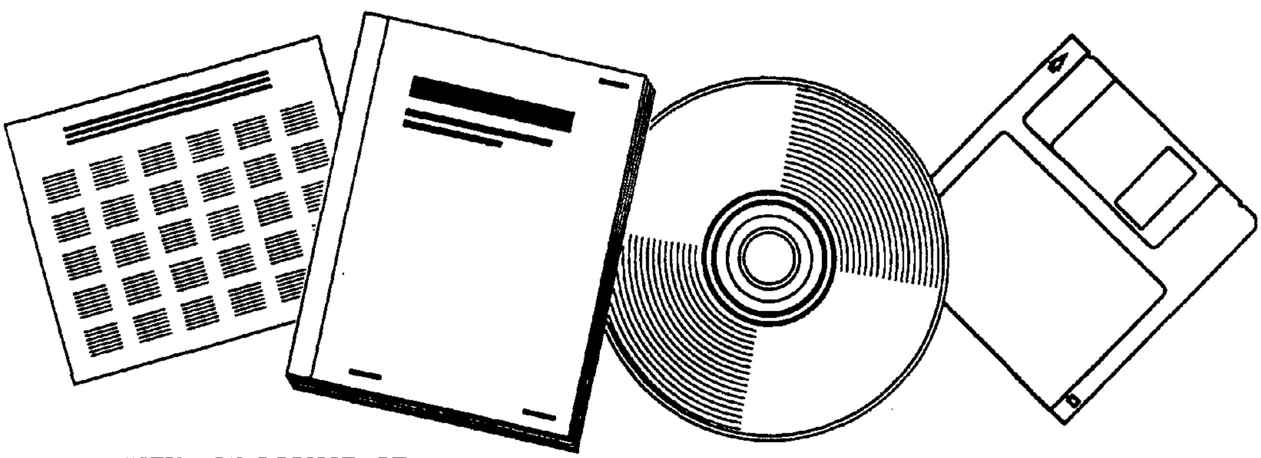

U.S. DEPARTMENT OF COMMERCE
National Technical Information Service

NATIONAL CENTER FOR EARTHQUAKE ENGINEERING RESEARCH
Headquartered at the State University of New York at Buffalo

ISSN 1088-3800

Investigation of Seismic Response of Buildings with Linear and Nonlinear Fluid Viscous Dampers

by

A.A. Seleemah and M.C. Constantinou
State University of New York at Buffalo
Department of Civil Engineering
Buffalo, New York 14261

Technical Report NCEER-97-0004

May 21, 1997

This research was conducted at the State University of New York at Buffalo and was supported in whole or in part by the National Science Foundation under Grant No. BCS 90-25010 and other sponsors.

NOTICE

NATIONAL CENTER FOR EARTHQUAKE ENGINEERING RESEARCH
Headquartered at the State University of New York at Buffalo

Investigation of Seismic Response of Buildings with Linear and Nonlinear Fluid Viscous Dampers

by

A.A. Seleemah[1] and M.C. Constantinou[2]

Publication Date: May 21, 1997
Submittal Date: January 24, 1997

Technical Report NCEER-97-0004

NCEER Task Number 95-5104A

NSF Master Contract Number BCS 90-25010

1 Visiting Scholar, Department of Civil Engineering, State University of New York at Buffalo and Assistant Lecturer, Benha Higher Institute of Technology, Ministry of Higher Education, Egypt.
2 Professor, Department of Civil Engineering, State University of New York at Buffalo

NATIONAL CENTER FOR EARTHQUAKE ENGINEERING RESEARCH
State University of New York at Buffalo
Red Jacket Quadrangle, Buffalo, NY 14261

50272-101

REPORT DOCUMENTATION PAGE	1. REPORT NO. NCEER-97-0004	2.	PB98-109002
4. Title and Subtitle: Investigation of Seismic Response of Buildings with Linear and Nonlinear Fluid Viscous Dampers			5. Report Date: May 21, 1997
			6.
7. Author(s): A.A. Seleemah and M.C. Constantinou			8. Performing Organization Rept. No.
9. Performing Organization Name and Address: State University of New York at Buffalo, Department of Civil Engineering, Buffalo, New York 14261			10. Project/Task/Work Unit No.
			11. Contract(C) or Grant(G) No. (C) BCS 90-25010 (G)
12. Sponsoring Organization Name and Address: National Center for Earthquake Engineering Research, State University of New York at Buffalo, Red Jacket Quadrangle, Buffalo, New York 14261			13. Type of Report & Period Covered: Technical report
			14.

15. Supplementary Notes

This research was conducted at the State University of New York at Buffalo and was supported in whole or in part by the National Science Foundation under Grant No. BCS 90-25010 and other sponsors.

16. Abstract (Limit: 200 words)

This report presents results of the first systematic experimental study of nonlinear fluid viscous dampers. Earthquake simulation tests have been performed on one- and three-story model structures with and without linear and nonlinear viscous dampers. The experimental results demonstrated significant reductions in response when dampers, whether linear or nonlinear, were added to the structural frame. Moreover, direct comparisons of responses of the structure with linear and nonlinear dampers elucidated further benefits offered by the nonlinear devices and identified potential drawbacks. The experimental response has been compared with predictions of response history and simplified methods of analysis. The latter methods has been based on the linear static procedure of the NEHRP Guidelines for the Seismic Rehabilitation of Buildings. Comparisons of analytical and experimental responses showed good agreement.

17. Document Analysis a. Descriptors

b. Identifiers/Open-Ended Terms

Earthquake engineering. Linear fluid viscous dampers. Nonlinear fluid viscous dampers. Shaking table tests. Analytical models. Time history analysis.

c. COSATI Field/Group

18. Availability Statement	19. Security Class (This Report)	21. No. of Pages
Release unlimited	Unclassified	300
	20. Security Class (This Page) Unclassified	22. Price

(See ANSI-Z39.18) See Instructions on Reverse OPTIONAL FORM 272 (4-77)

PREFACE

The National Center for Earthquake Engineering Research (NCEER) was established in 1986 to develop and disseminate new knowledge about earthquakes, earthquake-resistant design and seismic hazard mitigation procedures to minimize loss of life and property. The emphasis of the Center is on eastern and central United States *structures*, and *lifelines* throughout the country that may be exposed to any level of earthquake hazard.

NCEER's research is conducted under one of four Projects: the Building Project, the Nonstructural Components Project, and the Lifelines Project, all three of which are principally supported by the National Science Foundation, and the Highway Project which is primarily sponsored by the Federal Highway Administration.

The research and implementation plan in years six through ten (1991-1996) for the Building, Nonstructural Components, and Lifelines Projects comprises four interdependent elements, as shown in the figure below. Element I, Basic Research, is carried out to support projects in the Applied Research area. Element II, Applied Research, is the major focus of work for years six through ten for these three projects. Demonstration Projects under Element III have been planned to support the Applied Research projects and include individual case studies and regional studies. Element IV, Implementation, will result from activity in the Applied Research projects, and from Demonstration Projects.

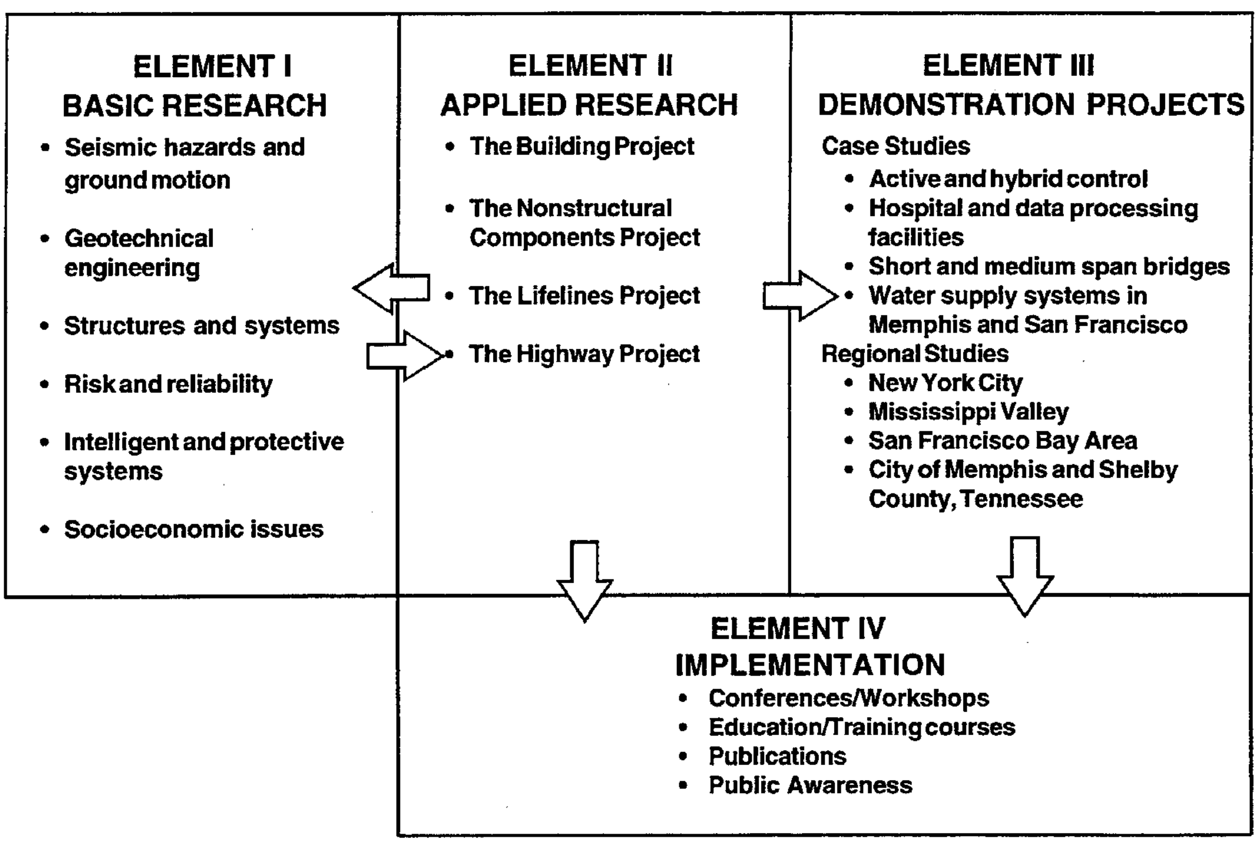

Research in the **Building Project** focuses on the evaluation and retrofit of buildings in regions of moderate seismicity. Emphasis is on lightly reinforced concrete buildings, steel semi-rigid frames, and masonry walls or infills. The research involves small- and medium-scale shake table tests and full-scale component tests at several institutions. In a parallel effort, analytical models and computer programs are being developed to aid in the prediction of the response of these buildings to various types of ground motion.

Two of the short-term products of the **Building Project** will be a monograph on the evaluation of lightly reinforced concrete buildings and a state-of-the-art report on unreinforced masonry.

The **protective and intelligent systems program** constitutes one of the important areas of research in the **Building Project**. Current tasks include the following:

1. Evaluate the performance of full-scale active bracing and active mass dampers already in place in terms of performance, power requirements, maintenance, reliability and cost.
2. Compare passive and active control strategies in terms of structural type, degree of effectiveness, cost and long-term reliability.
3. Perform fundamental studies of hybrid control.
4. Develop and test hybrid control systems.

The need for protection against earthquakes provided an incentive to adopt and adapt well-known military technology to structures in order to reduce their vulnerability to earthquakes. The work presented in this paper is entirely dedicated to verification of hardware, and understanding its complex behavior in order to make it applicable to reduce vibrations of buildings. The nonlinear dampers verified herein are an extension of application of linear devices for reduction of earthquake generated forces and deformations. This field of study, one of the most advanced in the industry, was encouraged, supported, and developed by researchers of NCEER. Many applications to existing structures are the result of their efforts. Moreover, the applications were much supported by reports of NCEER, traveling seminars (Passive Energy Dissipation for Seismic/Wind Design and Retrofit Short Course), and publications such as this. This work is a natural extension of previous work done on linear nonlinear damping in linear or nonlinear structures.

ABSTRACT

Among the many supplemental energy dissipation devices proposed and implemented for earthquake hazard mitigation, fluid viscous dampers have found a significant number of recent applications. At first the interest has been in dampers with linear viscous behavior. Accordingly, a number of experimental and analytical studies has been conducted that demonstrated the effectiveness of these devices for earthquake hazard mitigation. More recently, interest has been increasing for the use of nonlinear viscous damping devices. This report represents the first systematic experimental study of nonlinear viscous damping devices.

Earthquake simulation tests have been performed on one-story and three-story model structures without and with linear and nonlinear viscous dampers. The experimental results demonstrated, once more, significant reductions in response when dampers, whether linear or nonlinear, are added to the structural frame. Moreover, direct comparisons of responses of the structure with linear and nonlinear dampers elucidated further benefits offered by the nonlinear devices and identified potential drawbacks.

The experimental response has been compared with predictions of response history and simplified methods of analysis. The latter method has been based on the linear static procedure of the NEHRP Guidelines for the Seismic Rehabilitation of Buildings. Comparisons of analytical and experimental responses showed good agreement.

ACKNOWLEDGMENTS

Financial support for this project has been provided by the National Center for Earthquake Engineering Research (Project No. 95-5104A) and Taylor Devices, Inc., N. Tonawanda, New York.

Ayman Seleemah's stay and study at the State University of New York at Buffalo has been supported by the Ministry of Higher Education of the Arab Republic of Egypt. This report represents a major portion of the doctoral dissertation of Ayman Seleemah at Cairo University in Egypt. The dissertation committee consists of Professors Hasan M. Emam, Vice President of Cairo University, Amr W. Sadek, Structural Engineering Dept., Cairo University, and El Sayed A. El Kasaby, Head, Civil Engineering Dept., Benha Higher Institute of Technology.

Messrs. Mark Pitman, Dan Walch and R. Cizdziel, the technicians of the structural dynamics laboratory and earthquake simulator at the State University of New York, assisted in the experimental part of this work. Their assistance is greatly appreciated.

TABLE OF CONTENTS

TABLE OF CONTENTS (Cont'd)

LIST OF ILLUSTRATIONS

LIST OF ILLUSTRATIONS (Cont'd)

LIST OF ILLUSTRATIONS (Cont'd)

LIST OF ILLUSTRATIONS (Cont'd)

LIST OF ILLUSTRATIONS (Cont'd)

LIST OF ILLUSTRATIONS (Cont'd)

LIST OF ILLUSTRATIONS (Cont'd)

LIST OF ILLUSTRATIONS (Cont'd)

LIST OF ILLUSTRATIONS (Cont'd)

LIST OF TABLES

LIST OF TABLES (Cont'd)

SECTION 1

INTRODUCTION

1.1 General

Structures located in seismically active areas must be designed to resist earthquake loading. However, absolute safety and no damage cannot be achieved economically even in earthquakes likely to occur within the lifetime of a structure. Accordingly, it is an acceptable practice to design most structures with the objectives of life safety in the design basis earthquake and collapse prevention in stronger earthquakes. That is, it is acceptable that structures suffer significant structural and nonstructural damage. Exception to this philosophy are design standards for critical facilities, hospitals and schools, for which an attempt is made to minimize damage as well as protect life.

The level of damping in structures is typically very low and hence the amount of energy dissipated during elastic behavior is very small. During a severe earthquake, the design philosophy seeks to prevent collapse at the expense of allowing inelastic action in specially detailed critical regions of the structural system such as beams near or adjacent to the beam-column joints. Although such regions may be well detailed, their hysteretic behavior will degrade with repeated inelastic cycling. That is, the inelastic behavior in these regions, though able to dissipate substantial energy, often results in significant damage to the structural members. In addition, interstory drifts required to achieve significant hysteretic energy dissipation in the critical regions are large and usually result in permanent deformations and substantial damage to the nonstructural elements such as infill walls, partitions, doorways and sensitive equipment attached to the structure.

A novel approach for earthquake hazard mitigation is the use of earthquake protective systems, either at the foundation of the structure (seismic isolation, e.g. see Skinner et. al. 1993; Kelly 1993; Soong and Constantinou 1994), or throughout the height of the structure (supplemental damping systems). The objective of the latter approach is to preferentially dissipate earthquake-induced energy in devices designed especially for this purpose, and to eliminate or minimize energy dissipation demand and inelastic action in primary structural members. This way of controlling the response usually results in elimination or reduction of inelastic action in structural members and reduction of interstory drift.

Supplemental damping devices dissipate energy by different means, such as yield of mild steel, sliding friction, viscoelastic action in polymeric materials, piston or plate movement within fluids, or fluid flow through orifices. Considerable research has been conducted on energy dissipation systems. Reviews of these efforts and specific descriptions of energy dissipation systems may be found in Soong and Constatinou (1994), Soong and Dargush (1996) and Constantinou et. al. (1997). The Federal Emergency Management Agency (1996) issued in September of 1996 the ballot version of the National Earthquake Hazards Reduction Program Guidelines and Commentary for the Seismic Rehabilitation of Buildings. These documents contain a chapter devoted to energy dissipation systems. Being the collective effort of a number of consultants in a three-year project, this chapter contains the most up-to-date analysis and design guidelines for such systems.

This report focuses on the supplemental damping devices that operate on the principle of fluid flow through orifices, which are commonly called viscous damping devices or viscous dampers. Experimental and analytical studies of buildings and bridge structures incorporating linear viscous damping devices have been performed by Constantinou et. al. (1992), Tsopelas et. al. (1994) and Reinhorn et. al. (1995). The work described in this report represents the first systematic experimental study of nonlinear viscous damping devices.

1.2 Objectives and Scope

The objectives of this study were to experimentally study the behavior of a structural systems with added nonlinear viscous dampers, and to analytically predict its seismic response by response history and simplified methods of analysis.

To achieve these objectives, a number of tasks have been performed as follows:

a) An available 3-story steel model structure with damage from previous testing has been repaired to a condition with sufficient strength to resist weak earthquakes without damage. The repaired structure exhibited brittle behavior and could not be expected to resist stronger earthquakes without the use of an earthquake protective system.

b) Testing of the model structure without dampers has been conducted to establish a basis for comparison.

c) Linear viscous dampers have been selected and tested within the model structure in order to establish a basis for comparison of linear and nonlinear viscous damper effects.

d) Linear and nonlinear viscous dampers have been tested for determination of properties and for development of analytical models.

e) Testing of the model structure with nonlinear viscous dampers has been conducted.

f) Recorded response quantities have been compared to analytical results produced by response history and simplified analysis procedures.

g) Recorded response quantities of the structure without and with linear and nonlinear viscous dampers have been compared.

SECTION 2

MECHANICAL PROPERTIES OF FLUID DAMPERS

2.1 Introduction

Fluid viscous dampers operate on the principle of flow of viscous fluid through orifices. These devices have been originally developed for military applications and later used for various applications such as energy absorbing buffers in steel mills, canal lock buffers, offshore oil leg suspension and in shock and vibration isolation. For some of these applications the input is severe with peak velocity reaching 5 m/sec and peak acceleration reaching 200g with a very small rise time of the order of a few milliseconds (Constantinou 1992). Some notable examples of military applications are launch gantry dampers for the U.S. Navy with force output of up to 8900 kN and travel of 5 m, seismic dampers in nuclear power plants with force output of 1335 to 4450 kN, payload dampers for the space shuttle, wind dampers for the Atlas and Saturn-V rockets and shock isolators for most tactical and strategic missiles of the U.S. Armed Forces (Soong and Constantinou 1994).

Recently, these devices have been utilized in a number of buildings either as elements of a seismic isolation system or as wind or seismic energy absorbing elements through out the height of the building. Table 2-I summarizes these applications. Moreover, a study for retrofitting the suspended part of the Golden Gate Bridge in California concluded that the use of nonlinear viscous dampers will produce the desired performance (Rodriquez 1994).

Table 2-I **Recent Structural Applications of Fluid Viscous Dampers**

Name and Type of Structure	Location	Type and Number of Dampers	Date of Installation	Load	Additional Information
North American Air Defense Command	Cheyenne Mountain, WO USA	Quantity, Type, and Size Classified	1984	Nuclear Attack	Classified
Rich Stadium	Buffalo, NY USA	Total = 12 50 kN, 460 mm stroke	1993	Wind	Wind dampers connect light poles to the stadium parapet wall to eliminate base plate anchor bolt fatigue
Pacific Bell North Area Operation Center	Sacramento, CA USA	Total = 62 130 kN, 50 mm stroke	1995	Seismic	New construction, three story steel braced frame, dampers used to dissipate seismic energy
San Bernardino County Medical Center (5 Buildings)	San Bernardino, CA USA	Total = 186 1400 kN, 600 mm stroke	1995	Seismic	New construction, dampers used to add energy dissipation to rubber bearing isolation system in five independently isolated buildings
Hotel Woodland	Woodland, CA USA	Total = 16 450 kN, 50 mm stroke	1996	Seismic	Seismic retrofit of four story historic masonry structure with fluid dampers
28 State Street	Boston, MA USA	Total = 40 670 kN, 25 mm stroke	1996	Wind	Wind dampers used in diagonal bracing for comfort level improvements to a completely renovated high rise office building
Langenbach House	Oakland, CA USA	Total = 4 130 kN, 150 mm stroke	1995	Seismic	Seismic dampers used to provide energy dissipation in rubber bearing isolation system

Table 2-I **Recent Structural Applications of Fluid Viscous Dampers (Continued)**

Name and Type of Structure	Location	Type and Number of Dampers	Date of Installation	Load	Additional Information
CSUS Science II Building	Sacramento, CA USA	Total = 40 220 kN, 50mm stroke	1996	Seismic	Seismic dampers used in chevron bracing of this new structure to dissipate seismic energy
San Francisco Opera House	San Francisco, CA USA	Total = 16 1780 kN, 75 mm stroke	1996	Seismic	Retrofit application, Dampers used to add energy dissipation
Kaiser Data Center	Corona, CA USA	Total = 16 425 kN, 560 mm stroke	1996	Seismic	Retrofit application, dampers used to add energy dissipation to rubber bearing isolation system
The Money Store National Headquarters	Sacramento, CA USA	Total = 120 710 kN, 64 mm stroke 1290 kN, 64 mm stroke	1996	Seismic	New construction, pyramid shaped 11-story office building, moment frame structure with dampers in diagonal braces
Quebec Iron and Titanium Smelter	Tracy Canada	Total = 22 450 kN, 64 mm stroke 225 kN, 100 mm stroke 130 kN, 100 mm stroke	1996	Seismic and Wind	Dual purpose spring dampers for seismic and wind protection of two smelter buildings. Dampers used to prevent building from impacting during a seismic event
Hayward City Hall	Hayward, CA USA	Total = 15 1400 kN, 600 mm stroke	To be installed 1997	Seismic	Seismic retrofit, dampers used to add energy dissipation to friction pendulum bearing isolation system

Table 2-I **Recent Structural Applications of Fluid Viscous Dampers (Continued)**

Name and Type of Structure	Location	Type and Number of Dampers	Date of Installation	Load	Additional Information
Rockwell Building 505	Newport Beach, CA USA	Total = 6 320 kN, 64 mm stroke	To be installed 1997	Seismic	Retrofit of a long building with multiple expansion gaps.Dampers restrict relative movements between building sections
Cape Girardeau Bridge	Cape Girardeau, MO USA	Total = 8 6700 kN, 180 mm stroke	To be installed 1997	Seismic	New construction of a cable-stayed bridge. Dampers control longitudinal earthquake movement while allowing free thermal movement
San Francisco Civic Center	San Francisco, CA USA	Total = 292 1000 kN, 100 mm stroke 550 kN, 100 mm stroke	To be installed 1997	Seismic	New construction, 14-story 8000 square meter Government office building with dampers in diagonal bracing elements to dissipate seismic energy
Rio Vista Bridge	Rio Vista, CA USA	Total = 8 685 kN, 254 mm stroke	To be installed 1997	Seismic	Retrofit of highway bridge
CSULA Administration Building	Los Angeles, CA USA	Total=14 1100 kN, 150 mm stroke	To installed 1997	Seismic	Seismic upgrade of office building. Dampers installed in Chevron bracing to dissipate seismic energy
Alaska Building	Alaska USA	Total = 2 445 kN, 128 mm stroke	To be installed 1997	Seismic	Retrofit to timber frame structure. Dampers installed in diagonal bracing to dissipate seismic energy

2.2 Construction of the Dampers

Figure 2-1 shows a longitudinal cross section of one of the dampers used in this study. The damper consists of a stainless steel piston with a bronze orifice head and an accumulator. These are contained in a stainless steel cylinder filled with silicone oil and closed by a high strength acetal resin seal and a seal retainer. The fluid flows through specially shaped orifices in the bronze head. This flow is compensated by a passive bi-metallic thermostat that allows stable operation of the device over a wide temperature range (-40^0 C to 70^0 C). The orifice configuration and mechanical construction can be adjusted to produce various flow characteristics with different resisting force properties. The construction of fluid dampers with an accumulator is not common for large size dampers. Rather, constructions with a run-through rod have been used in all of the applications listed in Table 2-I.

2.3 Operation of the Dampers

The damping force results from the pressure differential across the piston head. In Figure 2-1 assume that the piston moves towards the right. This results in fluid flow from chamber 2 to chamber 1, creating a pressure differential between the two chambers. However, another phenomenon also takes place: a volume equal to the piston rod area multiplied by the piston travel is forced into the cylinder. Since the fluid is compressible, its volume will decrease by this amount and thus a restoring (stiffness) force will develop. This phenomenon can be prevented by either using an accumulator or using a run-through rod design strategy for the dampers. In the tested dampers an accumulator was used to prevent the occurrence of fluid compression. For low frequency motions (below a certain cut-off frequency that can be specified in the accumulator design), the accumulator valve can properly operate and prevent fluid compression. However, for high frequency motions (above the cut-off frequency), the accumulator valve is unable to properly function and the dampers develop restoring force.

The existence of this restoring force for frequencies higher than the cut-off frequency may be a desirable property. The dampers can provide additional viscous type damping to the fundamental mode of the structure (typically with frequency lower than the cut-off frequency), and can provide additional damping and stiffness to the higher modes. This typically results in suppression of the contribution of higher modes to the structural response. A variety of design of fluid dampers has been developed. Figure 2-2 illustrates the four basic design characteristics (Soong and Constantinou, 1994). All four are shown with an accumulator although it is possible to avoid its use with a design incorporating a run-through rod. The fluidic device uses specially shaped orifices to achieve a force output of the type

$$p = C_o |\dot{u}|^{\alpha} \operatorname{sgn}(\dot{u}) \tag{2-1}$$

where p is the force, C_o is the damping constant, $\dot{u}$ is the piston velocity, and α is a coefficient in the range 0.3 to 2.0. The value $\alpha = 2$ is achieved with cylindrical orifices, a design which is typically unacceptable in structural applications. Small values of α, say around 0.5, are effective in attenuating high velocity shocks, whereas a design with $\alpha = 1$ (linear damper) is usually desirable in wind and seismic applications.

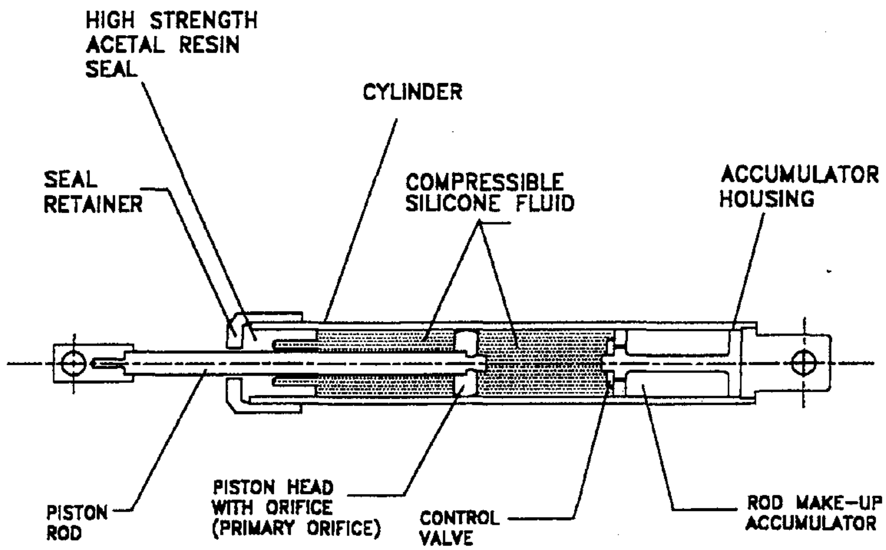

FIGURE 2-1 Longitudinal Cross Section of a Fluid Damper

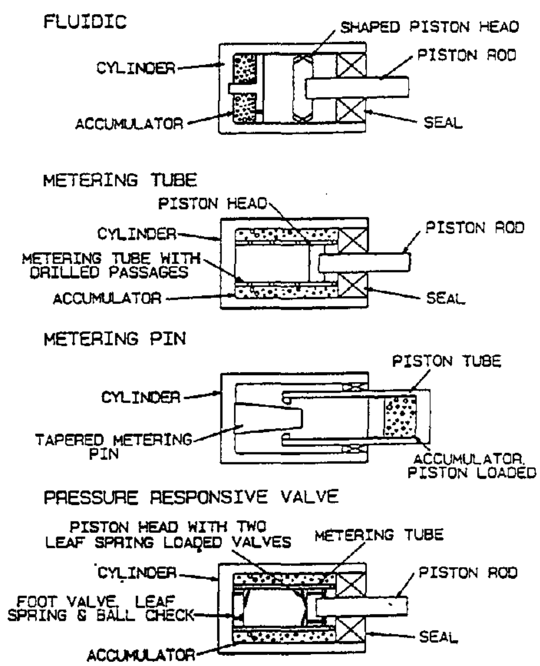

FIGURE 2-2 Design Characteristics of Fluid Dampers

The metering tube and metering pin designs can produce force output of the type

$$p = C_o \dot{u}^2 f(u)\,\mathrm{sgn}(\dot{u}) \tag{2-2}$$

where $f(u)$ is a function of displacement. The design can be effective when tuned for a particular displacement signature.

The pressure responsive valve design uses multiple spring loaded puppet valves that can achieve an output force of the type of Equation (2-1). Its performance may be limited by the dynamic characteristics of the valves.

Two types of dampers were used in this study. First, linear dampers (α = 1) with fluidic control orifices were utilized. The second set of dampers was specified to be nonlinear with exponent α in the range of 0.4 to 0.6. and output force equal to that of the linear dampers at the velocity of 150 mm/sec. The nonlinear dampers were produced from the linear ones, which were tested first, by modifying their flow characteristics. However, due to the small size of the dampers, difficulties were encountered in achieving the desired performance. It was found necessary to use for the nonlinear dampers a combined fluidic orifice - pressure responsive valve design. Dimensions for the dampers were: extended length = 330 mm, and diameter = 38 mm. Stroke was ± 50 mm and rated maximum force output was 9 kN. They weighted 10.4 N each.

2.4 Experimental Setup

Component testing was conducted first for determining the characteristics of the dampers. The tested dampers were connected to a hydraulic actuator that applied a dynamic force along the damper's axis. This applied force was such that the piston rod moved in harmonic motion with specific amplitude and frequency. The displacement was measured through a linear variable differential transformer (LVDT) that was located within the actuator. The damper force was measured through a load cell connected between the damper and a reaction frame.

Both the force and displacement records were collected through a data acquisition system. The data collection rate varied between 10 readings per second for low frequency motions (f = 0.1 Hz) to 1600 readings per second for high frequency motions (f = 16 Hz and above). The measured signals were filtered using a low pass filter with a cut-off frequency of 50 Hz. The recorded force-displacement relationships were used to extract the mechanical properties of the dampers.

2.5 Determination of Mechanical Properties of Dampers

Testing is typically conducted with displacement controlled command such that the resulting motion of the damper piston is sinusoidal, that is the damper displacement is given by

$$u = u_0 \sin(\Omega t) \tag{2-3}$$

where u_o and Ω are the specified amplitude and frequency of motion, respectively, and t is the time. Recorded loops of force versus displacement reveal characteristics of the tested devices, such as basic behavior (viscous or viscoelastic), behavior in tension and compression (symmetry of loop), dependency of behavior on temperature, frequencies, etc.

Moreover, the experimental results can be used to calibrate a mathematical model of the device provided that its basic form has been identified.

Assuming that the behavior is purely viscous, that is, force output is only related to velocity (e.g. Equation 2-1), it is sufficient to record the force output of the device at selected velocities for the model calibration. For the tested devices, the behavior has been identified to be purely viscous for frequencies of motion below a cut-off frequency of about 4 Hz. Accordingly, viscous models for the two types of utilized dampers could be easily calibrated. These models were found to be sufficient for the prediction of the seismic response of the tested structures given that the response was dominated by contributions from the first mode of vibration, which was characterized by a frequency lesser than the cut-off frequency of 4 Hz.

The development of mathematical models capable of describing the behavior of the tested dampers within a wider range of frequencies requires first the identification of the general form of the model and second the collection of more refined data on the behavior of the devices. For linear dampers it is possible to apply principles of the theory of viscoelasticity in determining mechanical properties and in constructing mathematical models that are valid over a wide range of frequencies. The usefulness of such models for the tested structures is in the identification of the damped structure (see Section 4).

The theory that follows applies to devices that have viscoelastic behavior. It is thus restricted to linear dampers. Moreover, the application of this theory to the determination of mechanical properties requires considerable caution because indiscriminate use may lead to erroneous conclusions. It is assumed that motion of the form described by Equation (2-3) is imposed to the damper and under steady-state conditions the force needed to maintain this motion is also described by a sinusoidal function, that is,

$$p = p_0 \sin(\Omega t + \Theta) \tag{2-4}$$

or

$$p = p_o \sin \Omega t . \cos \Theta + p_o \cos \Omega t . \sin \Theta \tag{2-5}$$

where p_o is the amplitude of the force and Θ is the phase angle. It should be noted that Equations (2-3) and (2-4) describe force-displacement loops of the type shown in Figure 2-3. Note that for purely viscous behavior, the loop is a perfect ellipse.

The energy dissipated by the damper in a single cycle can be evaluated as the area of the force-displacement loop. The result is

$$W_d = \pi . p_o u_o \sin \Theta \tag{2-6}$$

Introducing the terms

$$K_1 = \frac{p_o}{u_o} \cos \Theta \tag{2-7}$$

and

$$K_2 = \frac{p_o}{u_o} \sin \Theta \tag{2-8}$$

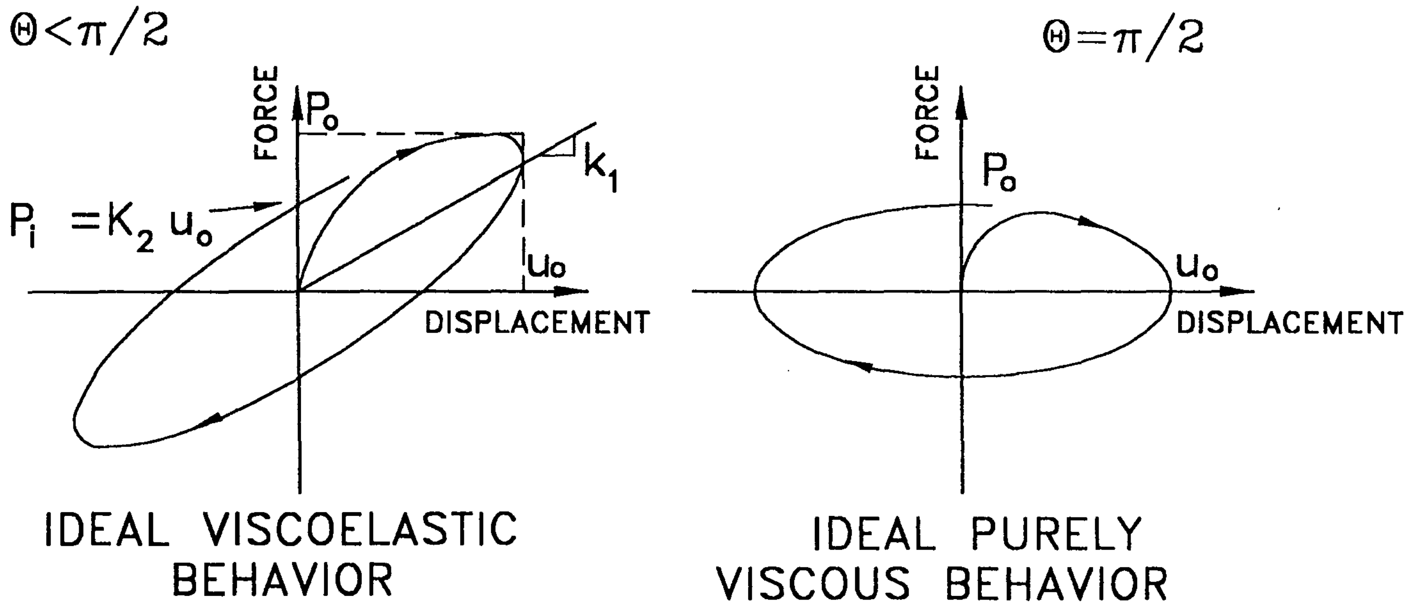

FIGURE 2-3 Idealized Force-Displacement Loops of Viscoelastic Energy Dissipation Devices

the following relation is established upon substitution into Equation (2-5)

$$p = K_1 u_o \sin \Omega t + K_2 u_o \cos \Omega t \tag{2-9}$$

or

$$p = K_1 u + \frac{K_2}{\Omega} \dot{u} \tag{2-10}$$

It is evident that the first term in this equation represents the restoring (spring like) force of the damper, which is in phase with the displacement. It is termed the storage stiffness. The second term in the equation represents the damping force, which is in phase with the velocity or is 90^0 out of phase with the displacement. The quantity K_2 is termed the loss stiffness. Thus, the damping constant, C, of the device is given by

$$C = \frac{K_2}{\Omega} \tag{2-11}$$

Equations (2-6) through (2-8) can be combined to give

$$\Theta = \sin^{-1}\left(\frac{K_2 u_o}{p_o}\right) \tag{2-12}$$

and

$$K_2 = \frac{W_d}{\pi . u_o^2} \tag{2-13}$$

A number of other useful relations may be derived. Equation (2-5) may be used to obtain the phase angle as

$$\Theta = \sin^{-1}(\frac{p_i}{P_o}) \tag{2-14}$$

where p_i is the ordinate of force at zero displacement. Furthermore, Equation (2-9) may be used to derive that the force at maximum displacement is equal to $K_1 u_o$ leading to interpretation of K_1 as the slope of the line shown in Figure 2-3. The same equation may be used to show that

$$p_i = K_2 u_o \tag{2-15}$$

When an experiment is conducted, values of Ω, u_o, p_o, p_i and W_d can be either directly measured or calculated from experimental data. Equations (2-7) to (2-15) may be used to extract the mechanical properties K_1, K_2, C and Θ. Provided that the behavior is truly viscous or viscoelastic (as depicted in Figure 2-3), anyone of these equations may be used and the results will be identical. However, actual behavior may deviate from the ideal one, in which case indiscriminate use of these equations may lead to erroneous properties and misinterpretation of behavior.

For example, Figure 2-4a shows recorded force-displacement loops of a damper for sinusoidal displacement input of 4 Hz frequency and amplitude of 6.2 mm. It may be observed that behavior is nearly purely viscous but not ideal. Data extracted from the recorded loop are $u_o = 6.2$ mm, $p_o = p_i =$ 2902 N, $W_d = 54282$ N.mm, and peak velocity

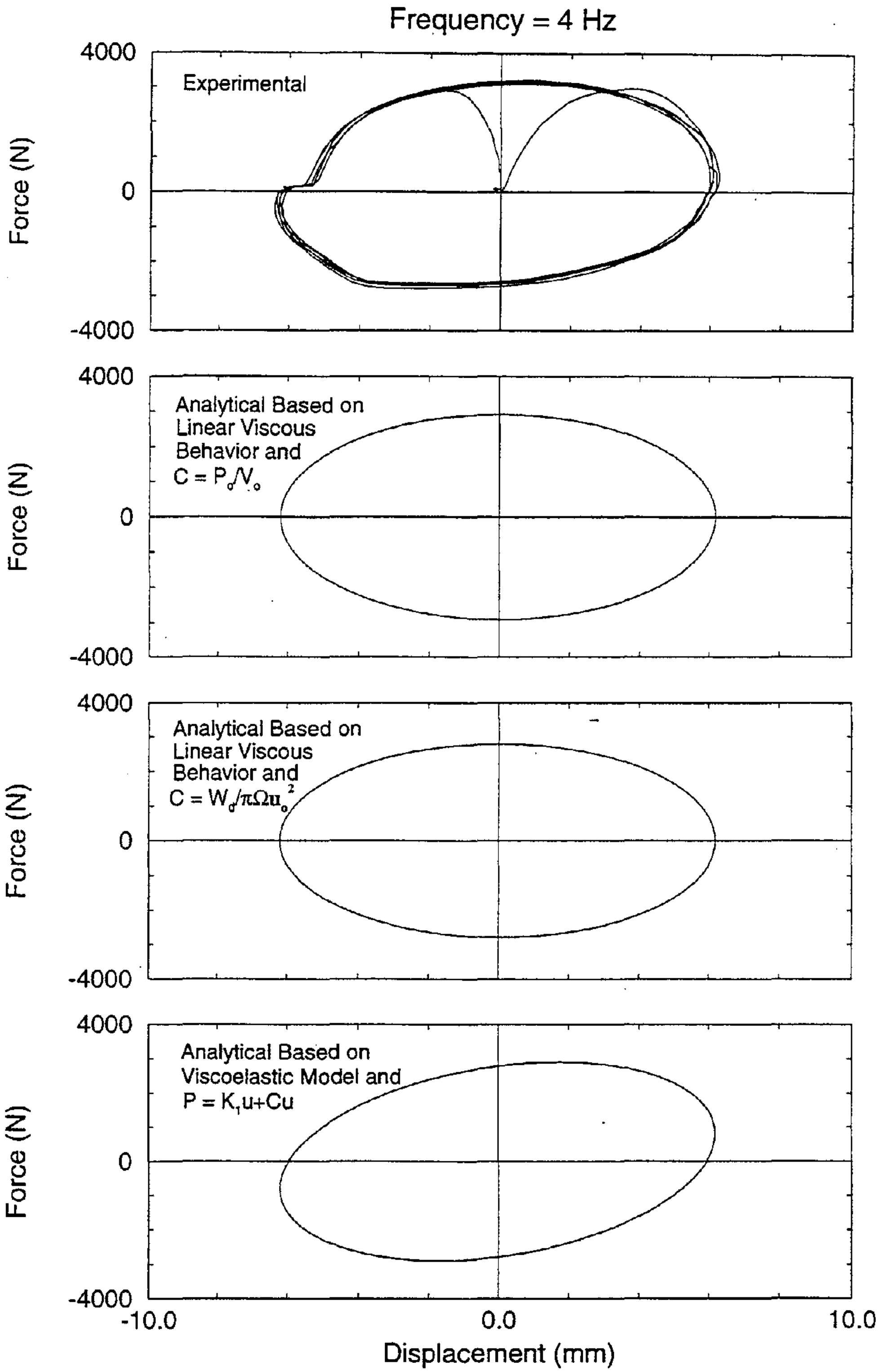

FIGURE 2-4 Example of Model Calibration

$v_o = 155.6$ mm/sec. We may proceed in establishing the mechanical properties and then, based on these properties, analytically reconstruct the loop for only the specific conditions of this test. For this we use the following procedures :

(a) Based on the observation of purely viscous behavior and assuming linear behavior, we calculate the damping constant as the ratio of peak force to peak velocity, that is, C = 2902/155.6 = 18.65 N.s/mm. The analytical model is then simply described by $p = C\dot{u}$ (the reader is cautioned that such model cannot be calibrated by a single test unless behavior is truly linear viscous). Figure 2-4b depicts the loop produced by the model. The model predicts the correct peak force (against which it was calibrated) but it overestimates the energy dissipated per cycle (56495 vs. 54282 N.mm).

(b) Based on the observation of purely viscous behavior and assuming linear behavior, Equations (2-11) and (2-13) are used to calculate the damping constant C. The result is 17.9 N.s/mm. The analytical loop is depicted in Figure 2-4c. It may be seen that peak force is under-predicted but the loop contains the same area (energy dissipated) as the actual loop.

(c) Equations (2-7), (2-11), (2-12) and (2-13) are used to calculate $C = 17.9$ N.s/mm, $\Theta = 73.9^{o}$ and $K_1 = 129.9$ N/mm. Equation (2-10) is then used to analytically construct the loop, which is shown in Figure 2-4d. The model exhibits viscoelastic behavior, which while mild, is in clear contradiction with experimental observations. Simply in this case, indiscriminate use of theory resulted in an erroneous prediction.

2.6 Mathematical Modeling of Dampers

An acceptable model of behavior of the tested dampers is the viscous model described by Equation (2-1). This model is valid for purely viscous behavior, which is typically found in fluid dampers with run-through rod. For the tested dampers this behavior is valid over a limited range of frequencies, approximately 0 to 4 Hz. Viscous models for both the tested linear and nonlinear dampers were calibrated and used in the analytical prediction of response of the tested structure.

For the case of linear dampers, an analytical model valid over a wider range of frequencies has been calibrated. The model is the standard Maxwell model which has been previously found to describe well the behavior of linear dampers with accumulators (Constantinou and Symans 1992). The model is described by

$$p + \lambda \dot{p} = C_o \dot{u} \tag{2-16}$$

where p is the force, $\dot{u}$ is the velocity, C_o is the damping constant at essentially zero frequency and λ is the relaxation time constant.

Application of Fourier transform to Equation (2-16) results in

$$\overline{p}(\Omega) = \left[K_1(\Omega) + iK_2(\Omega)\right].\overline{u}(\Omega) \tag{2-17}$$

where

$$K_1 = \frac{C_o \lambda \Omega^2}{1+\lambda^2\Omega^2} \tag{2-18}$$

$$K_2 = \frac{C_o \Omega}{1+\lambda^2\Omega^2} \tag{2-19}$$

are the storage and loss stiffness, respectively. Moreover, a bar denotes the Fourier amplitude.

It follows that the damping constant and phase angle are, respectively, given by

$$C = \frac{K_2}{\Omega} = \frac{C_o}{1+\lambda^2\Omega^2} \tag{2-20}$$

$$\Theta = \tan^{-1}\left(\frac{K_2}{K_1}\right) = \tan^{-1}\left(\frac{1}{\lambda\Omega}\right) \tag{2-21}$$

2.7 Test Results and Model Calibration

Three of the linear dampers (numbered 1, 4 and 6) and all six nonlinear dampers were tested by the procedure described in Section 2.4. Temperature of testing was about 22^{o} C (normal room temperature). The frequency of testing was in the range of 0.1 to 25 Hz with peak velocity in the range of 4 to 430 mm/sec.

Figure 2-5 shows recorded force displacement loops for linear damper No. 1. Various interesting features may be observed in these loops:

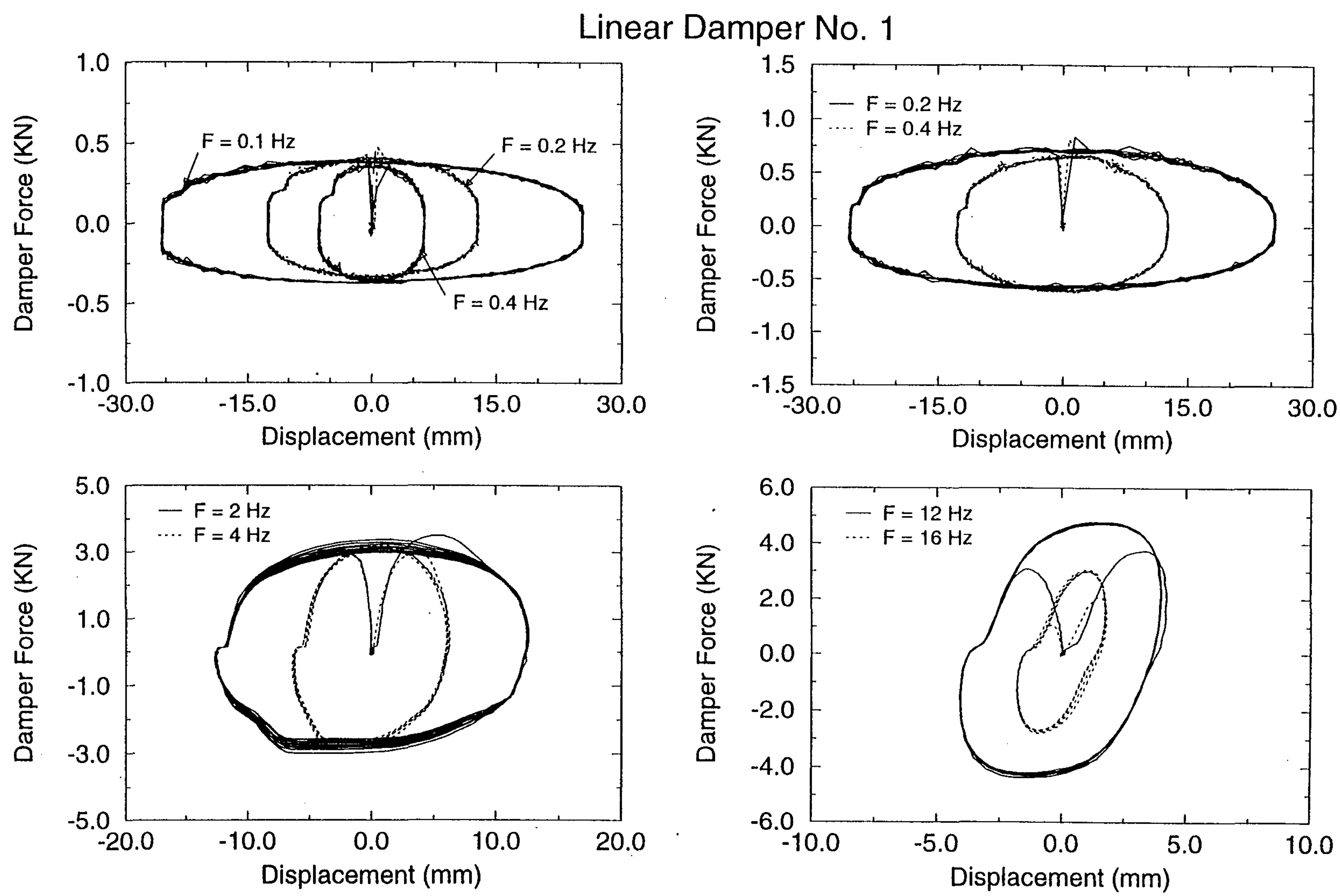

FIGURE 2-5 Typical Recorded Loops of Linear Dampers

(a) The devices exhibit, in addition to viscous, frictional behavior that originates in the seals. Static tests determined this friction force to be equal to about 60 N on the average.

(b) The behavior is indeed viscous as observed in a comparison of peak force in tests with double the frequency and half the stroke (that is, same velocity).

(c) Evidence of stiffness is seen in the right-bottom graph for testing at high frequencies.

Figure 2-6 shows recorded loops of nonlinear dampers. It may be observed that behavior is viscous (same peak force at same peak velocity when frequency and stroke are different). The behavior is easily recognized as being nonlinear from the shape of the loops that resemble rectangular rather than elliptical shape.

A comparison of loops of linear and nonlinear dampers under identical testing conditions is provided in Figure 2-7. Noting that the two dampers were designed to produce the same peak force at velocity of 150 mm/sec, we observe this to be indeed the case. As intended in the design, the nonlinear damper exhibit much higher force at lower velocities than the linear ones. We also observe some anomalies in the loop of the nonlinear damper at high velocities. We believe this to have been caused by the operation of the pressure responsive valves used in the construction of the devices.

Figure 2-8 presents graphs of force at zero displacement (that is when velocity is maximum) versus peak velocity for the tested dampers. The shown force represents the viscous component only. The frictional component of about 60 N has been subtracted. Data are shown only for the range of velocity that is relevant to the shake table testing, for which

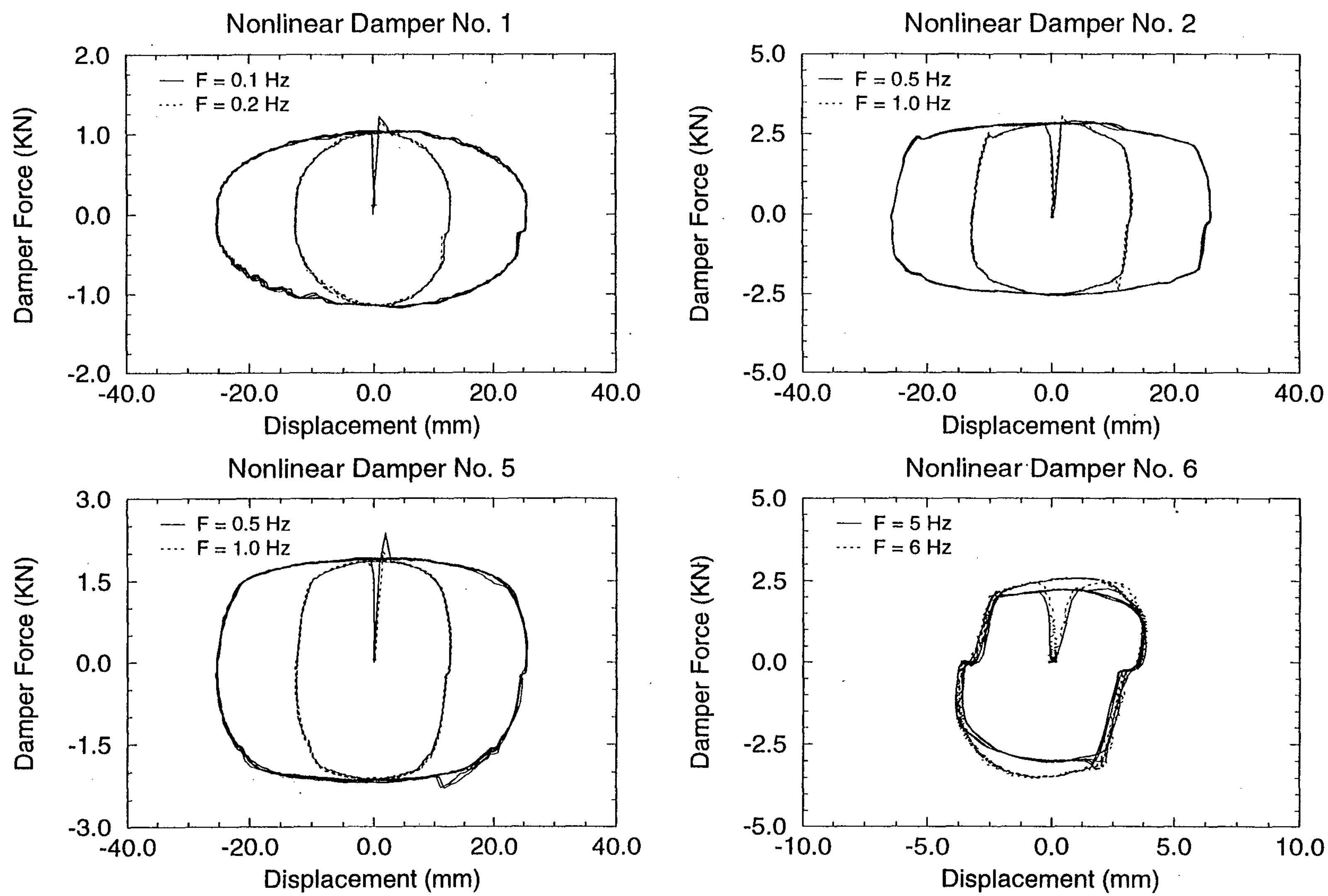

FIGURE 2-6 Typical Recorded Loops of Nonlinear Dampers

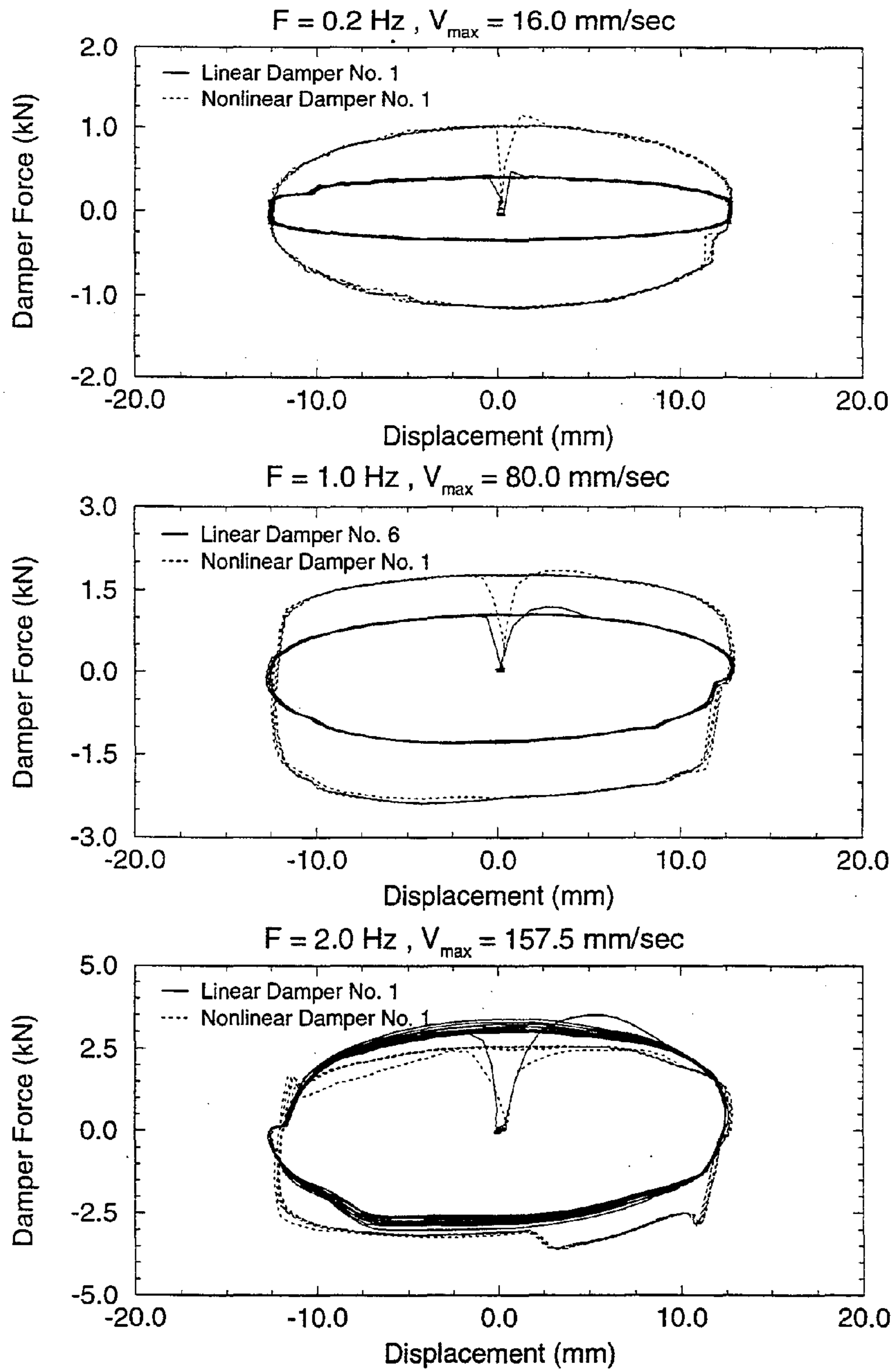

FIGURE 2-7 Comparison between Linear and Nonlinear Damper Loops

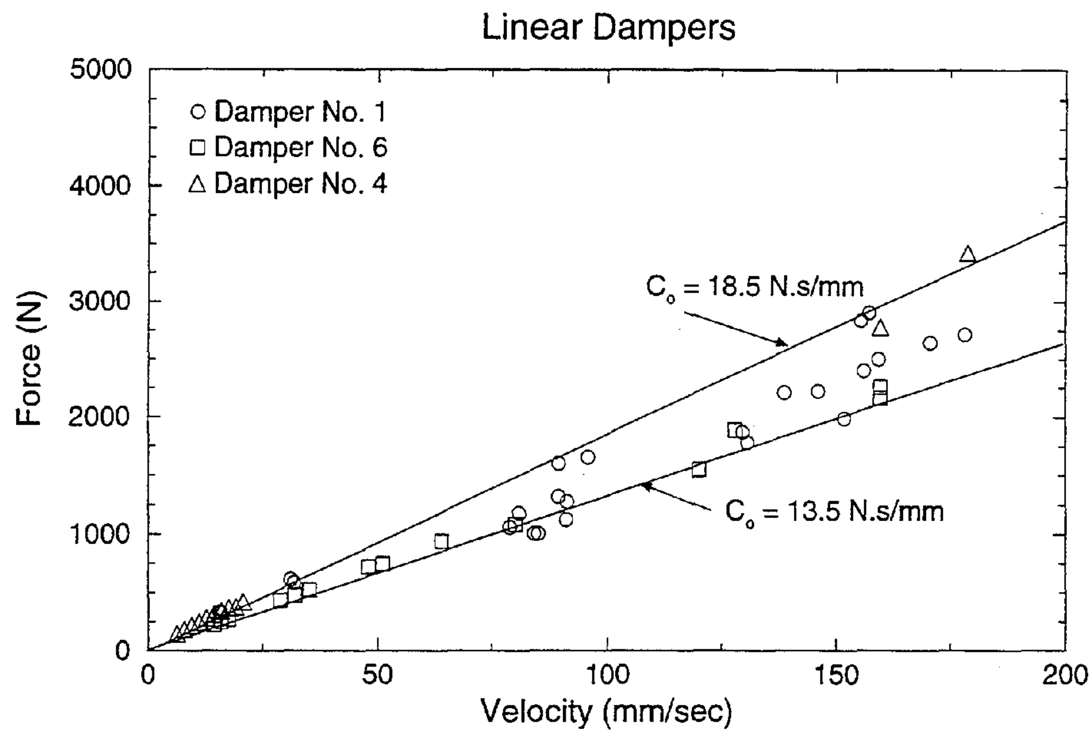

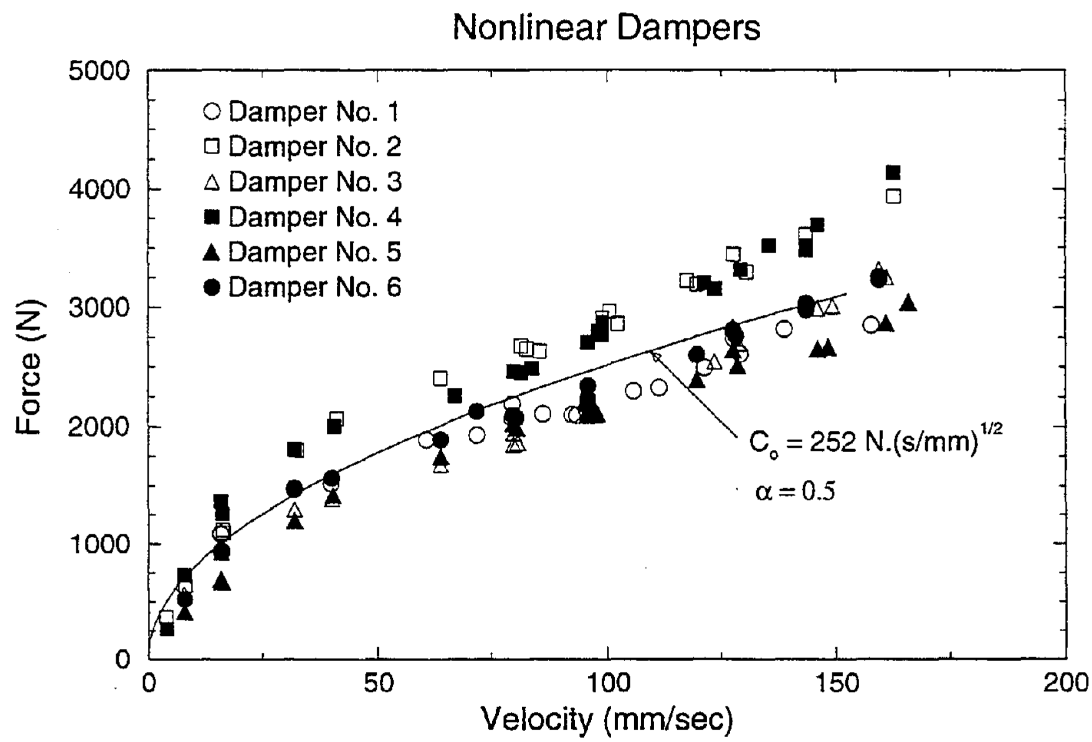

FIGURE 2-8 Force-Velocity Relationship of Linear and Nonlinear Dampers

peak velocity in the dampers did not exceed 150 mm/sec. For the linear dampers, it may be observed that data follow a linear trend and are bound by straight lines for which the slopes (the damping constant) are 13.5 and 18.5 N.sec/mm. On the average, the damping constant is $C_o = 16$ N.sec/mm and the scatter of data is within $\pm 15\%$ of this value. The same values were obtained when data over a large range of velocities were considered, as seen in Figure 2-9. Evidently the linear damper may be modeled by Equation (2-1) with $\alpha = 1$ and $C_o = 16$ N.sec/mm. More specifically, this model is valid for damper No. 1, whereas for dampers 4 and 6, the upper and lower limits on the damping constant, respectively, would better fit the experimental data. For the nonlinear dampers, the data fit well, on the average, the model of Equation (2-1) with $\alpha = 0.5$ and C_o = 252 $N.(\sec/mm)^{1/2}$. Again the scatter of data around the force-velocity curve predicted by this model is within $\pm 15\%$. More specifically, Figure 2-10 shows that more refined modeling is possible. Grouped in pairs with nearly identical properties, the six dampers may, more appropriately, be modeled to have a damping constant within the range of 220 to 300 $N.(\sec/mm)^{1/2}$. That is one pair of dampers (No. 2 and 4) exhibited approximately 30% more force output than the other four. This pair was placed at the first story of the tested structure.

It is worthy of noting in Figure 2-10 that the calibrated model of nonlinear dampers does not represent well the actual behavior at very low velocity (less than about 15 mm/s). It appears that the low velocity behavior of the devices is nearly linear. That is, an even more refined model for the nonlinear dampers is possible and it has been developed and calibrated. It contained a simple modification for linear behavior at low velocities. The model predicted the behavior of the tested model slightly better than the purely nonlinear

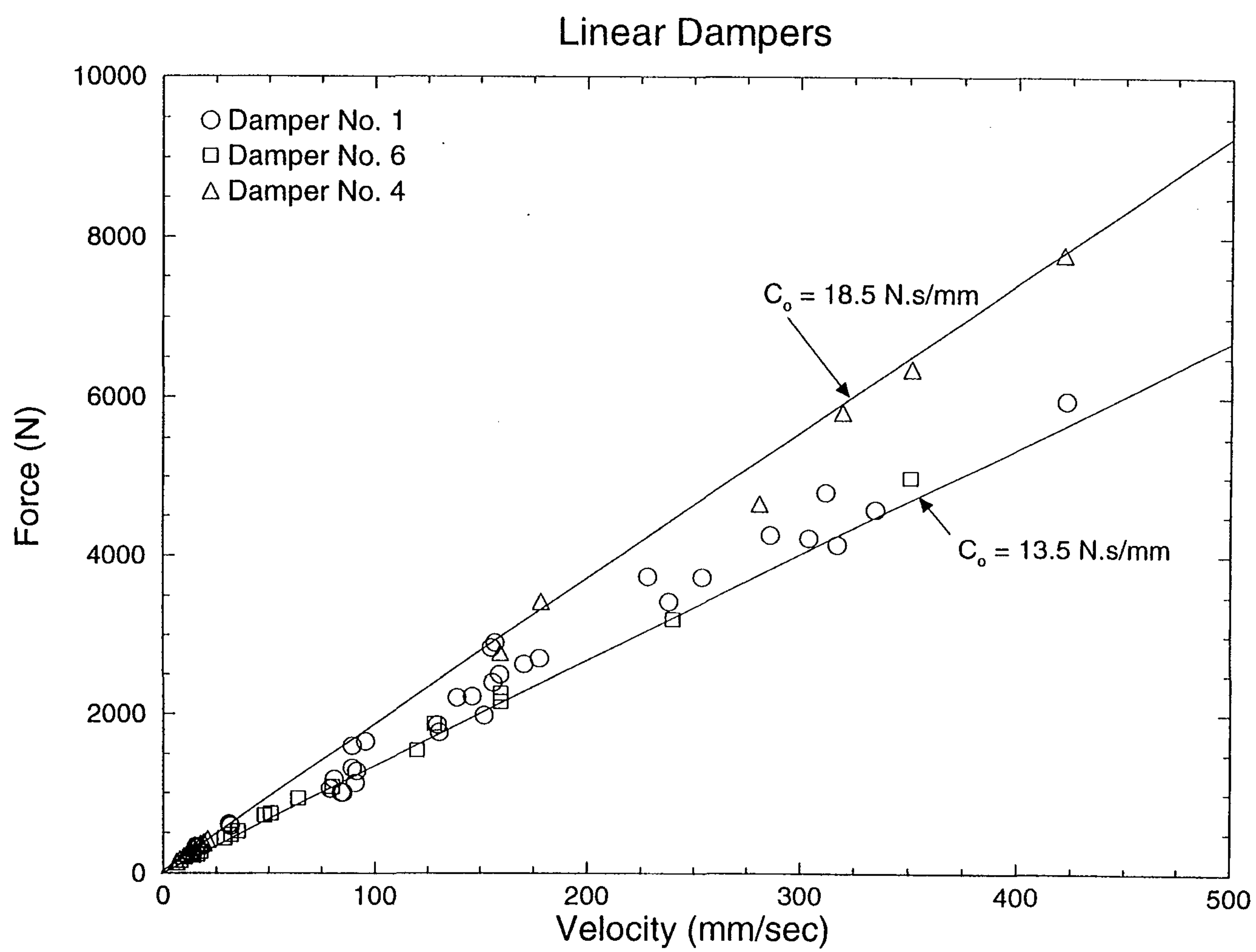

FIGURE 2-9 Force-Velocity Relationship of Linear Dampers over a Wide Range of Velocity

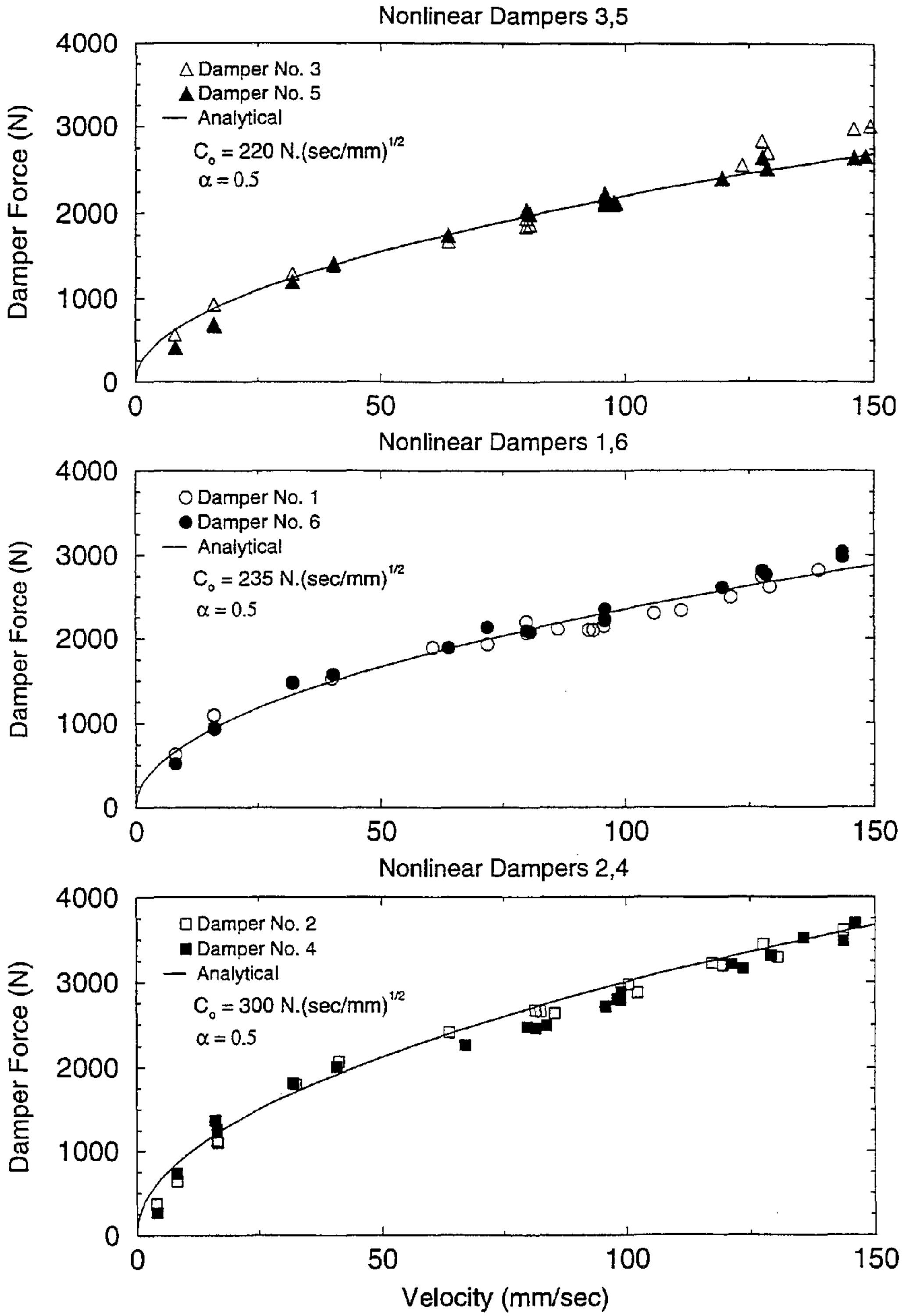

FIGURE 2-10 Refined Model for Nonlinear Dampers

model. Particularly, it predicted better the response in weak earthquakes, in which the drift and velocity were low.

The calibrated viscous models of linear and nonlinear dampers have been used for the analytical prediction of the response history of the tested structure on the shake table with satisfactory results. That is, the modeling has been adequate despite the neglect of stiffening effects at higher frequencies due to the insignificant contribution of higher modes to the seismic response of the tested structure. However, the prediction of dynamic characteristics (frequency and damping ratio) of the tested structure with linear dampers required a more refined model for the dampers. For this, the Maxwell model of Equation (2-16) has been found to adequately describe the behavior of the linear dampers within the frequency range of 0 to 25 Hz.

For the calibration of the Maxwell model, the theory of Sections 2.5 and 2.6 has been used. Based on the experimental results, the damping constant C has been determined by use of Equations (2-11) and (2-13) with energy W_d calculated from the recorded loops. The damping constant represented a mechanical property that could be determined from the experimental data without much ambiguity. The storage stiffness K_1 and phase angle Θ were also determined through the use of Equation 2-7 and either Equation 2-12 or 2-14, respectively. That is, judgment was exercised in the use of these equations based on observation of loops.

Figure 2-11 presents these mechanical properties for linear damper No.1. As noted earlier, this damper exhibited a behavior that was in-between that of the other tested dampers. A

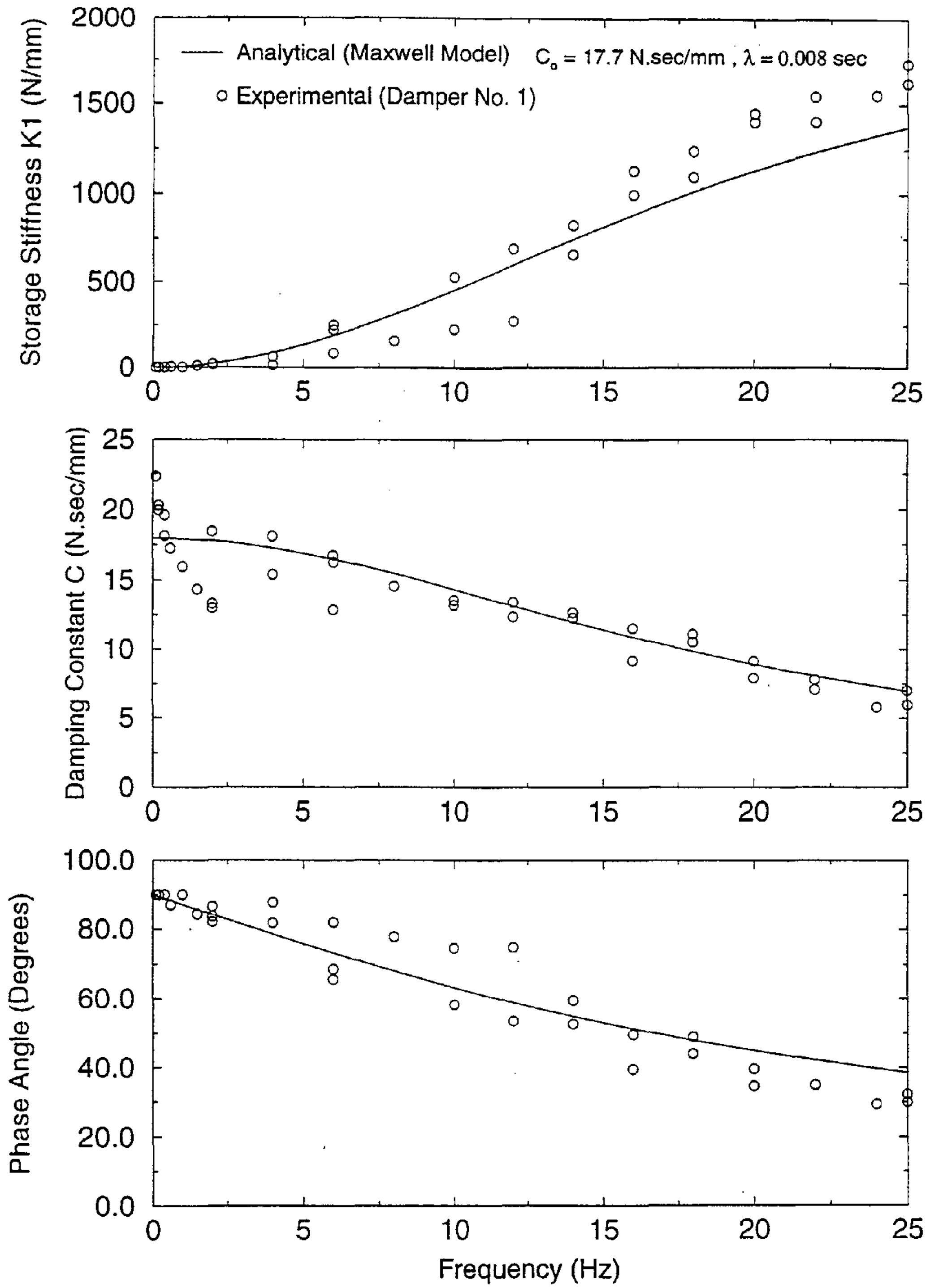

FIGURE 2-11 Comparison of Experimental and Analytically Derived Values of Storage Stiffness, Damping Constant and Phase Angle for Linear Dampers

good fit of the data on damping constant could be achieved with model parameters being $C_o = 17.7$ N.sec/mm and $\lambda = 0.008$ sec. As seen in Figure 2-11 this choice of model parameters results in a good prediction of the other mechanical properties.

The results of Figure 2-11 demonstrate that the linear dampers do not exhibit storage stiffness for frequencies below 4 Hz. The calibrated Maxwell model predicts some small storage stiffness for low frequencies, although this is of insignificant practical importance. It should be noted that the relaxation time λ is so small such that for the damping constant to change by more than 5% from its zero frequency value (C_o) it would require frequencies of more than 4.5 Hz (see Equation 2-20).

SECTION 3

STRUCTURAL MODEL FOR SHAKE TABLE TESTING

3.1 Tested Model

The tested model is a 3-story quarter length scale steel structure that was previously used in a number of studies at the University at Buffalo (Chung 1988, Soong 1990, Constantinou and Symans 1992, Symans and Constantinou 1995). The structure was originally designed not to represent a similitude scale replica of a full scale structure but rather, it was designed as a small versatile structural testing system. In its tested configuration, it had limited seismic capacity and exhibited non-ductile behavior that is representative of existing buildings in many parts of the world. Figure 3-1 shows drawings of the model structure.

The model was previously used in a large number of studies during which the structure has been damaged. The first story columns of the model were cracked at their tops and bottoms. The structure was repaired in such a way that it did not significantly change its dynamic characteristics. Welding of a longitudinal plate to each column tee section was found to be suitable. Welding of the plates was performed in such a way that concentration of heat at each section was avoided. This was achieved by alternating among the four columns during the welding process and allowing the columns to cool down after each welding phase. Figure 3-1 shows a section of the repaired first story columns.

Following repair, a total of 25 preliminary tests were conducted on the three story structure. The structure was tested either without any dampers (denoted from here on as the bare frame) or with two linear fluid dampers attached diagonally at the first story. During one of

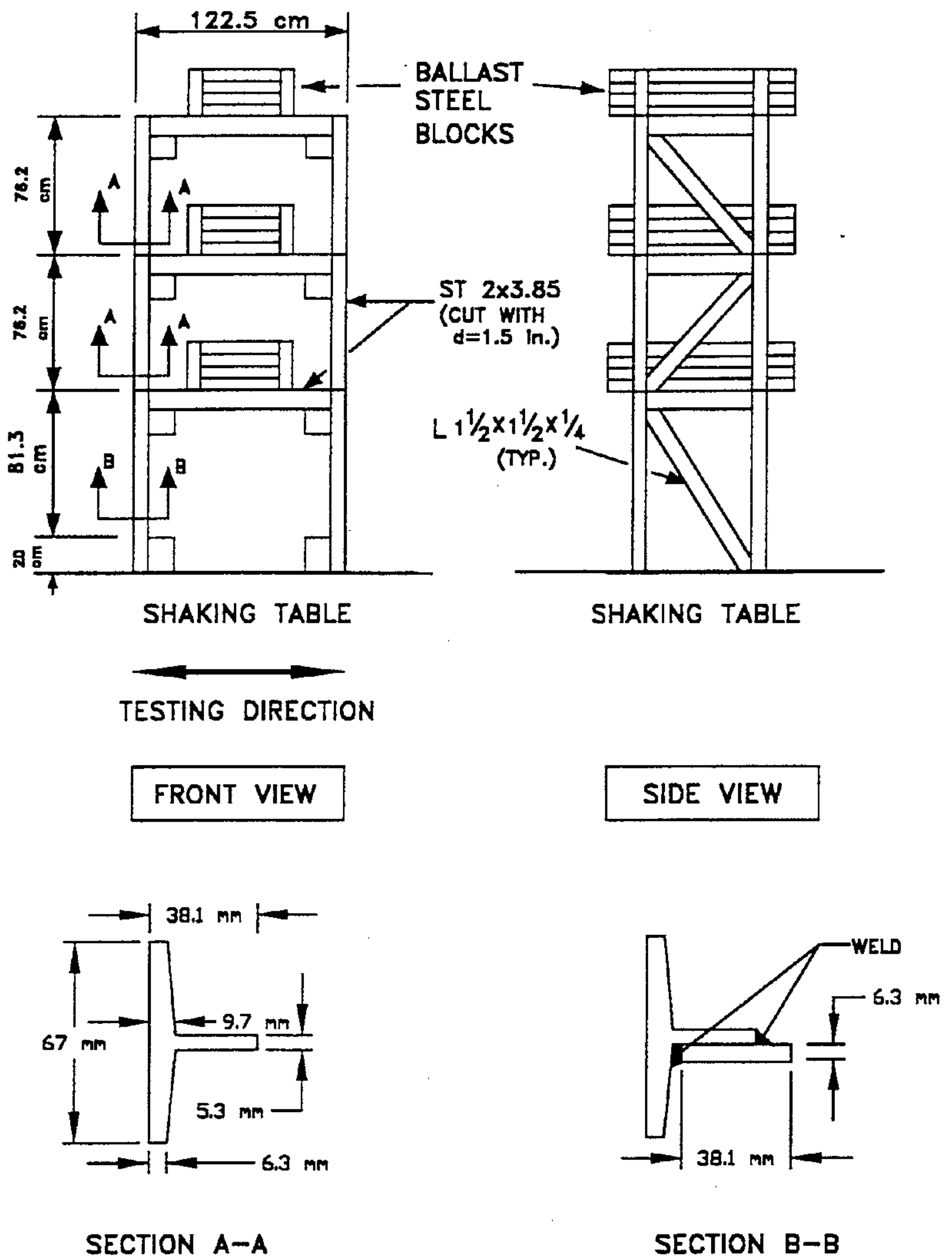

FIGURE 3-1 Schematic of Tested Model

these tests, the frame developed cracks at the first and the second story beams and at the top and the bottom of the second story columns. After investigation, it was recognized that these points were already fatigued during hundreds of tests conducted on the frame in previous studies. This was evident in recorded story shear force-drift loops which showed no evidence of any yielding of the frame that could have taken place. Once again the structure was repaired by drilling a hole at the tip of each crack and then welding 16 tapered plates as shown schematically in Figure 3-2. The tapered configuration was selected to assure gradual transition of stresses and to avoid concentration of welding over a single cross section. The repaired frame exhibited sufficient strength to remain elastic in subsequent testing. Care has been taken to avoid excessive story drifts for it was known that the frame exhibited brittle behavior.

The main set of tests began with the 3-story structure (denoted from here on as the repaired frame) without dampers, with 2 dampers placed diagonally in the second story (story of maximum drift), with 4 dampers placed at both the second and the third stories (two at each story), and with 6 dampers at all stories (two at each story). Figure 3-3 shows schematically the different configurations of the tested structure.

The structure was also tested in a single-degree-of-freedom configuration with the second and third stories braced. This configuration was tested without and with two dampers as shown schematically in Figure 3-4.

Views of the three story structure without dampers, with 2, 4, and 6 dampers are shown in Figures 3-5 through 3-8. Moreover, Figures 3-9 and 3-10 show views of the one-story

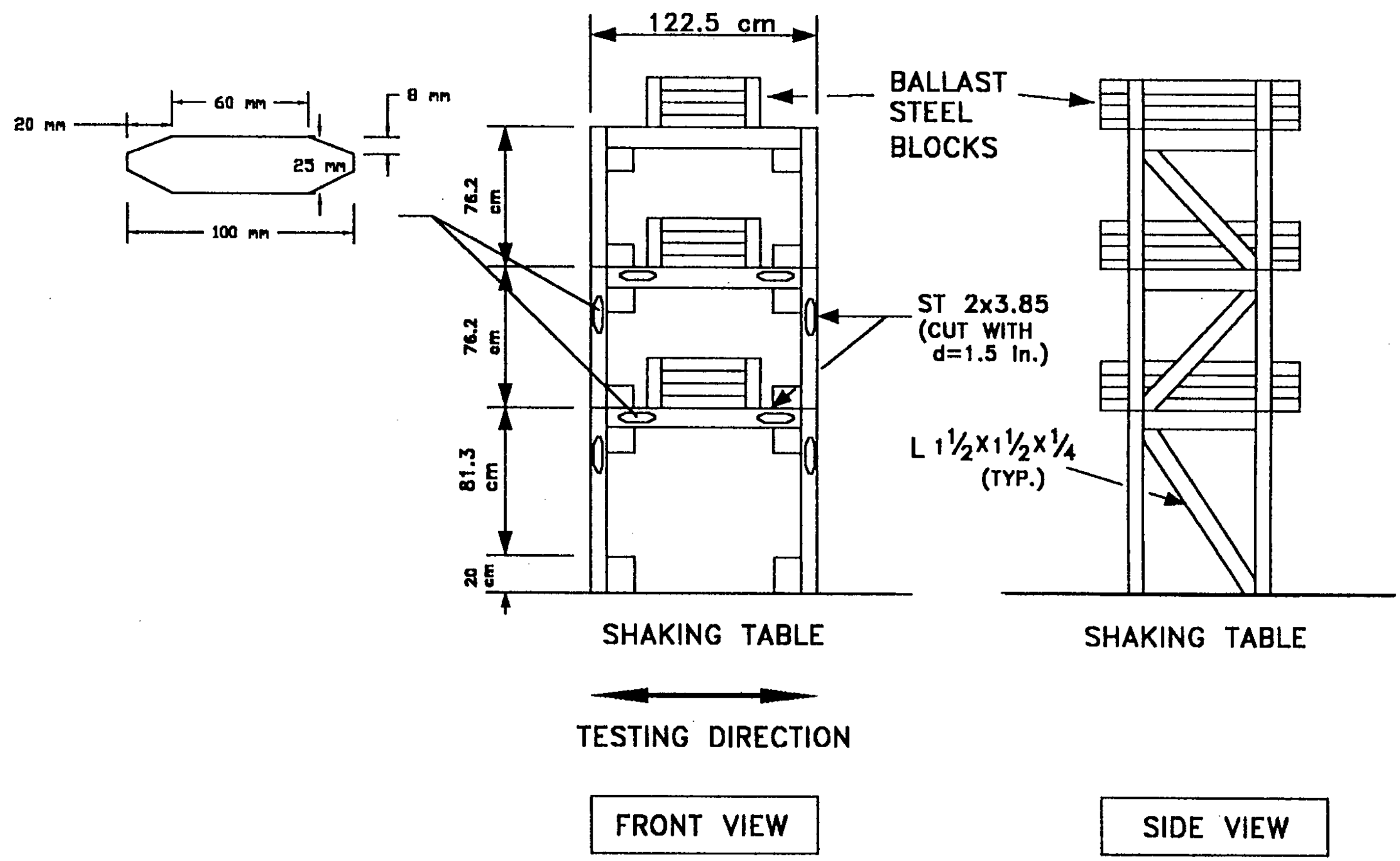

FIGURE 3-2 Schematic of Tested Model Showing Repair with 16 Tapered Plates

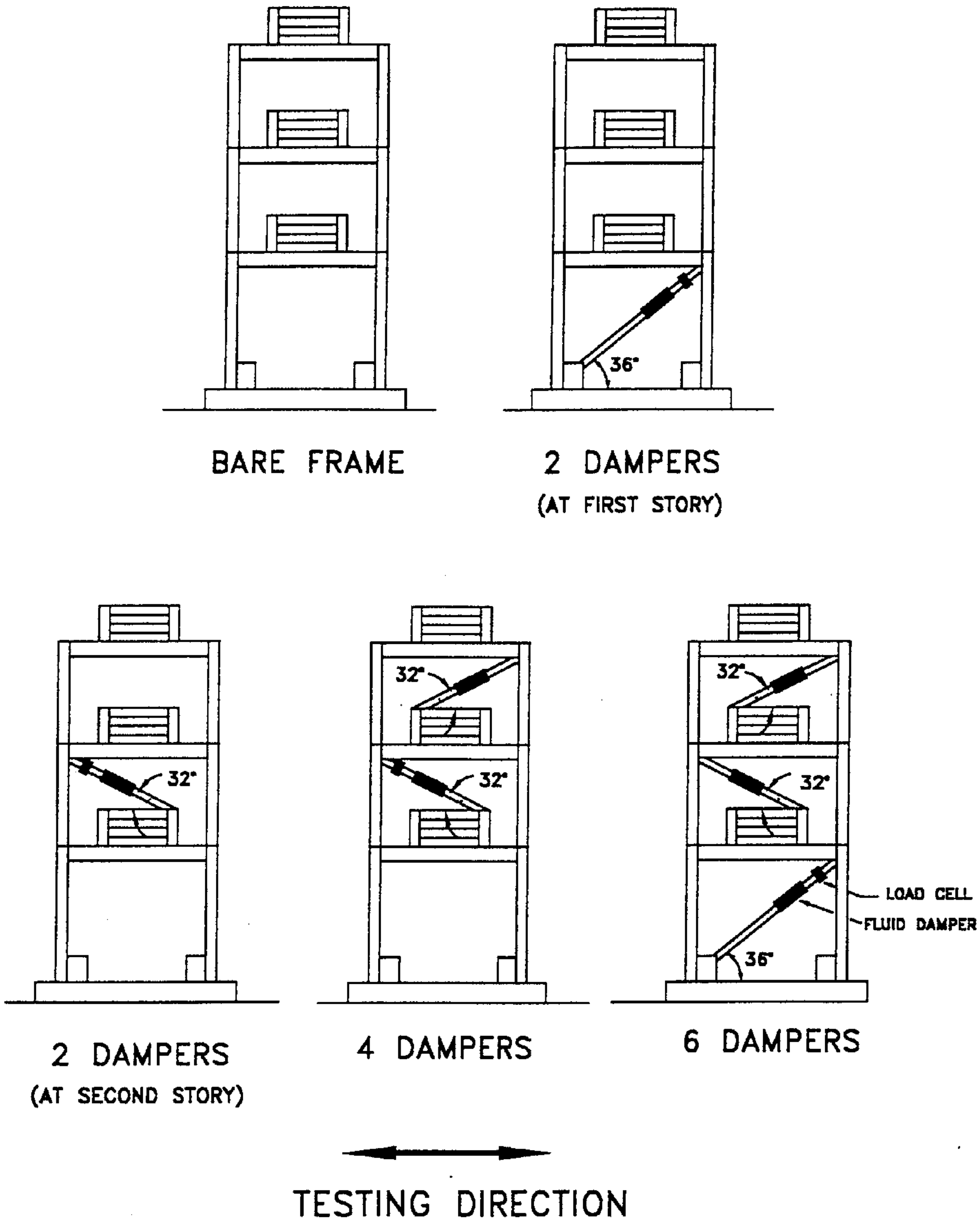

FIGURE 3-3 Schematic of Different Configurations of the Tested 3-Story Structure

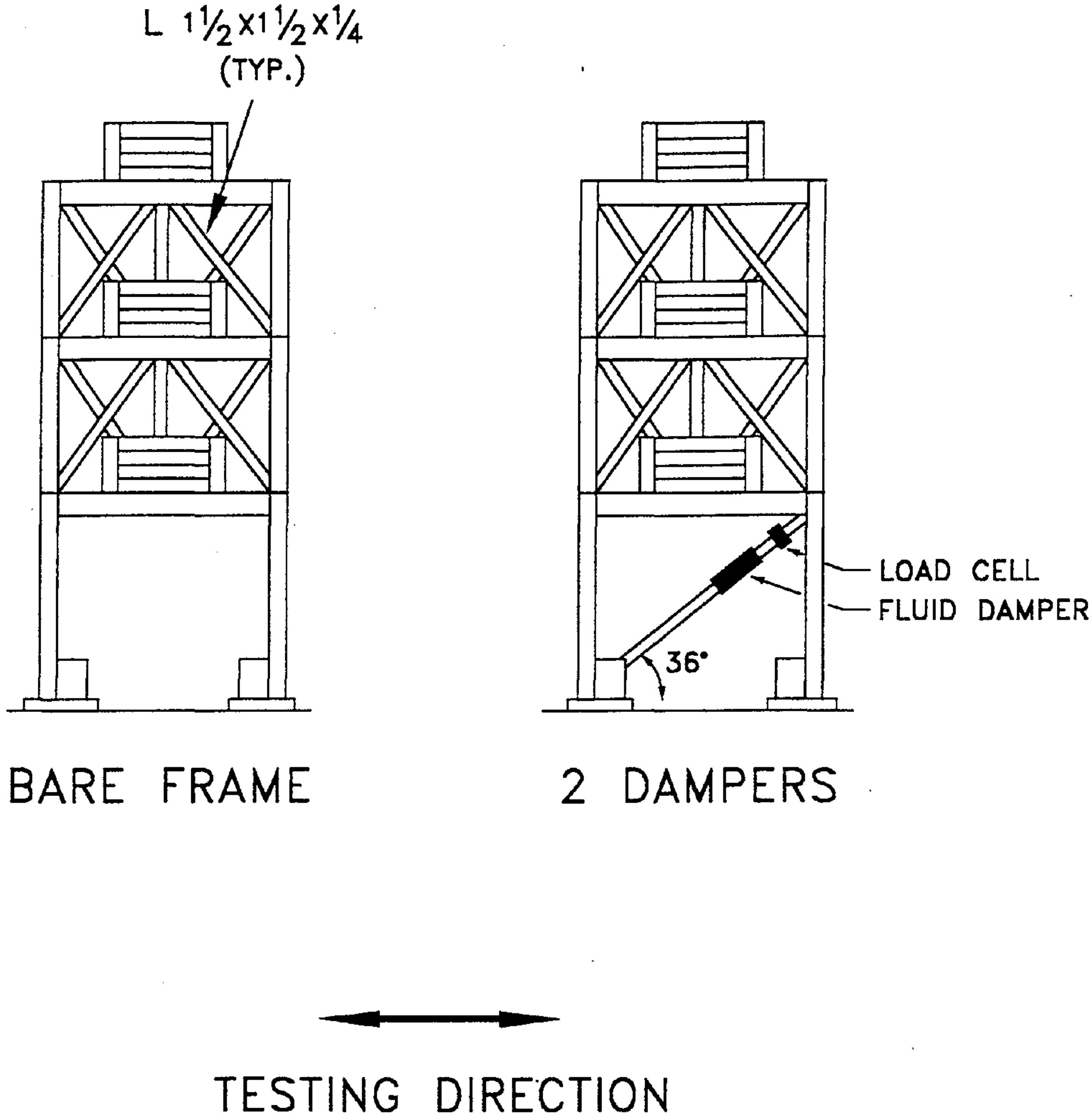

FIGURE 3-4 Schematic of Different Configurations of the Tested 1-Story Structure

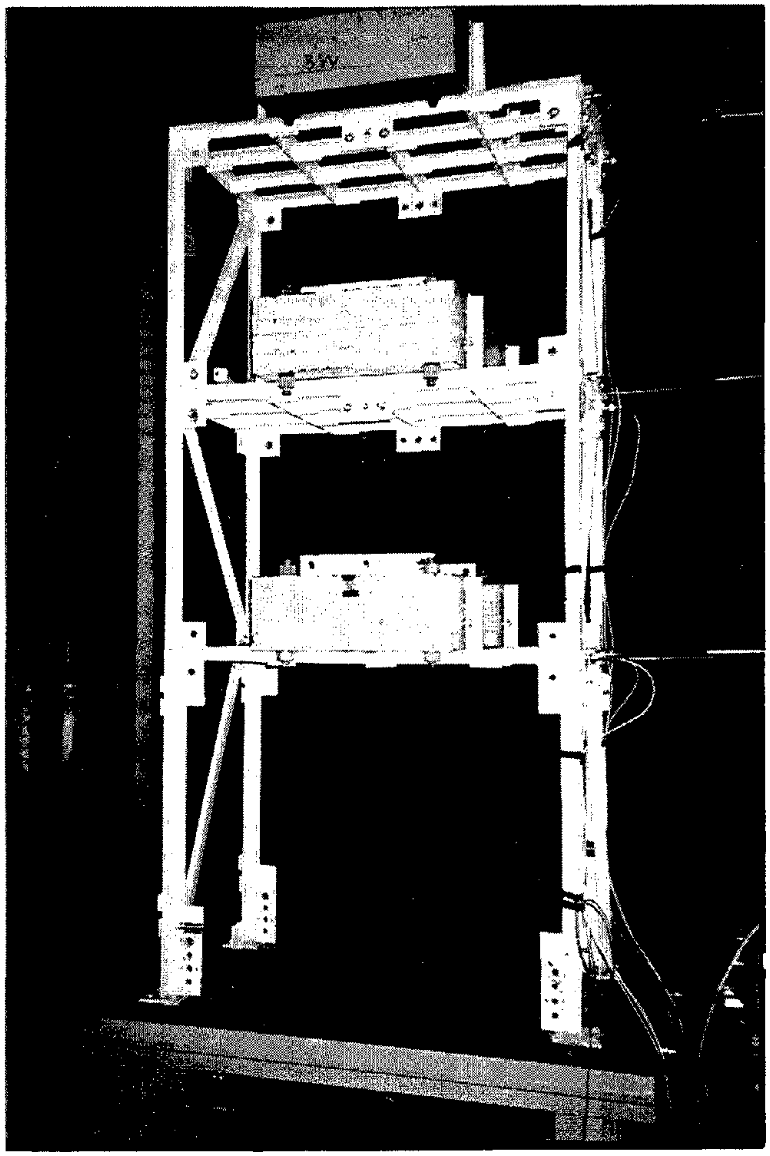

FIGURE 3-5 View of the 3-Story Structure without Dampers

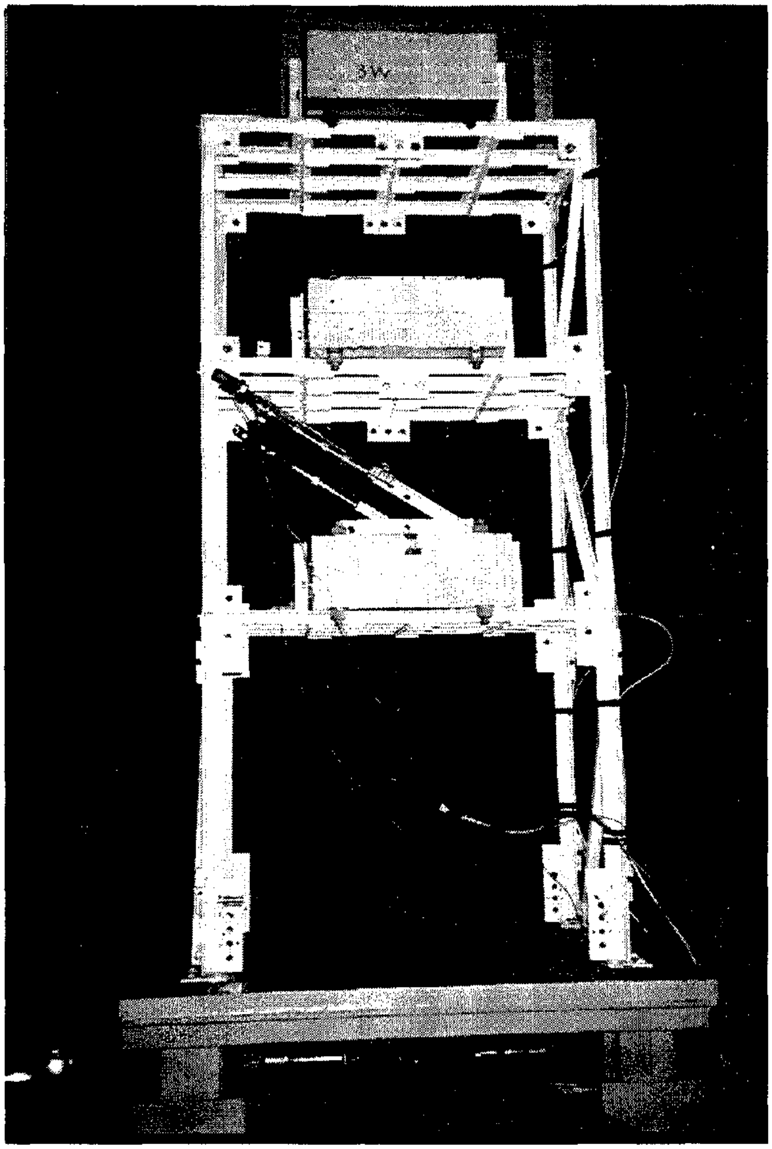

FIGURE 3-6 View of the 3-Story Structure with Two Dampers at the Second Story

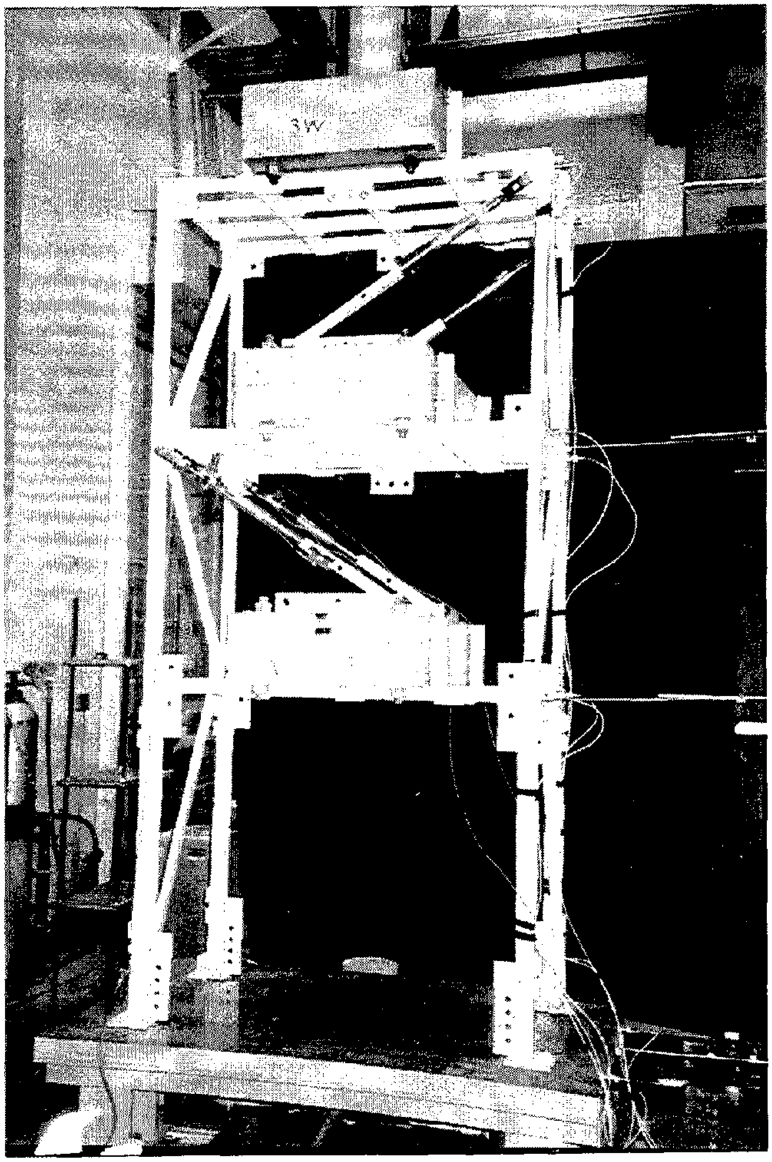

FIGURE 3-7 View of the 3-Story Structure with Four Dampers at the Second and Third Stories

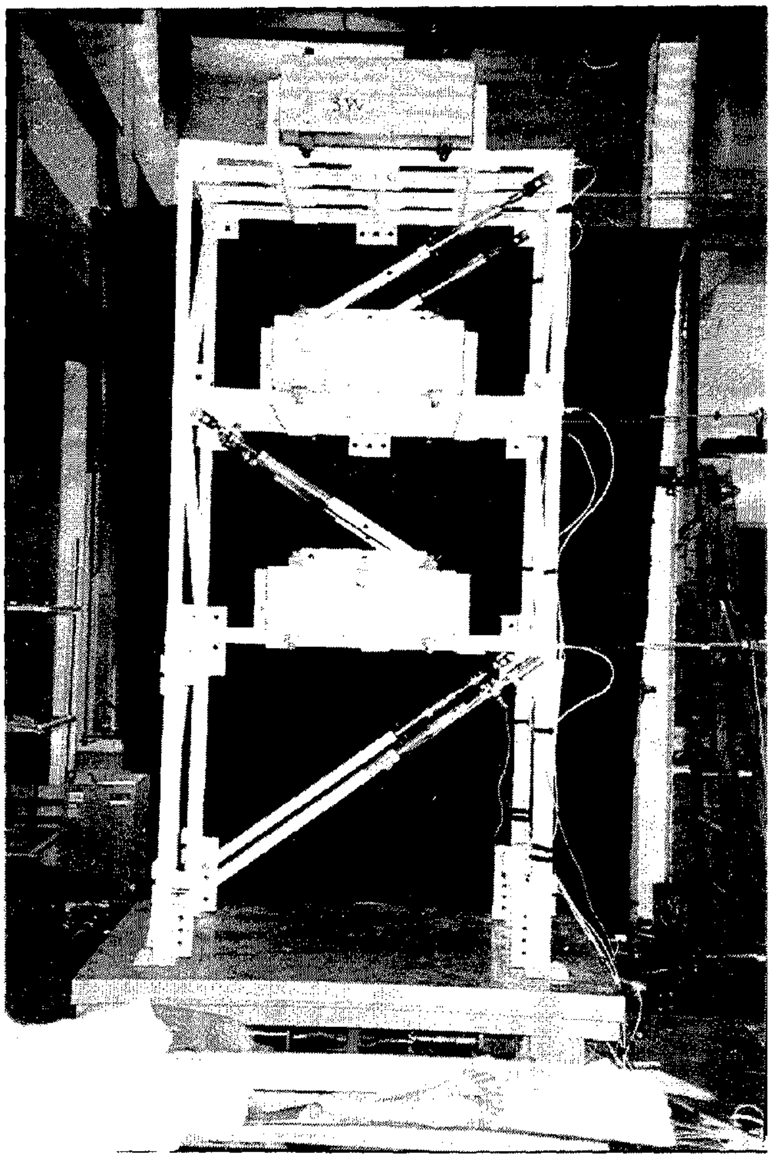

FIGURE 3-8 View of the 3-Story Structure with a Complete Vertical Distribution of Dampers (Six Dampers)

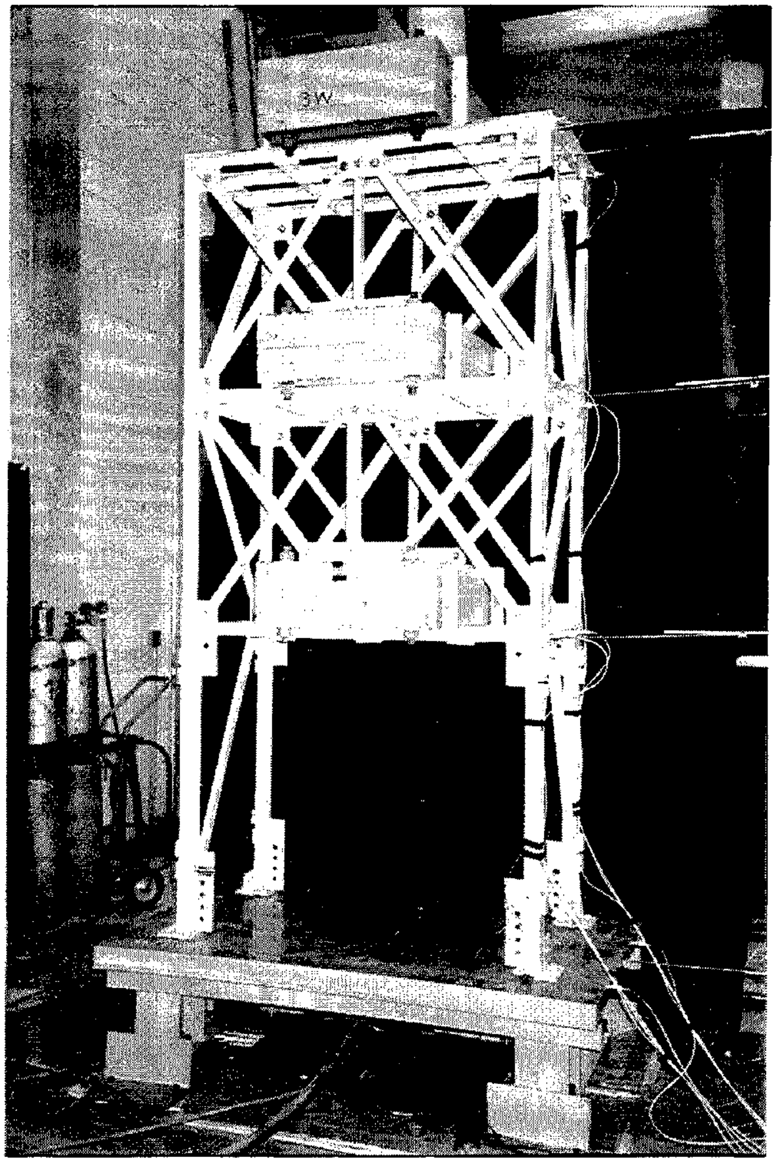

FIGURE 3-9 View of the One-Story Structure

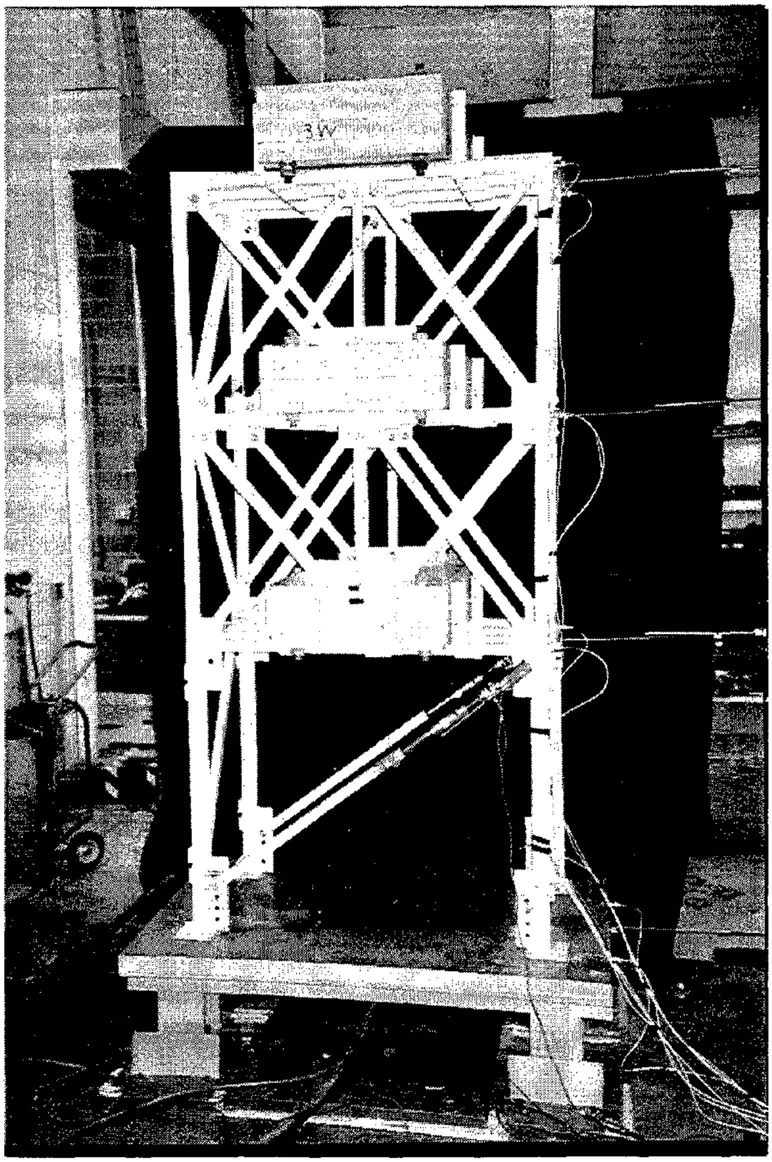

FIGURE 3-10 View of the One-Story Structure with Two Dampers

structure without and with dampers, respectively. A close up view of the dampers is shown in Figure 3-11. Finally Figure 3-12 shows a schematic of the damper connection details.

A set of identification and seismic tests was carried out using linear viscous dampers and then the set of tests was repeated using nonlinear viscous dampers.

3.2 Test Program

A total of 244 earthquake simulation tests have been conducted. Ten different earthquake records were used in these tests. Moreover, white noise excitations as well as sinusoidal waves at different frequencies were used. Table 3-I lists the earthquake ground motions used in this study. For each record the time scale was compressed by a factor of 2 to satisfy the similitude requirements of the quarter length scale model. Table 3-II summarizes all other similitude laws for this scale.

Figures 3-13 through 3-22 show recorded time histories of the table motion in tests with input being the earthquake signals of Table 3-I. The displacement and acceleration records were directly measured whereas the velocity record was obtained by numerical differentiation of the displacement record. Moreover, the 5% damped response spectra of the actual and table produced records are plotted in the same figures.

The shaking table used in this study was a small, custom made table that was driven in displacement-controlled mode. Accordingly, ground displacement was very well reproduced by the shaking table. Moreover, accelerations were reasonably well reproduced except for the Pacoima Dam record for which the peak acceleration and high frequency

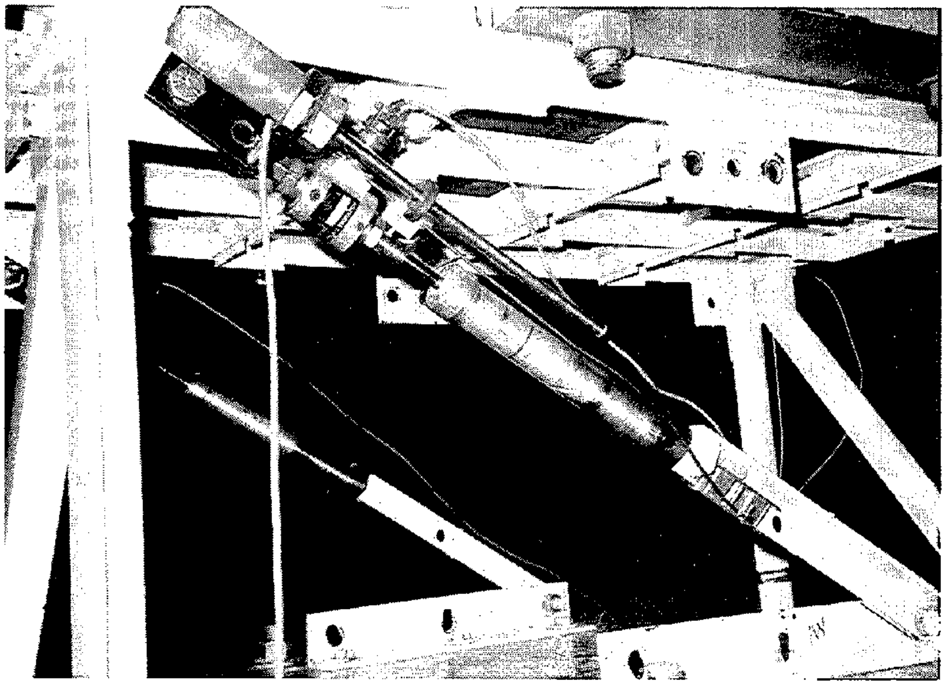

FIGURE 3-11 Close-up View of the Dampers

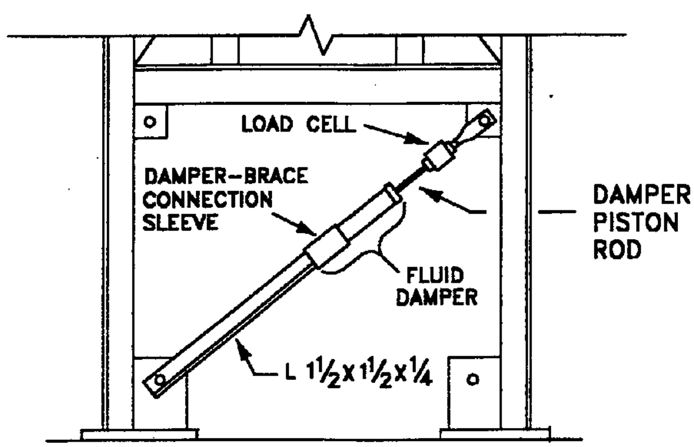

FIGURE 3-12 Schematic of Damper Connection Details

Table 3-I Characteristics of Earthquake Motions Used in the Test Program (in Prototype Scale)

Ground Motion	Record	Magnitude	Peak Acceleration (g's)	Peak Velocity (mm/sec)	Peak Displacement (mm)
El Centro S00E	Imperial Valley, May 18, 1940, Component S00E	6.7	0.348	334.5	108.7
Taft N21E	Kern County, July 21, 1952, Component N21E	7.2	0.156	157.2	67.1
Pacoima Dam S74W	San Fernando, Los Angeles, February 9, 1971, Component S74W	6.4	1.080	577.3	108.2
Miyagi-Ken-Oki EW	Tohoku University,Sendai, Japan, June 12, 1978, Component EW	7.4	0.160	141.0	50.8
Hachinohe NS	Tokachi-Oki earthquake, Japan, May 16, 1968, Component NS	7.9	0.229	357.1	118.9
Northridge (Newhall 90)	San Fernando, Los Angeles, January 17, 1994, Newhall site, 90 deg.	6.7	0.610	748.4	176.0
Northridge (Newhall 360)	San Fernando, Los Angeles, January 17, 1994, Newhall site, 360 deg.	6.7	0.598	947.0	305.0
Northridge (Sylmar 90)	San Fernando, Los Angeles, January 17, 1994, Sylmar site, 90 deg.	6.7	0.610	769.4	152.0
Eilat NS	Gulf of Aquba, Middle East, November 22, 1995, Component NS	5.4	0.081	99.9	44.6
Eilat EW	Gulf of Aquba, Middle East, November 22, 1995, Component EW	5.4	0.093	114.5	54.5

Table 3-II Summary of Similitude Laws of Quarter Length Scale Model

Parameter	Dimension	Scale	Conversion Factor
Linear Dimension	L	S_L	4
Gravitational Acceleration (g)	L/T^2	1	1
Time	T	$\sqrt{S_L}$	2
Displacement	L	S_L	4
Velocity	L/T	$\sqrt{S_L}$	2
Acceleration	L/T^2	1	1
Frequency	$1/T$	$1/\sqrt{S_L}$	0.5
Mass Density	FL^4T^2	*	*
Modulus of Elasticity	F/L^2	S_E	1
Stress	F/L^2	S_E	1
Strain	-----	1	1
Poisson Ratio	-----	1	1
Force	F	$S_E S_L^2$	16
Pressure	F/L^2	S_E	1
Energy	FL	$S_E S_L^3$	64
Period	T	$\sqrt{S_L}$	2

* Artificial Mass Simulation

Conversion Factor = Prototype Quantity / Model Quantity

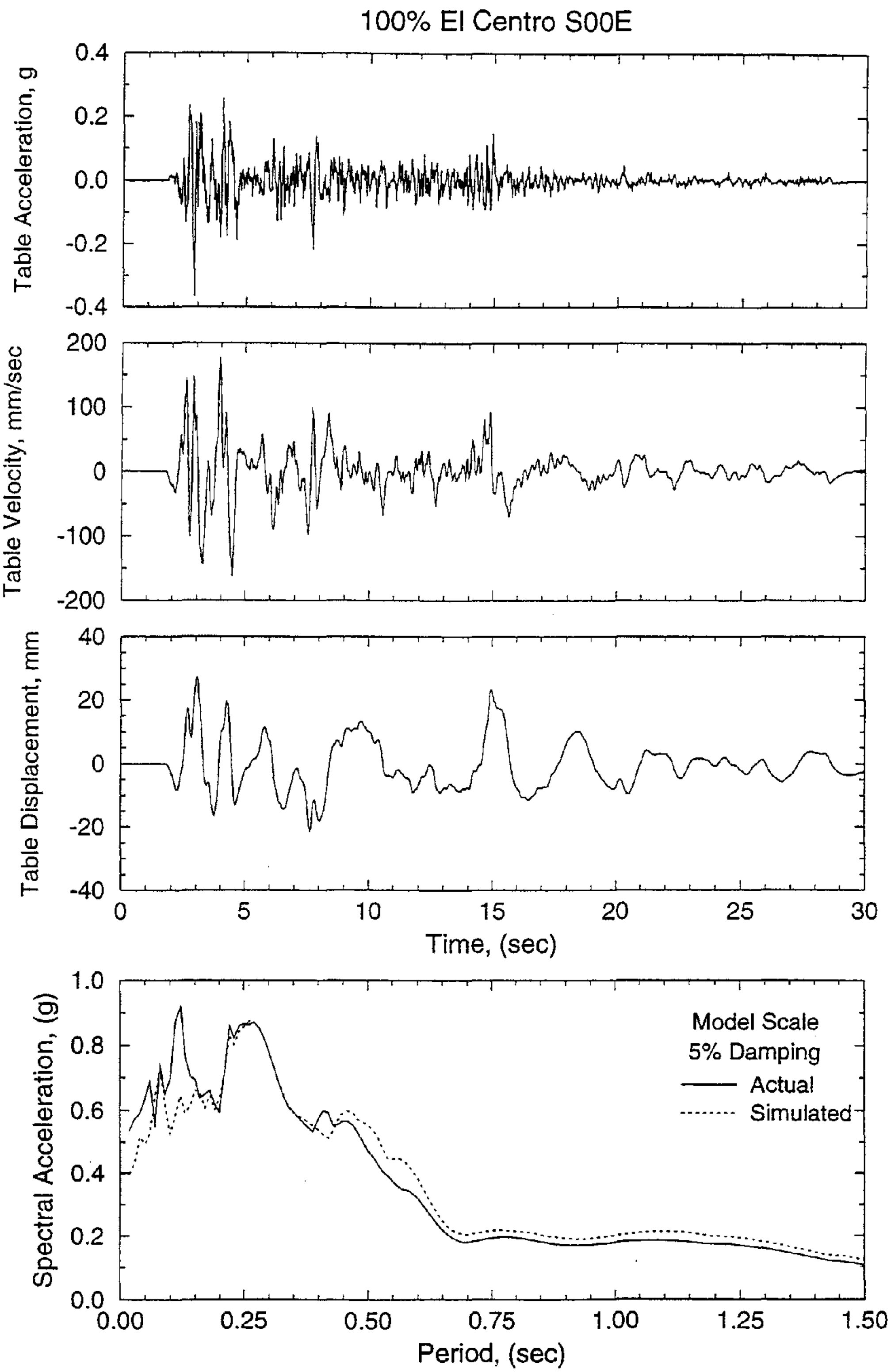

FIGURE 3-13 Time Histories of Displacement, Velocity, and Acceleration and Spectra of Acceleration and Displacement of Shaking Table Motion in 100% El Centro S00E

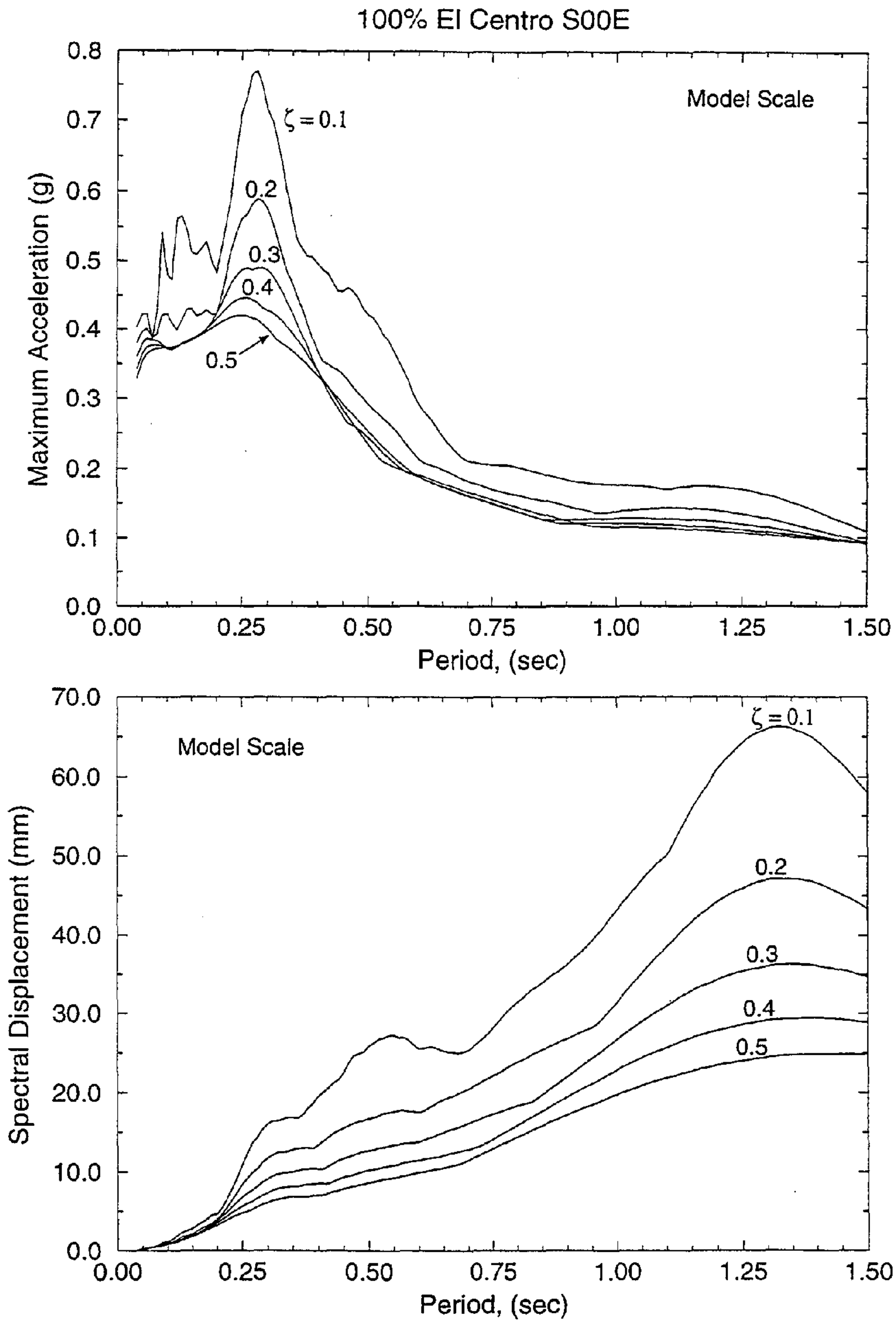

FIGURE 3-13 Time Histories of Displacement, Velocity, and Acceleration and Spectra of Acceleration and Displacement of Shaking Table Motion in 100% El Centro S00E (Continued)

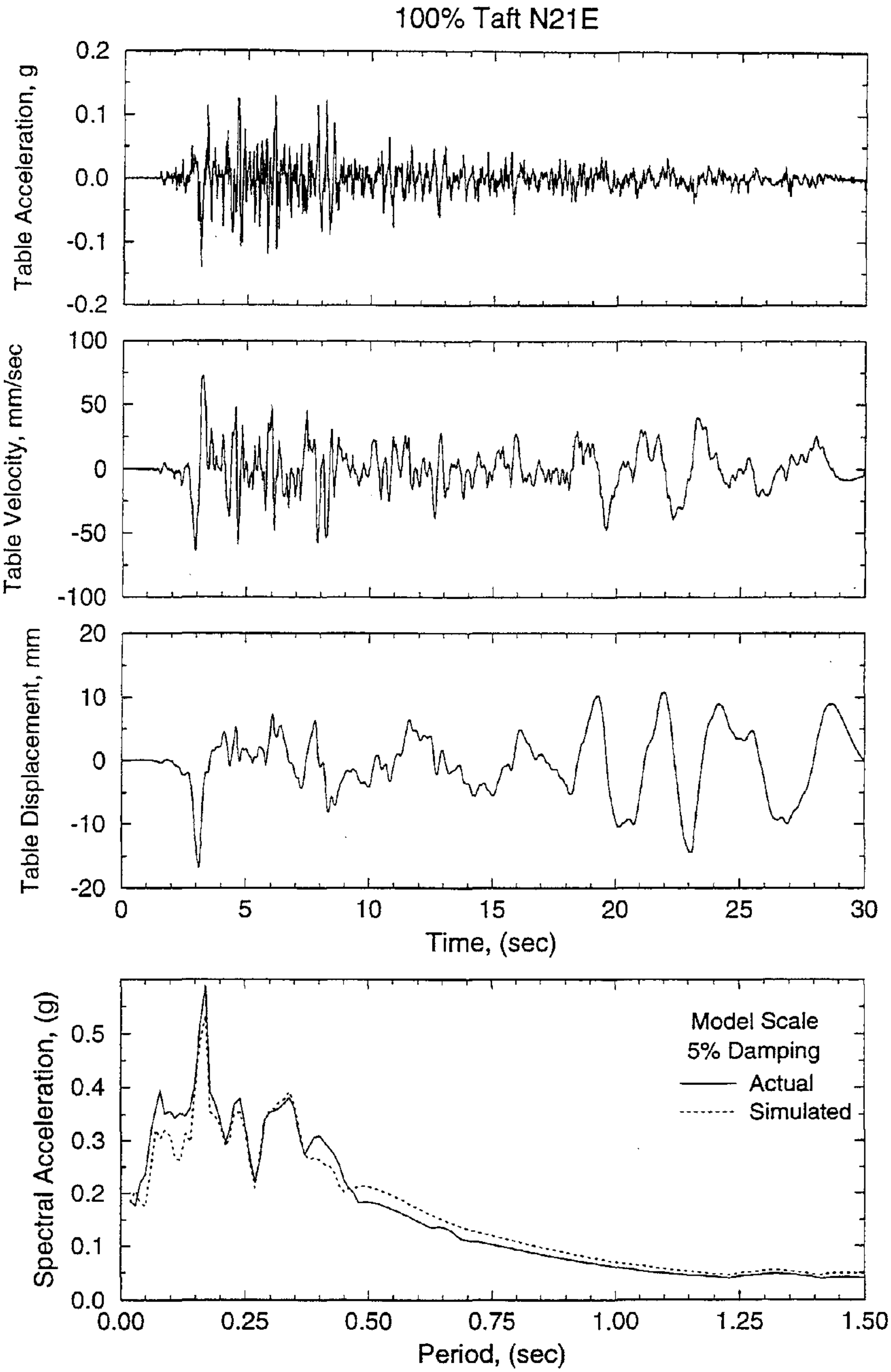

FIGURE 3-14 Time Histories of Displacement, Velocity, and Acceleration and Spectra of Acceleration and Displacement of Shaking Table Motion in 100% Taft N21E

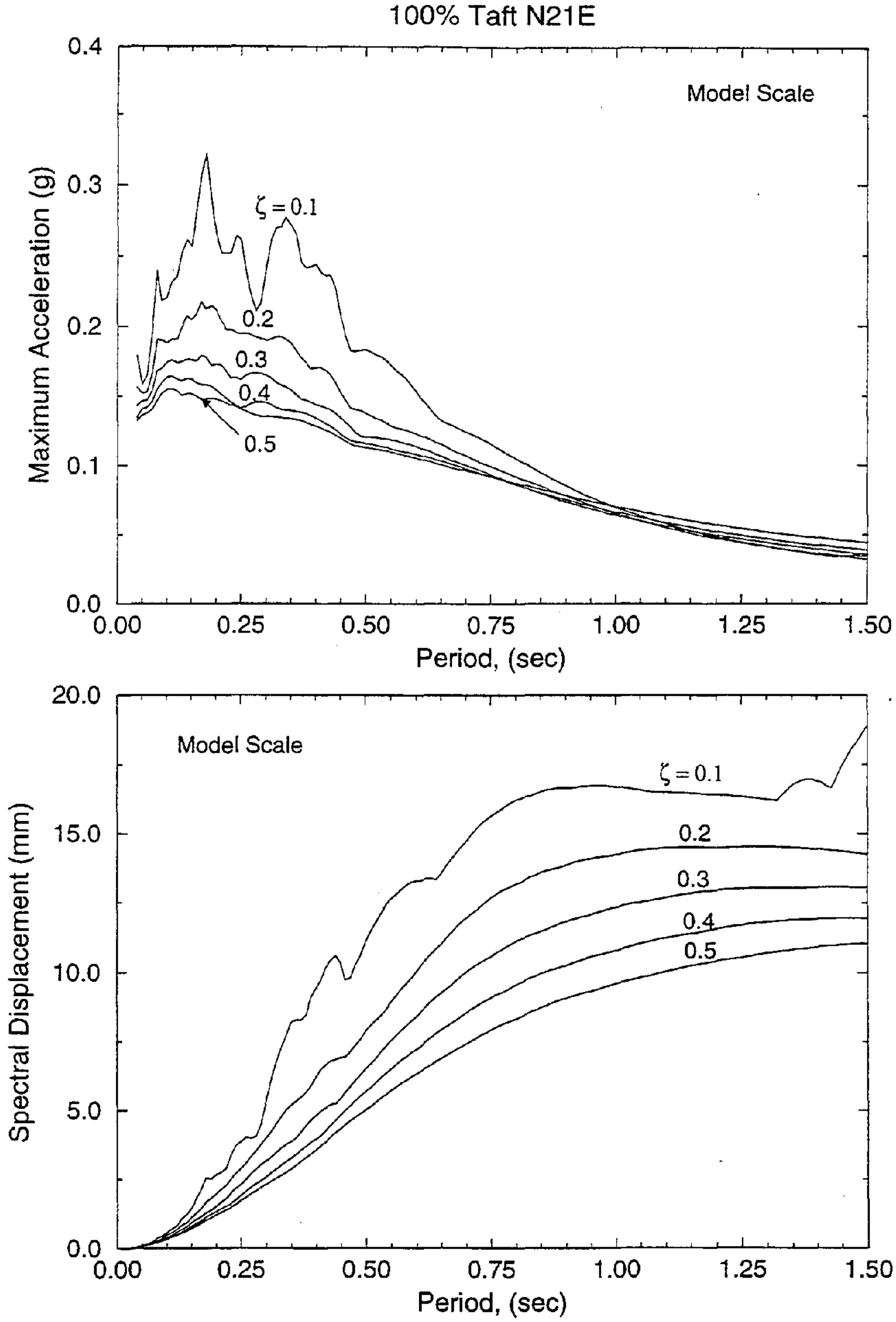

FIGURE 3-14 Time Histories of Displacement, Velocity, and Acceleration and Spectra of Acceleration and Displacement of Shaking Table Motion in 100% Taft N21E (Continued)

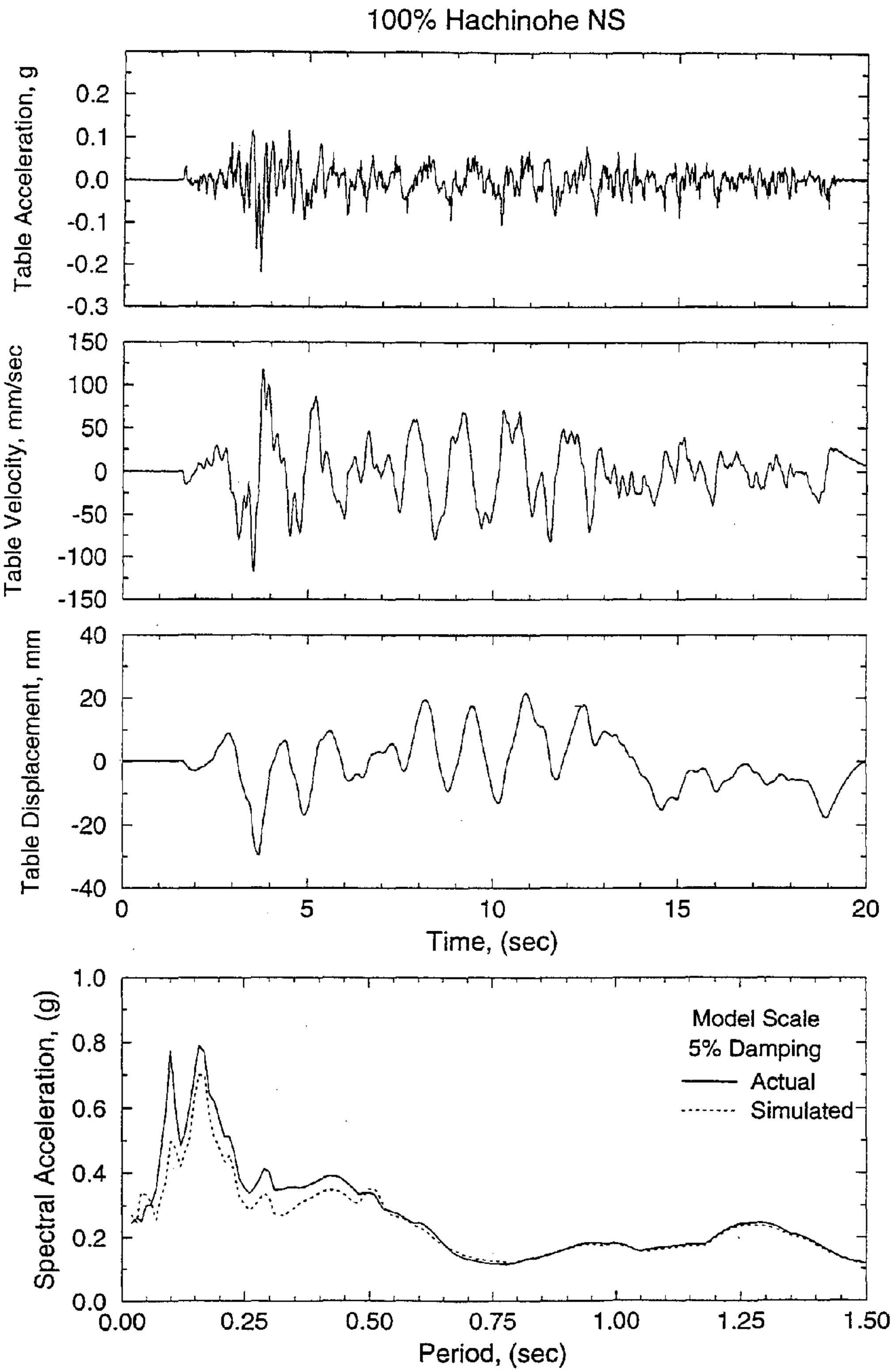

FIGURE 3-15 Time Histories of Displacement, Velocity, and Acceleration and Spectra of Acceleration and Displacement of Shaking Table Motion in 100% Hachinohe NS

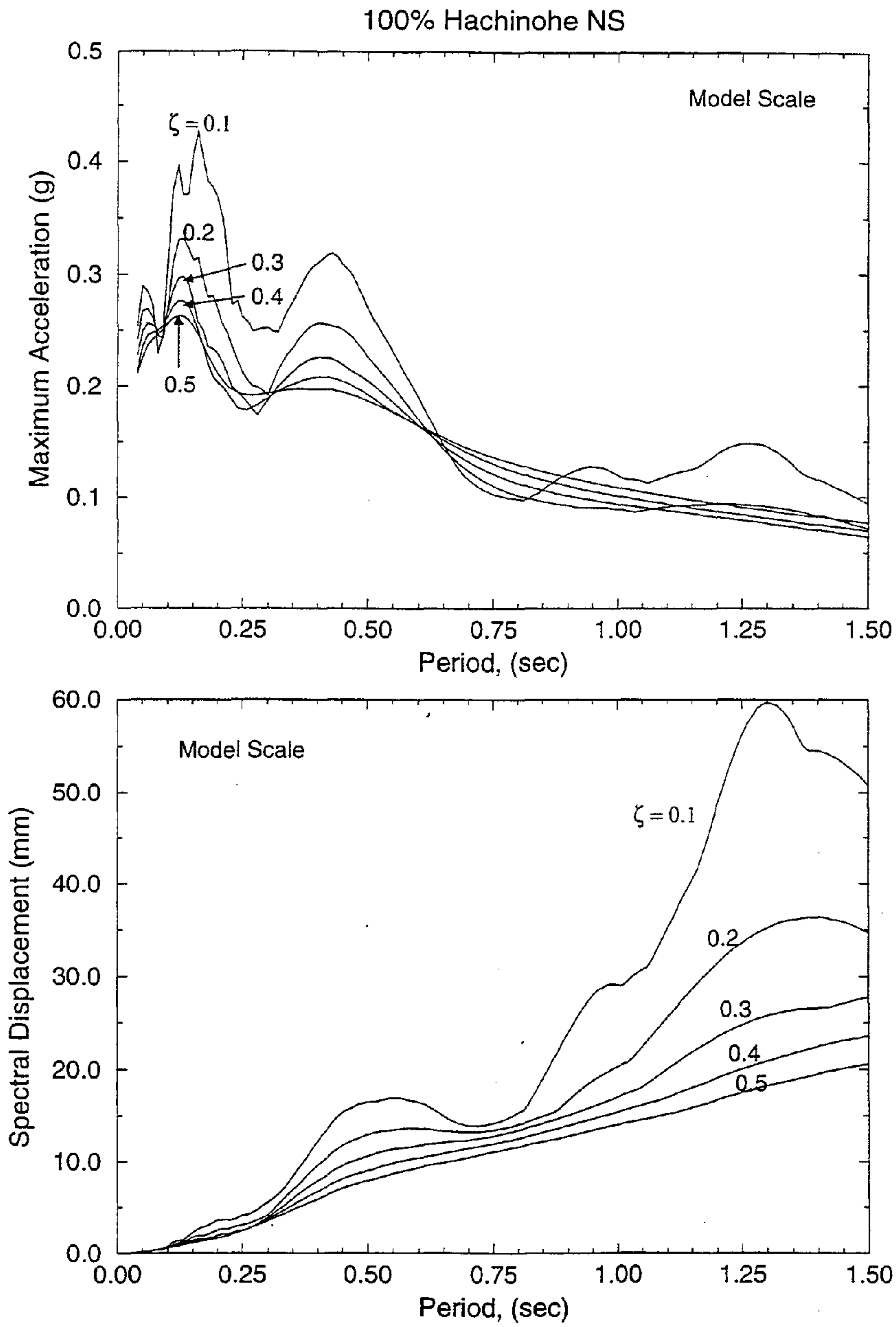

FIGURE 3-15 Time Histories of Displacement, Velocity, and Acceleration and Spectra of Acceleration and Displacement of Shaking Table Motion in 100% Hachinohe NS (Continued)

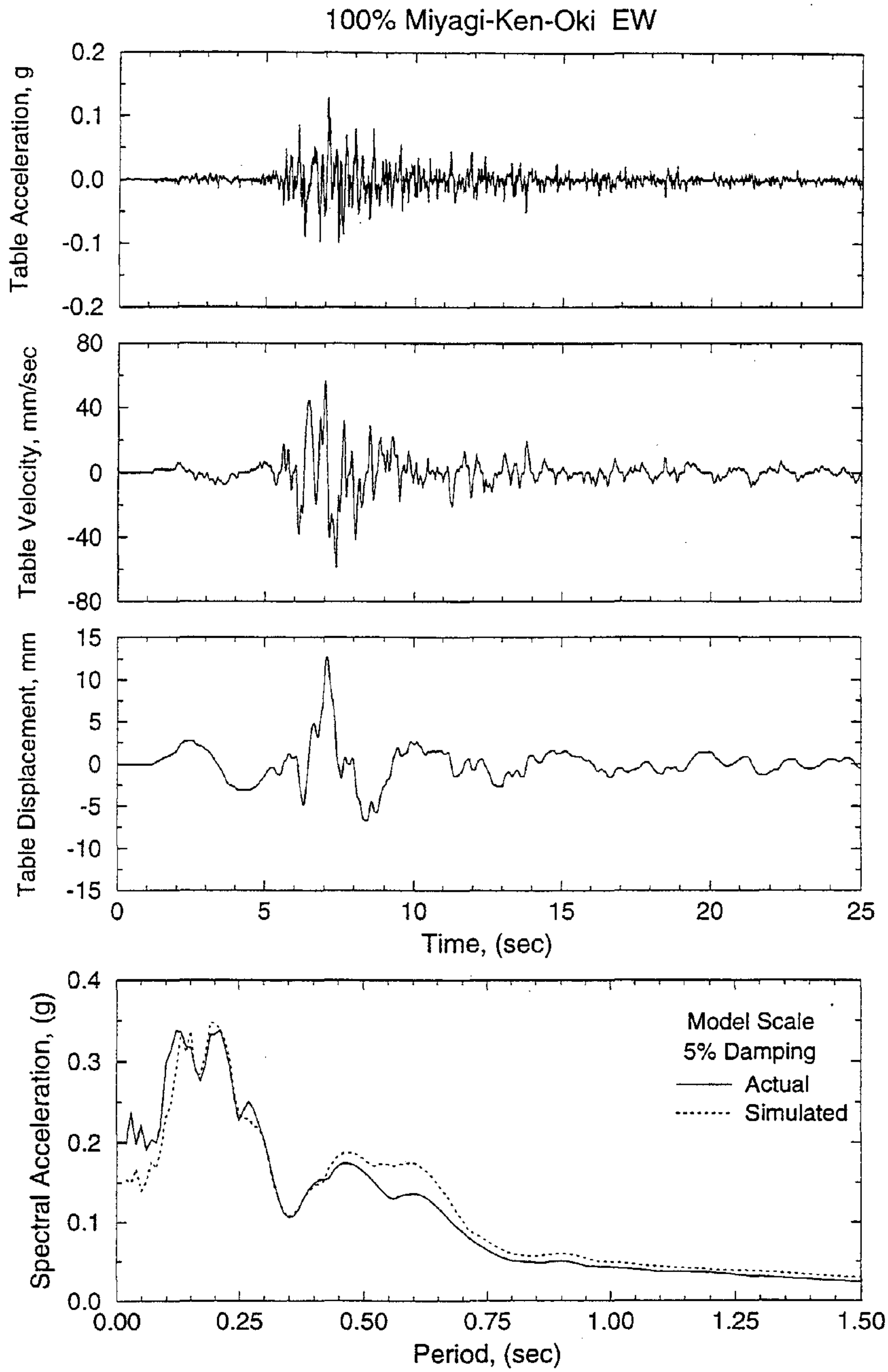

FIGURE 3-16 Time Histories of Displacement, Velocity, and Acceleration and Spectra of Acceleration and Displacement of Shaking Table Motion in 100%Miyagi-Ken-Oki EW

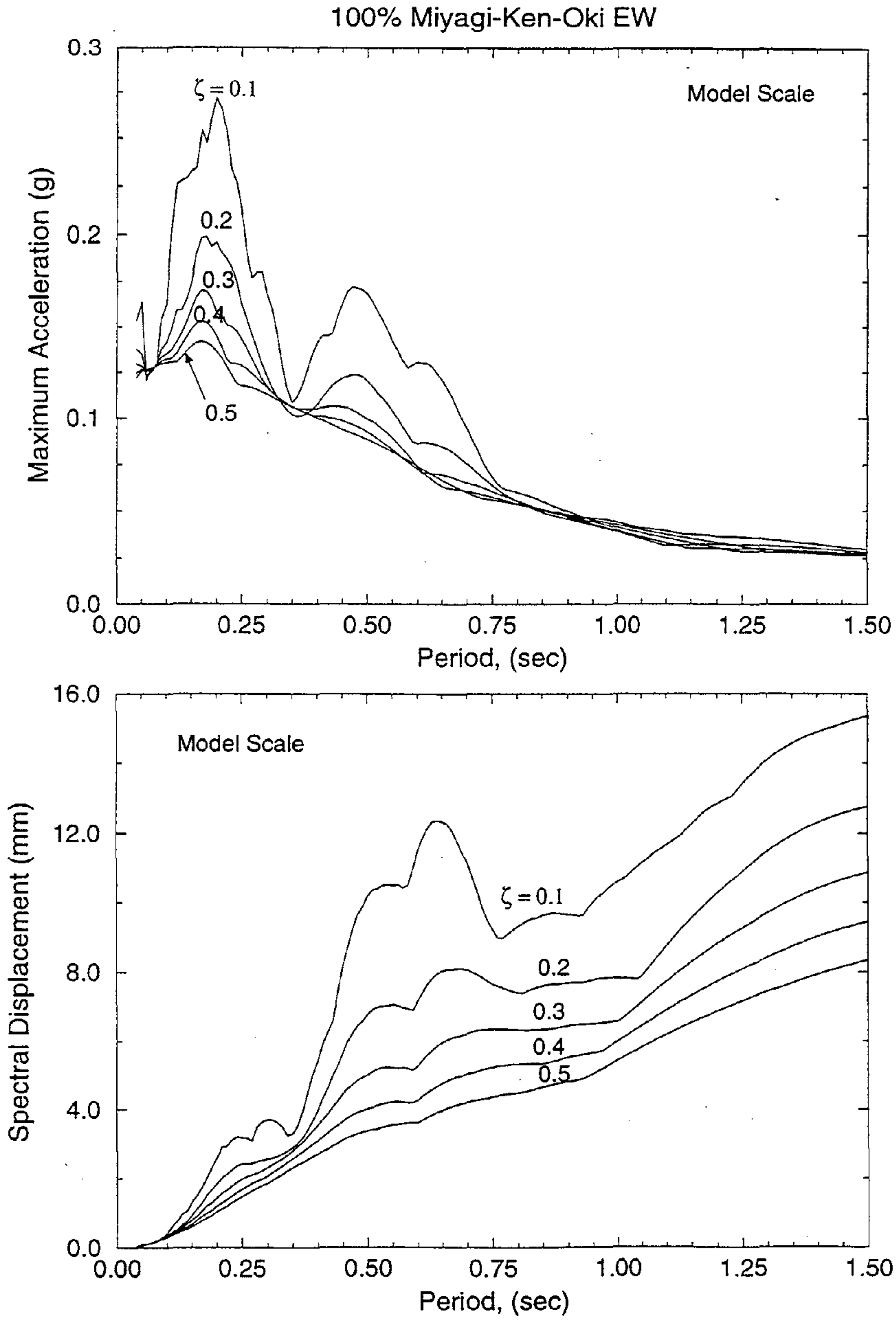

FIGURE 3-16 Time Histories of Displacement, Velocity, and Acceleration and Spectra of Acceleration and Displacement of Shaking Table Motion in 100%Miyagi-Ken-Oki EW (Continued)

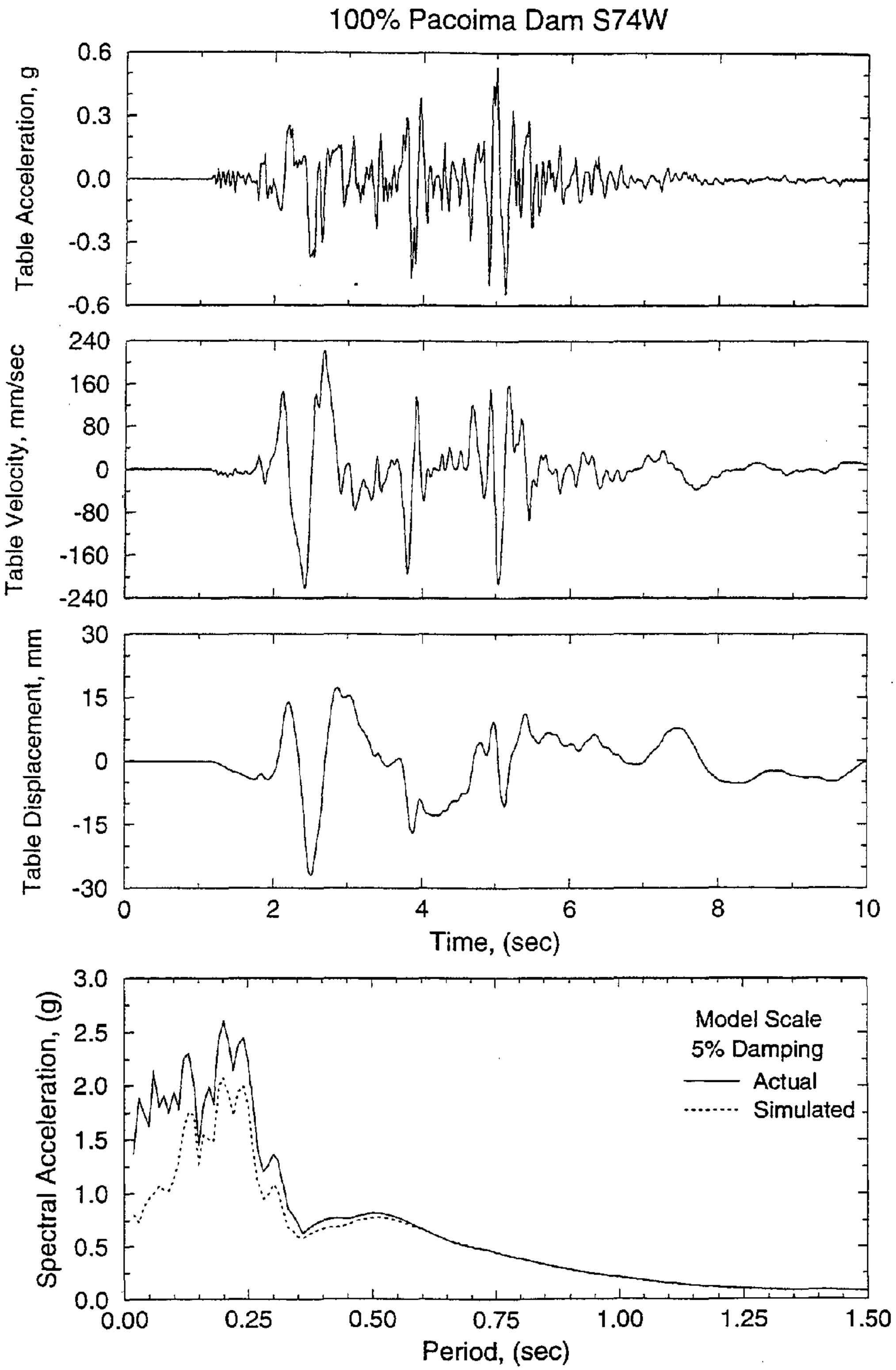

FIGURE 3-17 Time Histories of Displacement, Velocity, and Acceleration and Spectra of Acceleration and Displacement of Shaking Table Motion in 100% Pacoima Dam S74W

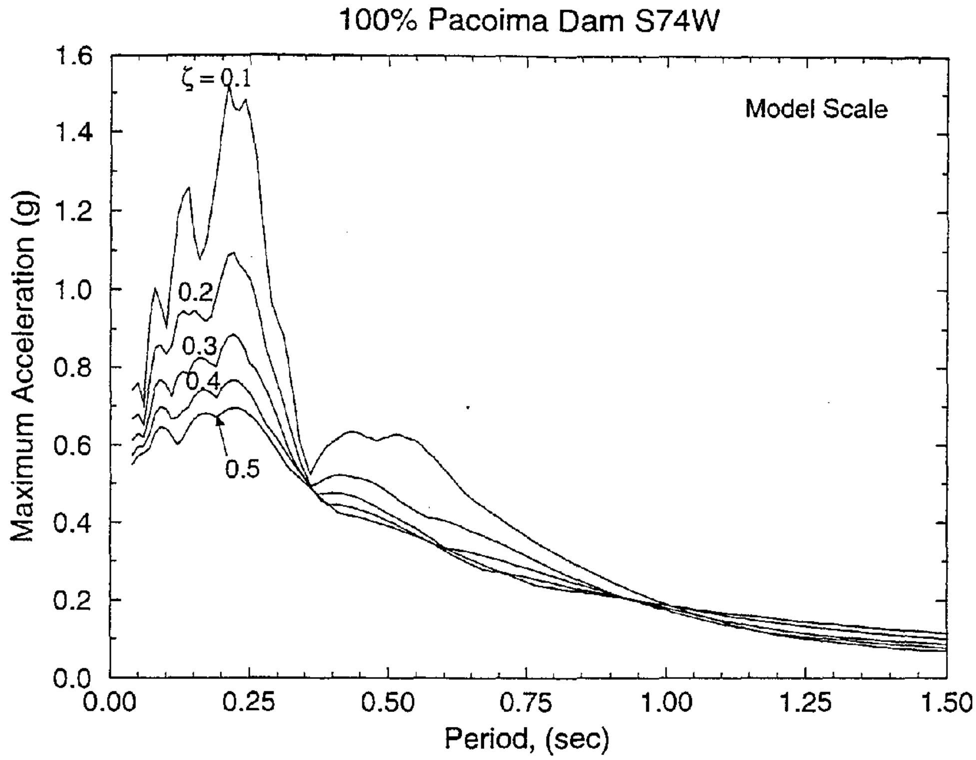

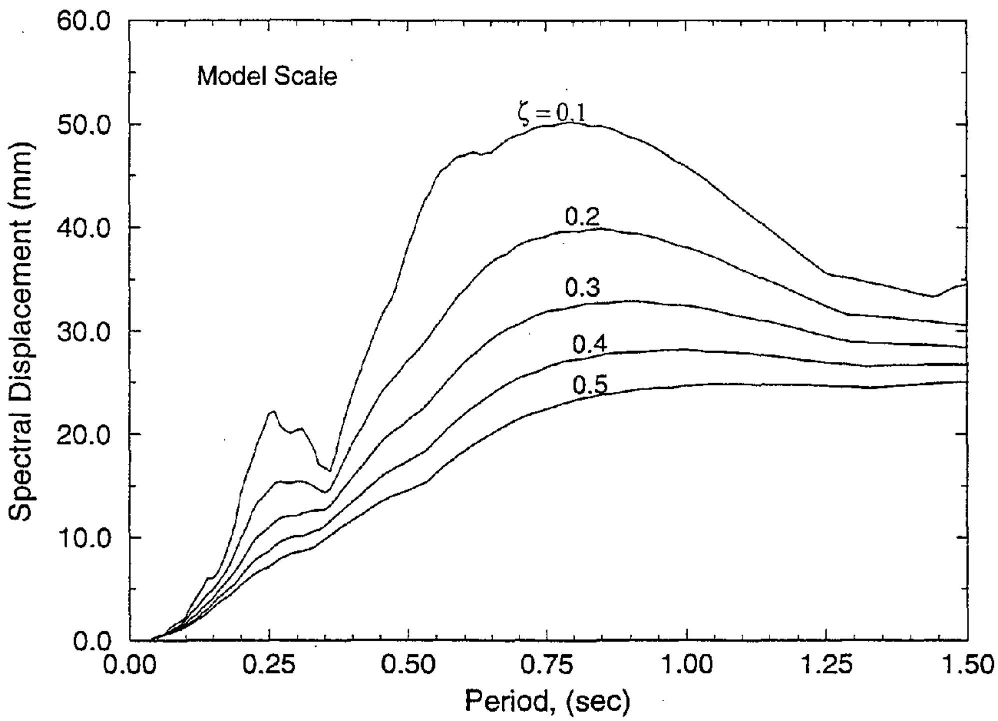

FIGURE 3-17 Time Histories of Displacement, Velocity, and Acceleration and Spectra of Acceleration and Displacement of Shaking Table Motion in 100% Pacoima Dam S74W (Continued)

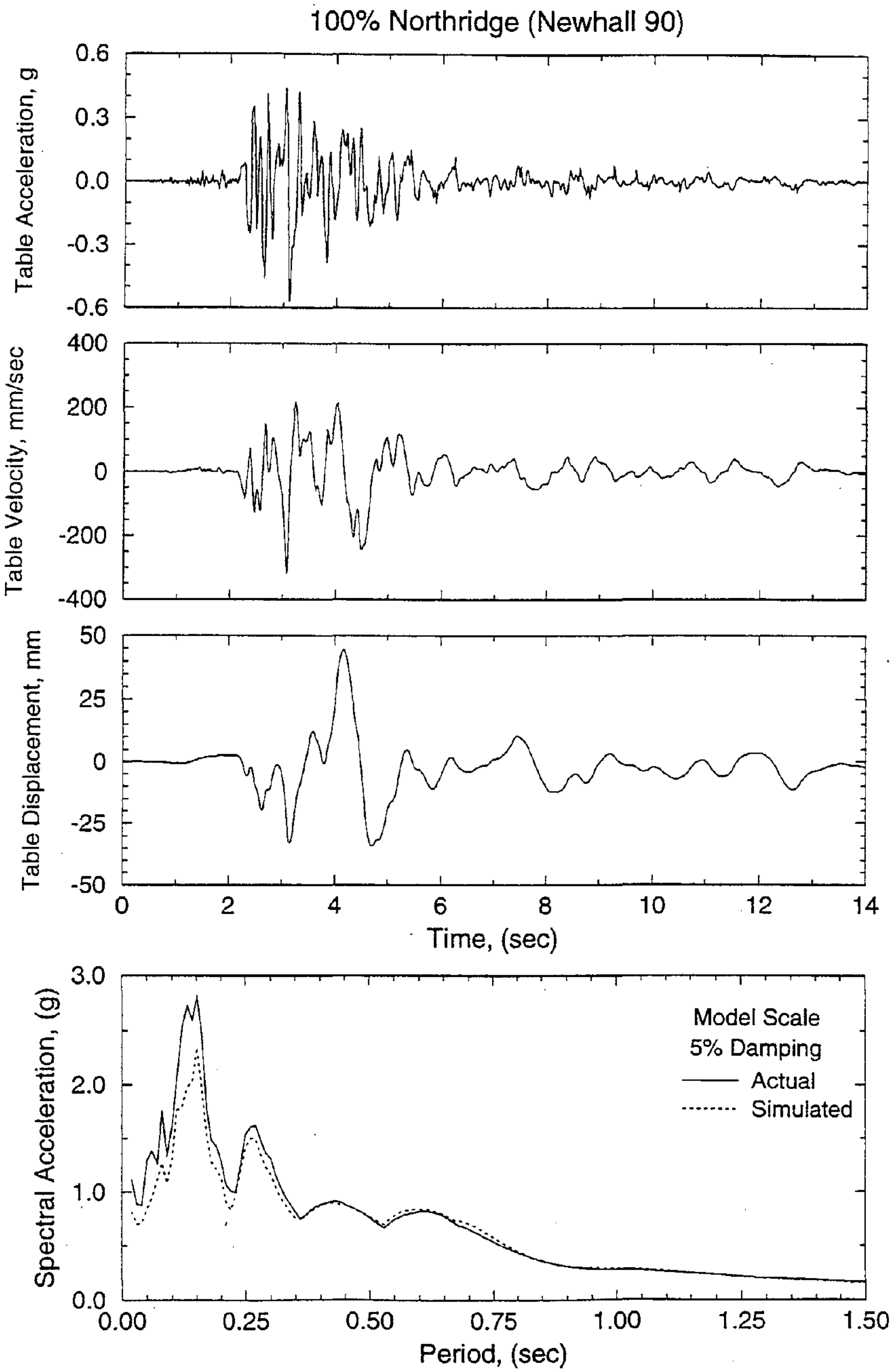

FIGURE 3-18 Time Histories of Displacement, Velocity, and Acceleration and Spectra of Acceleration and Displacement of Shaking Table Motion in 100% Northridge (Newhall 90)

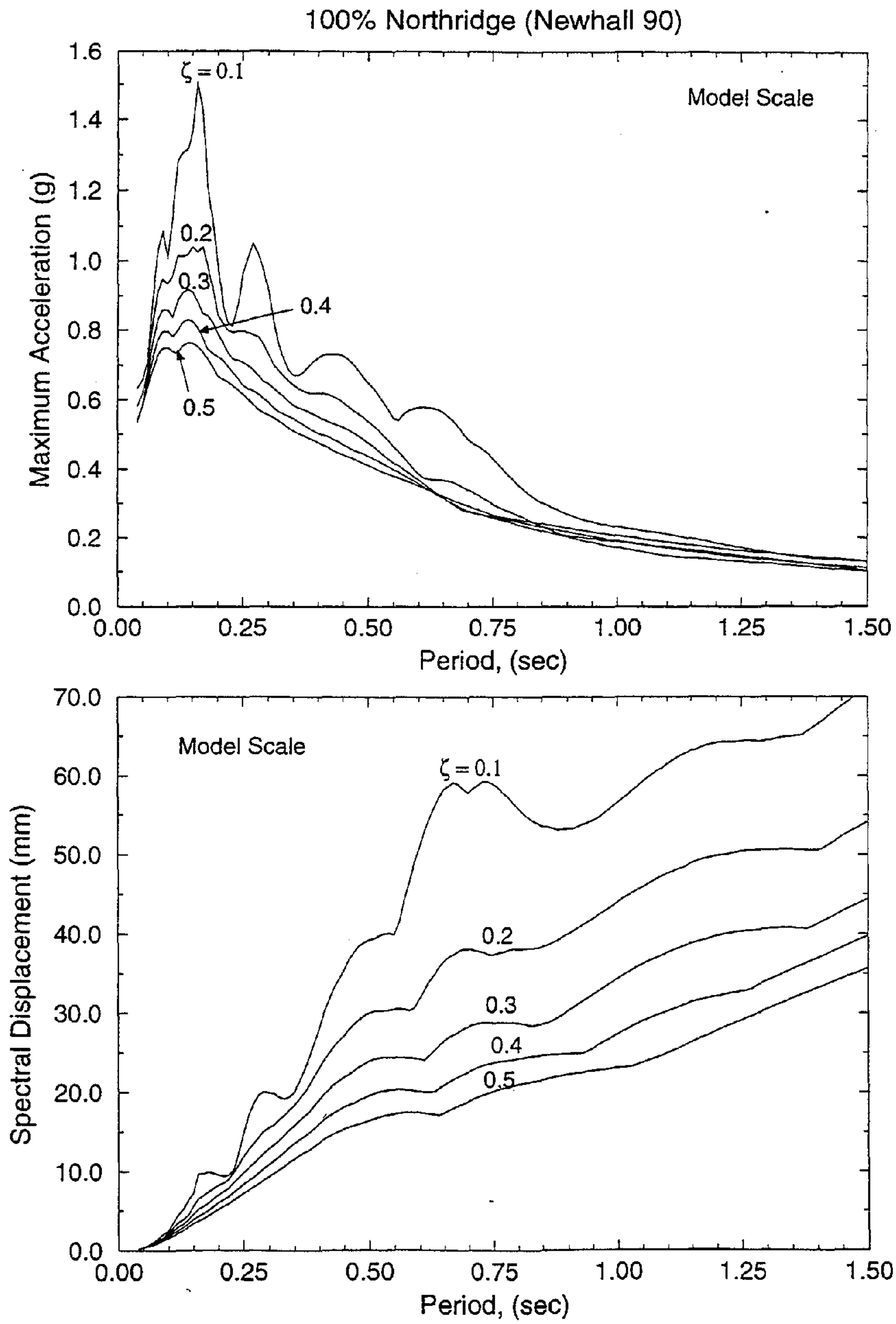

FIGURE 3-18 Time Histories of Displacement, Velocity, and Acceleration and Spectra of Acceleration and Displacement of Shaking Table Motion in 100% Northridge (Newhall 90) (Continued)

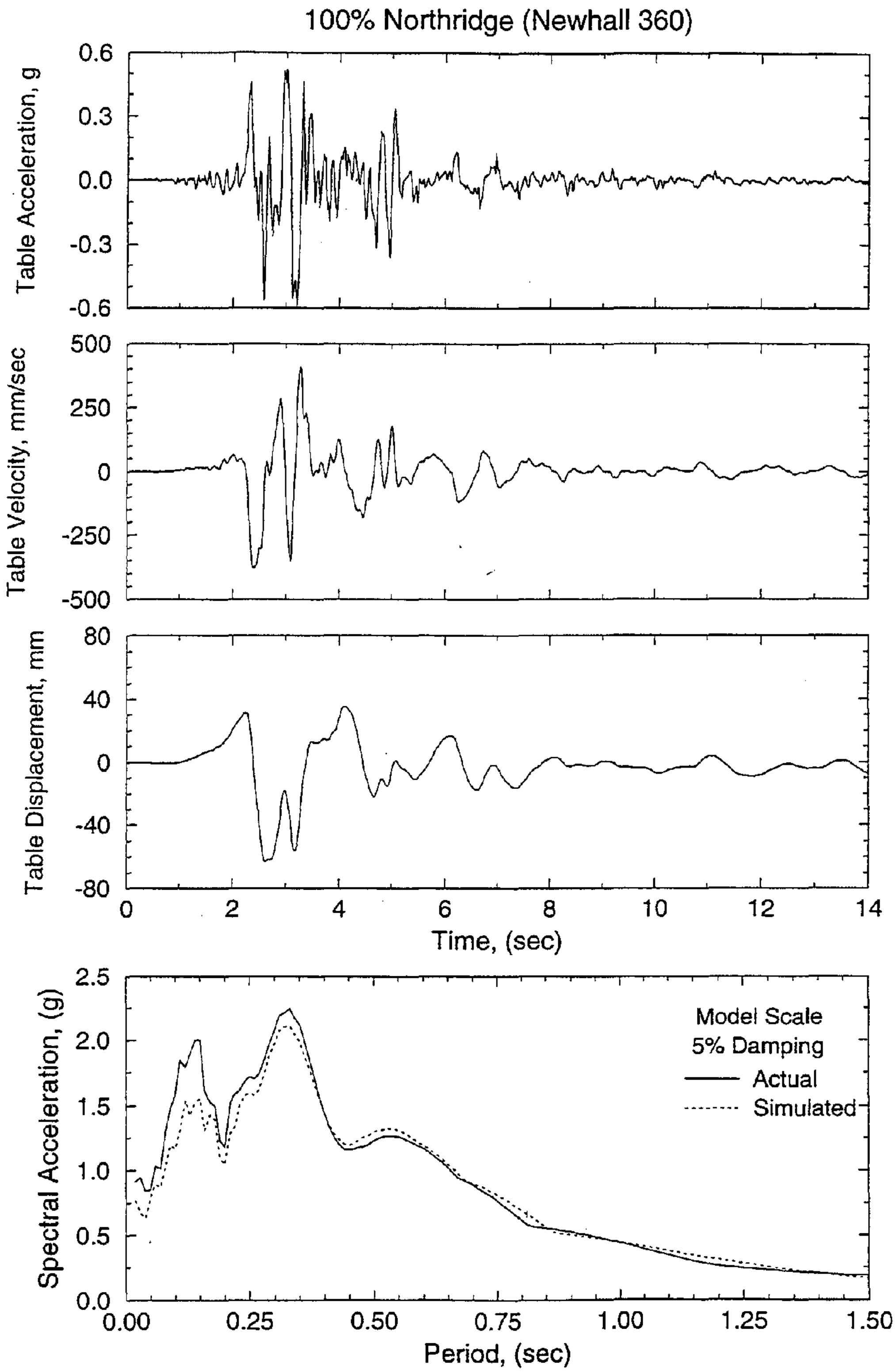

FIGURE 3-19 Time Histories of Displacement, Velocity, and Acceleration and Spectra of Acceleration and Displacement of Shaking Table Motion in 100% Northridge (Newhall 360)

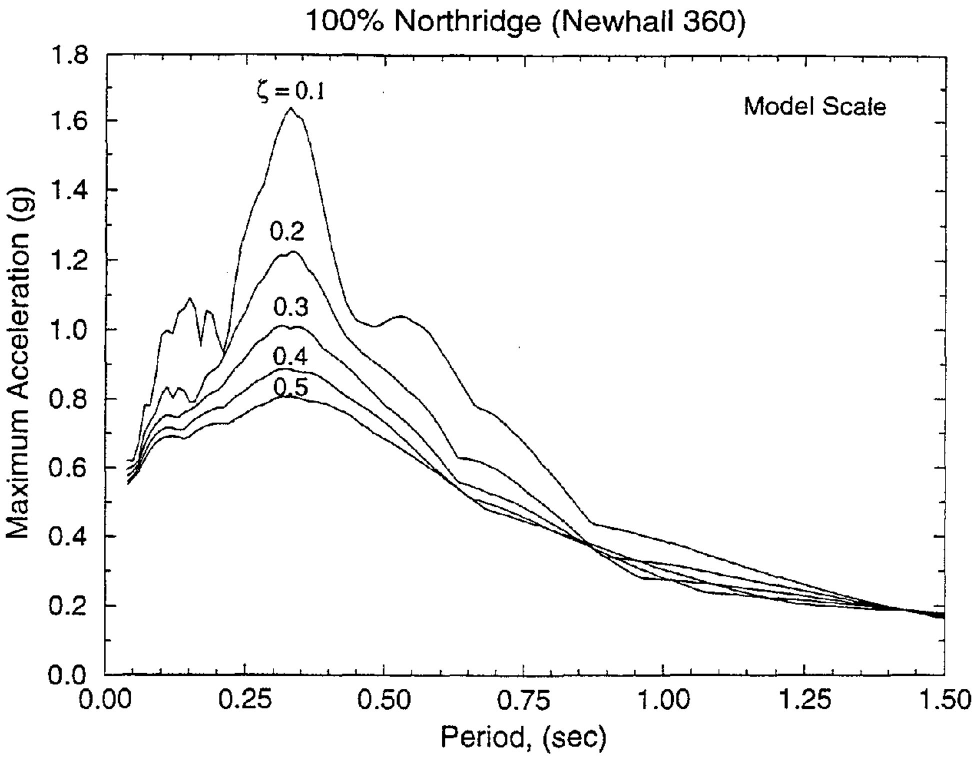

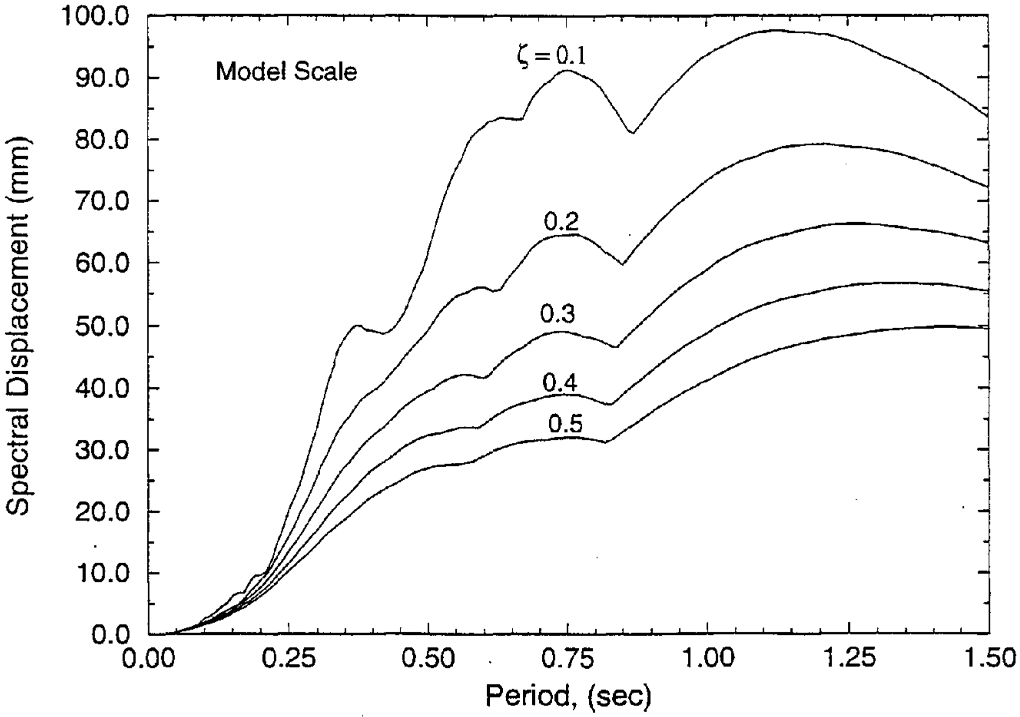

FIGURE 3-19 Time Histories of Displacement, Velocity, and Acceleration and Spectra of Acceleration and Displacement of Shaking Table Motion in 100% Northridge (Newhall 360) (Continued)

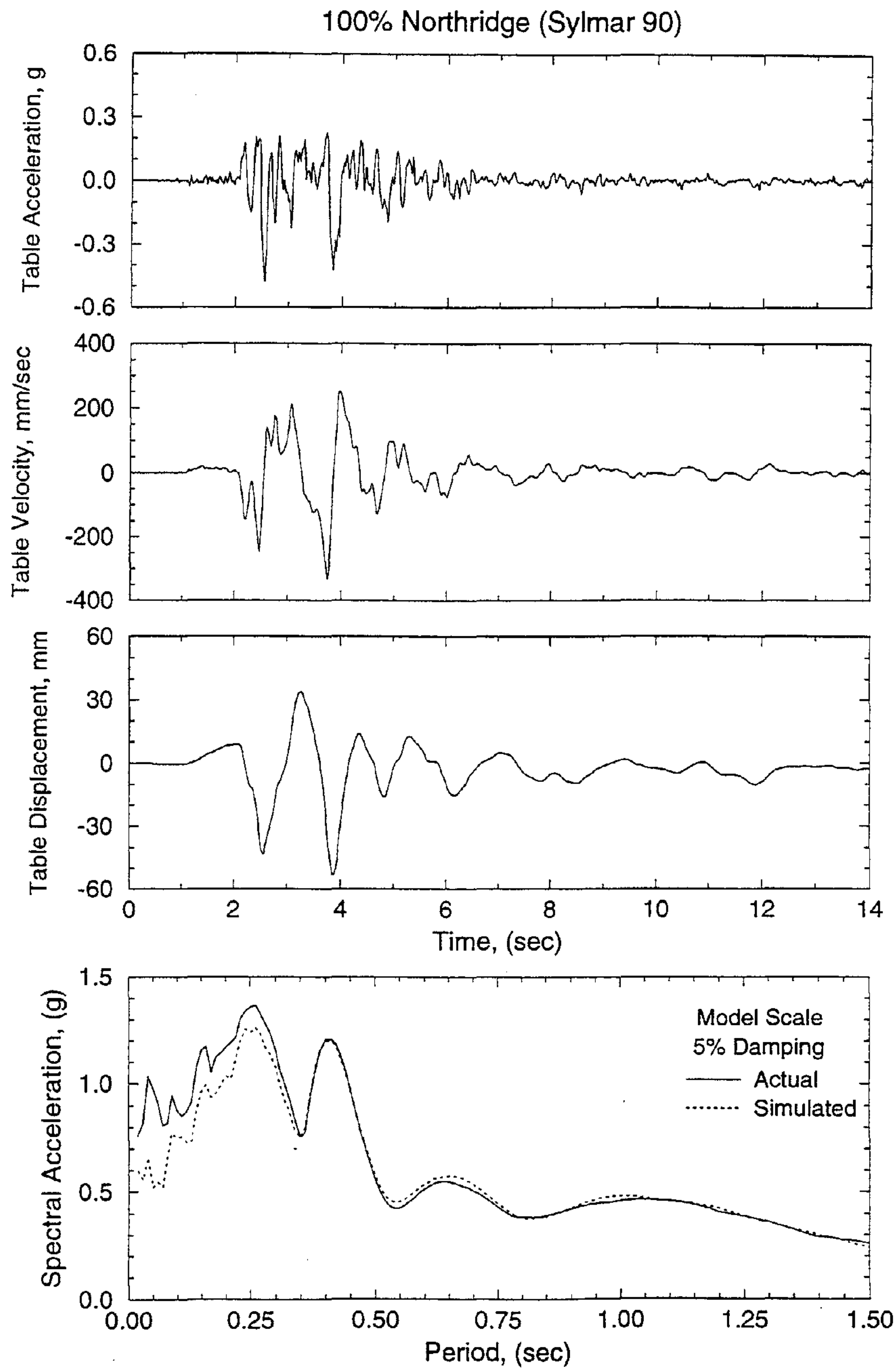

FIGURE 3-20 Time Histories of Displacement, Velocity, and Acceleration and Spectra of Acceleration and Displacement of Shaking Table Motion in 100% Northridge (Sylmar 90)

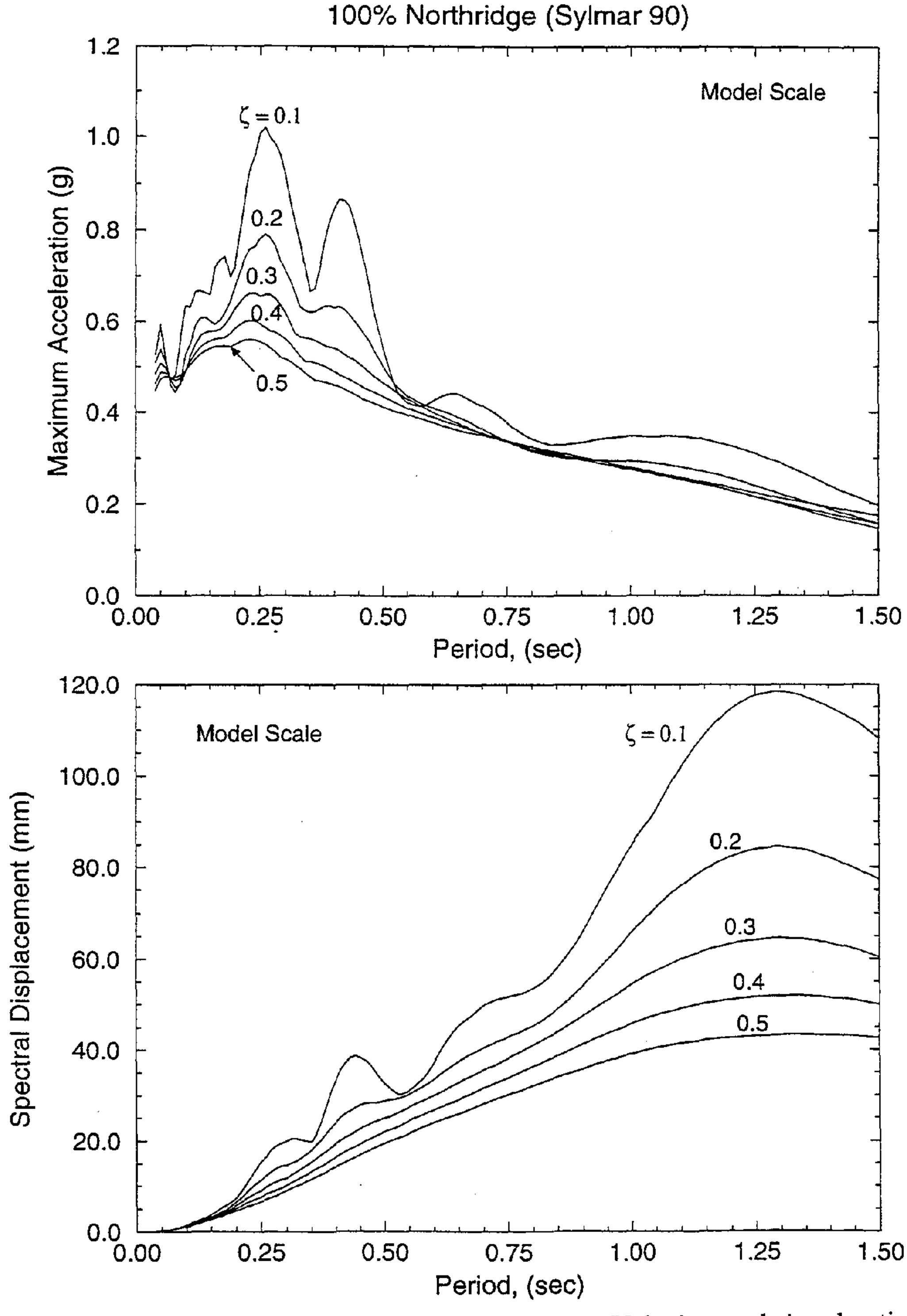

FIGURE 3-20 Time Histories of Displacement, Velocity, and Acceleration and Spectra of Acceleration and Displacement of Shaking Table Motion in 100% Northridge (Sylmar 90) (Continued)

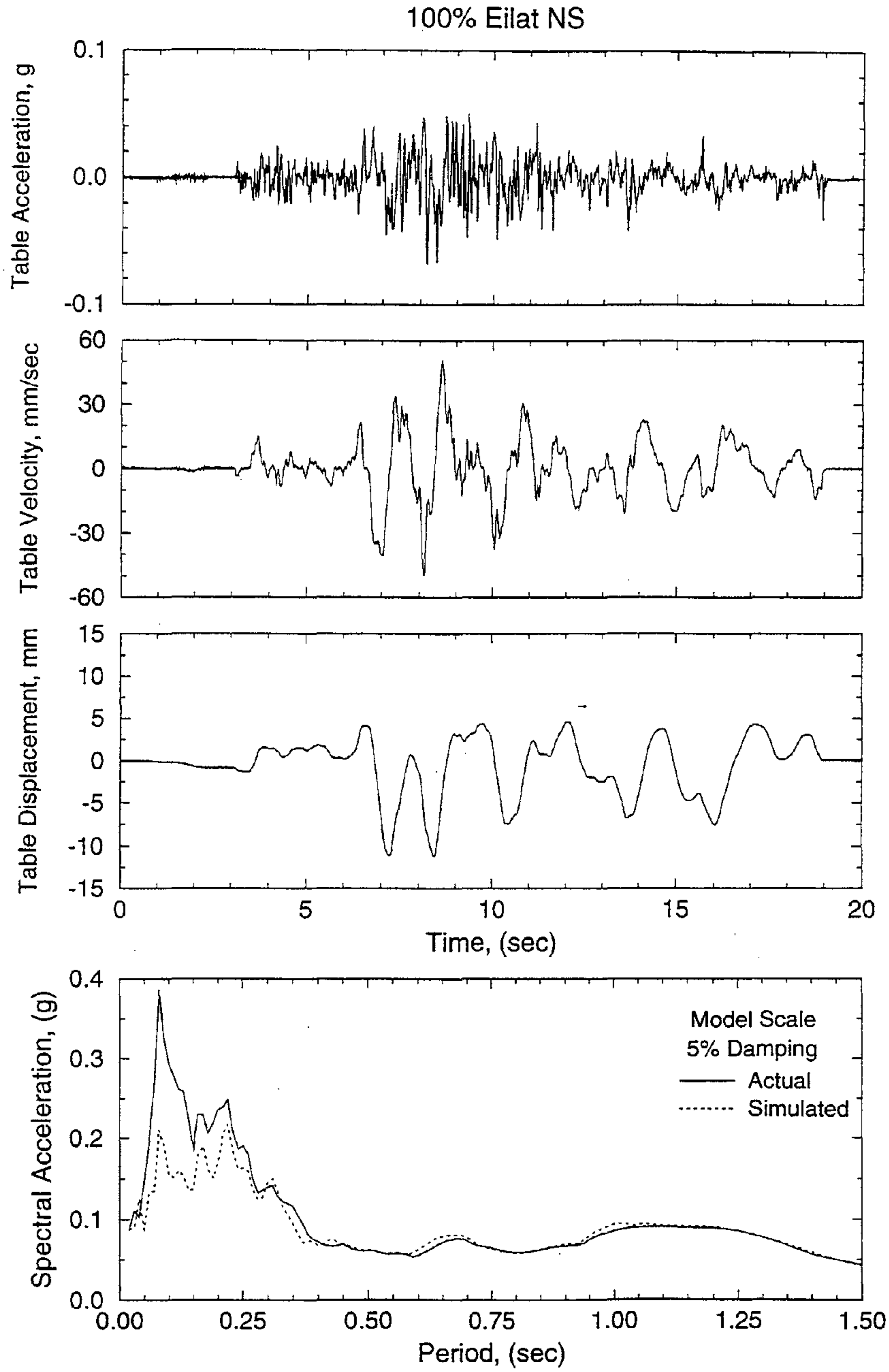

FIGURE 3-21 Time Histories of Displacement, Velocity, and Acceleration and Spectra of Acceleration and Displacement of Shaking Table Motion in 100% Eilat NS

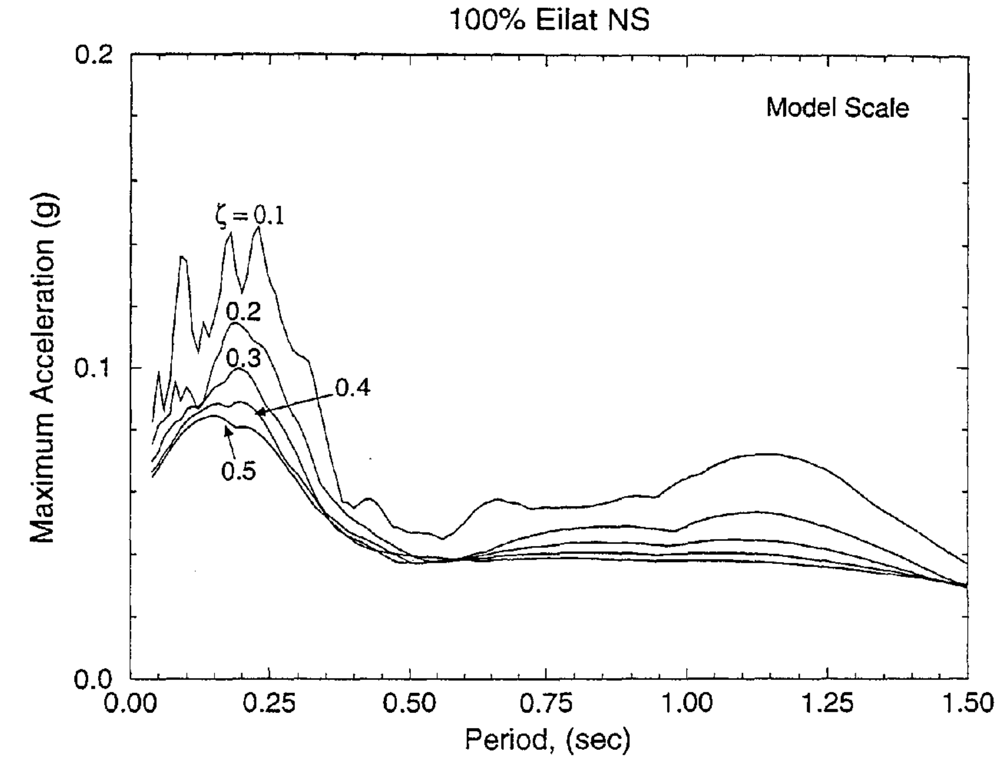

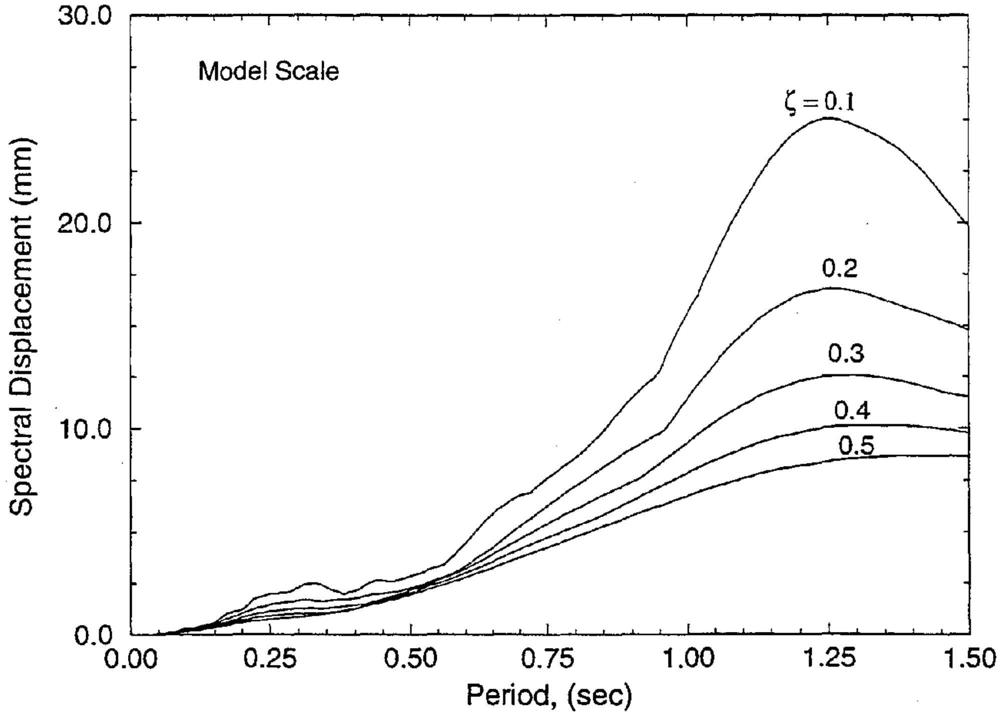

FIGURE 3-21 Time Histories of Displacement, Velocity, and Acceleration and Spectra of Acceleration and Displacement of Shaking Table Motion in 100% Eilat NS (Continued)

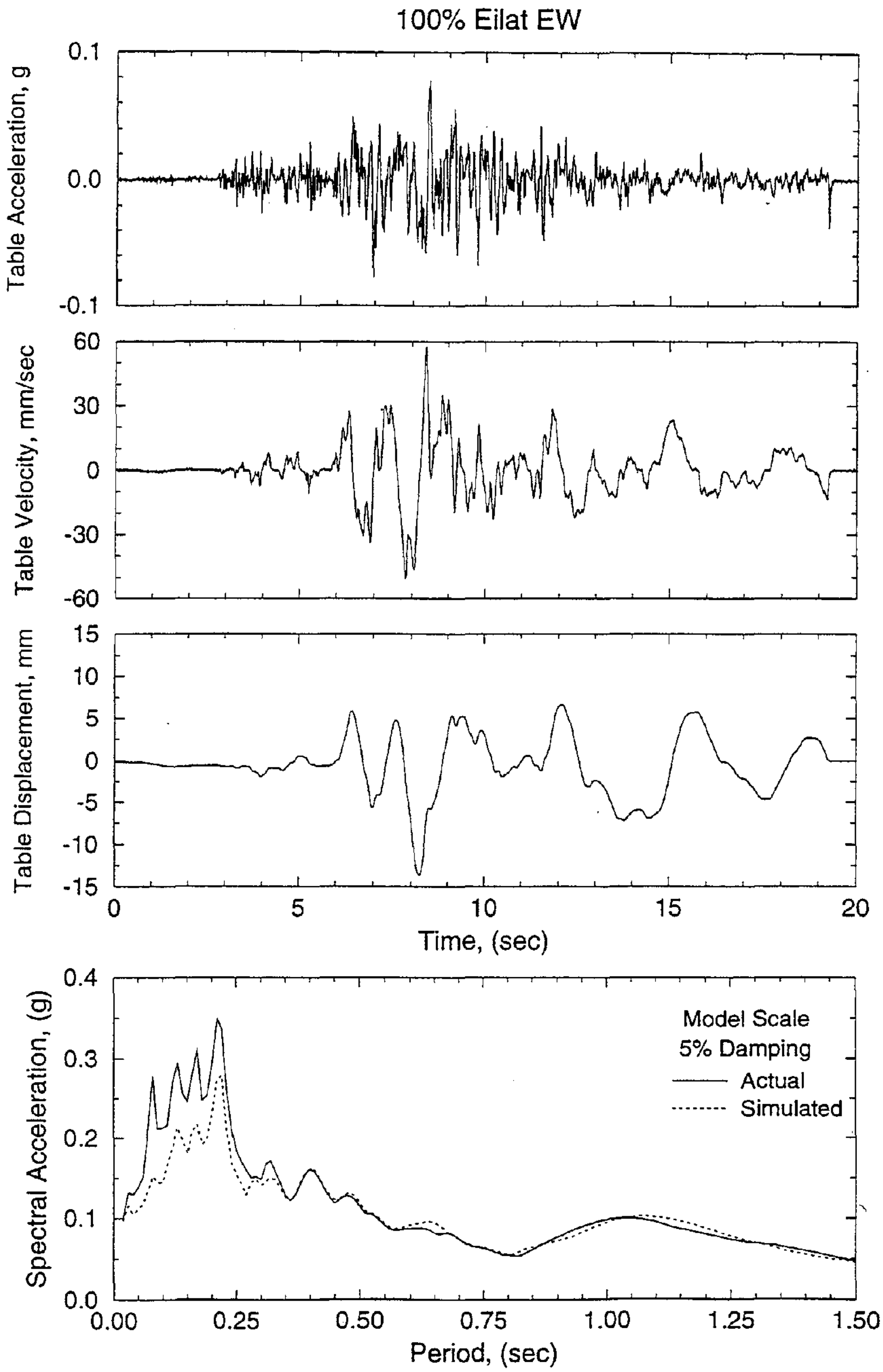

FIGURE 3-22 Time Histories of Displacement, Velocity, and Acceleration and Spectra of Acceleration and Displacement of Shaking Table Motion in 100% Eilat EW

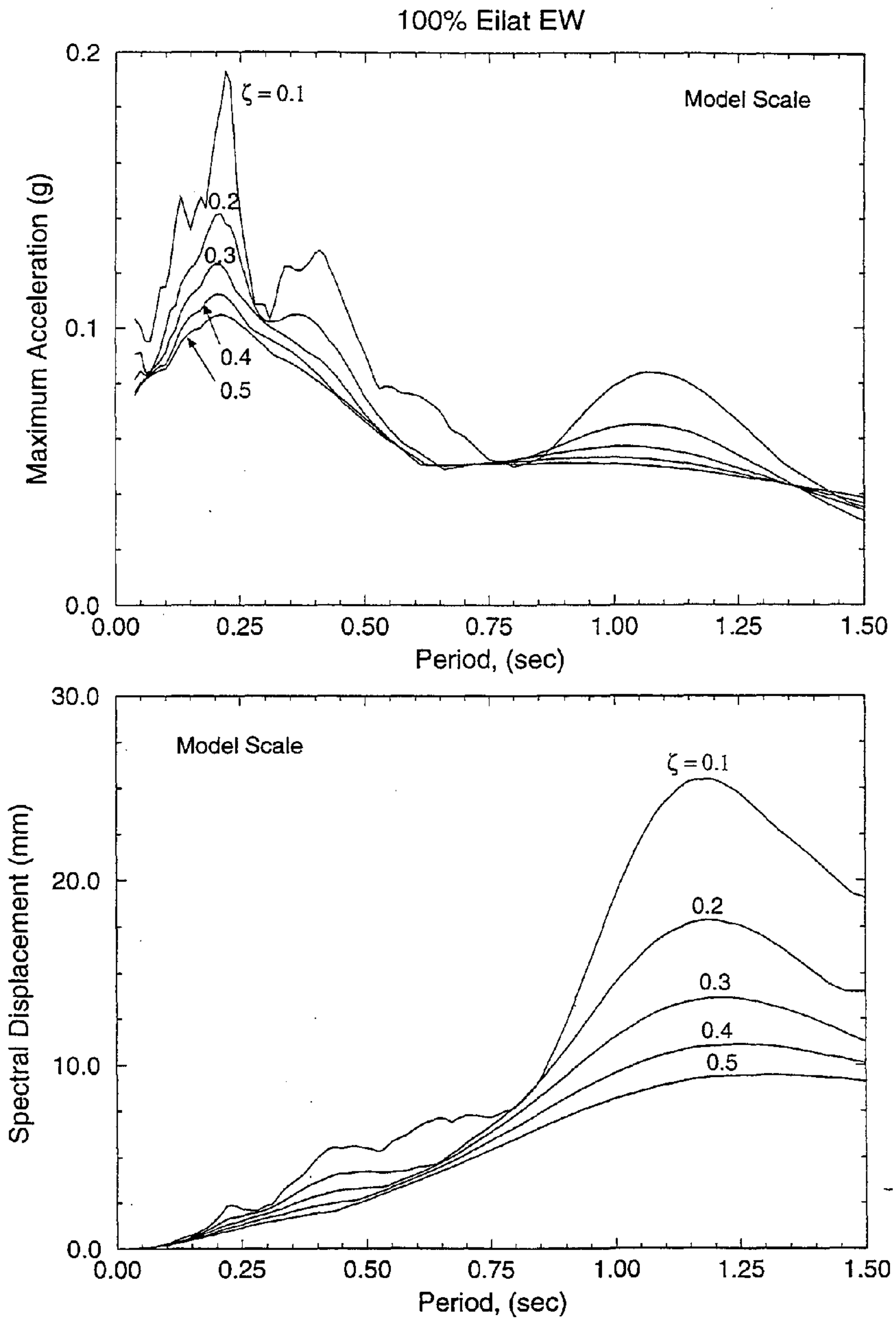

FIGURE 3-22 Time Histories of Displacement, Velocity, and Acceleration and Spectra of Acceleration and Displacement of Shaking Table Motion in 100% Eilat EW (Continued)

content could not be reproduced well (see Figure 3-17). However, the 5% damped response spectra of the actual records and the table motions compared very well specially in the period range of interest, that is 0.25 to 0.5 sec.

Figures 3-13 though 3-22 contain also the high damping response spectra of displacement and acceleration (exact, not pseudo-acceleration) of the table motions. These high damping spectra will be useful in analytical calculations presented later in Section 6.

Table 3-III lists the conducted shaking table tests together with information on the structural system configuration and excitation. It should be pointed out that the excitations are identified with percentage figures which represent the scaling factor used to amplify or deamplify displacements, velocities, and accelerations of the actual record.

3.3 Data Acquisition System

A total of 17 channels was used to monitor the structural response. Table 3-IV lists these channels and Figure 3-23 illustrates the placement of the instruments. Note that transducers 9 to 12 measured the displacement of the table and of each floor with respect to a fixed reaction frame.

Two load cells were placed diagonally along the axis of the two dampers at either the first story (1-story configuration or 3-story with 6 dampers) or the second story (3-story with 2 or 4 dampers configuration). The axial damper displacement was recorded using a displacement transducer placed along the axis of a single damper as shown in Figure 3-11.

Table 3-III Summary of Shaking Table Tests

Test No.	File Name	Structure	Dampers	Excitation
3-Story, Bare Frame Configuration				
1	B30WN2.1	3 - Story	0	White Noise
2	ELCENO	3 - Story	0	10% Elcentro S00E
3	B30E33	3 - Story	0	33% Elcentro S00E
4	B30E50	3 - Story	0	50% Elcentro S00E
5	B30T75	3 - Story	0	75% Taft N21E
6	B30T100	3 - Story	0	100% Taft N21E
7	B30M75	3 - Story	0	75% Miyagi-Ken-Oki EW
8	B30M100	3 - Story	0	100% Miyagi-Ken-Oki EW
9	B30H50	3 - Story	0	50% Hachinohe NS
10	B30P25	3 - Story	0	25% Pacoima Dam S74W
Two Linear Dampers Added at the First Story (3-Story, 2-Damper Configuration)				
11	L32WN.5	3 - Story	2LD	White Noise
12	FR1.1	3 - Story	2LD	Sinusoidal (F=1Hz)
13	FR15.2	3 - Story	2LD	Sinusoidal (F=1.5Hz)
14	FR2.2	3 - Story	2LD	Sinusoidal (F=2Hz)
15	FR25.1	3 - Story	2LD	Sinusoidal (F=2.5Hz)
16	FR15.3	3 - Story	2LD	Sinusoidal (F=1.5Hz)
17*	FR2.3	3 - Story	2LD	Sinusoidal (F=2Hz)
18	FR25.2	3 - Story	2LD	Sinusoidal (F=2.5Hz)
Dampers Removed (3-Story, Bare Frame Configuration)				
19	B30WNC	3 - Story	0	White Noise
20	B30S05	3 - Story	0	Sinusoidal (F=0.5Hz)
21	B30S10	3 - Story	0	Sinusoidal (F=1Hz)
22	B30S15	3 - Story	0	Sinusoidal (F=1.5Hz)
23	B30S20	3 - Story	0	Sinusoidal (F=2Hz)
24	B30S25	3 - Story	0	Sinusoidal (F=2.5Hz)

LD = Linear Damper ND = Nonlinear Damper

Table 3-III Summary of Shaking Table Tests (Continued)

Test No.	File Name	Structure	Dampers	Excitation
25	B30S30	3 - Story	0	Sinusoidal (F=3Hz)
Frame Repaired (Using 16 Tapered Plates)				
26	B30WNR.1	3 - Story	0	White Noise
27	R30T75.1	3 - Story	0	150% Taft N21E
28	R30T75.2	3 - Story	0	75% Taft N21E
29	R30H50	3 - Story	0	50% Hachinohe NS
30	R30M75	3 - Story	0	75% Miyagi-Ken-Oki EW
31	R30P25	3 - Story	0	25% Pacoima Dam S74W
32	R30E20	3 - Story	0	20% Elcentro S00E
33	R30S10	3 - Story	0	Sinusoidal (F=1Hz)
34	R30S15	3 - Story	0	Sinusoidal (F=1.5Hz)
35	R30S30	3 - Story	0	Sinusoidal (F=3Hz)
36	R30WNR	3 - Story	0	White Noise
Two Linear Dampers Added at the Second Story (3-Story, 2-Damper Configuration)				
37	L232WN.5	3 - Story	2LD	White Noise
38	L232WN.6	3 - Story	2LD	White Noise
39	L232T75	3 - Story	2LD	75% Taft N21E
40	L232H50	3 - Story	2LD	50% Hachinohe NS
41	L232M75	3 - Story	2LD	75% Miyagi-Ken-Oki EW
42	L232P25	3 - Story	2LD	25% Pacoima Dam S74W
43	L232E20	3 - Story	2LD	20% Elcentro S00E
44	L232S10	3 - Story	2LD	Sinusoidal (F=1Hz)
45	L232S15	3 - Story	2LD	Sinusoidal (F=1.5Hz)
46	L232S30	3 - Story	2LD	Sinusoidal (F=3Hz)
Two More Linear Dampers Added at the Third Story (3-Story, 4-Damper Configuration)				
47	L34WN.1	3 - Story	4LD	White Noise

LD = Linear Damper ND = Nonlinear Damper

Table 3-III Summary of Shaking Table Tests (Continued)

Test No.	File Name	Structure	Dampers	Excitation
48	L34WN.2	3 - Story	4LD	White Noise
49	L34T75	3 - Story	4LD	75% Taft N21E
50	L34N75	3 - Story	4LD	75% Miyagi-Ken-Oki EW
51	L34H50	3 - Story	4LD	50% Hachinohe NS
52	L34P25	3 - Story	4LD	25% Pacoima Dam S74W
53	L34E20	3 - Story	4LD	20% Elcentro S00E
54	L34S10	3 - Story	4LD	Sinusoidal (F=1Hz)
55	L34S15	3 - Story	4LD	Sinusoidal (F=1.5Hz)
56	L34S30	3 - Story	4LD	Sinusoidal (F=3Hz)
57	L34T100	3 - Story	4LD	100% Taft N21E
58	L34M100	3 - Story	4LD	100% Miyagi-Ken-Oki EW
59	L34H75	3 - Story	4LD	75% Hachinohe NS
60	L34P40	3 - Story	4LD	40% Pacoima Dam S74W
61	L34E33	3 - Story	4LD	33% Elcentro S00E
62	L34E50	3 - Story	4LD	50% Elcentro S00E
63	L34T150	3 - Story	4LD	150% Taft N21E
64	L34E75	3 - Story	4LD	75% Elcentro S00E
65	L34T200	3 - Story	4LD	200% Taft N21E
66	L34E100	3 - Story	4LD	100% Elcentro S00E
Two More Linear Dampers Added at the First Story (3-Story, 6-Damper Configuration)				
67	L36WN.1	3 - Story	6LD	White Noise
68	L36WN.2	3 - Story	6LD	White Noise
69	L36T75	3 - Story	6LD	75% Taft N21E
70	L36M75	3 - Story	6LD	75% Miyagi-Ken-Oki EW
71	L36H50	3 - Story	6LD	50% Hachinohe NS
72	L36P25.	3 - Story	6LD	25% Pacoima Dam S74W

LD = Linear Damper ND = Nonlinear Damper

Table 3-III Summary of Shaking Table Tests (Continued)

Test No.	File Name	Structure	Dampers	Excitation
73	L36E20	3 - Story	6LD	20% Elcentro S00E
74	L36T100	3 - Story	6LD	100% Taft N21E
75	L36M100	3 - Story	6LD	100% Miyagi-Ken-Oki EW
76	L36H75	3 - Story	6LD	75% Hachinohe NS
77	L36P40	3 - Story	6LD	40% Pacoima Dam S74W
78	L36E33	3 - Story	6LD	33% Elcentro S00E
79	L36E50	3 - Story	6LD	50% Elcentro S00E
80	L36T150	3 - Story	6LD	150% Taft N21E
81	L36E75	3 - Story	6LD	75% Elcentro S00E
82	L36T200	3 - Story	6LD	200% Taft N21E
83	L36E100	3 - Story	6LD	100% Elcentro S00E
84	L361N30	3 - Story	6LD	30% Northridge (Newhall 90)
85	L362N20	3 - Story	6LD	20% Northridge (Newhall 360)
86	L36Y30	3 - Story	6LD	30% Northridge (Sylmar 90)
87	L361N60	3 - Story	6LD	60% Northridge (Newhall 90)
88	L362N40	3 - Story	6LD	40% Northridge (Newhall 360)
89	L36Y60	3 - Story	6LD	60% Northridge (Sylmar 90)
90	L36LN10	3 - Story	6LD	100% Eilat NS
91	L36LE10	3 - Story	6LD	100% Eilat EW
92	L36LN20	3 - Story	6LD	200% Eilat NS
93	L36LE20	3 - Story	6LD	200% Eilat EW
94	L36LN30	3 - Story	6LD	300% Eilat NS
95	L36LE30	3 - Story	6LD	300% Eilat EW
96	L36LS10	3 - Story	6LD	Sinusoidal (F=1Hz)
97	L36S15	3 - Story	6LD	Sinusoidal (F=1.5Hz)
98	L36S30	3 - Story	6LD	Sinusoidal (F=3Hz)

LD = Linear Damper ND = Nonlinear Damper

Table 3-III Summary of Shaking Table Tests (Continued)

Test No.	File Name	Structure	Dampers	Excitation
Two Linear Dampers Removed from the First Story (3-Story, 4-Damper Configuration)				
99	L341N30	3 - Story	4LD	30% Northridge (Newhall 90)
100	L342N20	3 - Story	4LD	20% Northridge (Newhall 360)
101	L34Y30	3 - Story	4LD	30% Northridge (Sylmar 90)
102	L34LN10	3 - Story	4LD	100% Eilat NS
103	L34LE10	3 - Story	4LD	100% Eilat EW
104	L34LN20	3 - Story	4LD	200% Eilat NS
105	L34LE20	3 - Story	4LD	200% Eilat EW
Two Linear Dampers Removed from the Third Story (3-Story, 2-Damper Configuration)				
106	L321N30	3 - Story	2LD	30% Northridge (Newhall 90)
107	L322N20	3 - Story	2LD	20% Northridge (Newhall 360)
108	L32Y30	3 - Story	2LD	30% Northridge (Sylmar 90)
109	L32LN10	3 - Story	2LD	100% Eilat NS
110	L32LE10	3 - Story	2LD	100% Eilat EW
Two Linear Dampers Removed from the Second Story (3-Story, Bare Frame Configuration)				
111	R301N20	3 - Story	0	20% Northridge (Newhall 90)
112	R302N15	3 - Story	0	15% Northridge (Newhall 360)
113	R30Y20	3 - Story	0	20% Northridge (Sylmar 90)
114	R30LN10	3 - Story	0	100% Eilat NS
115	R30LE10	3 - Story	0	100% Eilat EW
Second and Third Stories Braced and Two Linear Dampers Added to the First Story (1-Story, 2-Damper Configuration)				
116	R12WN	1 - Story	2LD	White Noise
117	R12WN2	1 - Story	2LD	White Noise
118	R12T100	1 - Story	2LD	100% Taft N21E
119	R12E50	1 - Story	2LD	50% Elcentro S00E
120	R12M100	1 - Story	2LD	100% Miyagi-Ken-Oki EW

LD = Linear Damper ND = Nonlinear Damper

Table 3-III Summary of Shaking Table Tests (Continued)

Test No.	File Name	Structure	Dampers	Excitation
121	R12H75	1 - Story	2LD	75% Hachinohe NS
122	R12P25	1 - Story	2LD	25% Pacoima Dam S74W
123	R12T150	1 - Story	2LD	150% Taft N21E
124	R12E75	1 - Story	2LD	75% Elcentro S00E
125	R12M150	1 - Story	2LD	150% Miyagi-Ken-Oki EW
126	R12H100.2	1 - Story	2LD	100% Hachinohe NS
127	R121N30	1 - Story	2LD	30% Northridge (Newhall 90)
128	R122N20	1 - Story	2LD	20% Northridge (Newhall 360)
129	R12Y30	1 - Story	2LD	30% Northridge (Sylmar 90)
130	R12LN10	1 - Story	2LD	100% Eilat NS
131	R12LE10	1 - Story	2LD	100% Eilat EW
132	R12LN20	1 - Story	2LD	200% Eilat NS
133	R12LE20	1 - Story	2LD	200% Eilat EW
Dampers Removed (1-Story, Bare Frame Configuration)				
134	B10WN	1 - Story	0	White Noise
135	B10WN2	1 - Story	0	White Noise
136	B10H75	1 - Story	0	75% Hachinohe NS
137	B10M75	1 - Story	0	75% Miyagi-Ken-Oki EW
138	B10T75	1 - Story	0	75% Taft N21E
139	B10M100	1 - Story	0	100% Miyagi-Ken-Oki EW
140	B10T100	1 - Story	0	100% Taft N21E
141	B10E20	1 - Story	0	20% Elcentro S00E
142	B10LN10	1 - Story	0	100% Eilat NS
143	B10LE10	1 - Story	0	100% Eilat EW
144	B101N20	1 - Story	0	20% Northridge (Newhall 90)
145	B102N15	1 - Story	0	15% Northridge (Newhall 360)

LD = Linear Damper ND = Nonlinear Damper

Table 3-III Summary of Shaking Table Tests (Continued)

Test No.	File Name	Structure	Dampers	Excitation
146	B10Y20	1 - Story	0	20% Northridge (Sylmar 90)
147	B10P20	1 - Story	0	20% Pacoima Dam S74W
148	B10E39	1 - Story	0	40% Elcentro S00E
Two Nonlinear Dampers Added at the First Story (1-Story, 2-Damper Configuration)				
149	N10WN1.1	1 - Story	2ND	White Noise
150	N10WN2.1	1 - Story	2ND	White Noise
151	N12WN3.1	1 - Story	2ND	White Noise
152	N12T100	1 - Story	2ND	100% Taft N21E
153	N12E50	1 - Story	2ND	50% Elcentro S00E
154	N12M100	1 - Story	2ND	100% Miyagi-Ken-Oki EW
155	N12H75	1 - Story	2ND	75% Hachinohe NS
156	N12P25	1 - Story	2ND	25% Pacoima Dam S74W
157	N12T150	1 - Story	2ND	150% Taft N21E
158	N12E75	1 - Story	2ND	75% Elcentro S00E
159	N12M150	1 - Story	2ND	150% Miyagi-Ken-Oki EW
160	N12H100	1 - Story	2ND	100% Hachinohe NS
161	N121N30	1 - Story	2ND	30% Northridge (Newhall 90)
162	N122N20	1 - Story	2ND	20% Northridge (Newhall 360)
163	N12Y30	1 - Story	2ND	30% Northridge (Sylmar 90)
164	N12LN10	1 - Story	2ND	100% Eilat NS
165	N12LE10	1 - Story	2ND	100% Eilat EW
166	N12LN20	1 - Story	2ND	200% Eilat NS
167	N12LE20	1 - Story	2ND	200% Eilat EW
Bracing and Dampers Removed (3-Story, Bare Frame Configuration)				
168	R30WNR2	3 - Story	0	White Noise
Two Nonlinear Dampers Added at the Second Story (3-Story, 2-Damper Configuration)				

LD = Linear Damper   ND = Nonlinear Damper

Table 3-III Summary of Shaking Table Tests (Continued)

Test No.	File Name	Structure	Dampers	Excitation
169	N30WN1	3 - Story	2ND	White Noise
170	N30WN2	3 - Story	2ND	White Noise
171	N32T75	3 - Story	2ND	75% Taft N21E
172	N32H50	3 - Story	2ND	50% Hachinohe NS
173	N32M75	3 - Story	2ND	75% Miyagi-Ken-Oki EW
174	N32P25	3 - Story	2ND	25% Pacoima Dam S74W
175	N32E20	3 - Story	2ND	20% Elcentro S00E
176	N321N30	3 - Story	2ND	30% Northridge (Newhall 90)
177	N322N20	3 - Story	2ND	20% Northridge (Newhall 360)
178	N30Y30	3 - Story	2ND	30% Northridge (Sylmar 90)
179	N32LN10	3 - Story	2ND	100% Eilat NS
180	N32LE10	3 - Story	2ND	100% Eilat EW
181	N32T100	3 - Story	2ND	100% Taft N21E
182	N32E33	3 - Story	2ND	33% Elcentro S00E
183	N32E50	3 - Story	2ND	50% Elcentro S00E
Two More Nonlinear Dampers Added at the Third Story (3-Story, 4-Damper Configuration)				
184	N34WN3	3 - Story	4ND	White Noise
185	N34WN4	3 - Story	4ND	White Noise
186	N34T75	3 - Story	4ND	75% Taft N21E
187	N34M75	3 - Story	4ND	75% Miyagi-Ken-Oki EW
188	N34H50	3 - Story	4ND	50% Hachinohe NS
189	N34P25	3 - Story	4ND	25% Pacoima Dam S74W
190	N34E21	3 - Story	4ND	20% Elcentro S00E
191	N34T100	3 - Story	4ND	100% Taft N21E
192	N34M100	3 - Story	4ND	100% Miyagi-Ken-Oki EW
193	N34H75	3 - Story	4ND	75% Hachinohe NS

LD = Linear Damper ND = Nonlinear Damper

Table 3-III Summary of Shaking Table Tests (Continued)

Test No.	File Name	Structure	Dampers	Excitation
194	N34P40	3 - Story	4ND	40% Pacoima Dam S74W
195	N34E33	3 - Story	4ND	33% Elcentro S00E
196	N34E50	3 - Story	4ND	50% Elcentro S00E
197	N34T150	3 - Story	4ND	150% Taft N21E
198	N34E75	3 - Story	4ND	75% Elcentro S00E
199	N34T201	3 - Story	4ND	200% Taft N21E
200	N34E100	3 - Story	4ND	100% Elcentro S00E
201	N341N30	3 - Story	4ND	30% Northridge (Newhall 90)
202	N342N20	3 - Story	4ND	20% Northridge (Newhall 360)
203	N34Y30	3 - Story	4ND	30% Northridge (Sylmar 90)
204	N34LN10	3 - Story	4ND	100% Eilat NS
205	N34LE10	3 - Story	4ND	100% Eilat EW
206	N34LN20	3 - Story	4ND	200% Eilat NS
207	N34LE20	3 - Story	4ND	200% Eilat EW
Two More Nonlinear Dampers Added at the First Story (3-Story, 6-Damper Configuration)				
208	N36WN2	3 - Story	6ND	White Noise
209	N36WN3	3 - Story	6ND	White Noise
210	N36T75	3 - Story	6ND	75% Taft N21E
211	N36M75	3 - Story	6ND	75% Miyagi-Ken-Oki EW
212	N36H50	3 - Story	6ND	50% Hachinohe NS
213	N36P25	3 - Story	6ND	25% Pacoima Dam S74W
214	N36E20	3 - Story	6ND	20% Elcentro S00E
215	N36T100	3 - Story	6ND	100% Taft N21E
216	N36M100	3 - Story	6ND	100% Miyagi-Ken-Oki EW
217	N36H75	3 - Story	6ND	75% Hachinohe NS
218	N36P40	3 - Story	6ND	40% Pacoima Dam S74W

LD = Linear Damper   ND = Nonlinear Damper

Table 3-III Summary of Shaking Table Tests (Continued)

Test No.	File Name	Structure	Dampers	Excitation
219	N36E33	3 - Story	6ND	33% Elcentro S00E
220	N36E50	3 - Story	6ND	50% Elcentro S00E
221	N36T150	3 - Story	6ND	150% Taft N21E
222	N36E75	3 - Story	6ND	75% Elcentro S00E
223	N36T200	3 - Story	6ND	200% Taft N21E
224	N36E100	3 - Story	6ND	100% Elcentro S00E
225	N361N30	3 - Story	6ND	30% Northridge (Newhall 90)
226	N362N20	3 - Story	6ND	20% Northridge (Newhall 360)
227	N36Y30	3 - Story	6ND	30% Northridge (Sylmar 90)
228	N361N60	3 - Story	6ND	60% Northridge (Newhall 90)
229	N362N40	3 - Story	6ND	40% Northridge (Newhall 360)
230	N36Y60	3 - Story	6ND	60% Northridge (Sylmar 90)
231	N36LN10	3 - Story	6ND	100% Eilat NS
232	N36LE10	3 - Story	6ND	100% Eilat EW
233	N36LN20	3 - Story	6ND	200% Eilat NS
234	N36LE20	3 - Story	6ND	200% Eilat EW
235	N36LN30	3 - Story	6ND	300% Eilat NS
236	N36LE30	3 - Story	6ND	300% Eilat EW
237	N36WN.2	3 - Story	6ND	White Noise
238	N36WN4	3 - Story	6ND	White Noise
239	N36WN5	3 - Story	6ND	White Noise
240	N36WN6	3 - Story	6ND	White Noise
Dampers Removed (3-Story, Bare Frame Configuration)				
241	R30T100	3 - Story	0	150% Taft N21E
242	R30E33	3 - Story	0	33% Elcentro S00E
243	R301N30	3 - Story	0	30% Northridge (Newhall 90)
244	R30WNF	3 - Story	0	White Noise

LD = Linear Damper ND = Nonlinear Damper

Table 3-IV List of Channels used to Measure Dynamic Response

Channel No.	Instrument	Notation	Measured Response
1	ACCL	AFE	Table Horizontal Acceleration - East
2	ACCL	AFW	Table Horizontal Acceleration - West
3	ACCL	A1E	1st Floor Horizontal Acceleration - East
4	ACCL	A1W	1st Floor Horizontal Acceleration - West
5	ACCL	A2E	2nd Floor Horizontal Acceleration - East
6	ACCL	A2W	2nd Floor Horizontal Acceleration - West
7	ACCL	A3E	3rd Floor Horizontal Acceleration - East
8	ACCL	A3W	3rd Floor Horizontal Acceleration - West
9	LDT	DHF	Table Horizontal Displacement - Center
10	LDT	DH1	1st Floor Horizontal Displacement - Center
11	LDT	DH2	2nd Floor Horizontal Displacement - Center
12	LDT	DH3	3rd Floor Horizontal Displacement - Center
13	Load Cell	LCE	Axial Damper Force - East Side
14	Load Cell	LCW	Axial Damper Force - West Side
15	LDT	DDW	Axial Damper Displacement - West Side
16*	LVDT	THD	Driving Actuator's Horizontal Displacement
17*	Load Cell	FA	Force in the Driving Actuator

ACCL = Accelerometer
LDT = Linear Displacement Transducer
LVDT = Linear Variable Differential Transformer
* = Table Controls

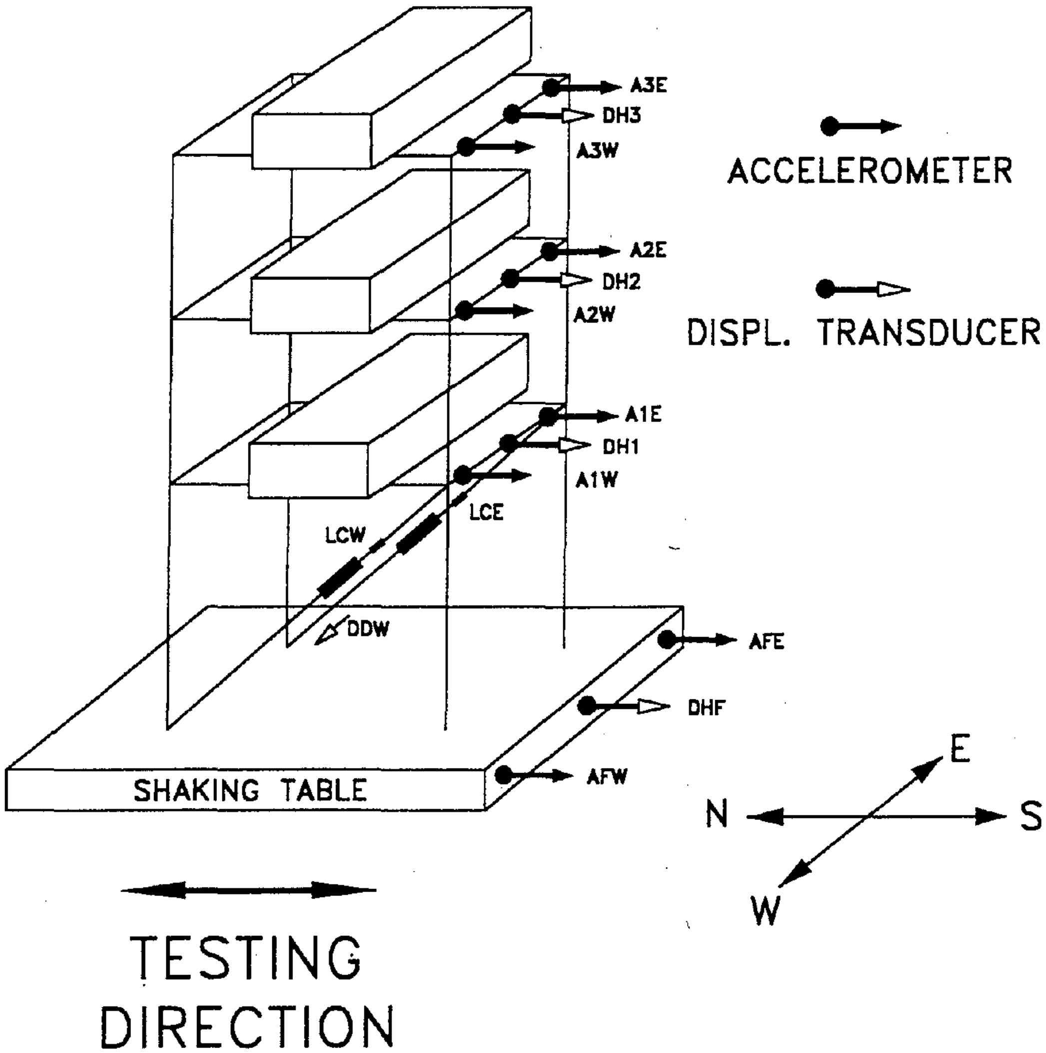

FIGURE 3-23 Instrumentation Diagram

It measured the relative displacement of one end of the damper with respect to the other end.

The data was collected simultaneously from all the channels at a rate of 100 readings per second. The measured signals were filtered at the data acquisition system using integrated low pass filters with cut-off frequency of 22 Hz.

SECTION 4

IDENTIFICATION OF STRUCTURAL PROPERTIES

4.1 Introduction

Identification of the properties of the structure without dampers could be easily accomplished using established procedures. The amplitude of the total acceleration transfer function of such lightly damped structures, when excited by a wide frequency range white noise vibration, contains sharp and narrow peaks which reveals the frequencies, damping ratios, and mode shapes. On the other hand, the transfer function of highly damped structures does not usually contains such sharp peaks and identification of such structures requires an indirect procedure.

The approach followed in this study for identification of the structure with linear dampers is based on a calibrated analytical model which is constructed as a combination of the identified properties of the structure without dampers plus the effect of the dampers. For this, analytical transfer functions of the structure without dampers are first compared to the experimental ones. When the comparison is satisfactory, the effect of the linear dampers is included to obtain an analytical model of the linearly damped structure. Verification of this analytical model is conducted by comparing the experimental and analytical transfer functions of the structure with dampers. The structural properties of the linearly damped structure can then be obtained by solving its eigenvalue problem.

Due to the existence of nonlinearities, the properties of the structure with nonlinear dampers are dependent on the amplitude and velocity of motion. Accordingly, identification of properties is not performed herein for the structure with nonlinear dampers. Rather, some insight into the behavior of the structure is provided through comparison of transfer functions at various levels of motion.

4.2 Identification of Single Story Structure with Linear Dampers

The equation of motion of the single story structure with dampers can be written in the following form

$$m\ddot{u} + C_u\dot{u} + ku + \eta p_d = -m\ddot{u}_g \tag{4-1}$$

where m is the mass of the structure, C_u and k are the damping constant and the stiffness of the structure without dampers, respectively; η is the number of dampers; p_d is the horizontal component of force in a single damper; and $u, \dot{u}$ and $\ddot{u}$ are the relative displacement, velocity, and acceleration of the mass m with respect to the ground, and $\ddot{u}_g$ is the ground acceleration.

The equation governing the behavior of a linear damper over a wide frequency range was given previously in Section 2 (Equation 2-16). For a damper inclined at an angle θ with respect to the horizontal, the equation in the horizontal direction is

$$p_d + \lambda\dot{p}_d = C_o\dot{u}\cos^2\theta \tag{4–2}$$

Application of Fourier transform to Equations (4-1) and (4-2) results in

$$-\Omega^2\overline{u} + 2i\xi_u\omega_n\Omega\overline{u} + \omega_n^2\overline{u} + \frac{\eta\overline{p}_d}{m} = -\overline{\ddot{u}}_g \tag{4-3}$$

$$\overline{p}_d = \frac{i\Omega C_o \cos^2\theta}{1 + i\lambda\Omega}\overline{u} \tag{4-4}$$

where $\overline{u}$ and $\overline{p}_d$ are the Fourier transforms of the displacement u and the damper force p_d, respectively, and ω_n and ξ_u are the natural frequency and damping ratio of the structure without dampers, respectively.

The amplitude of the total acceleration transfer function, T, is defined as the ratio of the steady state total acceleration $(\overline{\ddot{u}} + \overline{\ddot{u}}_g)$ amplitude to the amplitude of the ground motion acceleration $\overline{\ddot{u}}_g$.

$$T = \frac{\overline{\ddot{u}} + \overline{\ddot{u}}_g}{\overline{\ddot{u}}_g} = 1 - \frac{\Omega^2\overline{u}}{\overline{\ddot{u}}_g} \tag{4-5}$$

Substituting Equations (4-3) and (4-4) into (4-5) we obtain

$$T = \left| 1 + \frac{\Omega^2}{-\Omega^2 + \omega_n^2 + 2i\Omega\omega_n\xi_u + \left\{ \dfrac{i\eta\Omega C_o \cos^2\theta}{m(1 + i\lambda\Omega)} \right\}} \right| \tag{4-6}$$

where the vertical lines stands for the modulus of the contained complex quantity.

To obtain the experimental transfer function, the structure is excited by a stationary banded white noise vibration and records of total acceleration of the mass are obtained. The transfer function is then calculated as the ratio of the Fourier amplitude of the measured total acceleration to the Fourier amplitude of the ground excitation.

In the case of the structure without dampers ($\eta = 0$), the single sharp peak of the experimental transfer function occurs at ($\Omega = \omega_n$) and Equation (4-6) simplifies to

$$T^2(\omega_n) \approx 1 + \frac{1}{4\xi_u^2} \tag{4-7}$$

Knowing the experimental value of $T(\omega_n)$, ξ_u can be obtained directly from Equation (4-7). Knowing the properties of the undamped structure, ω_n and ξ_u, the eigenvalue problem of the linearly damped structure can be solved to obtain the structural properties. For this, Equations (4-1) and (4-2) with $\ddot{u}_g$ set equal to zero can be rewritten in the following form

$$[A]\{\dot{Z}\} + [B]\{Z\} = \{0\} \tag{4-8}$$

where

$$[A] = \begin{bmatrix} 1 & 0 & 0 \\ 0 & 1 & 0 \\ 0 & 0 & \lambda \end{bmatrix} \tag{4-9}$$

$$[B] = \begin{bmatrix} 2\xi_u\omega_n & \omega_n^2 & \frac{1}{m} \\ -1 & 0 & 0 \\ -\eta C_o \cos^2\theta & 0 & 1 \end{bmatrix} \tag{4-10}$$

$$\{Z\} = \begin{Bmatrix} \dot{u} \\ u \\ p_d \end{Bmatrix} \tag{4-11}$$

For a solution in the form $\{Z\} = \{Z_o\}e^{\Psi t}$, Equation (4-8) becomes

$$[B]\{Z_o\} + \Psi[A]\{Z_o\} = \{0\} \tag{4-12}$$

This is a generalized eigenvalue problem. It can be solved numerically by using standard software (e.g., MATLAB or IMSL) to obtain the eigenvalues Ψ (complex numbers). Recalling the expression of the characteristic roots of the equation of free vibration of a viscously damped SDOF system, namely

$$\Psi = -\xi\omega \pm i\omega\sqrt{1-\xi^2} \tag{4-13}$$

the frequency and damping ratio of our linearly viscous damped structure can be obtained as follows :

$$\omega = |\Psi| \tag{4-14}$$

$$\xi = \frac{-\Re(\Psi)}{\omega} \tag{4-15}$$

where the vertical lines stands for the modulus and $\Re$ stands for the real part of the complex number Ψ.

4.3 Identification of Multistory Structures

4.3.1 Structure without Dampers

The equation of motion of a multistory elastic structure when subjected to an earthquake ground excitation can be written in the following form

$$[M]\{\ddot{U}\}+[C_u]\{\dot{U}\}+[K]\{U\}=-[M]\{R\}\ddot{u}_g \tag{4-16}$$

Where $[M]$ is the lumped mass matrix, $[C_u]$ and $[K]$ are the damping and stiffness matrices, respectively; and $\{U\}$, $\{\dot{U}\}$ and $\{\ddot{U}\}$ are the vectors of relative displacements, velocities, and accelerations, respectively, of the lumped masses with respect to the ground. Moreover, $\{R\}$ is a vector which contains units in the case of a structure with one degree of freedom per floor.

The displacement vector $\{U\}$ of a system which has k degrees of freedom can be expressed in terms of modal coordinates $q_k(t)$ as follows :

$$\{U\}=\sum_{k=1}^{k}\{\varphi_k\}q_k(t) \tag{4-17}$$

where $\{\varphi_k\}$ is the k-th modal vector or mode shape.

Substituting for $\{U\}$ and its derivatives into Equation (4-16) and applying Fourier transform, the amplitude of the transfer function of degree of freedom j can be expressed as

$$T_j = \left| \sum_{k=1}^{k} \frac{-\Gamma_k (2i\Omega\,\omega_k \xi_k + \omega_k^2)}{\omega_k^2 - \Omega^2 + 2i\xi_k \Omega\,\omega_k} \varphi_{jk} \right| \tag{4-18}$$

where Γ_k is the k-th modal participation factor given by

$$\Gamma_k = \frac{\{\varphi_k\}^T [M]\{R\}}{\{\varphi_k\}^T [M]\{\varphi_k\}} \tag{4-19}$$

and ω_k and ξ_k are the k-th mode frequency and damping ratio, respectively. Moreover, φ_{jk} is the component of vector $\{\varphi_k\}$ corresponding to degree of freedom j. However, for small damping and well separated modes, T_j will have negligible value for all frequencies $\Omega \neq \omega_k$, hence Equation (4-18) can be approximated by

$$T_j(\omega_k) \approx \frac{\Gamma_k \sqrt{1 + 4\xi_k^2}}{2\xi_k} \varphi_{jk} \tag{4-20}$$

or

$$\xi_k = \frac{1}{2\sqrt{\left\{ \frac{T_j(\omega_k)}{\varphi_{jk}\Gamma_k} \right\}^2 - 1}} \tag{4-21}$$

where $T_j(\omega_k)$ is the peak value of the transfer function of floor j at frequency ω_k.

It should be pointed out that the term in front of φ_{jk} in Equation (4-20) is constant for each mode, therefore

$$T_j(\omega_k) \text{ is proportional to } \varphi_{jk} \tag{4-22}$$

Equation (4-22) implies that for a certain frequency ω_k, the magnitude of the peak of the transfer function corresponding to the *j*-th degree of freedom is directly proportional to the mode shape component φ_{jk}. Thus, the position of the peaks of the transfer function determine directly the modal frequencies and their values determine the corresponding mode shape. Equation (4-21) can then be used to obtain the modal damping ratios.

4.3.2 Experimental Stiffness and Damping Matrices

The stiffness matrix [K] and the damping matrix $[C_u]$ can be determined using the experimentally obtained natural frequencies, damping ratios and mode shapes and utilizing the procedure presented by Clough and Penzien (1993). Let define the generalized damping and mass matrices $\left[C_g\right]$ and $\left[M_g\right]$

$$[C_g] = [\Phi]^T [C_u][\Phi] \tag{4-23}$$

and

$$[M_g] = [\Phi]^T [M][\Phi] \tag{4-24}$$

where $[\Phi]$ is the mode shape matrix. Matrix $\left[M_g\right]$ is diagonal with elements equal to M_{gi}. Moreover, matrix $[C_g]$ is assumed diagonal (proportional damping) with elements equal to $2\xi_i\omega_i M_{gi}$.

Matrix $[C_u]$ can be obtained by pre-multiplying Equation (4-23) by $\left[\Phi^T\right]^{-1}$ and post-multiplying it by $[\Phi]^{-1}$, that is,

$$\left[\Phi^T\right]^{-1}[C_g][\Phi]^{-1} = \left[\Phi^T\right]^{-1}[\Phi]^T[C_u][\Phi][\Phi]^{-1} \tag{4-25}$$

or

$$[C_u] = \left[\Phi^T\right]^{-1}[C_g][\Phi]^{-1} \tag{4-26}$$

Taking advantage of the orthogonality properties of mode shapes relative to the mass matrix, pre-multiplication of Equation (4-24) by $[M_g]^{-1}$ results in

$$[M_g]^{-1}[M_g] = [I] = \left[[M_g]^{-1}[\Phi]^T[M]\right][\Phi] = [\Phi]^{-1}[\Phi] \tag{4-27}$$

from which it is evident that

$$[\Phi]^{-1} = [M_g]^{-1}[\Phi]^T[M] \tag{4-28}$$

and

$$\left[\Phi^T\right]^{-1} = [M][\Phi][M_g]^{-1} \tag{4-29}$$

Substituting Equations (4-28) and (4-29) into (4-26), the result is

$$[C_u] = [M][\Phi]\left[[M_g]^{-1}[C_g][M_g]^{-1}\right][\Phi]^T[M] \tag{4-30}$$

$$[C_u] = [M][\Phi][F][\Phi]^T[M] \tag{4-31}$$

where $[F]$ is a diagonal matrix containing elements $f_i = \dfrac{2\xi_i\omega_i}{M_{gi}}$. It is now useful to note that each modal damping ratio provides an independent contribution to the damping matrix, that is,

$$[c_i] = [M]\{\varphi_i\} f_i \{\varphi_i\}^T [M] \tag{4-32}$$

where $[c_i]$ is the matrix of contribution of mode i to the total damping matrix. The total damping matrix can now be obtained as the sum of the modal contribution matrices, that is,

$$[C_u] = \sum_{i=1}^{k} [c_i] = [M]\left[\sum_{i=1}^{k} \{\varphi_i\} f_i \{\varphi_i\}^T\right][M] \tag{4-33}$$

or

$$[C_u] = [M]\left[\sum_{i=1}^{k} \frac{2\xi_i\omega_i}{M_{gi}} \{\varphi_i\}\ \{\varphi_i\}^T\right][M] \tag{4-34}$$

Similarly, the stiffness matrix is constructed as

$$[K] = [M]\left[\sum_{i=1}^{k} \frac{\omega_i^2}{M_{gi}} \{\varphi_i\}\ \{\varphi_i\}^T\right][M] \tag{4-35}$$

where k is the number of modes and ξ_i, ω_i are the damping ratio and frequency of mode i, respectively.

4.3.3 Equation of Motion of Structure with Linear Dampers

The equations of motion of the structure with dampers can be obtained by adding a vector $\{PD\}$ to the equation of motion of the structure without dampers. This vector contains the horizontal component of damper forces at each floor. That is, the equations of motion are

$$[M]\{\ddot{U}\} + [C_u]\{\dot{U}\} + [K]\{U\} + \{PD\} = -[M]\{R\}\ddot{u}_g \tag{4-36}$$

$$\{PD\} = \begin{Bmatrix} \eta_k p_k \\ \vdots \\ \eta_j p_j - \eta_{j+1} p_{j+1} \\ \vdots \\ \eta_1 p_1 - \eta_2 p_2 \end{Bmatrix} \tag{4-37}$$

where η_j is the number of dampers at the j-th story and p_j is the horizontal component of force in a single damper at the j-th story. It is assumed that all dampers at the j-th story are identical. Moreover, vector {R} is replaced by a vector containing unites for the remainder of this section.

The equation describing the damper force p_j is given by

$$p_j + \lambda \dot{p}_j = C_{oj} \cos^2 \theta_j \frac{d}{dt}(u_j - u_{j-1}) \tag{4-38}$$

where C_{oj} is the damping constant of a damper at the j-th floor and θ_j is the angle of inclination of dampers at the floor j with respect to the horizontal. Application of Fourier transform to Equations (4-36) and (4-38) results in

$$\left[-\Omega^2[M]+i\Omega[C_u]+[K]+\frac{i\Omega}{1+i\Omega\lambda}[CD]\right]\{\overline{U}\}=-[M]\{1\}\ddot{\overline{u}}_g \tag{4-39}$$

In the above equation, the term in front of the Fourier transform of the displacement vector $\{\overline{U}\}$ is the dynamic stiffness matrix $[K_D(\Omega)]$, that is

$$[K_D(\Omega)]=-\Omega^2[M]+i\Omega[C_u]+[K]+\frac{i\Omega}{1+i\Omega\lambda}[CD] \tag{4-40}$$

where the term $\frac{i\Omega}{1+i\Omega\lambda}[CD]$ represents the contribution of the damper forces to the dynamic stiffness matrix. In the case of installing two linear dampers at each story of the 3-story frame, matrix $[CD]$ is given by

$$[CD]=\begin{bmatrix} C_3 & -C_3 & 0 \\ -C_3 & C_2+C_3 & -C_2 \\ 0 & -C_2 & C_1+C_2 \end{bmatrix} \tag{4-41}$$

For the case of two dampers at each of the second and the third stories, C_1=0 and $[CD]$ takes the form

$$[CD]=\begin{bmatrix} C_3 & -C_3 & 0 \\ -C_3 & C_2+C_3 & -C_2 \\ 0 & -C_2 & C_2 \end{bmatrix} \tag{4-42}$$

For the case of only two dampers installed at the second story ($C_1=C_3=0$), $[CD]$ takes the form

$$[CD] = \begin{bmatrix} 0 & 0 & 0 \\ 0 & C_2 & -C_2 \\ 0 & -C_2 & C_2 \end{bmatrix} \tag{4-43}$$

where $C_i = 2C_{oi}\cos^2\theta_i$; $i = 1, 2$ and 3.

4.3.4 Identification of the Structure with Linear Dampers

4.3.4.1Transfer Function

Equation (4-39) can be rewritten in the following form

$$\{\overline{U}\} = -[K_D(\Omega)]^{-1}[M]\{1\}\overline{\ddot{u}}_g \tag{4-44}$$

Defining the inverse of the dynamic stiffness matrix $[K_D(\Omega)]$ as $[H(\Omega)]$ and multiplying Equation (4-44) by $-\Omega^2$, the Fourier transform of the relative acceleration vector is obtained as

$$\{\overline{\ddot{U}}\} = \Omega^2[H(\Omega)][M]\{1\}\overline{\ddot{u}}_g \tag{4-45}$$

The amplitude of the transfer function of the j-th floor is given by

$$T_j = \frac{\overline{\ddot{u}}_g + \overline{\ddot{U}}_j}{\overline{\ddot{u}}_g} \tag{4-46}$$

Use of Equation (4-45), results in

$$T_j = \left| 1 + \Omega^2 \sum_{i=1}^{k} H_{ji}(\Omega).m_i \right| \qquad (4\text{-}47)$$

where $H_{ji}(\Omega)$ are the elements of the matrix $\left[H(\Omega)\right]$ and m_i is the lumped mass of the i-th floor.

4.3.4.2 Eigenvalue Problem

The eigenvalue problem is formulated in the same way as that of the single degree of freedom structure. Equation (4-8) is valid with the vector $\{Z\}$ given by

$$\{Z\} = \begin{Bmatrix} \{\dot{U}\} \\ \{U\} \\ \{PD\} \end{Bmatrix} \qquad (4\text{-}48)$$

and matrices $[A]$ and $[B]$ defined as

$$[A] = \begin{bmatrix} [M] & [0] & [0] \\ [0] & [I] & [0] \\ [0] & [0] & \lambda[I] \end{bmatrix} \qquad (4\text{-}49)$$

$$[B] = \begin{bmatrix} [C_u] & [K] & [I] \\ -[I] & [0] & [0] \\ [CD] & [0] & [I] \end{bmatrix} \qquad (4\text{-}50)$$

The solution of Equation (4-8) results in the complex eigenvalues Ψ, and eigenvectors $\{Z_o\}$ of the structure with linear dampers. Equations (4-14) and (4-15) are then used to obtain the frequency and damping ratio for each mode of vibration.

4.4 Identification Tests

Identification of the structural properties was conducted by exciting the base of the structure with a banded, 0 to 22 Hz white noise vibration. Identification of the structure without dampers was performed by the procedures of Sections 4.2 and 4.3. In the case of structures with linear dampers, the properties were obtained by the analytical procedures of Sections 4.2 and 4.3 and utilizing the identified properties of the bare frame and the calibrated Maxwell model of the dampers (see Figure 2-11).

4.4.1 Single Story Structure

Table 4-I summarizes the identified properties of the single story frame without and with two linear dampers.

Table 4-I Properties of One-Story Model Structure

	Bare Frame	2 Linear Dampers
Frequency (Hz)	4.30	4.40
Damping Ratio (%)	2.36	16.16

It may be noted that the presence of dampers has a minor effect on the structural frequency. This effect corresponds to a 5% increase in stiffness. That is, the dampers behave, effectively, as viscous devices. Figure 4-1 shows the transfer function of the structure for the cases, without, with two linear, and with two non-linear dampers. For the case of the structure without or with two linear dampers, the experimental and analytical transfer functions are plotted against each other. The comparison is seen to be very good. This

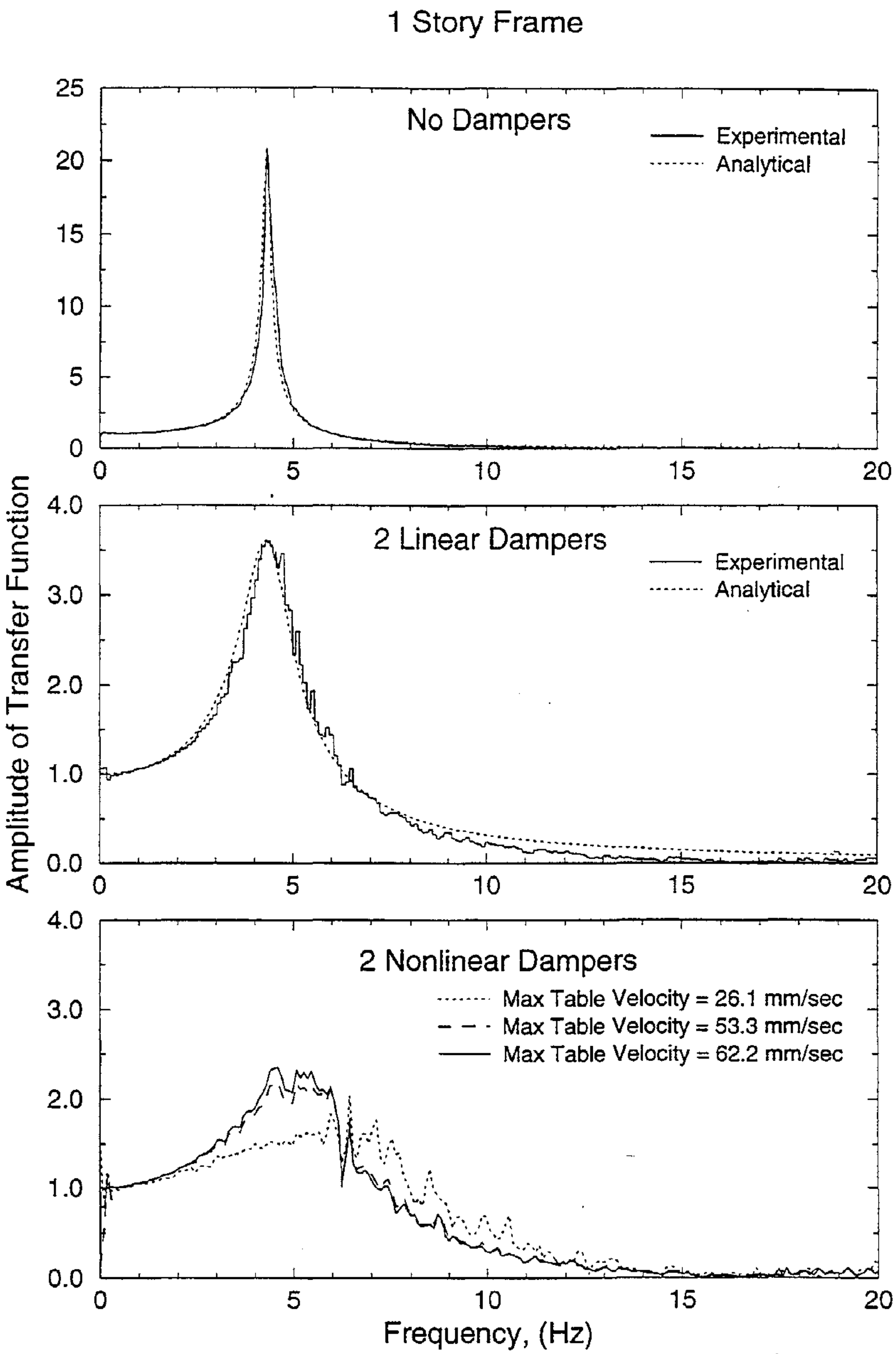

FIGURE 4-1 Transfer Functions of One-Story Frame without and with Two Linear and Two Nonlinear Dampers

demonstrate the validity of the analytical model for the single story structure with linear dampers.

In the case of the structure with two non-linear dampers, the experimental transfer function is plotted for different levels of the white noise excitation. It is observed that the amplitude of the transfer function increases with increasing level of excitation, that is, also increasing level of structural response. This implies that the effective damping ratio reduces with increasing level of structural response (i.e., amplitude of the motion). This has been analytically demonstrated by Soong and Constantinou (1994) for structures with nonlinear dampers with exponent α less than unity.

4.4.2 Three Story Structure

Table 4-II presents a summary of identified properties of the three story structure without dampers. Identified modal properties of the structure during various test stages are presented in Table 4-III. The results of Table 4-III demonstrate minor change in the modal properties of frame without dampers in the various test stages in which the frame was damaged and subsequently repaired. It can also be seen that the existence of the dampers has a very small effect on the fundamental frequency of the structure, but it significantly increases its damping. For the higher modes, the dampers introduce both significant stiffness and damping to the system. This was expected since the dampers exhibited storage stiffness for frequencies above about 4 Hz (see Section 2). This behavior leads to the suppression of the higher modes and consequently the system primarily responds in its fundamental mode.

Table 4-II Summary of Structural Properties of 3-Story Repaired Frame without Dampers

Mode		1	2	3
Frequency (Hz)		2.28	7.52	14.26
Damping Ratio (%)		2.71	1.02	1.04
Mode Shape	Floor1	0.360	-1.016	3.174
	Floor2	0.736	-0.843	-2.727
	Floor3	1	1	1
Mass Matrix $(N.s^2/cm)$		9.56	0	0
		0	9.56	0
		0	0	9.56
Stiffness Matrix *(kN/cm)*		13.10	-16.99	5.67
		-16.99	36.98	-28.89
		5.67	-28.89	49.9
Damping Matrix *(N.s/cm)*		8.76	-2.19	1.24
		-2.19	11.94	-4.27
		1.24	-4.27	13.73

Table 4-III Identified Modal Properties of the 3-Story Frame During Different Test Stages

		Frame Following Repair of Columns			Cracked Frame (Prior to Repair with 16 Plates)			Repaired Frame (with 16 Tapered Plates)		
	Mode	1	2	3	1	2	3	1	2	3
Frequency (Hz)		2.15	7.47	13.65	2.14	7.32	13.48	2.28	7.52	14.26
Damping Ratio (%)		3.66	1.06	0.78	2.20	0.75	0.81	2.71	1.02	1.04
Mode Shapes	Floor 3	1	1	1	1	1	1	1	1	1
	Floor 2	0.771	-0.889	-2.583	0.742	-0.840	-2.482	0.736	-0.843	-2.727
	Floor 1	0.377	-1.052	3.200	0.342	-1.040	2.850	0.360	-1.016	3.174
		Repaired Frame								
		2 LD at 2nd Story			4 LD at 2nd and 3rd Story			6 LD at all Stories		
	Mode	1	2	3	1	2	3	1	2	3
Frequency (Hz)		2.32	7.53	16.77	2.34	8.81	18.77	2.32	9.26	19.85
Damping Ratio (%)		12.57	1.34	23.57	15.44	33.14	32.85	21.79	47.10	33.50

LD = Linear Dampers

Of interest is the case of two dampers at the second story where the dampers could not add any significant stiffness nor damping to the second mode of the structure. This can be explained by observing that the second story modal drift in the second mode is very small. This demonstrates potential for problems in the case of incomplete vertical distribution of dampers.

Figures 4-2 to 4-4 present transfer functions of the structure without dampers. It should be mentioned that the frame has its first story columns already strengthened, whereas the so-called repaired frame has all its cracked locations repaired by welding of plates (16 tapered plates - see Section 3).

Figure 4-5 shows the transfer functions of the frame prior to its repair with the 16 plates in the case of two linear dampers added to its first story. It may be seen in this figure that the analytically predicted transfer function for the third floor exhibits a shorter primary peak than the experimental one. This indicates that the analytical model over-predicts damping in the fundamental mode. The reason for this difference was found to be in the value of damping constant used in the analytical model. This value was determined from testing of one damper but it was later realized that dampers exhibited differences in their properties.

Figure 4-6 shows the transfer functions of the repaired frame with two linear dampers added to its second story. These functions demonstrate that the addition of dampers significantly changes the first and the third mode damping ratio (compare Figure 4-6 to Figure 4-4) but they have almost no effect on the second mode. As previously explained, this is the result of the small second mode second story modal drift of the structure.

3 Story Bare Frame - No Dampers

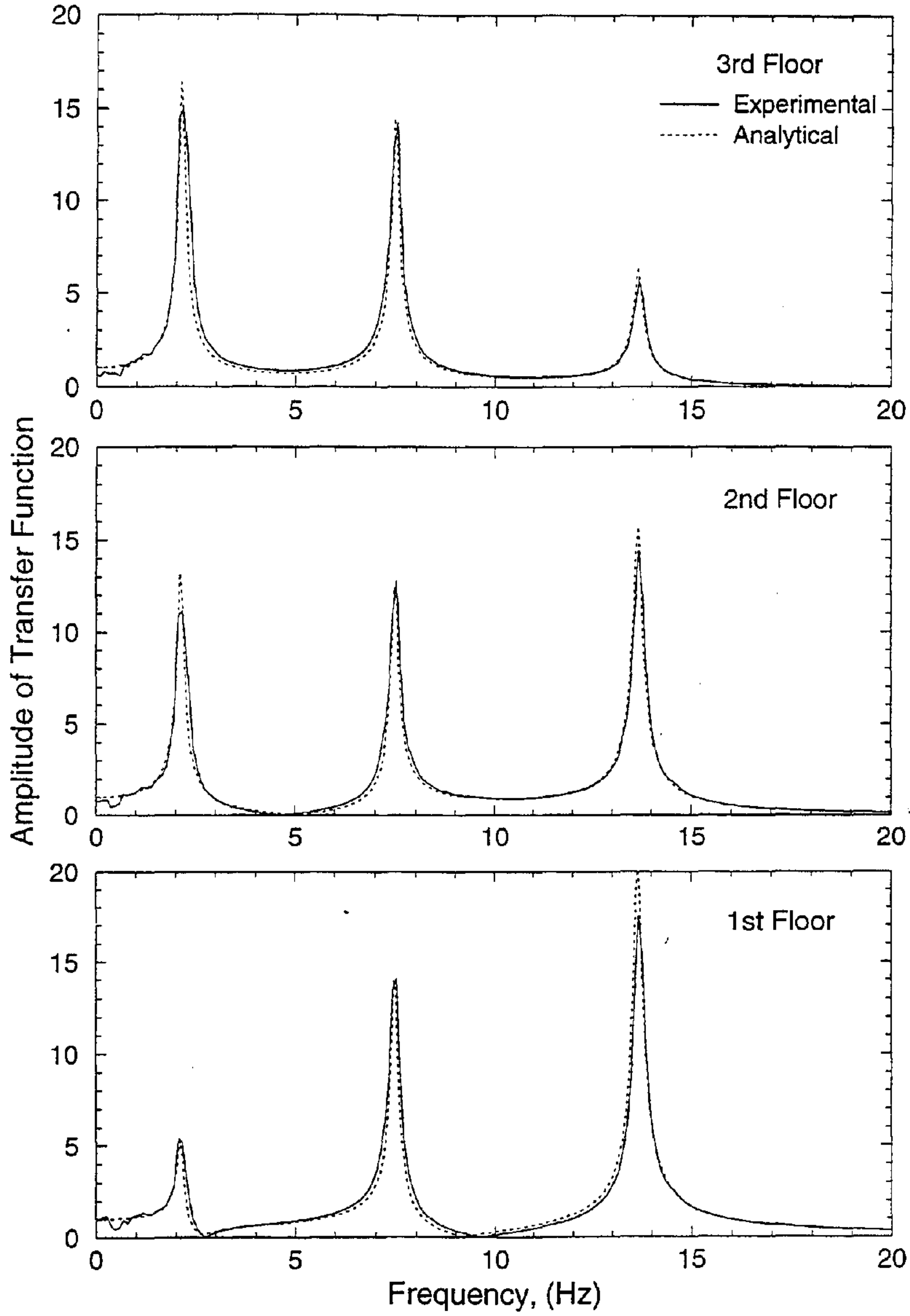

FIGURE 4-2 Comparison of Analytical and Experimental Transfer Functions of 3-Story Bare Frame without Dampers (Following Repair of Columns)

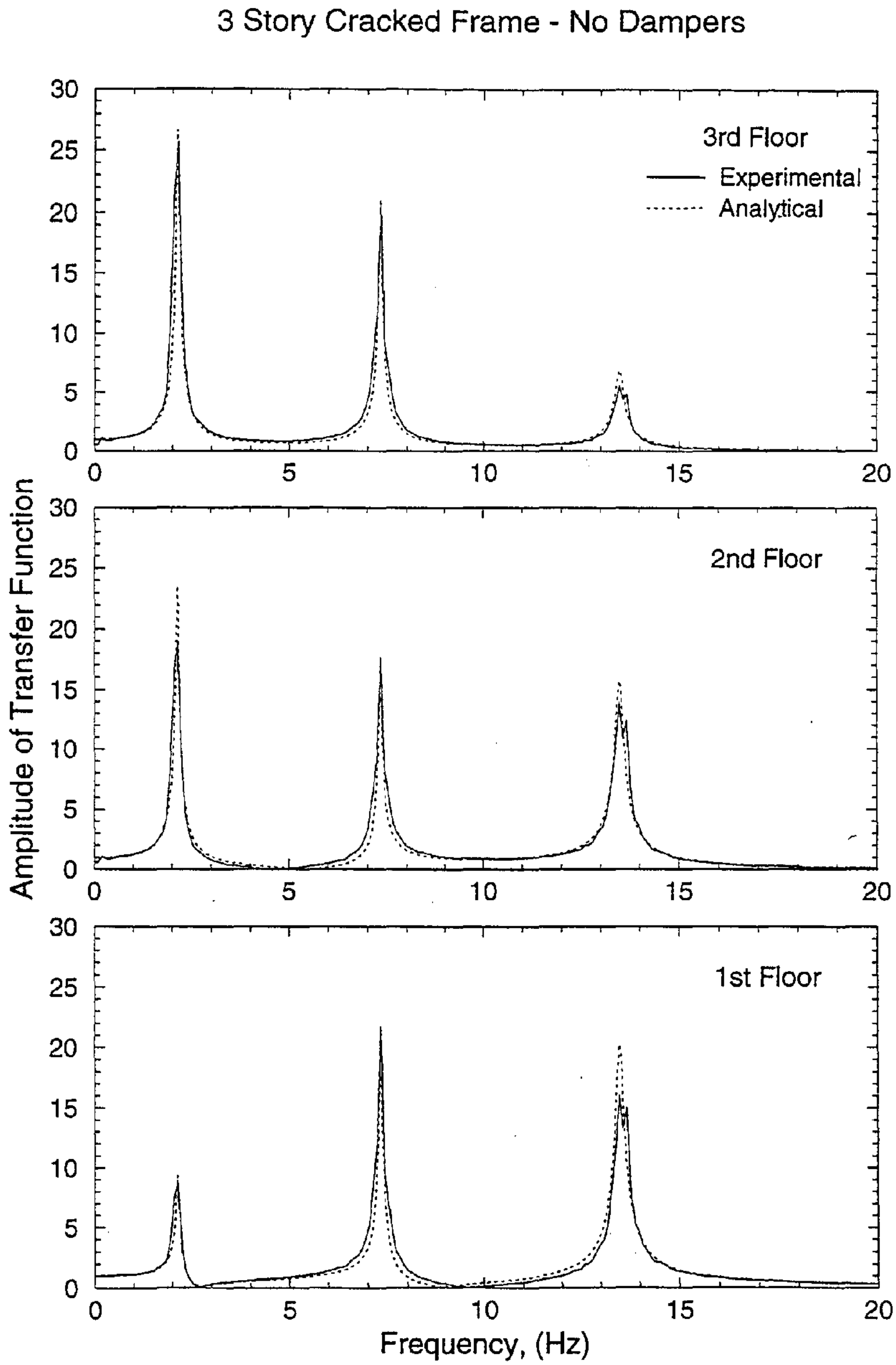

FIGURE 4-3 Comparison of Analytical and Experimental Transfer Functions of 3-Story Cracked Frame without Dampers (Prior to Repair with 16 Tapered Plates)

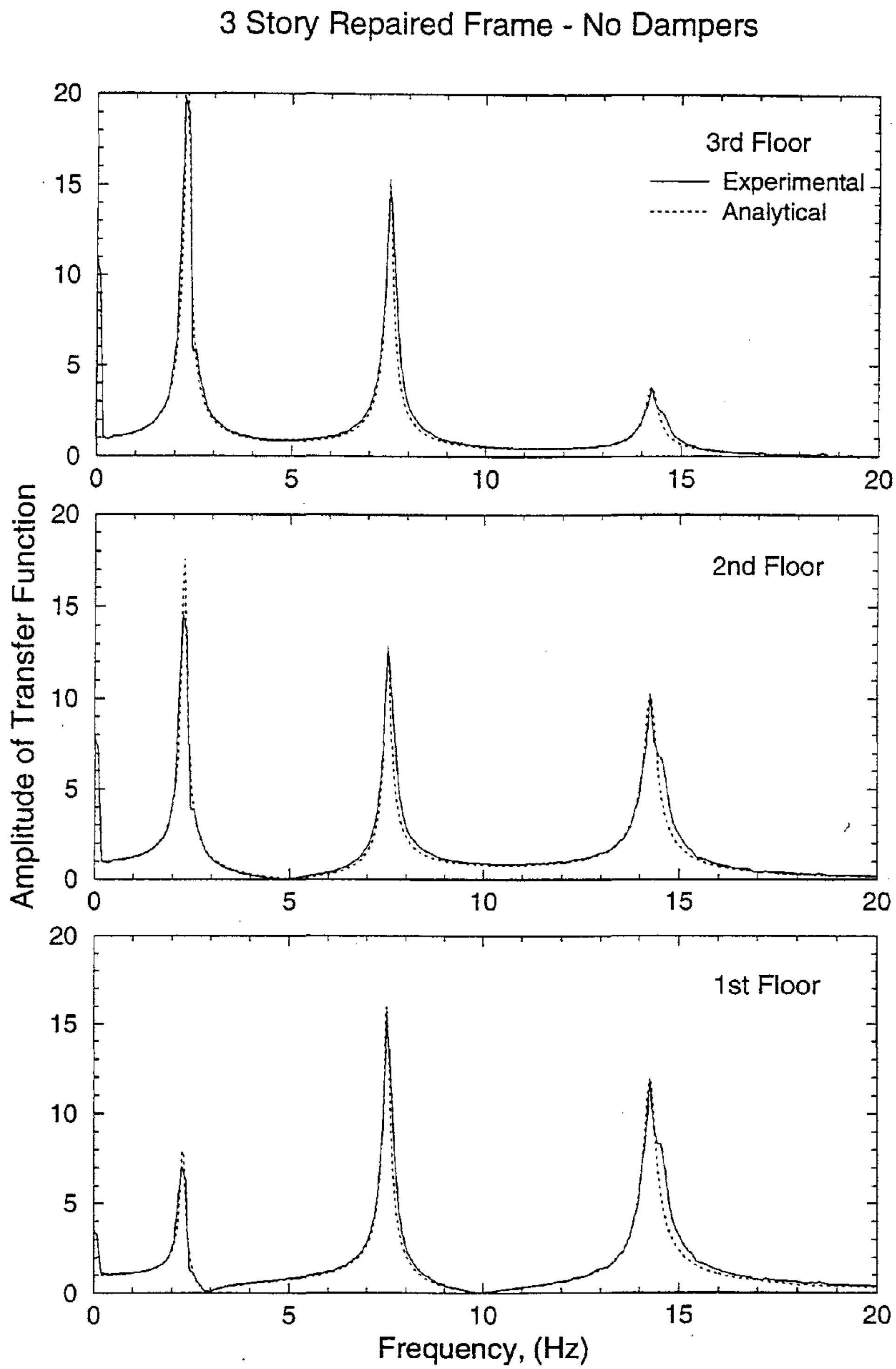

FIGURE 4-4 Comparison of Analytical and Experimental Transfer Functions of 3-Story Repaired Frame without Dampers (Repaired with 16 Tapered Plates)

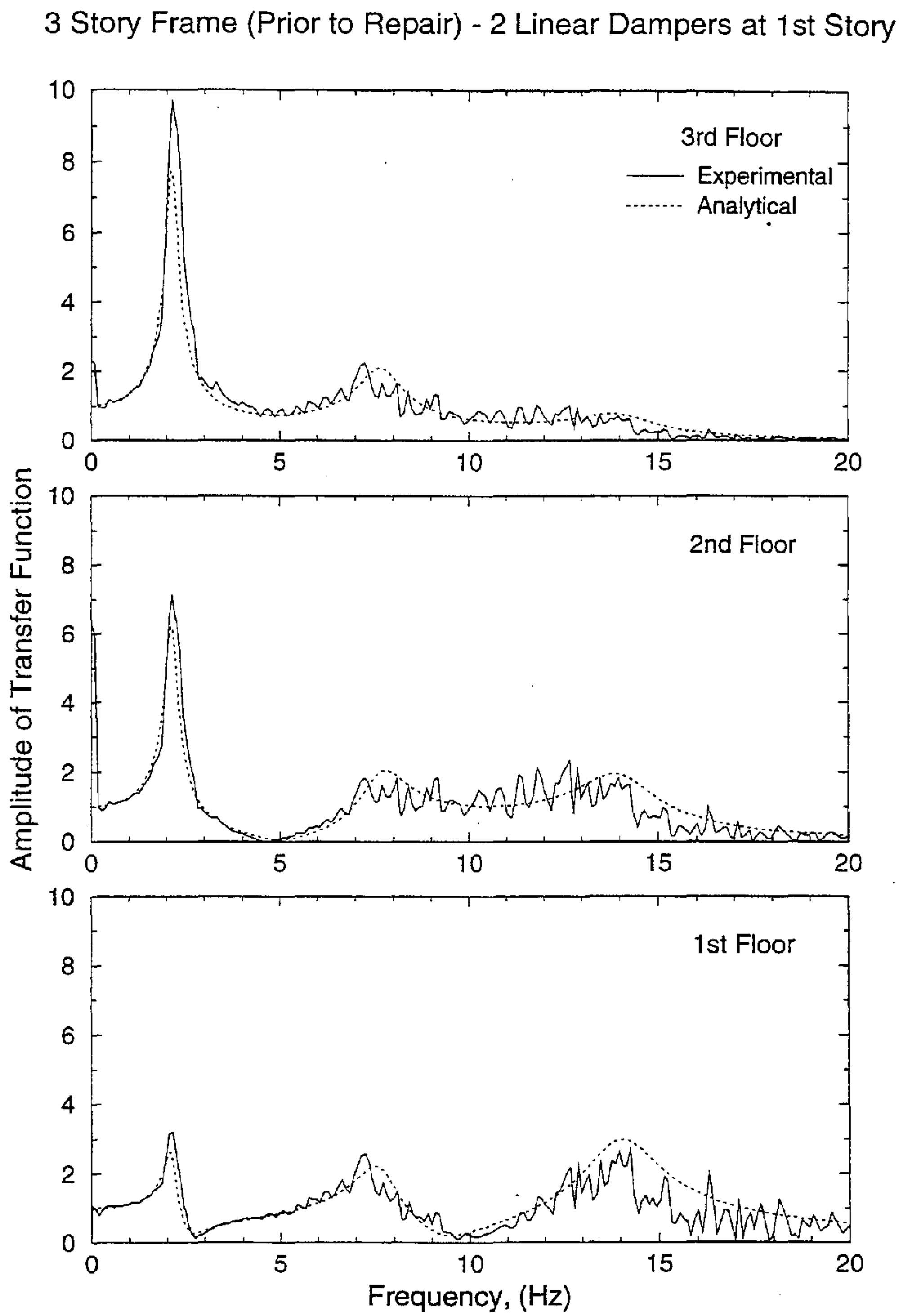

FIGURE 4-5 Comparison of Analytical and Experimental Transfer Functions of 3-Story Frame (Prior to Repair with 16 Tapered Plates) with Two Linear Dampers at First Story.

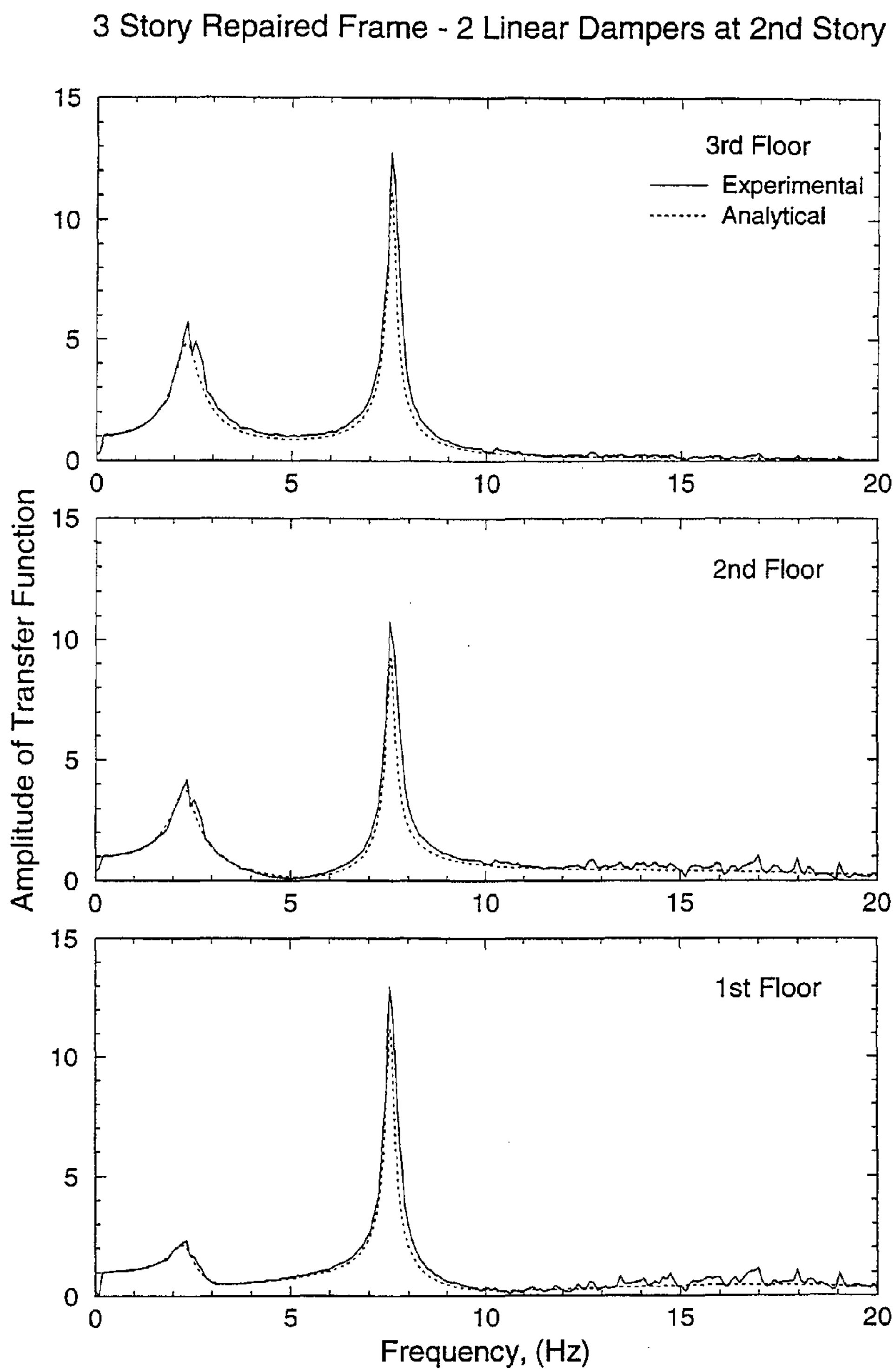

FIGURE 4-6 Comparison of Analytical and Experimental Transfer Functions of 3-Story Repaired Frame with Two Linear Dampers at Second Story

Figures 4-7 and 4-8 present transfer functions of the repaired frame with dampers installed either at the second and the third stories or over all stories. It is evident from these functions that the second and third modes are suppressed resulting essentially in a system with a single degree of freedom.

Figures 4-9 to 4-11 presents recorded transfer functions for the repaired frame with nonlinear dampers. The functions shown in Figure 4-9 again show a strong second mode component similar to the one seen in Figure 4-6 for the case of linear dampers. Of course the explanation is found in the small second mode second story modal drift of the structure.

Interesting is the behavior demonstrated in Figure 4-10 and 4-11 at high frequencies. The transfer functions exhibit noticeable high frequency confent that is not present in the case of linear dampers (see Figures 4-7 and 4-8). This behavior, that is caused by the nonlinearity of the dampers, will be further examined in the shake table tests by constructing floor response spectra. Finally, Figure 4-11 demonstrates again the expected reduction of effective damping ratio with increasing amplitude of deformation.

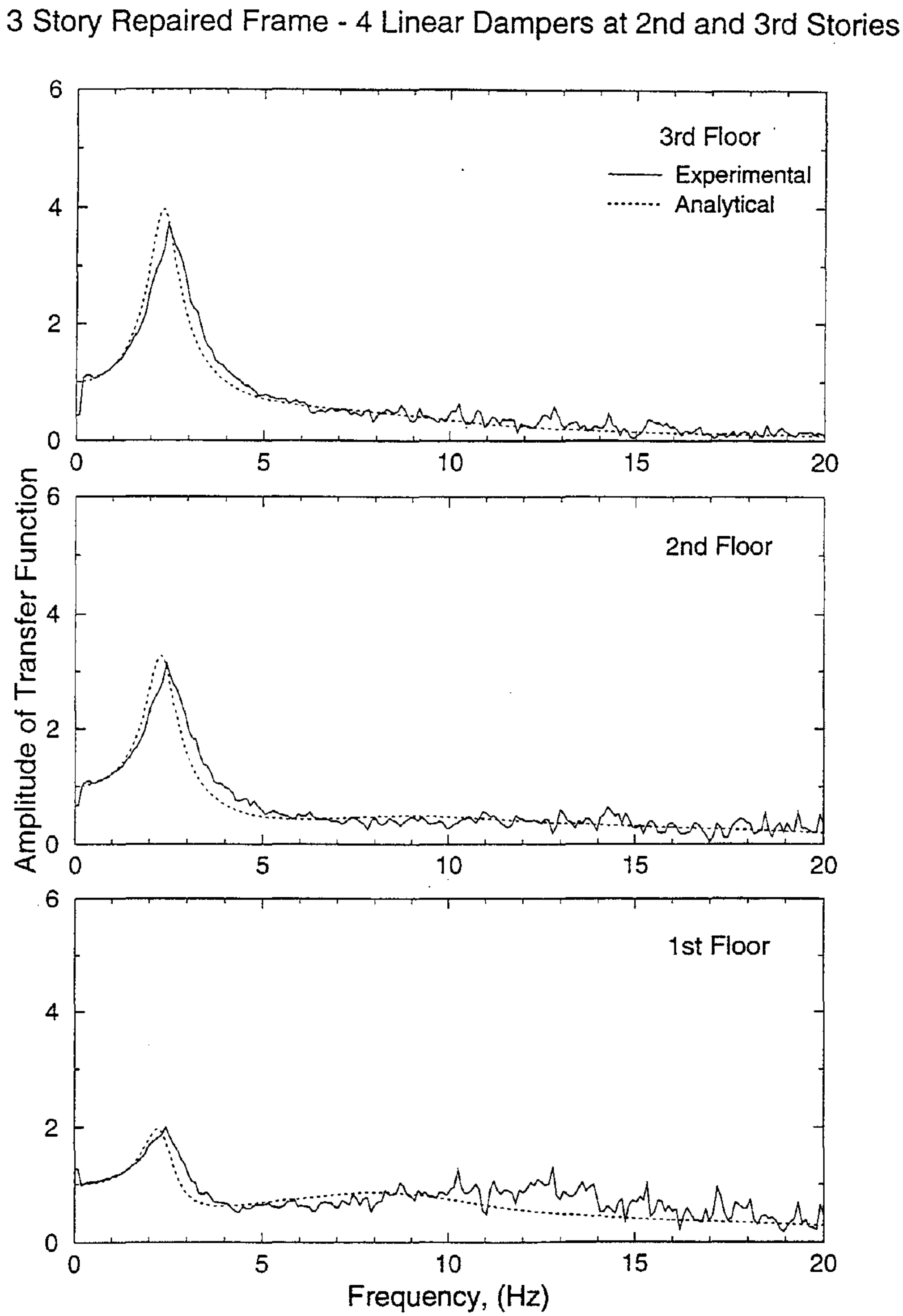

FIGURE 4-7 Comparison of Analytical and Experimental Transfer Functions of 3-Story Repaired Frame with Four Linear Dampers at the Second and Third Stories

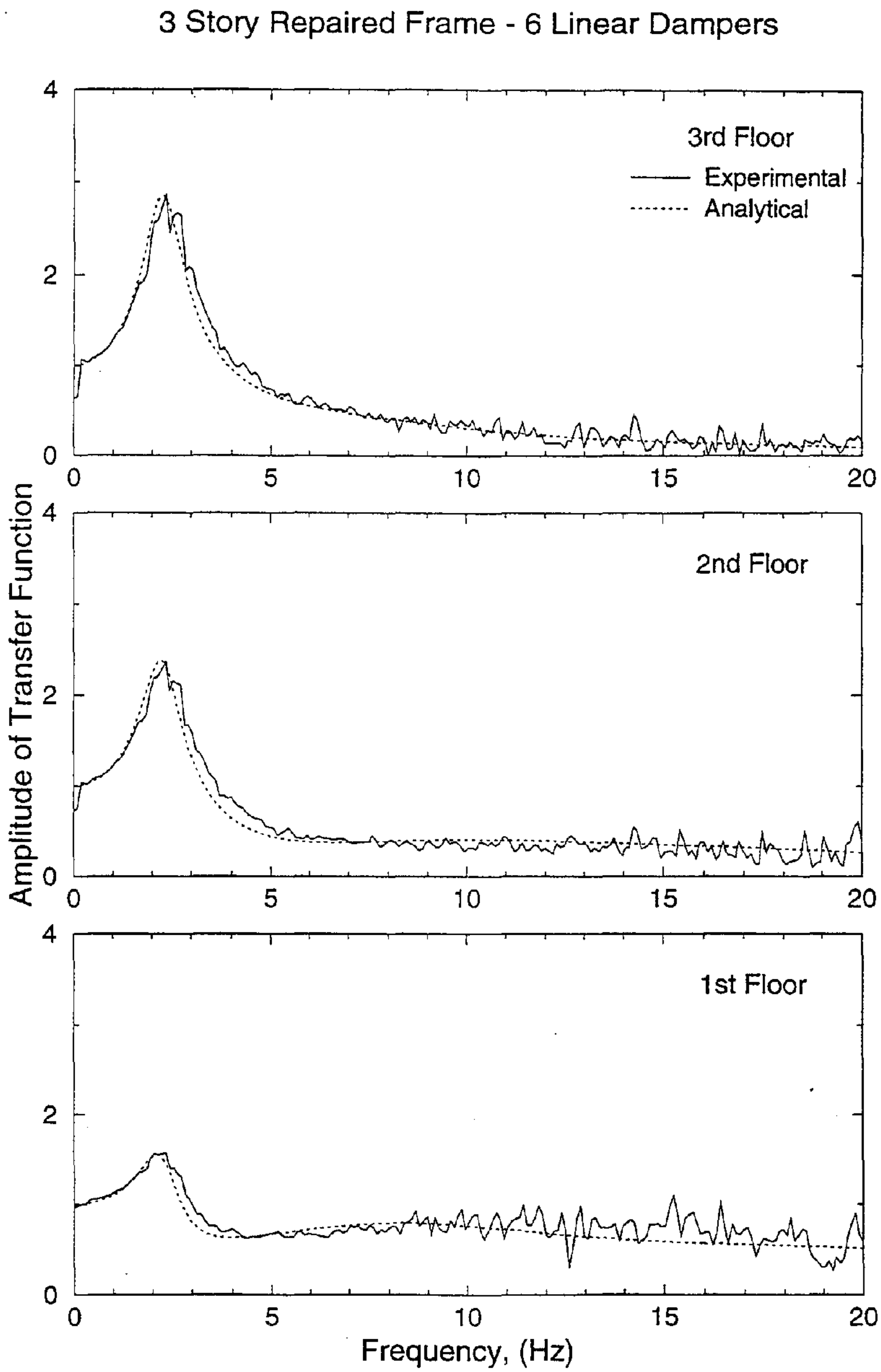

FIGURE 4-8 Comparison of Analytical and Experimental Transfer Functions of 3-Story Repaired Frame with Six Linear Dampers at All Stories (Two at Each Story)

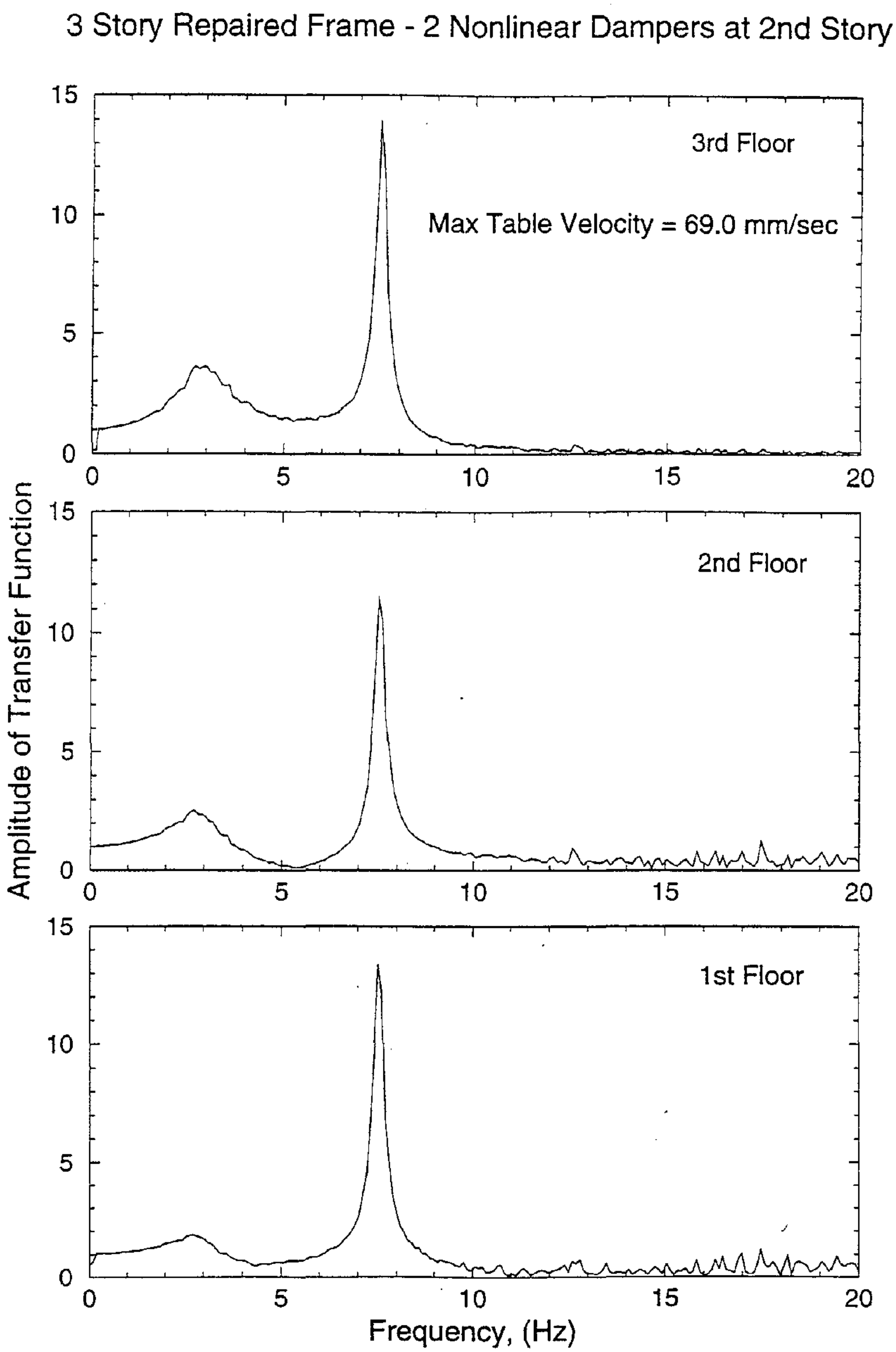

FIGURE 4-9 Experimental Transfer Functions of 3-Story Repaired Frame with Two Nonlinear Dampers at Second Story

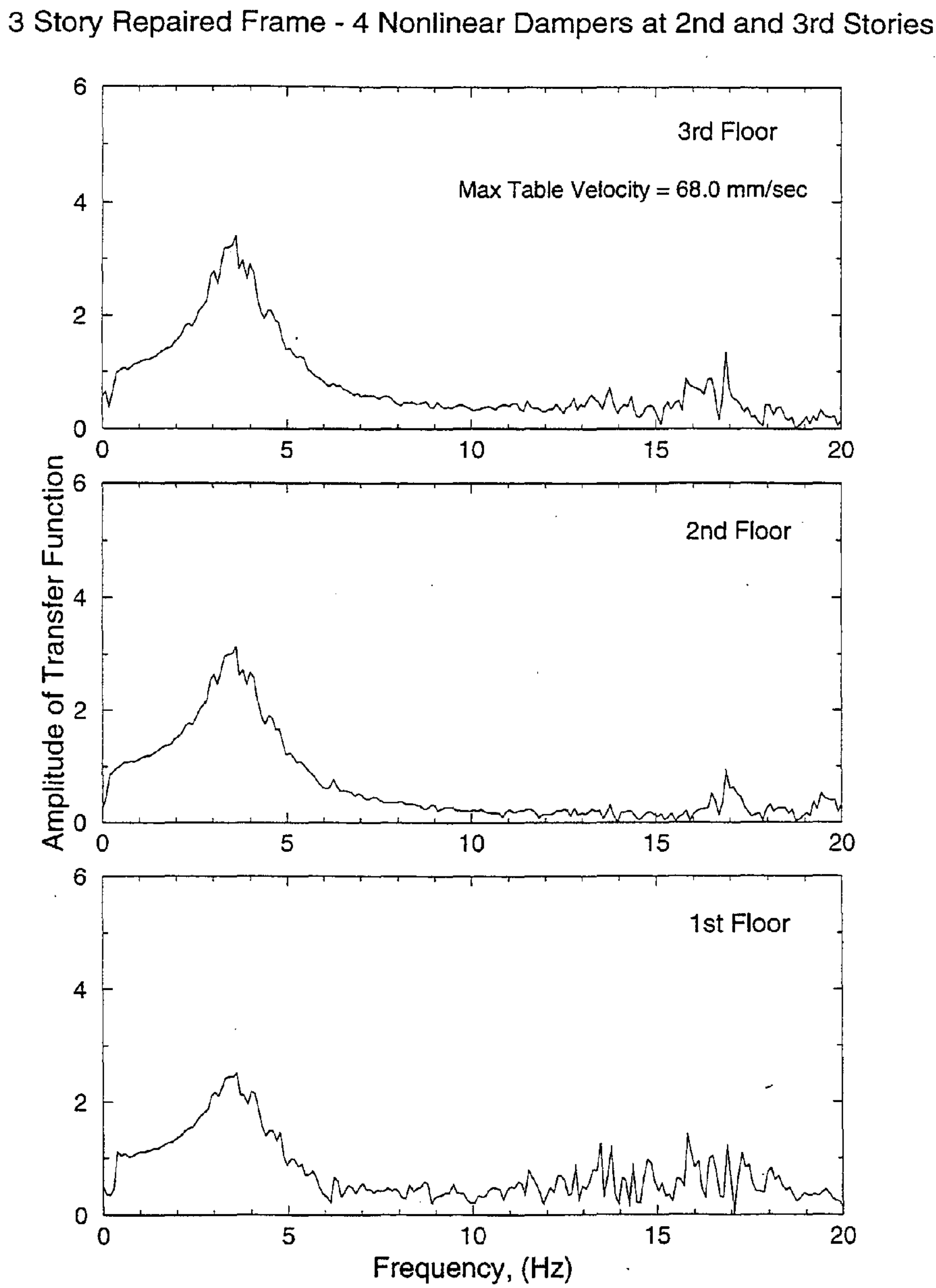

FIGURE 4-10 Experimental Transfer Functions of 3-Story Repaired Frame with Four Nonlinear Dampers at the Second and Third Stories

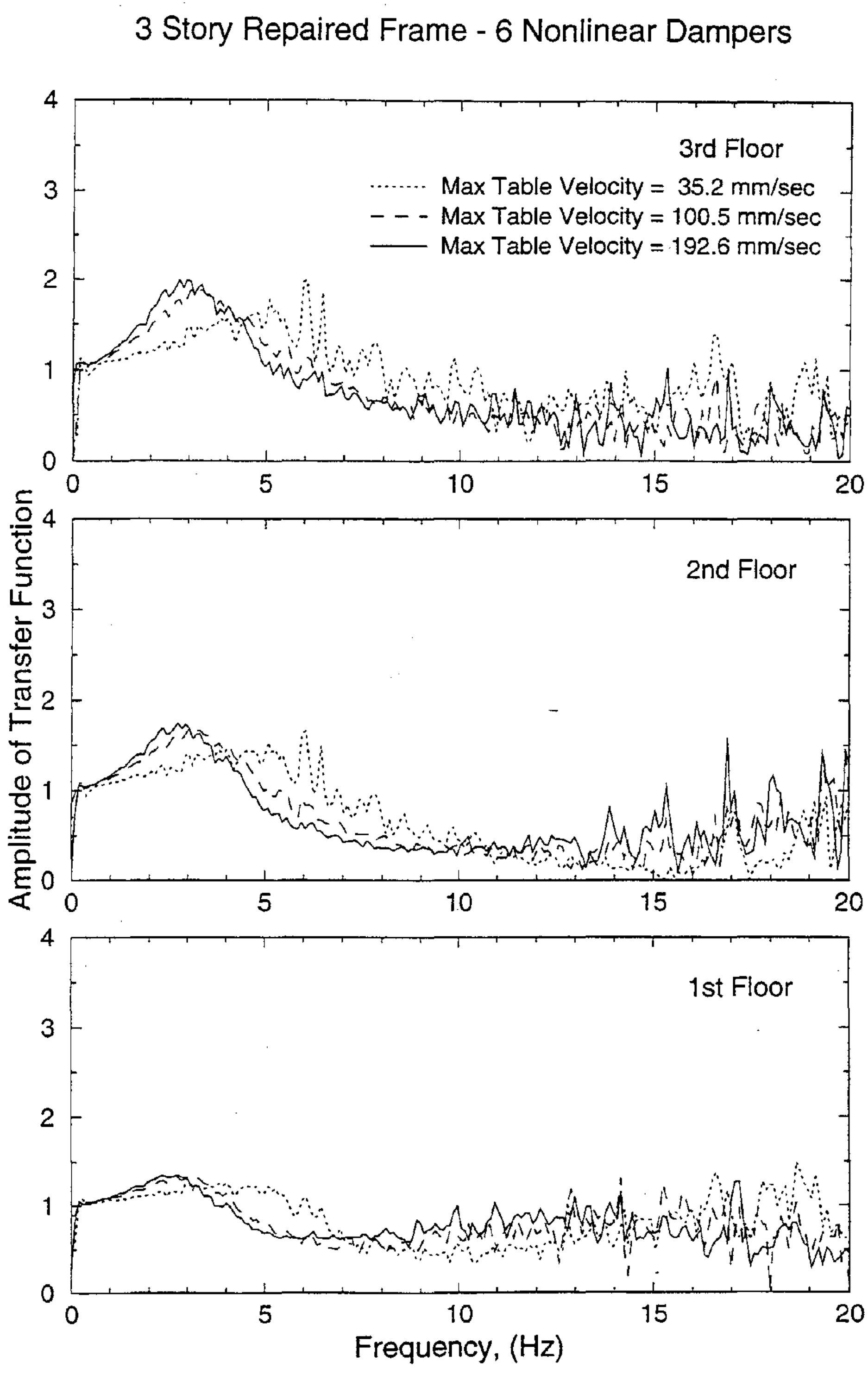

FIGURE 4-11 Experimental Transfer Functions of 3-Story Repaired Frame with Six Nonlinear Dampers at All Stories (Two at Each Story) for Different Levels of White Noise Excitation

SECTION 5

SHAKING TABLE TEST RESULTS AND INTERPRETATION

5.1 Single Story Structure

The experimental results for the single story structure are summarized in Tables 5-I through 5-III. These tables present the experimental results for the structure without dampers, with two linear dampers, and with two nonlinear dampers, together with information on the structural properties of the system (natural frequency and damping ratio) and the maximum recorded table displacement, velocity, and acceleration. The structural response is presented in terms of the maximum shear force normalized by the total weight of the structure (28743 N) and the maximum drift normalized by story height (813 mm). The story shear force was calculated from the recorded floor total acceleration and the known structural mass. Moreover, the table displacement and acceleration were directly measured, whereas the velocity was calculated by numerical differentiation of the displacement record.

5.2 Three Story Structure

Table 5-IV summarizes the experimental results for the 25 preliminary tests conducted on the 3-story structure. This set of tests was carried out for the following purpose :

1. To investigate the behavior of the bare frame after welding the longitudinal plates to the cracked sections of the first story columns.

Table 5-I **Summary of Experimental Results for Single Story Frame**

Test No.	File Name	Excitation	DMP	System Parameters Freq. Hz	System Parameters Damping	Maximum Table Motion Displacement (mm)	Maximum Table Motion Velocity (mm/sec)	Maximum Table Motion Acceleration (g)	Peak Shear Force / Total Weight	Peak Drift / Height (%)
134	B10WN	White Noise	0	4.30	0.024	4.48	26.43	0.061	0.113	0.167
135	B10WN2	White Noise	0	4.30	0.024	8.88	53.34	0.110	0.238	0.356
136	B10H75	75% Hachinohe NS	0	4.30	0.024	22.02	86.28	0.160	0.270	0.399
137	B10M75	75% Miyagi-Ken-Oki EW	0	4.30	0.024	8.95	34.61	0.085	0.250	0.365
138	B10T75	75% Taft N21E	0	4.30	0.024	12.22	56.04	0.112	0.313	0.467
139	B10M100	100% Miyagi-Ken-Oki EW	0	4.30	0.024	12.00	46.75	0.114	0.330	0.486
140	B10T100	100% Taft N21E	0	4.30	0.024	16.59	74.85	0.144	0.414	0.630
141	B10E20	20% Elcentro S00E	0	4.30	0.024	5.31	35.00	0.092	0.186	0.273
142	B10LN10	100% Eilat NS	0	4.30	0.024	10.86	53.42	0.062	0.168	0.248
143	B10LE10	100% Eilat EW	0	4.30	0.024	13.66	53.18	0.070	0.209	0.313
144	B101N20	20% Northridge (Newhall 90)	0	4.30	0.024	8.78	65.80	0.109	0.260	0.383
145	B102N15	15% Northridge (Newhall 360)	0	4.30	0.024	9.19	70.09	0.131	0.253	0.369
146	B10Y20	20% Northridge (Sylmar 90)	0	4.30	0.024	10.85	68.42	0.110	0.268	0.396
147	B10P20	20% Pacoima Dam S74W	0	4.30	0.024	5.10	47.86	0.109	0.418	0.628
148	B10E39	40% Elcentro S00E	0	4.30	0.024	10.90	70.88	0.178	0.382	0.576
149	B10WN3	White Noise	0	4.30	0.024	8.84	54.45	0.110	0.225	0.342

DMP = No. of Dampers

Table 5-II Summary of Experimental Results for Single Story Frame with Two Linear Dampers

Test No.	File Name	Excitation	DMP	System Parameters		Maximum Table Motion			Peak Shear Force / Total Weight	Peak Drift (%) / Height
				Freq. Hz	Damping	Displacement (mm)	Velocity (mm/sec)	Acceleration (g)		
116	R12WN	White Noise	2LD	4.40	0.162	5.12	29.61	0.067	0.080	0.094
117	R12WN2	White Noise	2LD	4.40	0.162	10.39	60.64	0.115	0.167	0.233
118	R12T100	100% Taft N21E	2LD	4.40	0.162	16.47	74.22	0.135	0.266	0.373
119	R12E50	50% Elcentro S00E	2LD	4.40	0.162	13.29	83.19	0.208	0.343	0.486
120	R12M100	100% Miyagi-Ken-Oki EW	2LD	4.40	0.162	12.17	53.82	0.105	0.212	0.301
121	R12H75	75% Hachinohe NS	2LD	4.40	0.162	22.11	86.28	0.159	0.212	0.282
122	R12P25	25% Pacoima Dam S74W	2LD	4.40	0.162	6.66	54.13	0.142	0.354	0.497
123	R12T150	150% Taft N21E	2LD	4.40	0.162	24.88	111.13	0.191	0.407	0.579
124	R12E75	75% Elcentro S00E	2LD	4.40	0.162	20.35	127.00	0.313	0.452	0.715
125	R12M150	150% Miyagi-Ken-Oki EW	2LD	4.40	0.162	18.28	80.80	0.151	0.331	0.477
126	R12H100.2	100% Hachinohe NS	2LD	4.40	0.162	29.46	114.54	0.199	0.277	0.393
127	R121N30	30% Northridge (Newhall 90)	2LD	4.40	0.162	13.27	92.63	0.147	0.295	0.415
128	R122N20	20% Northridge (Newhall 360)	2LD	4.40	0.162	12.20	90.57	0.155	0.262	0.365
129	R12Y30	30% Northridge (Sylmar 90)	2LD	4.40	0.162	16.06	98.74	0.161	0.307	0.436
130	R12LN10	100% Eilat NS	2LD	4.40	0.162	10.79	49.45	0.066	0.126	0.174
131	R12LE10	100% Eilat EW	2LD	4.40	0.162	13.64	53.42	0.079	0.156	0.217
132	R12LN20	200% Eilat NS	2LD	4.40	0.162	21.84	100.57	0.119	0.270	0.382
133	R12LE20	200% Eilat EW	2LD	4.40	0.162	27.29	106.52	0.156	0.317	0.454

DMP = No. of Dampers
2LD = 2 Linear Dampers

Table 5-III **Summary of Experimental Results for Single Story Frame with Two Nonlinear Dampers**

Test No.	File Name	Excitation	DMP	Maximum Table Motion			Peak Shear Force / Total Weight	Peak Drift / Height (%)
				Displacement (mm)	Velocity (mm/sec)	Acceleration (g)		
149A	N10WN1.1	White Noise	2ND	4.42	26.11	0.051	0.045	0.045
150	N10WN2.1	White Noise	2ND	8.88	53.34	0.091	0.101	0.112
151	N12WN3.1	White Noise	2ND	10.37	62.23	0.103	0.119	0.138
152	N12T100	100% Taft N21E	2ND	16.37	75.17	0.135	0.222	0.282
153	N12E50	50% Elcentro S00E	2ND	13.31	83.66	0.202	0.275	0.374
154	N12M100	100% Miyagi-Ken-Oki EW	2ND	12.34	59.45	0.107	0.179	0.211
155	N12H75	75% Hachinohe NS	2ND	21.96	88.98	0.146	0.195	0.233
156	N12P25	25% Pacoima Dam S74W	2ND	6.73	53.10	0.164	0.287	0.371
157	N12T150	150% Taft N21E	2ND	24.77	112.71	0.191	0.353	0.472
158	N12E75	75% Elcentro S00E	2ND	19.95	123.35	0.302	0.412	0.600
159	N12M150	150% Miyagi-Ken-Oki EW	2ND	18.49	89.14	0.154	0.282	0.363
160	N12H100	100% Hachinohe NS	2ND	29.36	118.59	0.184	0.273	0.341
161	N121N30	30% Northridge (Newhall) 90	2ND	13.08	87.87	0.154	0.260	0.333
162	N122N20	20% Northridge (Newhall) 360	2ND	12.24	88.82	0.150	0.213	0.270
163	N12Y30	30% Northridge (Sylmar) 90	2ND	15.88	97.47	0.161	0.239	0.305
164	N12LN10	100% Eilat NS	2ND	10.85	50.72	0.067	0.116	0.124
165	N12LE10	100% Eilat EW	2ND	13.46	55.56	0.099	0.149	0.170
166	N12LN20	200% Eilat NS	2ND	21.97	102.47	0.146	0.245	0.301
167	N12LE20	200% Eilat EW	2ND	27.03	110.97	0.192	0.300	0.386

DMP = No. of Dampers
2ND = 2 Nonlinear Dampers

Table 5-IV Summary of Experimental Results of Preliminary Tests for 3 Story Frame (Prior to Repair with 16 Tapered Plates)

Test	File			System Parameters		Maximum Table Motion			Peak Accelerations (g)		
No.	Name	Excitation	DMP	Frequency (Hz)	Damping	Displacement (mm)	Velocity (mm/sec)	Acceleration (g)	1st Floor	2nd Floor	3rd Floor
1	B30WN2.1	White Noise	0	2.15	0.037	5.61	33.50	0.061	0.158	0.207	0.302
2	ELCENO	10% Elcentro S00E	0	2.15	0.037	2.84	20.32	0.048	0.064	0.112	0.136
3	B30E33	33% Elcentro S00E	0	2.15	0.037	8.86	59.54	0.126	0.204	0.355	0.431
4	B30E50	50% Elcentro S00E	0	2.15	0.037	13.41	90.81	0.185	0.359	0.460	0.600
5	B30T75	75% Taft N21E	0	2.15	0.037	12.47	54.13	0.100	0.210	0.320	0.398
6	B30T100	100% Taft N21E	0	2.15	0.037	16.79	72.95	0.133	0.277	0.410	0.512
7	B30M75	75% Miyagi-Ken-Oki EW	0	2.15	0.037	9.40	47.14	0.098	0.198	0.236	0.303
8	B30M100	100% Miyagi-Ken-Oki EW	0	2.15	0.037	12.70	63.27	0.134	0.263	0.303	0.410
9	B30H50	50% Hachinohe NS	0	2.15	0.037	14.50	58.19	0.127	0.155	0.265	0.328
10	B30P25	25% Pacoima Dam S74W	0	2.15	0.037	6.88	57.23	0.147	0.297	0.323	0.440
Two Linear Dampers Added at First Story											
11	L32WN.5	White Noise	2 LD	2.16	0.078	5.82	29.13	0.058	0.083	0.113	0.152
12	FR1.1	Sinusoidal (F=1Hz)	2 LD	2.16	0.078	6.37	41.20	0.126	0.101	0.102	0.126
13	FR15.2	Sinusoidal (F=1.5Hz)	2 LD	2.16	0.078	6.66	63.02	0.181	0.165	0.214	0.251
14	FR2.2	Sinusoidal (F=2Hz)	2 LD	2.16	0.078	2.79	36.43	0.094	0.194	0.310	0.389
15	FR25.1	Sinusoidal (F=2.5Hz)	2 LD	2.16	0.078	2.33	35.40	0.122	0.118	0.186	0.313
16	FR15.3	Sinusoidal (F=1.5Hz)	2 LD	2.16	0.078	4.03	38.42	0.118	0.098	0.135	0.156

DMP = No. of Dampers
2LD = Two Linear Dampers at the 1st Story

Table 5-IV Summary of Experimental Results of Preliminary Tests for 3 Story Frame (Prior to Repair with 16 Tapered Plates) (Continued)

Test	File			System Parameters		Peak Shear Force/Total Weight			Peak Drift/Height (%)		
No.	Name	Excitation	DMP	Frequency (Hz)	Damping	1st Story	2nd Story	3rd Story	1st Story	2nd Story	3rd Story
1	B30WN2.1	White Noise	0	2.15	0.037	0.162	0.140	0.101	0.431	0.683	0.541
2	ELCENO	10% Elcentro S00E	0	2.15	0.037	0.098	0.078	0.045	0.264	0.391	0.264
3	B30E33	33% Elcentro S00E	0	2.15	0.037	0.299	0.236	0.144	0.845	1.225	0.811
4	B30E50	50% Elcentro S00E	0	2.15	0.037	0.407	0.335	0.200	1.236	1.777	1.181
5	B30T75	75% Taft N21E	0	2.15	0.037	0.252	0.209	0.133	0.711	1.085	0.735
6	B30T100	100% Taft N21E	0	2.15	0.037	0.312	0.268	0.171	0.911	1.398	0.960
7	B30M75	75% Miyagi-Ken-Oki EW	0	2.15	0.037	0.180	0.160	0.101	0.515	0.790	0.545
8	B30M100	100% Miyagi-Ken-Oki EW	0	2.15	0.037	0.241	0.212	0.137	0.693	1.063	0.739
9	B30H50	50% Hachinohe NS	0	2.15	0.037	0.223	0.180	0.109	0.619	0.938	0.617
10	B30P25	25% Pacoima Dam S74W	0	2.15	0.037	0.245	0.192	0.146	0.643	0.981	0.681
Two Linear Dampers Added at First Story											
11	L32WN.5	White Noise	2 LD	2.16	0.078	0.077	0.068	0.051	0.214	0.352	0.271
12	FR1.1	Sinusoidal (F=1Hz)	2 LD	2.16	0.078	0.081	0.060	0.042	0.214	0.289	0.219
13	FR15.2	Sinusoidal (F=1.5Hz)	2 LD	2.16	0.078	0.193	0.149	0.084	0.514	0.763	0.484
14	FR2.2	Sinusoidal (F=2Hz)	2 LD	2.16	0.078	0.289	0.225	0.130	0.800	1.200	1.602
15	FR25.1	Sinusoidal (F=2.5Hz)	2 LD	2.16	0.078	0.171	0.166	0.104	0.484	0.828	0.598
16	FR15.3	Sinusoidal (F=1.5Hz)	2 LD	2.16	0.078	0.117	0.089	0.052	0.312	0.456	0.296

DMP = No. of Dampers
2LD = Two Linear Dampers at the 1st Story

Table 5-IV Summary of Experimental Results of Preliminary Tests for 3 Story Frame (Prior to Repair with 16 Tapered Plates) (Continued)

Test	File			System Parameters		Maximum Table Motion			Peak Accelerations (g)		
No.	Name	Excitation	DMP	Frequency (Hz)	Damping	Displacement (mm)	Velocity (mm/sec)	Acceleration (g)	1st Floor	2nd Floor	3rd Floor
17*	FR2.3	Sinusoidal (F=2Hz)	2 LD	2.16	0.078	3.38	44.21	0.121	0.253	0.395	0.519
18	FR25.2	Sinusoidal (F=2.5Hz)	2 LD	2.16	0.078	3.44	53.50	0.178	0.211	0.297	0.386
Dampers Removed											
19	B30WNC	White Noise	0	2.14	0.022	3.65	22.15	0.050	0.111	0.155	0.208
20	B30S05	Sinusoidal (F=0.5Hz)	0	2.14	0.022	2.50	8.65	0.028	0.028	0.028	0.033
21	B30S10	Sinusoidal (F=1Hz)	0	2.14	0.022	2.53	17.22	0.049	0.060	0.066	0.067
22	B30S15	Sinusoidal (F=1.5Hz)	0	2.14	0.022	2.64	26.75	0.074	0.106	0.124	0.142
23	B30S20	Sinusoidal (F=2Hz)	0	2.14	0.022	1.78	23.18	0.048	0.185	0.342	0.426
24	B30S25	Sinusoidal (F=2.5Hz)	0	2.14	0.022	2.33	35.80	0.122	0.131	0.232	0.329
25	B30S30	Sinusoidal (F=3Hz)	0	2.14	0.022	1.20	23.89	0.073	0.080	0.083	0.132
Frame Repaired Using 16 Tapered Plates											

DMP = No. of Dampers
2LD = Two Linear Dampers at the 1st Story
* Caused Cracking

Table 5-IV Summary of Experimental Results of Preliminary Tests for 3 Story Frame (Prior to Repair with 16 Tapered Plates) (Continued)

Test No.	File Name	Excitation	DMP	System Parameters		Peak Shear Force/Total Weight			Peak Drift/Height (%)		
				Frequency (Hz)	Damping	1st Story	2nd Story	3rd Story	1st Story	2nd Story	3rd Story
17*	FR2.3	Sinusoidal (F=2Hz)	2 LD	2.16	0.078	0.365	0.292	0.173	1.070	1.598	1.034
18	FR25.2	Sinusoidal (F=2.5Hz)	2 LD	2.16	0.078	0.255	0.226	0.129	0.741	1.186	0.774
Dampers Removed											
19	B30WNC	White Noise	0	2.14	0.022	0.117	0.100	0.069	0.337	0.515	0.380
20	B30S05	Sinusoidal (F=0.5Hz)	0	2.14	0.022	0.018	0.013	0.011	0.048	0.056	0.050
21	B30S10	Sinusoidal (F=1Hz)	0	2.14	0.022	0.037	0.028	0.022	0.113	0.134	0.109
22	B30S15	Sinusoidal (F=1.5Hz)	0	2.14	0.022	0.099	0.075	0.047	0.282	0.384	0.265
23	B30S20	Sinusoidal (F=2Hz)	0	2.14	0.022	0.298	0.250	0.142	0.889	1.326	0.859
24	B30S25	Sinusoidal (F=2.5Hz)	0	2.14	0.022	0.198	0.173	0.110	0.588	0.928	0.630
25	B30S30	Sinusoidal (F=3Hz)	0	2.14	0.022	0.048	0.054	0.044	0.151	0.275	0.222
Frame Repaired Using 16 Tapered Plates											

DMP = No. of Dampers
2LD = Two Linear Dampers at the 1st Story
* Caused Cracking

2. To observe whether parts of the frame suffered fatigue due to the large number of tests conducted on the frame in previous studies.

3. To verify the ability of the shaking table (with table structure interaction included) to reproduce the input motion to a satisfactory degree of accuracy.

4. To assure that no torsional movement of the structure takes place, and

5. To gain experience regarding shaking table operation and data acquisition and reduction process.

Following conclusion of the preliminary tests, the frame was repaired using 16 tapered plates (see Section 3) and the main set of tests was conducted. Table 5-V summarizes the results of the tests conducted on the frame after its repair with 16 tapered plates (repaired frame). Tables 5-VI through 5-XI summarize the results of the tests with two linear dampers at the second story, four linear dampers at the second and third stories (two at each story), six linear dampers at all stories (two at each story), two nonlinear dampers at the second story, four nonlinear dampers at the second and third story (two at each story), and six nonlinear dampers at all stories (two at each story). In these tables, the presented results include the structural parameters (first mode frequency and damping ratio), the maximum table displacement, velocity and acceleration, and the maximum story accelerations. Furthermore, the tables include the maximum shear force of each story normalized by the total structural weight (28135 N) and the peak story drift normalized by the story height (813 mm for the first story and 762 mm for the second and third stories).

Table 5-V **Summary of Experimental Results for 3 Story Repaired Frame**

Test No.	File Name	Excitation	DMP	System Parameters		Maximum Table Motion			Peak Accelerations (g)		
				Freq. Hz	Damping	Displacement (mm)	Velocity (mm/sec)	Acceleration (g)	1st Floor	2nd Floor	3rd Floor
26	B30WNR.1	White Noise	0	2.28	0.027	N/A	N/A	0.073	0.169	0.200	0.254
27	R30T75.1	150% Taft N21E	0	2.28	0.027	20.39	99.30	0.238	0.351	0.483	0.594
28	R30T75.2	75% Taft N21E	0	2.28	0.027	12.43	54.45	0.111	0.225	0.355	0.458
29	R30H50	50% Hachinohe NS	0	2.28	0.027	13.98	57.47	0.124	0.180	0.254	0.342
30	R30M75	75% Miyagi-Ken-Oki EW	0	2.28	0.027	9.34	45.64	0.111	0.160	0.237	0.314
31	R30P25	25% Pacoima Dam S74W	0	2.28	0.027	6.65	55.64	0.133	0.296	0.384	0.444
32	R30E20	20% Elcentro S00E	0	2.28	0.027	5.15	37.23	0.080	0.132	0.219	0.269
33	R30S10	Sinusoidal (F=1Hz)	0	2.28	0.027	3.81	25.64	0.064	0.074	0.100	0.094
34	R30S15	Sinusoidal (F=1.5Hz)	0	2.28	0.027	2.57	26.27	0.073	0.094	0.113	0.133
35	R30S30	Sinusoidal (F=3Hz)	0	2.28	0.027	1.11	22.46	0.069	0.074	0.091	0.147
36	R30WNR	White Noise	0	2.28	0.027	5.76	34.29	0.066	0.156	0.186	0.223
111	R301N20	20% Northridge (Newhall 90)	0	2.28	0.027	8.77	62.23	0.114	0.222	0.209	0.312
112	R302N15	15% Northridge (Newhall 360)	0	2.28	0.027	9.34	55.80	0.111	0.185	0.232	0.322
113	R30Y20	20% Northridge (Sylmar 90)	0	2.28	0.027	10.07	59.45	0.092	0.172	0.291	0.395
114	R30LN10	100% Eilat NS	0	2.28	0.027	10.84	50.64	0.080	0.147	0.192	0.214
115	R30LE10	100% Eilat EW	0	2.28	0.027	13.25	56.20	0.081	0.170	0.204	0.278
168	R30WNR2	White Noise	0	2.28	0.027	5.39	33.26	0.067	0.162	0.174	0.209
241	R30T100	100% Taft N21E	0	2.28	0.027	16.59	72.79	0.148	0.425	0.551	0.662
242	R30E33	33% Elcentro S00E	0	2.28	0.027	8.58	63.58	0.131	0.213	0.349	0.452
243	R301N30	30% Northridge (Newhall 90)	0	2.28	0.027	13.07	79.29	0.146	0.254	0.332	0.452
244	R30WNF	White Noise	0	2.28	0.027	5.77	33.81	0.066	0.169	0.204	0.239

DMP = No. of Dampers

Table 5-V **Summary of Experimental Results for 3 Story Repaired Frame (Continued)**

Test No.	File Name	Excitation	DMP	System Parameters Freq. Hz	System Parameters Damping	Peak Shear Force/Total Weight 1st Story	Peak Shear Force/Total Weight 2nd Story	Peak Shear Force/Total Weight 3rd Story	Peak Drift/Height (%) 1st Story	Peak Drift/Height (%) 2nd Story	Peak Drift/Height (%) 3rd Story
26	B30WNR.1	White Noise	0	2.28	0.027	0.150	0.129	0.085	N/A	N/A	0.406
27	R30T75.1	150% Taft N21E	0	2.28	0.027	0.384	0.328	0.198	1.035	1.497	1.065
28	R30T75.2	75% Taft N21E	0	2.28	0.027	0.294	0.251	0.153	0.778	1.113	0.784
29	R30H50	50% Hachinohe NS	0	2.28	0.027	0.235	0.193	0.114	0.604	0.858	0.598
30	R30M75	75% Miyagi-Ken-Oki EW	0	2.28	0.027	0.180	0.150	0.105	0.468	0.673	0.510
31	R30P25	25% Pacoima Dam S74W	0	2.28	0.027	0.278	0.235	0.148	0.685	0.982	0.697
32	R30E20	20% Elcentro S00E	0	2.28	0.027	0.188	0.152	0.090	0.467	0.646	0.460
33	R30S10	Sinusoidal (F=1Hz)	0	2.28	0.027	0.056	0.043	0.031	0.134	0.187	0.151
34	R30S15	Sinusoidal (F=1.5Hz)	0	2.28	0.027	0.088	0.068	0.044	0.212	0.280	0.218
35	R30S30	Sinusoidal (F=3Hz)	0	2.28	0.027	0.068	0.074	0.049	0.179	0.302	0.235
36	R30WNR	White Noise	0	2.28	0.027	0.137	0.115	0.074	0.341	0.494	0.361
111	R301N20	20% Northridge (Newhall) 90	0	2.28	0.027	0.163	0.153	0.104	0.413	0.640	0.506
112	R302N15	15% Northridge (Newhall) 360	0	2.28	0.027	0.175	0.138	0.107	0.432	0.598	0.497
113	R30Y20	20% Northridge (Sylmar) 90	0	2.28	0.027	0.253	0.217	0.132	0.653	0.942	0.675
114	R30LN10	100% Eilat NS	0	2.28	0.027	0.121	0.094	0.071	0.295	0.404	0.336
115	R30LE10	100% Eilat EW	0	2.28	0.027	0.163	0.116	0.093	0.395	0.512	0.410
168	R30WNR2	White Noise	0	2.28	0.027	0.131	0.105	0.070	0.319	0.429	0.325
241	R30T100	100% Taft N21E	0	2.28	0.027	0.440	0.353	0.221	1.058	1.514	1.129
242	R30E33	33% Elcentro S00E	0	2.28	0.027	0.301	0.242	0.151	0.755	1.061	0.773
243	R301N30	30% Northridge (Newhall) 90	0	2.28	0.027	0.248	0.194	0.151	0.622	0.858	0.695
244	R30WNF	White Noise	0	2.28	0.027	0.143	0.105	0.080	0.341	0.455	0.360

DMP = No. of Dampers

Table 5-VI Summary of Experimental Results for 3-Story Repaired Frame with Two Linear Dampers at the 2nd Story

Test No.	File Name	Excitation	DMP	System Parameters		Maximum Table Motion			Peak Accelerations (g)		
				Freq. Hz	Damping	Displacement (mm)	Velocity (mm/sec)	Acceleration (g)	1st Floor	2nd Floor	3rd Floor
37	L232WN.5	White Noise	2LD	2.33	0.132	5.83	34.21	0.069	0.120	0.103	0.138
38	L232WN.6	White Noise	2LD	2.33	0.132	11.84	68.98	0.129	0.218	0.206	0.273
39	L232T75	75% Taft N21E	2LD	2.33	0.132	12.26	54.37	0.113	0.145	0.170	0.275
40	L232H50	50% Hachinohe NS	2LD	2.33	0.132	14.54	58.10	0.125	0.157	0.165	0.217
41	L232M75	75% Miyagi-Ken-Oki EW	2LD	2.33	0.132	9.24	42.55	0.106	0.114	0.129	0.159
42	L232P25	25% Pacoima Dam S74W	2LD	2.33	0.132	6.73	55.72	0.156	0.192	0.185	0.227
43	L232E20	20% Elcentro S00E	2LD	2.33	0.132	5.85	35.48	0.079	0.084	0.099	0.149
44	L232S10	Sinusoidal (F=1Hz)	2LD	2.33	0.132	3.79	24.84	0.073	0.059	0.056	0.082
45	L232S15	Sinusoidal (F=1.5Hz)	2LD	2.33	0.132	2.53	25.64	0.072	0.076	0.072	0.104
46	L232S30	Sinusoidal (F=3Hz)	2LD	2.33	0.132	1.11	21.75	0.072	0.070	0.090	0.122
106	L321N30	30% Northridge (Newhall 90)	2LD	2.33	0.132	13.24	91.52	0.159	0.293	0.252	0.382
107	L322N20	20% Northridge (Newhall 360)	2LD	2.33	0.132	12.46	75.57	0.141	0.240	0.290	0.326
108	L32Y30	30% Northridge (Sylmar 90)	2LD	2.33	0.132	15.61	95.96	0.142	0.169	0.247	0.274
109	L32LN10	100% Eilat NS	2LD	2.33	0.132	10.83	49.69	0.072	0.102	0.084	0.122
110	L32LE10	100% Eilat EW	2LD	2.33	0.132	13.40	57.15	0.077	0.138	0.120	0.193

2LD = 2 Linear Dampers

Table 5-VI Summary of Experimental Results for 3-Story Repaired Frame with Two Linear Dampers at the 2nd Story (Continued)

Test No.	File Name	Excitation	DMP	System Parameters		Peak Shear Force/Total Weight			Peak Drift/Height (%)		
				Freq. Hz	Damping	1st Story	2nd Story	3rd Story	1st Story	2nd Story	3rd Story
37	L232WN.5	White Noise	2LD	2.33	0.132	0.071	0.048	0.046	0.146	0.183	0.185
38	L232WN.6	White Noise	2LD	2.33	0.132	0.147	0.104	0.091	0.306	0.413	0.383
39	L232T75	75% Taft N21E	2LD	2.33	0.132	0.126	0.127	0.092	0.300	0.488	0.406
40	L232H50	50% Hachinohe NS	2LD	2.33	0.132	0.143	0.106	0.072	0.308	0.413	0.360
41	L232M75	75% Miyagi-Ken-Oki EW	2LD	2.33	0.132	0.095	0.073	0.053	0.220	0.300	0.234
42	L232P25	25% Pacoima Dam S74W	2LD	2.33	0.132	0.132	0.113	0.076	0.291	0.435	0.348
43	L232E20	20% Elcentro S00E	2LD	2.33	0.132	0.079	0.067	0.050	0.186	0.260	0.216
44	L232S10	Sinusoidal (F=1Hz)	2LD	2.33	0.132	0.038	0.029	0.027	0.080	0.118	0.111
45	L232S15	Sinusoidal (F=1.5Hz)	2LD	2.33	0.132	0.052	0.041	0.035	0.116	0.147	0.142
46	L232S30	Sinusoidal (F=3Hz)	2LD	2.33	0.132	0.073	0.059	0.041	0.165	0.226	0.182
106	L321N30	30% Northridge (Newhall 90)	2LD	2.33	0.132	0.191	0.168	0.127	0.416	0.643	0.583
107	L322N20	20% Northridge (Newhall 360)	2LD	2.33	0.132	0.221	0.167	0.109	0.497	0.640	0.506
108	L32Y30	30% Northridge (Sylmar 90)	2LD	2.33	0.132	0.229	0.173	0.091	0.526	0.690	0.492
109	L32LN10	100% Eilat NS	2LD	2.33	0.132	0.050	0.039	0.041	0.106	0.149	0.150
110	L32LE10	100% Eilat EW	2LD	2.33	0.132	0.087	0.086	0.064	0.204	0.327	0.282

2LD = 2 Linear Dampers

Table 5-VII Summary of Experimental Results for 3-Story Repaired Frame with Four Linear Dampers at 2nd and 3rd Stories

Test No.	File Name	Excitation	DMP	System Parameters Freq. Hz	System Parameters Damping	Maximum Table Motion Displacement (mm)	Maximum Table Motion Velocity (mm/sec)	Maximum Table Motion Acceleration (g)	Peak Accelerations (g) 1st Floor	Peak Accelerations (g) 2nd Floor	Peak Accelerations (g) 3rd Floor
47	L34WN.1	White Noise	4LD	2.35	0.163	5.93	34.37	0.070	0.062	0.060	0.072
48	L34WN.2	White Noise	4LD	2.35	0.163	11.87	69.53	0.129	0.125	0.129	0.149
49	L34T75	75% Taft N21E	4LD	2.35	0.163	12.24	53.10	0.108	0.114	0.138	0.183
50	L34N75	75% Miyagi-Ken-Oki EW	4LD	2.35	0.163	9.19	42.15	0.091	0.076	0.089	0.111
51	L34H50	50% Hachinohe NS	4LD	2.35	0.163	14.65	58.58	0.115	0.129	0.143	0.156
52	L34P25	25% Pacoima Dam S74W	4LD	2.35	0.163	6.76	55.72	0.139	0.139	0.138	0.167
53	L34E20	20% Elcentro S00E	4LD	2.35	0.163	5.18	33.97	0.081	0.108	0.104	0.123
54	L34S10	Sinusoidal (F=1Hz)	4LD	2.35	0.163	3.77	24.21	0.068	0.054	0.045	0.047
55	L34S15	Sinusoidal (F=1.5Hz)	4LD	2.35	0.163	2.55	25.08	0.072	0.059	0.056	0.056
56	L34S30	Sinusoidal (F=3Hz)	4LD	2.35	0.163	5.67	104.50	0.335	0.269	0.373	0.506
57	L34T100	100% Taft N21E	4LD	2.35	0.163	16.47	71.44	0.136	0.148	0.194	0.247
58	L34M100	100% Miyagi-Ken-Oki EW	4LD	2.35	0.163	12.21	56.12	0.125	0.112	0.120	0.152
59	L34H75	75% Hachinohe NS	4LD	2.35	0.163	21.92	86.68	0.162	0.191	0.215	0.236
60	L34P40	40% Pacoima Dam S74W	4LD	2.35	0.163	10.70	88.50	0.222	0.203	0.222	0.272
61	L34E33	33% Elcentro S00E	4LD	2.35	0.163	8.76	57.07	0.125	0.166	0.165	0.200
62	L34E50	50% Elcentro S00E	4LD	2.35	0.163	13.44	87.00	0.179	0.231	0.236	0.299
63	L34T150	150% Taft N21E	4LD	2.35	0.163	24.77	108.59	0.197	0.209	0.293	0.374
64	L34E75	75% Elcentro S00E	4LD	2.35	0.163	19.98	130.81	0.262	0.326	0.338	0.442
65	L34T200	200% Taft N21E	4LD	2.35	0.163	33.07	143.51	0.251	0.279	0.395	0.494

4LD = 4 Linear Dampers

Table 5-VII Summary of Experimental Results for 3-Story Repaired Frame with Four Linear Dampers at 2nd and 3rd Stories (Continued)

Test No.	File Name	Excitation	DMP	System Parameters Freq. Hz	System Parameters Damping	Peak Shear Force/Total Weight 1st Story	Peak Shear Force/Total Weight 2nd Story	Peak Shear Force/Total Weight 3rd Story	Peak Drift/Height (%) 1st Story	Peak Drift/Height (%) 2nd Story	Peak Drift/Height (%) 3rd Story
47	L34WN.1	White Noise	4LD	2.35	0.163	0.054	0.040	0.024	0.116	0.139	0.070
48	L34WN.2	White Noise	4LD	2.35	0.163	0.114	0.089	0.050	0.251	0.326	0.190
49	L34T75	75% Taft N21E	4LD	2.35	0.163	0.124	0.103	0.061	0.287	0.368	0.221
50	L34N75	75% Miyagi-Ken-Oki EW	4LD	2.35	0.163	0.079	0.064	0.037	0.181	0.226	0.125
51	L34H50	50% Hachinohe NS	4LD	2.35	0.163	0.130	0.096	0.052	0.287	0.339	0.238
52	L34P25	25% Pacoima Dam S74W	4LD	2.35	0.163	0.128	0.099	0.056	0.285	0.355	0.210
53	L34E20	20% Elcentro S00E	4LD	2.35	0.163	0.078	0.068	0.041	0.167	0.209	0.120
54	L34S10	Sinusoidal (F=1Hz)	4LD	2.35	0.163	0.035	0.028	0.016	0.076	0.103	0.041
55	L34S15	Sinusoidal (F=1.5Hz)	4LD	2.35	0.163	0.046	0.034	0.019	0.103	0.130	0.058
56	L34S30	Sinusoidal (F=3Hz)	4LD	2.35	0.163	0.325	0.285	0.169	0.763	1.012	0.672
57	L34T100	100% Taft N21E	4LD	2.35	0.163	0.173	0.140	0.082	0.396	0.510	0.315
58	L34M100	100% Miyagi-Ken-Oki EW	4LD	2.35	0.163	0.108	0.088	0.051	0.248	0.316	0.183
59	L34H75	75% Hachinohe NS	4LD	2.35	0.163	0.194	0.144	0.079	0.432	0.522	0.357
60	L34P40	40% Pacoima Dam S74W	4LD	2.35	0.163	0.208	0.162	0.091	0.464	0.584	0.386
61	L34E33	33% Elcentro S00E	4LD	2.35	0.163	0.123	0.108	0.067	0.287	0.365	0.221
62	L34E50	50% Elcentro S00E	4LD	2.35	0.163	0.185	0.159	0.100	0.434	0.551	0.350
63	L34T150	150% Taft N21E	4LD	2.35	0.163	0.259	0.213	0.125	0.608	0.788	0.503
64	L34E75	75% Elcentro S00E	4LD	2.35	0.163	0.276	0.237	0.147	0.658	0.826	0.531
65	L34T200	200% Taft N21E	4LD	2.35	0.163	0.352	0.287	0.165	0.824	1.063	0.670

4LD = 4 Linear Dampers

Table 5-VII Summary of Experimental Results for 3-Story Repaired Frame with Four Linear Dampers at 2nd and 3rd Stories (Continued)

Test No.	File Name	Excitation	DMP	System Parameters		Maximum Table Motion			Peak Accelerations (g)		
				Freq. Hz	Damping	Displacement (mm)	Velocity (mm/sec)	Acceleration (g)	1st Floor	2nd Floor	3rd Floor
66	L34E100	100% Elcentro S00E	4LD	2.35	0.163	26.80	174.70	0.343	0.405	0.438	0.590
99	L341N30	30% Northridge (Newhall 90)	4LD	2.35	0.163	13.44	89.93	0.168	0.155	0.199	0.254
100	L342N20	20% Northridge (Newhall 360)	4LD	2.35	0.163	12.36	79.61	0.138	0.173	0.235	0.291
101	L34Y30	30% Northridge (Sylmar 90)	4LD	2.35	0.163	15.74	96.84	0.143	0.171	0.206	0.250
102	L34LN10	100% Eilat NS	4LD	2.35	0.163	10.84	49.21	0.063	0.059	0.059	0.073
103	L34LE10	100% Eilat EW	4LD	2.35	0.163	13.49	57.39	0.076	0.091	0.110	0.135
104	L34LN20	200% Eilat NS	4LD	2.35	0.163	21.87	98.66	0.130	0.097	0.122	0.146
105	L34LE20	200% Eilat EW	4LD	2.35	0.163	26.90	115.81	0.158	0.156	0.219	0.282

4LD = 4 Linear Dampers

Table 5-VII Summary of Experimental Results for 3-Story Repaired Frame with Four Linear Dampers at 2nd and 3rd Stories (Continued)

Test No.	File Name	Excitation	DMP	System Parameters		Peak Shear Force/Total Weight			Peak Drift/Height (%)		
				Freq. Hz	Damping	1st Story	2nd Story	3rd Story	1st Story	2nd Story	3rd Story
66	L34E100	100% Elcentro S00E	4LD	2.35	0.163	0.365	0.311	0.197	0.873	1.104	0.710
99	L341N30	30% Northridge (Newhall 90)	4LD	2.35	0.163	0.191	0.151	0.085	0.432	0.554	0.373
100	L342N20	20% Northridge (Newhall 360)	4LD	2.35	0.163	0.214	0.171	0.097	0.478	0.615	0.416
101	L34Y30	30% Northridge (Sylmar 90)	4LD	2.35	0.163	0.194	0.151	0.083	0.447	0.564	0.369
102	L34LN10	100% Eilat NS	4LD	2.35	0.163	0.050	0.042	0.024	0.103	0.135	0.078
103	L34LE10	100% Eilat EW	4LD	2.35	0.163	0.094	0.079	0.045	0.210	0.270	0.150
104	L34LN20	200% Eilat NS	4LD	2.35	0.163	0.099	0.084	0.049	0.215	0.290	0.173
105	L34LE20	200% Eilat EW	4LD	2.35	0.163	0.196	0.164	0.094	0.451	0.578	0.358

4LD = 4 Linear Dampers

Table 5-VIII **Summary of Experimental Results for 3-Story Repaired Frame with Six Linear Dampers**

Test No.	File Name	Excitation	DMP	System Parameters Freq. Hz	System Parameters Damping	Maximum Table Motion Displacement (mm)	Maximum Table Motion Velocity (mm/sec)	Maximum Table Motion Acceleration (g)	Peak Accelerations (g) 1st Floor	Peak Accelerations (g) 2nd Floor	Peak Accelerations (g) 3rd Floor
67	L36WN.1	White Noise	6LD	2.33	0.231	11.80	70.25	0.130	0.119	0.116	0.128
68	L36WN.2	White Noise	6LD	2.33	0.231	17.76	103.66	0.181	0.174	0.174	0.208
69	L36T75	75% Taft N21E	6LD	2.33	0.231	12.18	54.13	0.116	0.107	0.114	0.145
70	L36M75	75% Miyagi-Ken-Oki EW	6LD	2.33	0.231	9.12	42.31	0.090	0.085	0.084	0.101
71	L36H50	50% Hachinohe NS	6LD	2.33	0.231	14.61	58.42	0.118	0.122	0.125	0.138
72	L36P25	25% Pacoima Dam S74W	6LD	2.33	0.231	6.75	55.40	0.137	0.117	0.124	0.155
73	L36E20	20% Elcentro S00E	6LD	2.33	0.231	5.21	33.73	0.089	0.091	0.086	0.104
74	L36T100	100% Taft N21E	6LD	2.33	0.231	16.48	71.44	0.139	0.134	0.160	0.197
75	L36M100	100% Miyagi-Ken-Oki EW	6LD	2.33	0.231	12.22	56.75	0.123	0.104	0.114	0.136
76	L36H75	75% Hachinohe NS	6LD	2.33	0.231	21.99	86.99	0.162	0.179	0.191	0.214
77	L36P40	40% Pacoima Dam S74W	6LD	2.33	0.231	10.70	87.95	0.216	0.188	0.202	0.246
78	L36E33	33% Elcentro S00E	6LD	2.33	0.231	8.75	56.12	0.139	0.136	0.135	0.169
79	L36E50	50% Elcentro S00E	6LD	2.33	0.231	13.43	86.60	0.199	0.191	0.200	0.259
80	L36T150	150% Taft N21E	6LD	2.33	0.231	24.57	108.90	0.190	0.196	0.246	0.304
81	L36E75	75% Elcentro S00E	6LD	2.33	0.231	19.98	130.25	0.285	0.280	0.293	0.385
82	L36T200	200% Taft N21E	6LD	2.33	0.231	33.07	143.11	0.253	0.258	0.341	0.419
83	L36E100	100% Elcentro S00E	6LD	2.33	0.231	26.71	174.23	0.360	0.348	0.383	0.522
84	L361N30	30% Northridge (Newhall 90)	6LD	2.33	0.231	13.17	90.96	0.168	0.143	0.179	0.225

6LD = 6 Linear Dampers

Table 5-VIII Summary of Experimental Results for 3-Story Repaired Frame with Six Linear Dampers (Continued)

Test No.	File Name	Excitation	DMP	System Parameters		Peak Shear Force/Total Weight			Peak Drift/Height (%)		
				Freq. Hz	Damping	1st Story	2nd Story	3rd Story	1st Story	2nd Story	3rd Story
67	L36WN.1	White Noise	6	2.33	0.231	0.105	0.076	0.043	0.209	0.263	0.174
68	L36WN.2	White Noise	6	2.33	0.231	0.158	0.123	0.069	0.342	0.422	0.276
69	L36T75	75% Taft N21E	6	2.33	0.231	0.099	0.081	0.048	0.214	0.285	0.171
70	L36M75	75% Miyagi-Ken-Oki EW	6	2.33	0.231	0.077	0.060	0.034	0.162	0.211	0.122
71	L36H50	50% Hachinohe NS	6	2.33	0.231	0.113	0.084	0.046	0.235	0.285	0.193
72	L36P25	25% Pacoima Dam S74W	6	2.33	0.231	0.115	0.089	0.052	0.238	0.302	0.186
73	L36E20	20% Elcentro S00E	6	2.33	0.231	0.069	0.058	0.035	0.127	0.168	0.099
74	L36T100	100% Taft N21E	6	2.33	0.231	0.146	0.118	0.066	0.313	0.406	0.251
75	L36M100	100% Miyagi-Ken-Oki EW	6	2.33	0.231	0.104	0.081	0.045	0.219	0.287	0.175
76	L36H75	75% Hachinohe NS	6	2.33	0.231	0.175	0.130	0.071	0.372	0.457	0.321
77	L36P40	40% Pacoima Dam S74W	6	2.33	0.231	0.189	0.147	0.082	0.407	0.518	0.333
78	L36E33	33% Elcentro S00E	6	2.33	0.231	0.110	0.093	0.056	0.227	0.287	0.179
79	L36E50	50% Elcentro S00E	6	2.33	0.231	0.163	0.140	0.086	0.351	0.450	0.295
80	L36T150	150% Taft N21E	6	2.33	0.231	0.225	0.182	0.101	0.493	0.645	0.416
81	L36E75	75% Elcentro S00E	6	2.33	0.231	0.241	0.209	0.128	0.544	0.686	0.451
82	L36T200	200% Taft N21E	6	2.33	0.231	0.308	0.250	0.140	0.683	0.890	0.577
83	L36E100	100% Elcentro S00E	6	2.33	0.231	0.324	0.280	0.174	0.750	0.947	0.629
84	L361N30	30% Northridge (Newhall 90)	6	2.33	0.231	0.173	0.135	0.075	0.364	0.482	0.306

6LD = 6 Linear Dampers

Table 5-VIII Summary of Experimental Results for 3-Story Repaired Frame with Six Linear Dampers (Continued)

Test No.	File Name	Excitation	DMP	System Parameters		Maximum Table Motion			Peak Accelerations (g)		
				Freq. Hz	Damping	Displacement (mm)	Velocity (mm/sec)	Acceleration (g)	1st Floor	2nd Floor	3rd Floor
85	L362N20	20% Northridge (Newhall 360)	6LD	2.33	0.231	12.39	80.33	0.132	0.165	0.213	0.260
86	L36Y30	30% Northridge (Sylmar 90)	6LD	2.33	0.231	15.72	97.16	0.141	0.158	0.180	0.211
87	L361N60	60% Northridge (Newhall 90)	6LD	2.33	0.231	24.99	175.90	0.321	0.273	0.342	0.437
88	L362N40	40% Northridge (Newhall 360)	6LD	2.33	0.231	24.13	156.92	0.227	0.308	0.404	0.502
89	L36Y60	60% Northridge (Sylmar 90)	6LD	2.33	0.231	30.35	189.55	0.274	0.277	0.350	0.425
90	L36LN10	100% Eilat NS	6LD	2.33	0.231	10.87	49.29	0.067	0.054	0.060	0.068
91	L36LE10	100% Eilat EW	6LD	2.33	0.231	13.54	57.39	0.077	0.081	0.097	0.118
92	L36LN20	200% Eilat NS	6LD	2.33	0.231	21.94	99.46	0.137	0.092	0.108	0.129
93	L36LE20	200% Eilat EW	6LD	2.33	0.231	26.94	115.41	0.159	0.149	0.200	0.250
94	L36LN30	300% Eilat NS	6LD	2.33	0.231	32.79	150.26	0.206	0.138	0.161	0.197
95	L36LE30	300% Eilat EW	6LD	2.33	0.231	40.34	171.37	0.237	0.227	0.293	0.378
96	L36*L* S10	Sinusoidal (F=1Hz)	6LD	2.33	0.231	3.72	23.89	0.066	0.049	0.041	0.037
97	L36S15	Sinusoidal (F=1.5Hz)	6LD	2.33	0.231	2.53	24.77	0.068	0.054	0.046	0.048
98	L36S30	Sinusoidal (F=3Hz)	6LD	2.33	0.231	1.14	22.78	0.069	0.081	0.083	0.096

6LD = 6 Linear Dampers

Table 5-VIII Summary of Experimental Results for 3-Story Repaired Frame with Six Linear Dampers (Continued)

Test No.	File Name	Excitation	DMP	System Parameters		Peak Shear Force/Total Weight			Peak Drift/Height (%)		
				Freq. Hz	Damping	1st Story	2nd Story	3rd Story	1st Story	2nd Story	3rd Story
85	L362N20	20% Northridge (Newhall 360)	6	2.33	0.231	0.198	0.155	0.087	0.413	0.557	0.360
86	L36Y30	30% Northridge (Sylmar 90)	6	2.33	0.231	0.170	0.130	0.070	0.360	0.492	0.305
87	L361N60	60% Northridge (Newhall 90)	6	2.33	0.231	0.331	0.260	0.146	0.702	0.953	0.629
88	L362N40	40% Northridge (Newhall 360)	6	2.33	0.231	0.375	0.294	0.167	0.796	1.070	0.737
89	L36Y60	60% Northridge (Sylmar 90)	6	2.33	0.231	0.333	0.256	0.142	0.710	0.992	0.659
90	L36LN10	100% Eilat NS	6	2.33	0.231	0.047	0.040	0.023	0.086	0.110	0.064
91	L36LE10	100% Eilat EW	6	2.33	0.231	0.084	0.069	0.039	0.176	0.238	0.121
92	L36LN20	200% Eilat NS	6	2.33	0.231	0.090	0.075	0.043	0.178	0.249	0.145
93	L36LE20	200% Eilat EW	6	2.33	0.231	0.176	0.145	0.083	0.376	0.499	0.307
94	L36LN30	300% Eilat NS	6	2.33	0.231	0.136	0.113	0.066	0.269	0.373	0.241
95	L36LE30	300% Eilat EW	6	2.33	0.231	0.266	0.221	0.126	0.570	0.751	0.482
96	L36L S10	Sinusoidal (F=1Hz)	6	2.33	0.231	0.031	0.024	0.012	0.056	0.060	0.026
97	L36S15	Sinusoidal (F=1.5Hz)	6	2.33	0.231	0.040	0.028	0.016	0.069	0.100	0.051
98	L36S30	Sinusoidal (F=3Hz)	6	2.33	0.231	0.065	0.053	0.032	0.128	0.180	0.108

6LD = 6 Linear Dampers

Table 5-IX Summary of Experimental Results for 3-Story Repaired Frame with Two Nonlinear Dampers at the 2nd Story

Test	File	Excitation	DMP	Maximum Table Motion			Peak Accelerations (g)			Peak Shear Force/Total Weight			Peak Drift/Height (%)		
No.	Name			Disp. (mm)	Velocity (mm/sec)	Acceleration (g)	1st Floor	2nd Floor	3rd Floor	1st story	2nd story	3rd story	1st Story	2nd Story	3rd Story
169	N30WN1	White Noise	2ND	5.50	33.26	0.063	0.099	0.096	0.115	0.062	0.046	0.038	0.115	0.105	0.128
170	N30WN2	White Noise	2ND	11.39	68.98	0.123	0.210	0.187	0.233	0.126	0.093	0.078	0.251	0.217	0.267
171	N32T75	75% Taft N21E	2ND	12.27	54.05	0.111	0.158	0.166	0.210	0.136	0.097	0.070	0.244	0.240	0.272
172	N32H50	50% Hachinohe NS	2ND	14.73	58.26	0.121	0.143	0.132	0.150	0.118	0.077	0.050	0.242	0.238	0.239
173	N32M75	75% Miyagi-Ken-Oki EW	2ND	9.08	41.99	0.091	0.120	0.101	0.140	0.080	0.062	0.047	0.161	0.153	0.175
174	N32P25	25% Pacoima Dam S74W	2ND	6.56	55.17	0.148	0.181	0.212	0.275	0.141	0.105	0.092	0.255	0.216	0.323
175	N32E20	20% Elcentro S00E	2ND	5.20	33.02	0.083	0.102	0.106	0.130	0.091	0.072	0.043	0.161	0.138	0.164
176	N321N30	30% Northridge (Newhall 90)	2ND	13.19	89.61	0.151	0.305	0.250	0.344	0.196	0.144	0.115	0.358	0.429	0.489
177	N322N20	20% Northridge (Newhall 360)	2ND	12.34	76.91	0.156	0.257	0.256	0.326	0.226	0.172	0.109	0.484	0.537	0.464
178	N30Y30	30% Northridge (Sylmar 90)	2ND	15.71	96.76	0.138	0.193	0.184	0.257	0.178	0.138	0.086	0.382	0.417	0.360
179	N32LN10	100% Eilat NS	2ND	10.72	49.45	0.068	0.113	0.093	0.152	0.061	0.053	0.051	0.117	0.106	0.180
180	N32LE10	100% Eilat EW	2ND	13.44	57.15	0.076	0.132	0.129	0.193	0.093	0.078	0.064	0.161	0.196	0.210
181	N32T100	100% Taft N21E	2ND	16.46	72.07	0.141	0.228	0.246	0.290	0.163	0.123	0.097	0.323	0.346	0.395
182	N32E33	33% Elcentro S00E	2ND	8.83	56.36	0.134	0.177	0.172	0.220	0.147	0.114	0.073	0.259	0.263	0.303
183	N32E50	50% Elcentro S00E	2ND	13.49	85.88	0.183	0.296	0.320	0.368	0.184	0.169	0.123	0.347	0.462	0.495

2ND = 2 Nonlinear Dampers

Table 5-X Summary of Experimental Results for 3 Story Repaired Frame with Four Nonlinear Dampers at the 2nd and 3rd Stories

Test	File			Maximum Table Motion			Peak Accelerations (g)			Peak Shear Force/Total Weight			Peak Drift/Height (%)		
No.	Name	Excitation	DMP	Disp. (mm)	Velocity (mm/sec)	Acceleration (g)	1st Floor	2nd Floor	3rd Floor	1st story	2nd story	3rd story	1st Story	2nd Story	3rd Story
184	N34WN3	White Noise	4ND	5.66	33.66	0.072	0.082	0.078	0.085	0.069	0.052	0.028	0.133	0.109	0.040
185	N34WN4	White Noise	4ND	11.46	67.95	0.129	0.175	0.143	0.176	0.133	0.101	0.059	0.251	0.222	0.111
186	N34T75	75% Taft N21E	4ND	12.24	53.98	0.108	0.145	0.163	0.167	0.136	0.099	0.056	0.249	0.201	0.099
187	N34M75	75% Miyagi-Ken-Oki EW	4ND	9.03	40.56	0.086	0.104	0.103	0.110	0.091	0.070	0.037	0.174	0.150	0.065
188	N34H50	50% Hachinohe NS	4ND	14.59	58.02	0.118	0.106	0.102	0.107	0.095	0.067	0.036	0.196	0.182	0.099
189	N34P25	25% Pacoima Dam S74W	4ND	6.66	54.53	0.141	0.187	0.206	0.191	0.158	0.126	0.064	0.284	0.228	0.100
190	N34E21	20% Elcentro S00E	4ND	5.39	32.54	0.092	0.113	0.119	0.128	0.104	0.077	0.043	0.192	0.130	0.059
191	N34T100	100% Taft N21E	4ND	16.38	72.07	0.130	0.186	0.216	0.217	0.168	0.127	0.072	0.330	0.288	0.142
192	N34M100	100% Miyagi-Ken-Oki EW	4ND	12.06	54.13	0.123	0.145	0.143	0.149	0.120	0.092	0.050	0.229	0.203	0.100
193	N34H75	75% Hachinohe NS	4ND	21.97	87.87	0.164	0.160	0.165	0.162	0.146	0.103	0.054	0.299	0.304	0.178
194	N34P40	40% Pacoima Dam S74W	4ND	10.63	88.58	0.215	0.283	0.334	0.299	0.207	0.182	0.100	0.394	0.391	0.199
195	N34E33	33% Elcentro S00E	4ND	8.83	54.61	0.137	0.196	0.191	0.206	0.168	0.126	0.069	0.307	0.243	0.114
196	N34E50	50% Elcentro S00E	4ND	13.51	83.19	0.200	0.304	0.310	0.323	0.215	0.183	0.108	0.427	0.428	0.228
197	N34T150	150% Taft N21E	4ND	24.69	108.27	0.190	0.251	0.319	0.320	0.237	0.189	0.107	0.495	0.502	0.277
198	N34E75	75% Elcentro S00E	4ND	20.04	126.21	0.292	0.345	0.415	0.474	0.304	0.255	0.158	0.634	0.705	0.444
199	N34T201	200% Taft N21E	4ND	32.85	144.07	0.248	0.307	0.368	0.463	0.319	0.262	0.154	0.675	0.754	0.445
200	N34E100	100% Elcentro S00E	4ND	26.77	169.39	0.374	0.366	0.500	0.659	0.393	0.334	0.220	0.815	0.970	0.704
201	N341N30	30% Northridge (Newhall 90)	4ND	13.12	89.22	0.150	0.229	0.255	0.250	0.195	0.153	0.083	0.397	0.388	0.203
202	N342N20	20% Northridge (Newhall 360)	4ND	12.12	80.80	0.142	0.227	0.263	0.280	0.230	0.171	0.093	0.463	0.468	0.258
203	N34Y30	30% Northridge (Sylmar 90)	4ND	15.77	97.39	0.139	0.231	0.233	0.234	0.189	0.148	0.078	0.367	0.357	0.190
204	N34LN10	100% Eilat NS	4ND	10.75	50.72	0.065	0.083	0.092	0.091	0.082	0.060	0.030	0.135	0.104	0.048
205	N34LE10	100% Eilat EW	4ND	13.53	58.10	0.074	0.095	0.107	0.121	0.101	0.075	0.040	0.183	0.170	0.063
206	N34LN20	200% Eilat NS	4ND	21.75	100.09	0.135	0.167	0.204	0.182	0.146	0.118	0.061	0.262	0.229	0.121
207	N34LE20	200% Eilat EW	4ND	26.93	115.89	0.157	0.207	0.233	0.247	0.174	0.147	0.082	0.382	0.388	0.167

4ND = 4 Nonlinear Dampers

Table 5-XI Summary of Experimental Results for 3-Story Repaired Frame with Six Nonlinear Dampers

Test	File			Maximum Table Motion			Peak Accelerations (g)			Peak Shear Force/Total Weight			Peak Drift/Height (%)		
No.	Name	Excitation	DMP	Disp. (mm)	Velocity (mm/sec)	Acceleration (g)	1st Floor	2nd Floor	3rd Floor	1st story	2nd story	3rd story	1st Story	2nd Story	3rd Story
208	N36WN2	White Noise	6ND	11.51	68.90	0.120	0.117	0.118	0.145	0.106	0.078	0.048	0.141	0.142	0.089
209	N36WN3	White Noise	6ND	17.38	100.49	0.178	0.179	0.182	0.221	0.158	0.118	0.074	0.219	0.248	0.142
210	N36T75	75% Taft N21E	6ND	12.23	55.17	0.104	0.103	0.122	0.124	0.105	0.074	0.041	0.145	0.133	0.086
211	N36M75	75% Miyagi-Ken-Oki EW	6ND	9.14	41.28	0.097	0.095	0.109	0.102	0.092	0.066	0.034	0.130	0.133	0.068
212	N36H50	50% Hachinohe NS	6ND	14.52	59.93	0.111	0.103	0.092	0.102	0.088	0.063	0.034	0.134	0.142	0.082
213	N36P25	25% Pacoima Dam S74W	6ND	6.70	53.50	0.132	0.166	0.171	0.183	0.157	0.112	0.061	0.181	0.173	0.089
214	N36E20	20% Elcentro S00E	6ND	5.16	33.60	0.089	0.088	0.091	0.096	0.081	0.058	0.032	0.100	0.083	0.036
215	N36T100	100% Taft N21E	6ND	16.34	72.79	0.128	0.141	0.172	0.170	0.144	0.100	0.057	0.189	0.185	0.116
216	N36M100	100% Miyagi-Ken-Oki EW	6ND	12.11	55.17	0.125	0.124	0.139	0.135	0.119	0.088	0.045	0.169	0.173	0.097
217	N36H75	75% Hachinohe NS	6ND	21.88	88.82	0.155	0.153	0.140	0.154	0.132	0.095	0.051	0.211	0.227	0.149
218	N36P40	40% Pacoima Dam S74W	6ND	10.67	85.96	0.230	0.250	0.303	0.275	0.205	0.176	0.092	0.282	0.322	0.170
219	N36E33	33% Elcentro S00E	6ND	8.72	55.17	0.138	0.144	0.152	0.166	0.138	0.101	0.055	0.168	0.154	0.074
220	N36E50	50% Elcentro S00E	6ND	13.45	84.14	0.196	0.226	0.234	0.242	0.197	0.146	0.081	0.251	0.278	0.153
221	N36T150	150% Taft N21E	6ND	24.62	110.57	0.186	0.196	0.278	0.264	0.198	0.148	0.088	0.298	0.333	0.178
222	N36E75	75% Elcentro S00E	6ND	19.97	127.08	0.288	0.291	0.352	0.384	0.276	0.212	0.128	0.404	0.495	0.288
223	N36T200	200% Taft N21E	6ND	32.66	143.75	0.246	0.244	0.343	0.349	0.264	0.199	0.116	0.428	0.519	0.276
224	N36E100	100% Elcentro S00E	6ND	26.71	168.91	0.352	0.352	0.436	0.530	0.363	0.285	0.177	0.572	0.746	0.488
225	N361N30	30% Northridge (Newhall 90)	6ND	13.15	89.61	0.159	0.187	0.215	0.204	0.178	0.135	0.068	0.266	0.277	0.144
226	N362N20	20% Northridge (Newhall 360)	6ND	12.33	84.69	0.131	0.179	0.201	0.200	0.173	0.125	0.067	0.281	0.284	0.150

6ND = 6 Nonlinear Dampers

Table 5-XI Summary of Experimental Results for 3-Story Repaired Frame with Six Nonlinear Dampers (Continued)

Test	File			Maximum Table Motion			Peak Accelerations (g)			Peak Shear Force/Total Weight			Peak Drift/Height (%)		
No.	Name	Excitation	DMP	Disp. (mm)	Velocity (mm/sec)	Acceleration (g)	1st Floor	2nd Floor	3rd Floor	1st story	2nd story	3rd story	1st Story	2nd Story	3rd Story
227	N36Y30	30% Northridge (Sylmar 90)	6ND	15.75	98.35	0.140	0.173	0.181	0.187	0.168	0.118	0.062	0.253	0.258	0.144
228	N361N60	60% Northridge (Newhall 90)	6ND	25.62	178.99	0.312	0.290	0.394	0.431	0.326	0.247	0.114	0.593	0.710	0.443
229	N362N40	40% Northridge (Newhall 360)	6ND	24.11	161.77	0.233	0.340	0.414	0.462	0.362	0.283	0.154	0.660	0.799	0.518
230	N36Y60	60% Northridge (Sylmar 90)	6ND	30.99	194.31	0.297	0.323	0.394	0.408	0.306	0.228	0.136	0.558	0.651	0.409
231	N36LN10	100% Eilat NS	6ND	10.79	49.93	0.065	0.070	0.073	0.086	0.070	0.049	0.029	0.083	0.082	0.038
232	N36LE10	100% Eilat EW	6ND	13.44	57.23	0.085	0.100	0.108	0.115	0.097	0.074	0.038	0.132	0.131	0.058
233	N36LN20	200% Eilat NS	6ND	21.83	100.81	0.139	0.132	0.142	0.178	0.139	0.097	0.059	0.184	0.187	0.102
234	N36LE20	200% Eilat EW	6ND	26.93	115.17	0.183	0.192	0.225	0.224	0.173	0.139	0.075	0.282	0.311	0.137
235	N36LN30	300% Eilat NS	6ND	32.63	151.61	0.200	0.192	0.243	0.245	0.183	0.147	0.082	0.279	0.297	0.173
236	N36LE30	300% Eilat EW	6ND	40.37	168.99	0.263	0.268	0.324	0.334	0.248	0.200	0.111	0.443	0.528	0.255
237	N36WN.2	White Noise	6ND	5.92	35.24	0.066	0.061	0.056	0.061	0.051	0.037	0.020	0.064	0.055	0.027
238	N36WN4	White Noise	6ND	22.98	133.83	0.225	0.219	0.257	0.269	0.191	0.155	0.090	0.300	0.356	0.200
239	N36WN5	White Noise	6ND	28.08	162.56	0.269	0.276	0.306	0.309	0.220	0.186	0.103	0.388	0.449	0.247
240	N36WN6	White Noise	6ND	33.29	192.64	0.324	0.323	0.369	0.344	0.254	0.220	0.115	0.482	0.547	0.305

6ND = 6 Nonlinear Dampers

5.3 Interpretation of Results

5.3.1 Effectiveness of the Dampers

An assessment of the effectiveness of dampers in reducing dynamic response can be made by comparison of responses of the same structure without and with dampers for the same earthquake input. To aid in this comparison, Figures 5-1 to 5-6 for the case of linear dampers and Figures 5-7 to 5-12 for the case of nonlinear dampers have been prepared. These figures compare peak response quantities of the tested 3-story structure without and with various damper configurations and for either the same level of earthquake input or two substantially different levels of input for the same earthquake motion.

These figures, in general, demonstrate significant response reduction when dampers are added to the structural frame. As expected, best performance is achieved when a complete vertical distribution of dampers is used, although even an incomplete distribution produces substantial response reduction. However, it should be mentioned that these results apply for an essentially elastic structural system. Had the system been allowed to significantly yield, the reduction in acceleration and force response would have been much less, although the reduction in drift response and damage would have been equally significant.

Probably the most impressive results are seen in Figures 5-11 and 5-12 in which the structure with a complete vertical distribution of nonlinear dampers undergoes substantially less story drifts than the structure without dampers for significantly stronger earthquake input and for about the same force and acceleration response.

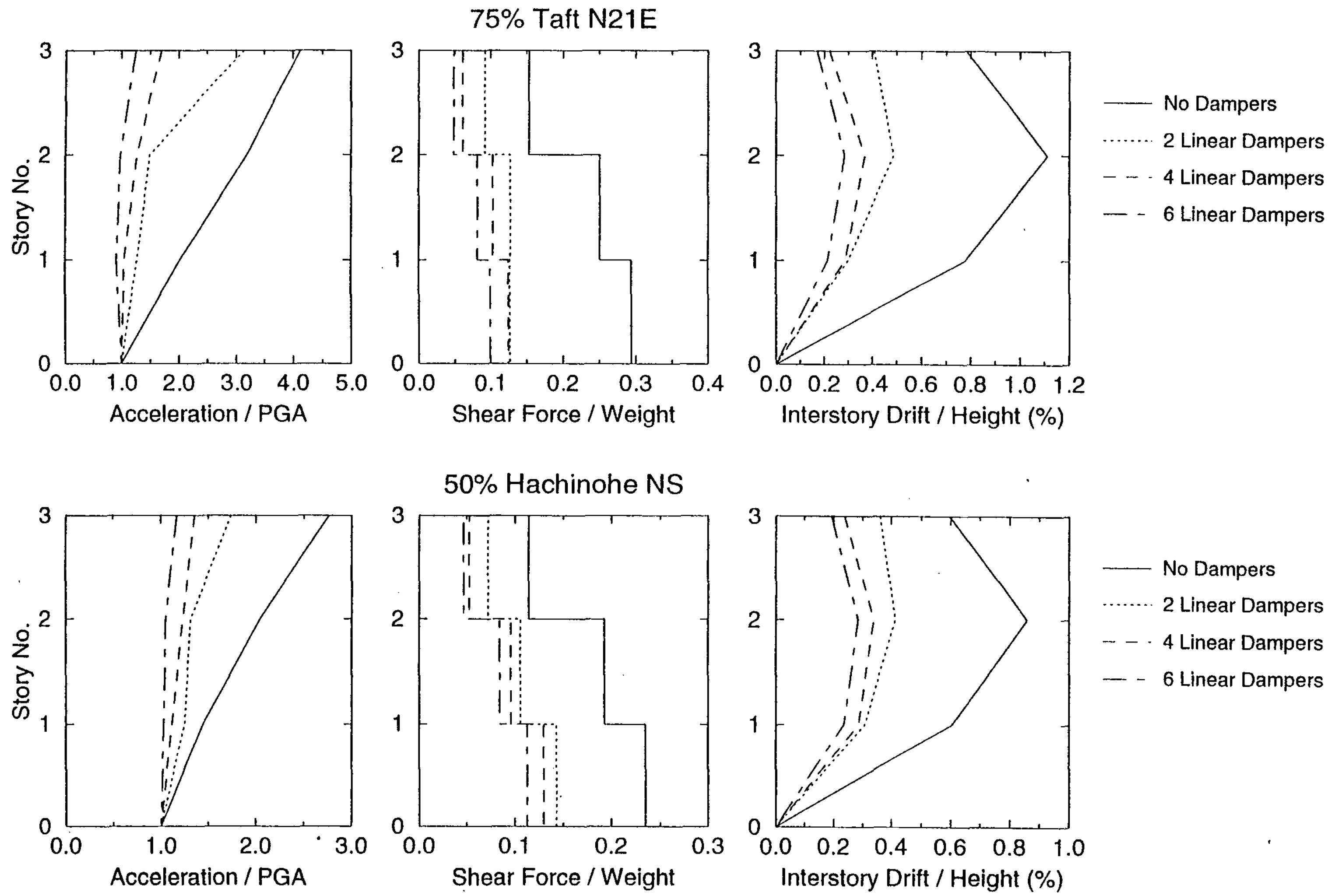

FIGURE 5-1 Acceleration, Story Shear and Interstory Drift Profiles of 3-Story Repaired Structure without Dampers and with Different Linear Dampers Configurations Subjected to 75% Taft and 50% Hachinohe Earthquakes

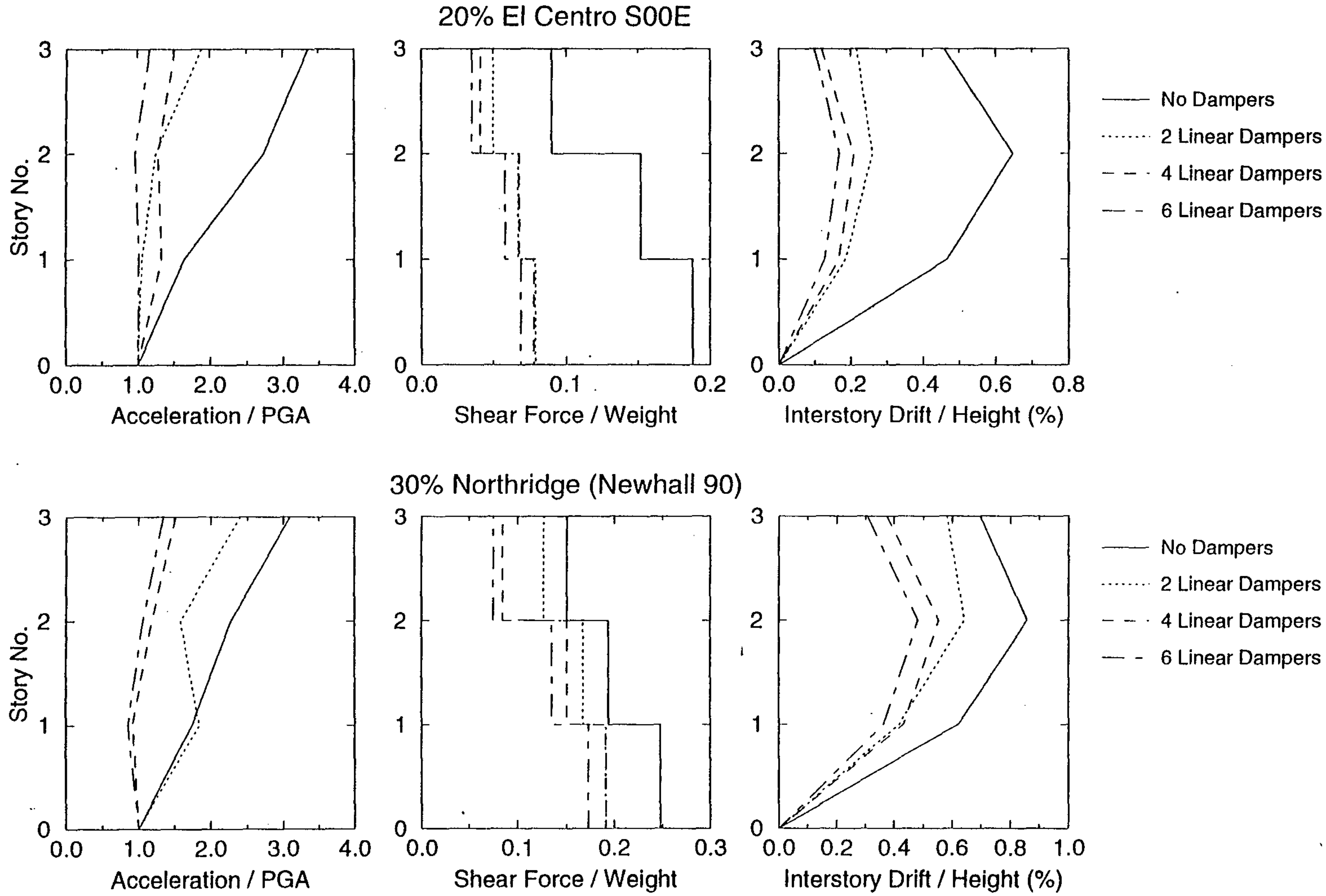

FIGURE 5-2 Acceleration, Story Shear and Interstory Drift Profiles of 3-Story Repaired Structure without Dampers and with Different Linear Dampers Configurations Subjected to 20% El Centro and 30% Northridge (Newhall 90) Earthquakes

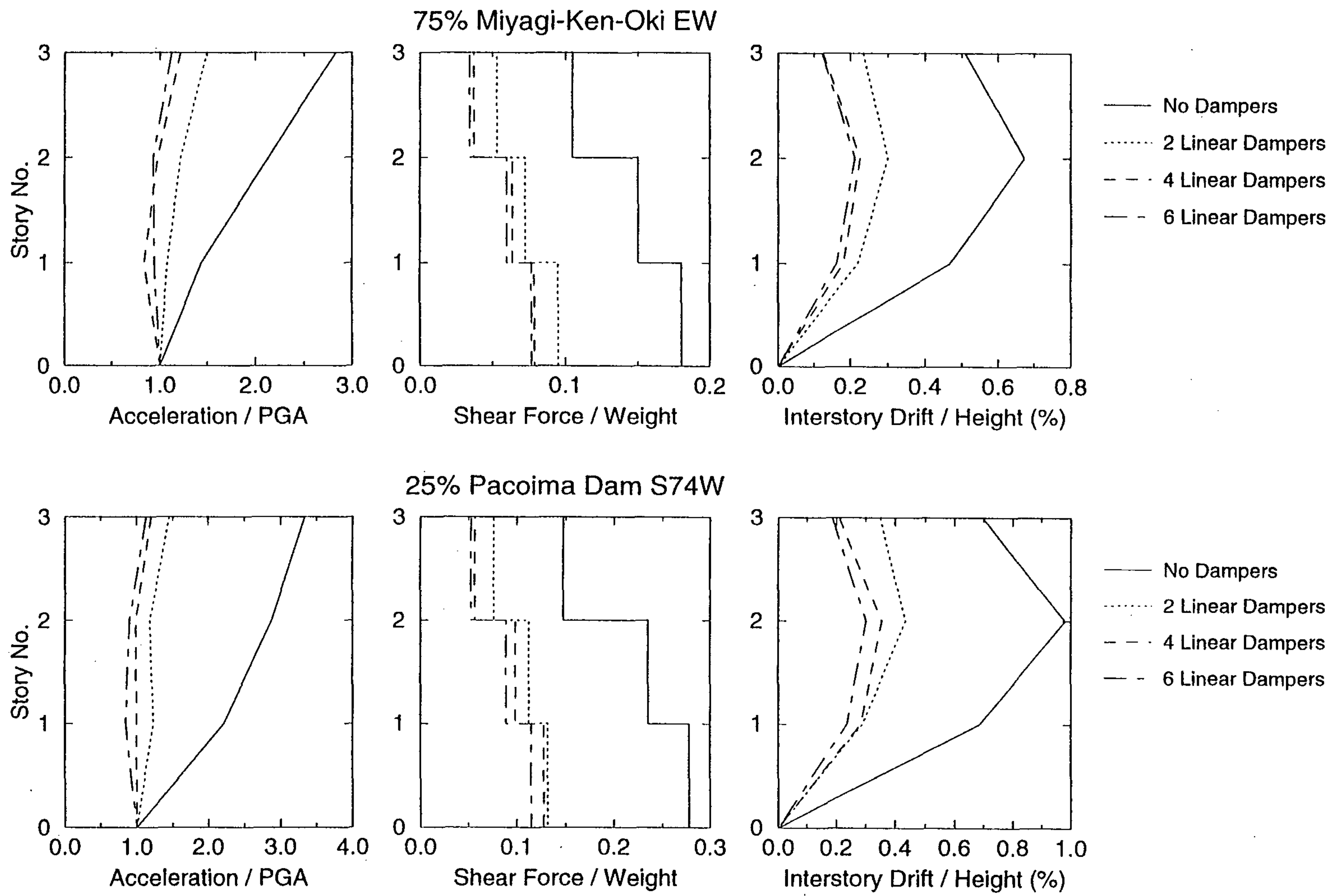

FIGURE 5-3 Acceleration, Story Shear and Interstory Drift Profiles of 3-Story Repaired Structure without Dampers and with Different Linear Dampers Configurations Subjected to 75% Miyagi-Ken-Oki and 25% Pacoima Dam Earthquakes

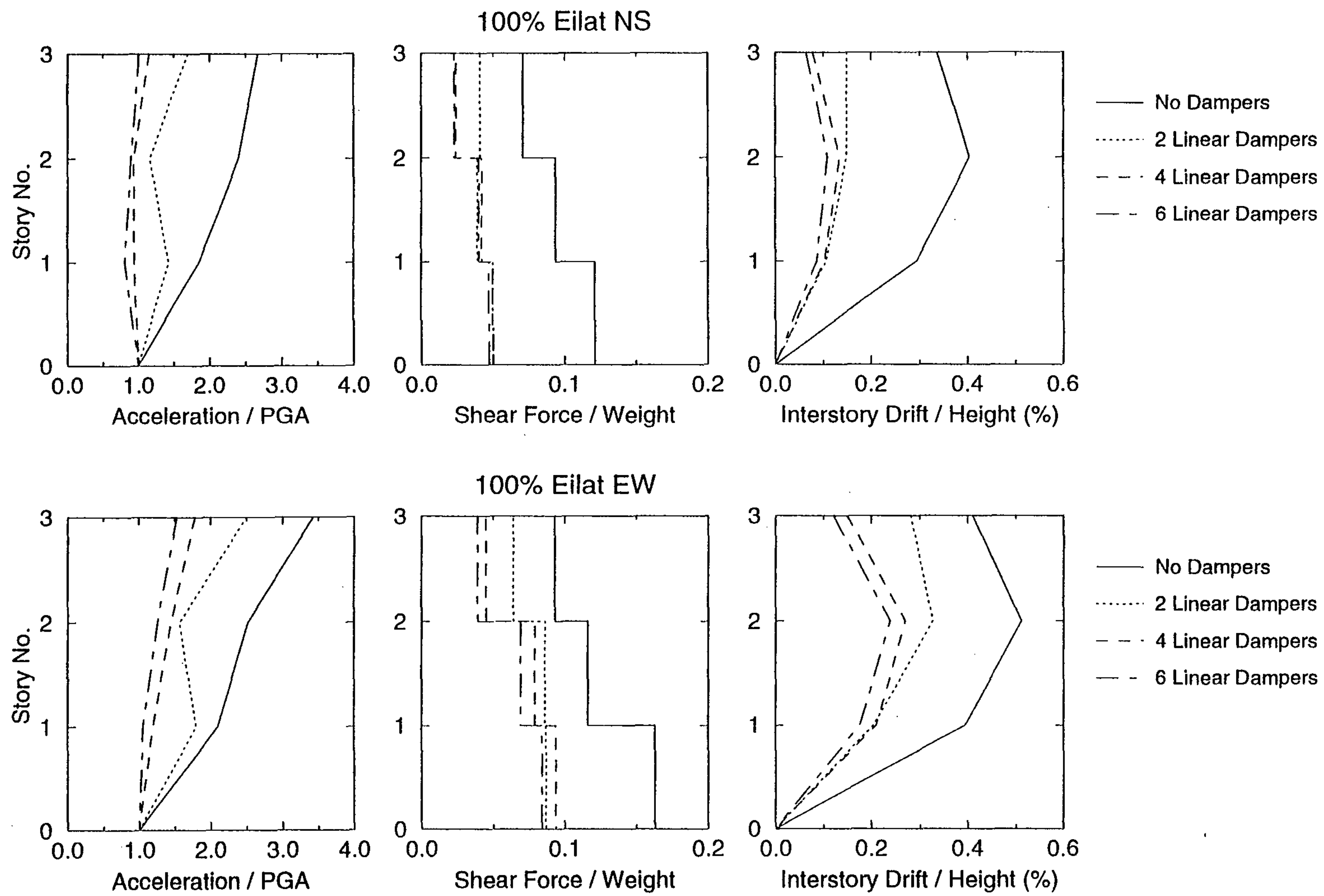

FIGURE 5-4 Acceleration, Story Shear and Interstory Drift Profiles of 3-Story Repaired Structure without Dampers and with Different Linear Dampers Configurations Subjected to 100% Eilat NS and 100% Eilat EW Earthquakes

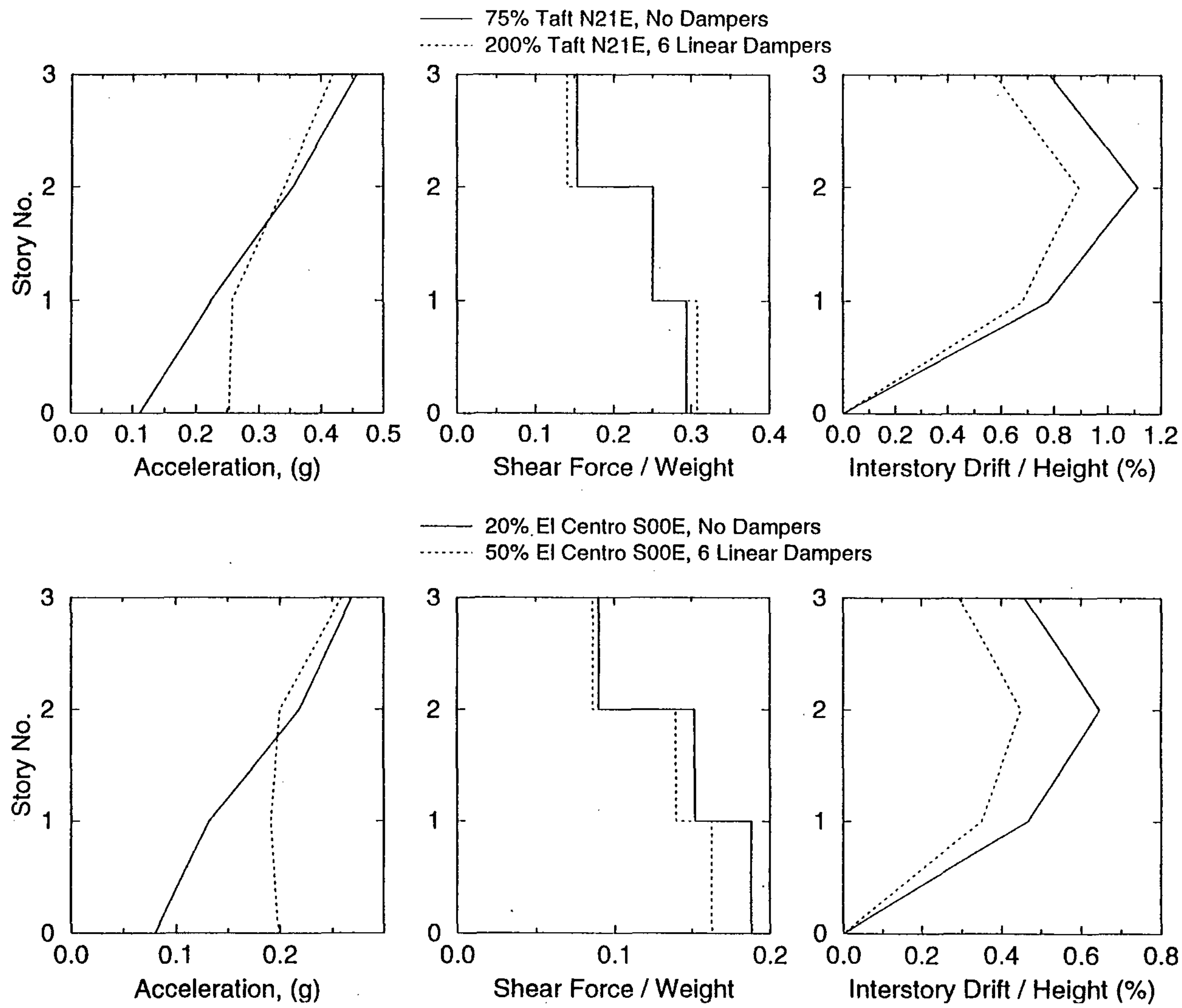

FIGURE 5-5 Comparison of Acceleration, Story Shear and Interstory Drift Profiles of 3-Story Repaired Structure without Dampers and with Six Linear Dampers Subjected to Different Levels of the Same Earthquake Input

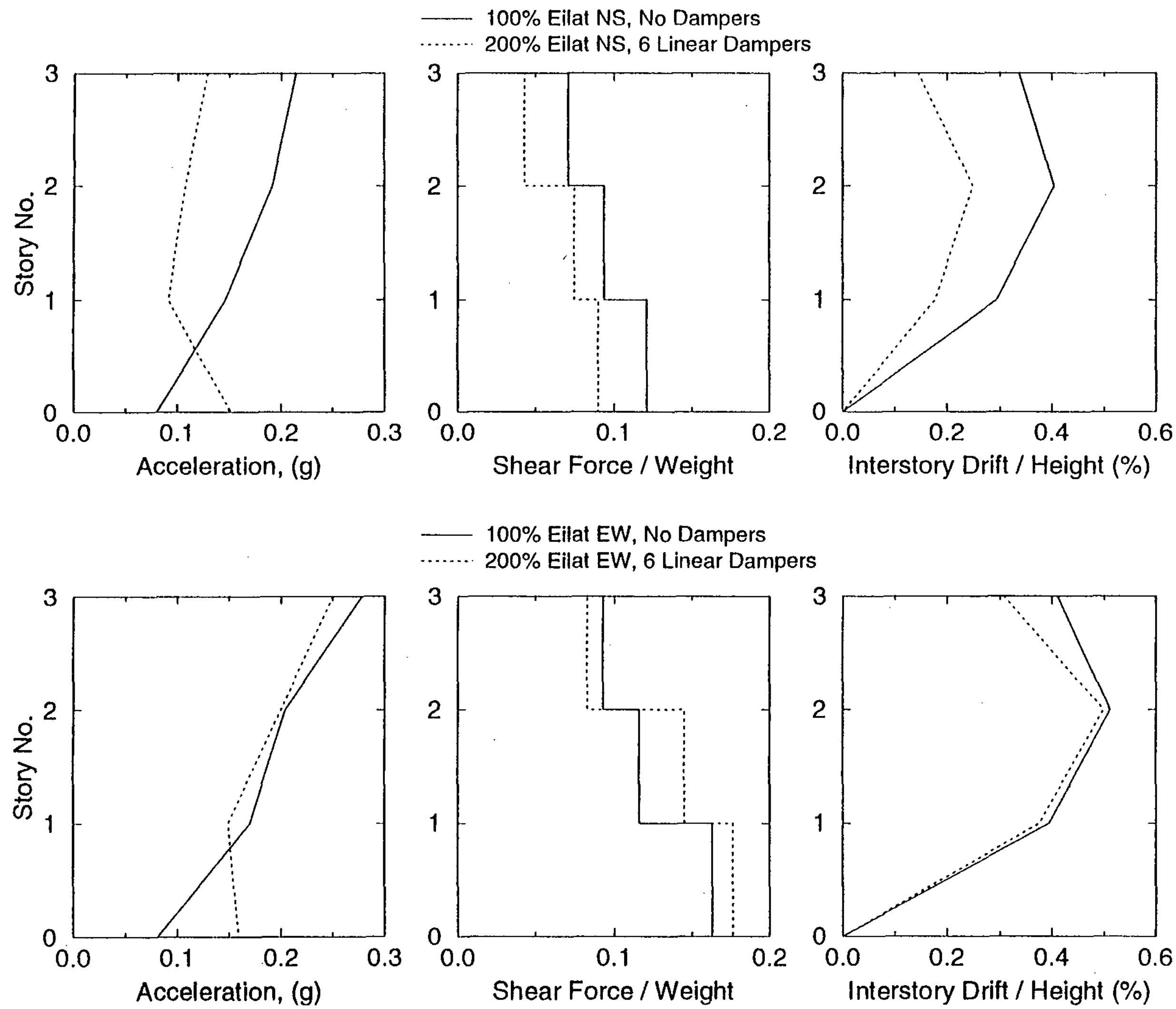

FIGURE 5-6 Comparison of Acceleration, Story Shear and Interstory Drift Profiles of 3-Story Repaired Structure without Dampers and with Six Linear Dampers Subjected to Different Levels of the Same Earthquake Input

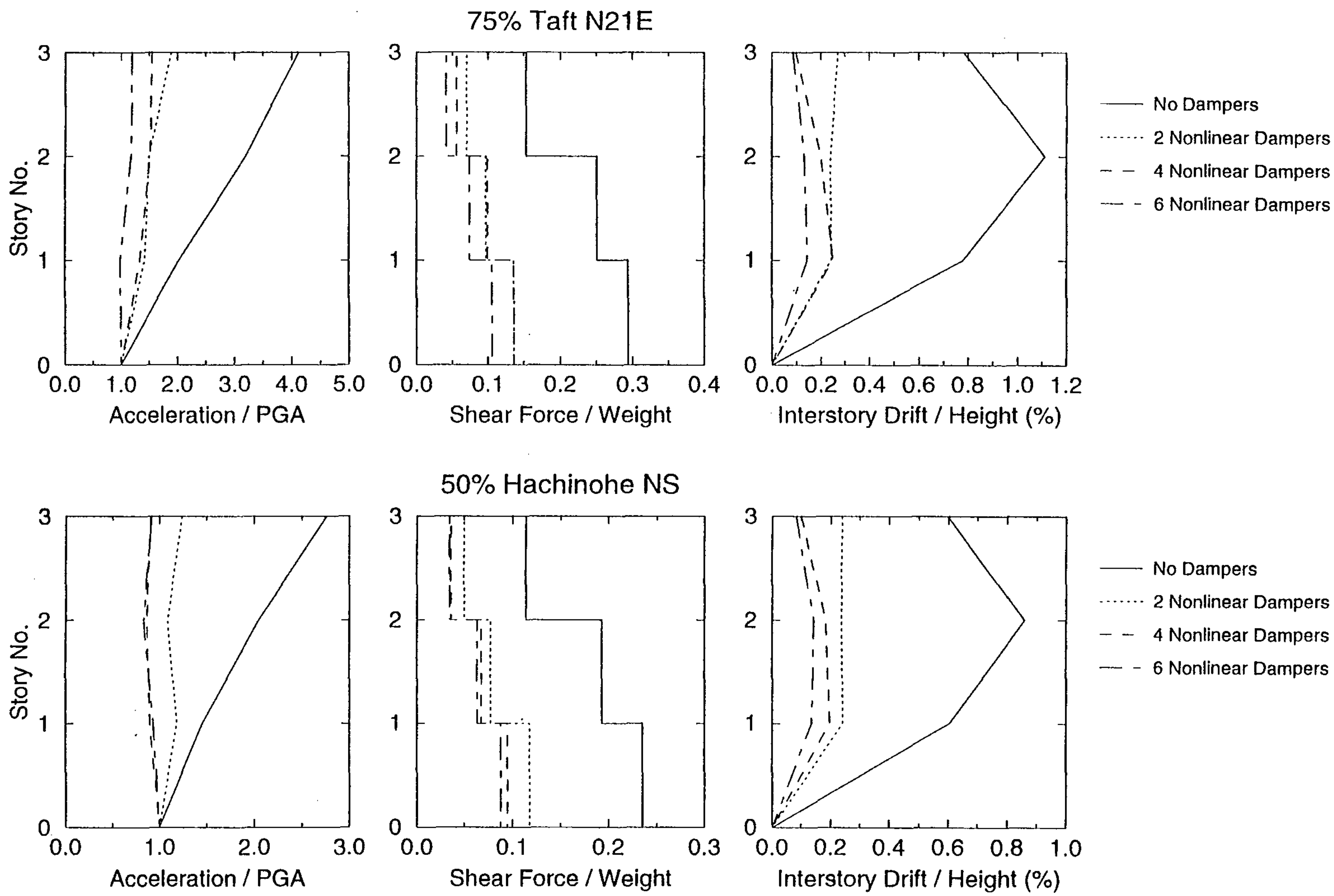

FIGURE 5-7 Acceleration, Story Shear and Interstory Drift Profiles of 3-Story Repaired Structure without Dampers and with Different Nonlinear Dampers Configurations Subjected to 75% Taft and 50% Hachinohe Earthquakes

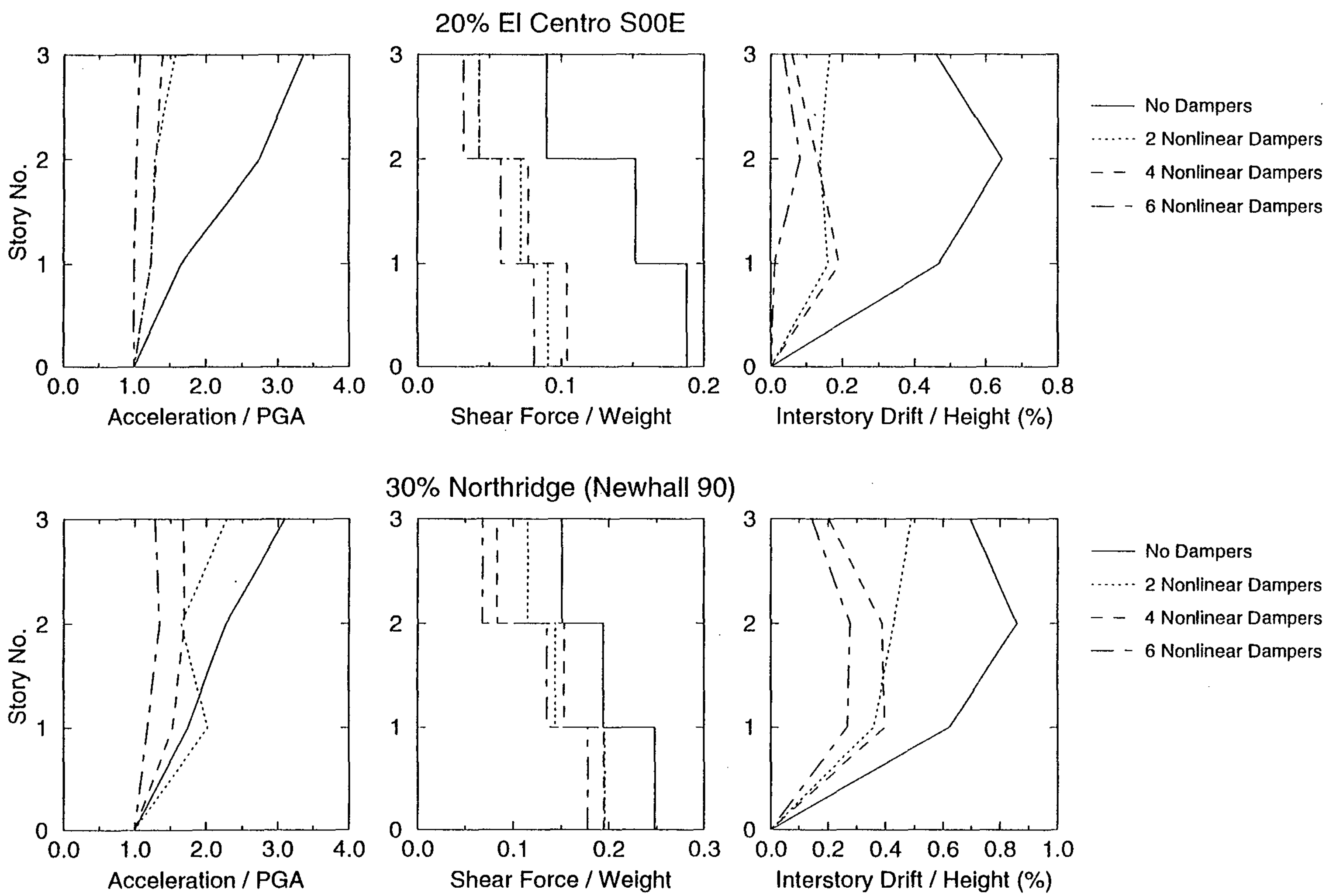

FIGURE 5-8 Acceleration, Story Shear and Interstory Drift Profiles of 3-Story Repaired Structure without Dampers and with Different Nonlinear Dampers Configurations Subjected to 20% El Centro and 30% Northridge (Newhall 90) Earthquakes

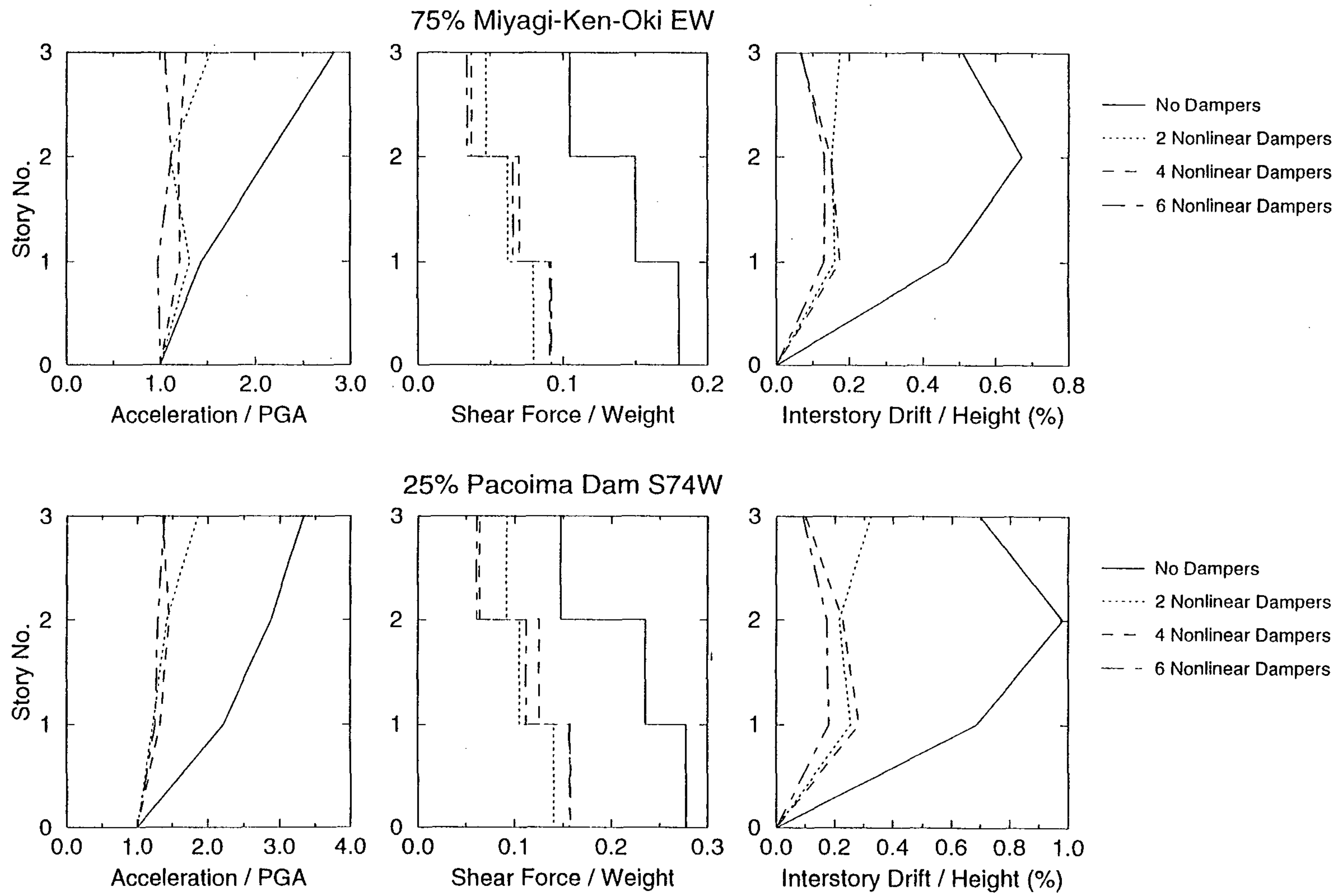

FIGURE 5-9 Acceleration, Story Shear and Interstory Drift Profiles of 3-Story Repaired Structure without Dampers and with Different Nonlinear Dampers Configurations Subjected to 75% Miyagi-Ken-Oki and 25% Pacoima Dam Earthquakes

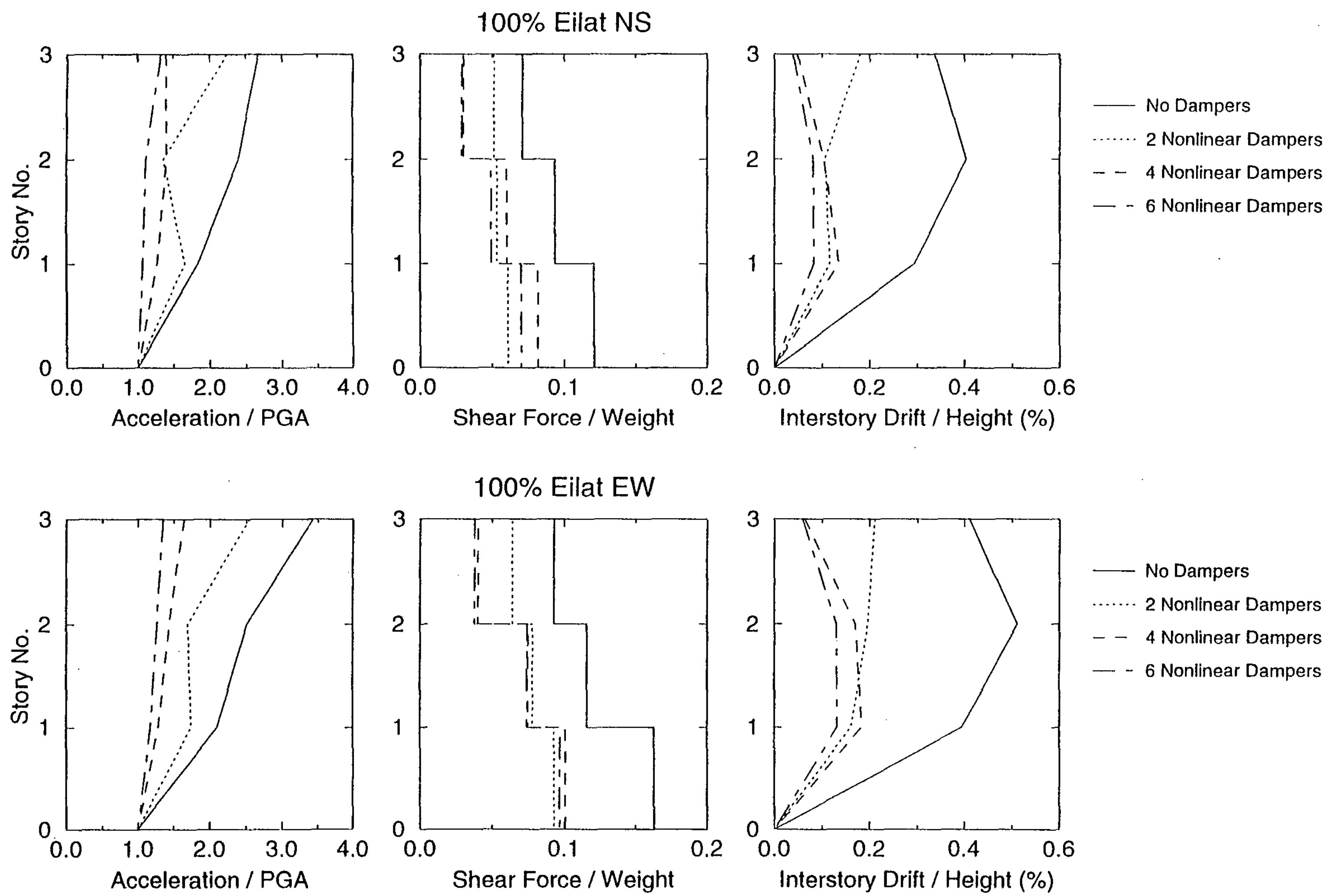

FIGURE 5-10 Acceleration, Story Shear and Interstory Drift Profiles of 3-Story Repaired Structure without Dampers and with Different Nonlinear Dampers Configurations Subjected to 100% Eilat NS and 100% Eilat EW Earthquakes

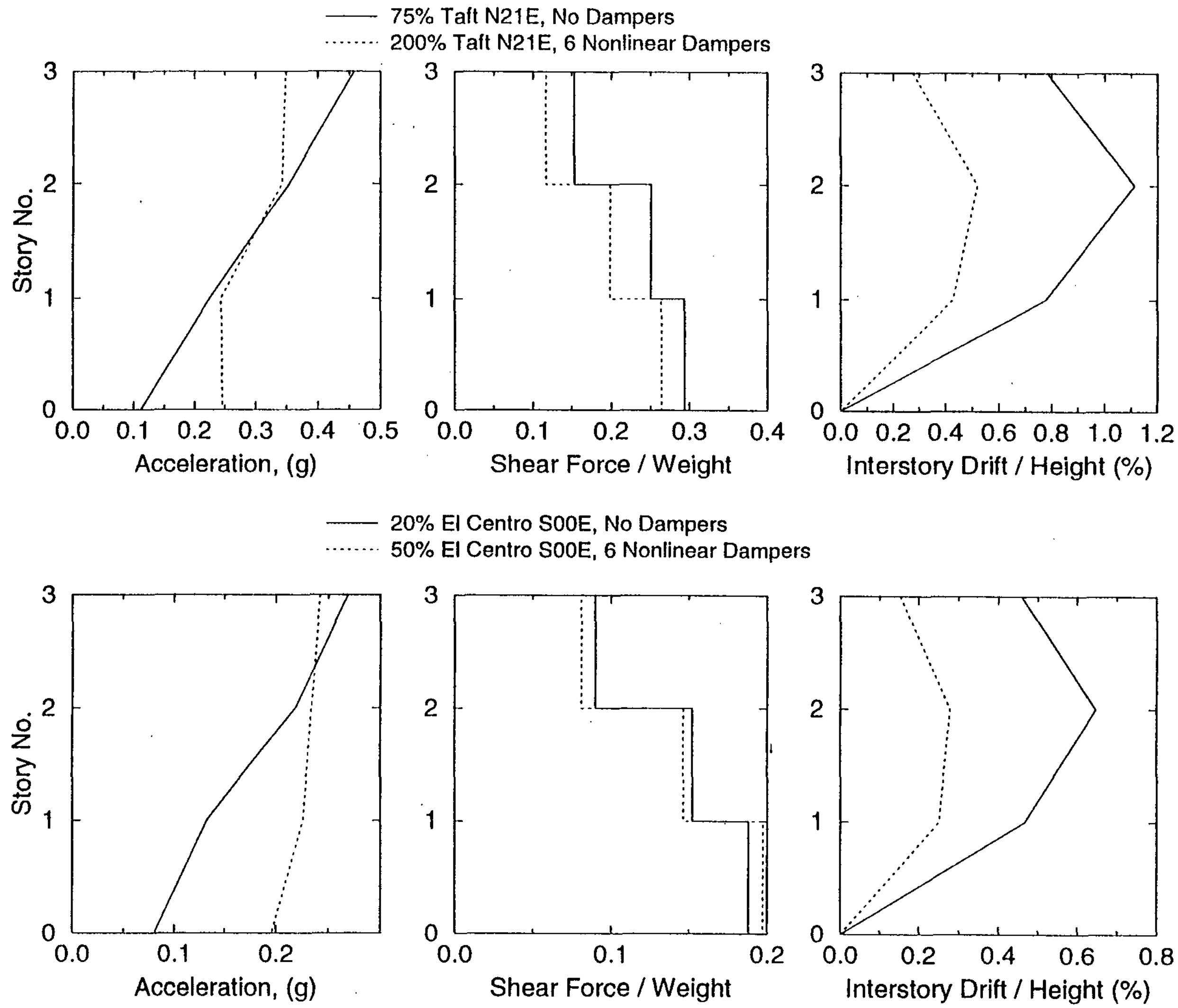

FIGURE 5-11 Comparison of Acceleration, Story Shear and Interstory Drift Profiles of 3-Story Repaired Structure without Dampers and with Six Nonlinear Dampers Subjected to Different Levels of the Same Earthquake Input

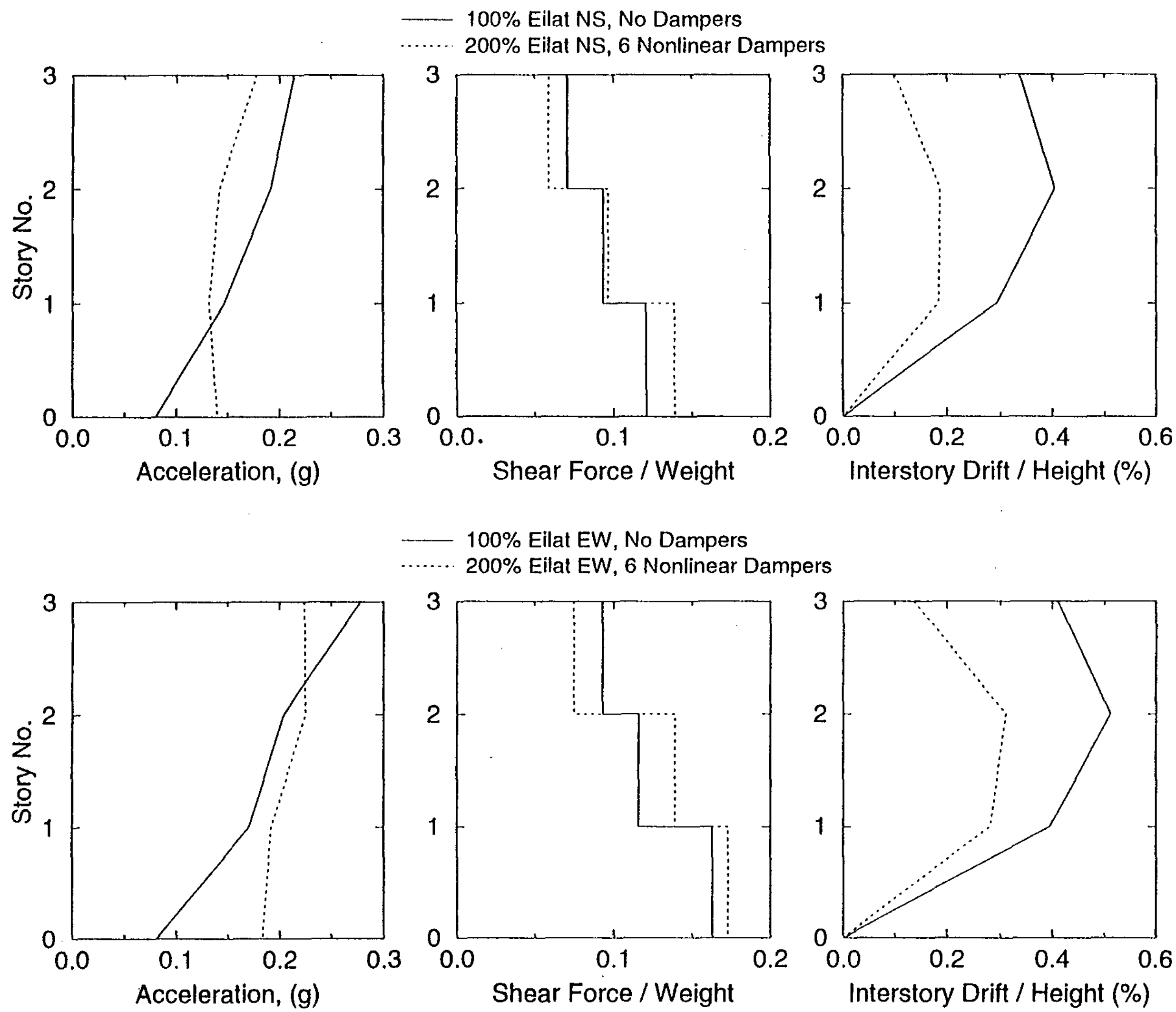

FIGURE 5-12 Comparison of Acceleration, Story Shear and Interstory Drift Profiles of 3-Story Repaired Structure without Dampers and with Six Nonlinear Dampers Subjected to Different Levels of the Same Earthquake Input

In a different type of comparison of response, Tables 5-XII and 5-XIII present ratios of peak story drift and peak shear force of the structure with dampers to the structure without dampers. These ratios are, respectively, designated as RD and RBS in these tables.

For the tested one-story structure, it is observed in Table 5-XII that nonlinear dampers achieve larger response reductions in both drift and shear force than linear dampers. For the case of the 3-story structure, nonlinear dampers achieve, in all tests, larger drift response reduction than linear dampers. However for the same input motions, nonlinear dampers result in larger base shear than linear dampers. This is expected in low velocity motions where the nonlinear dampers exhibit large damping force, thus, effectively appear as linear dampers with large damping constant. Overall, the response reduction ratios RD and RBS are within the ranges indicated in Table 5-XIV.

5.3.2 Comparison of Linear and Nonlinear Dampers

Direct comparison of story shear force-drift loops for the one-story and 3-story structure without and with linear or nonlinear dampers is provided in Figures 5-13 to 5-24 for selected earthquakes. These figures, in addition to elucidating the benefits offered by the addition of dampers, provide information on the behavior of dampers. Particularly, in Figures 5-13 to 5-17 for the one-story structure, the contribution to the base shear by the columns and dampers has been separated. It is evident in these figures that the force mobilized in the nonlinear dampers is systematically larger than that mobilized in the linear dampers. This was expected since the two types of dampers were designed to have about the same output damping force at velocity of 150 mm/sec. That is, for weak motions (such

Table 5-XII Reduction in Drift and Base Shear for Single Story Frame with Linear and Nonlinear Dampers

Excitation	2 Linear Dampers		2 Nonlinear Dampers	
	RD	RBS	RD	RBS
100% Taft N21E	0.59	0.64	0.45	0.54
100% Miyagi-Ken-Oki EW	0.62	0.64	0.43	0.54
75% Hachinohe NS	0.71	0.79	0.58	0.72
100% Eilat NS	0.70	0.75	0.50	0.69
100% Eilat EW	0.69	0.75	0.54	0.71

RD = Reduction in Drift
RBS = Reduction in Base Shear

Table 5-XIII Reduction in Drift and Base Shear for 3-Story Repaired Frame with Various Configurations of Linear and Nonlinear Dampers

Excitation	2 Linear Dampers				4 Linear Dampers				6 Linear Dampers			
	RD			RBS	RD			RBS	RD			RBS
	1st*	2nd*	3rd*		1st*	2nd*	3rd*		1st*	2nd*	3rd*	
75% Taft N21E	0.39	0.44	0.52	0.43	0.37	0.33	0.28	0.42	0.28	0.26	0.22	0.34
50% Hachinohe NS	0.50	0.48	0.60	0.61	0.48	0.40	0.40	0.55	0.39	0.33	0.32	0.48
75% Miyagi-Ken-Oki EW	0.47	0.45	0.46	0.53	0.39	0.34	0.25	0.44	0.35	0.31	0.24	0.43
25% Pacoima Dam S74W	0.43	0.44	0.50	0.47	0.42	0.36	0.30	0.46	0.35	0.31	0.27	0.41
20% El Centro S00E	0.40	0.40	0.47	0.42	0.36	0.32	0.26	0.41	0.27	0.26	0.22	0.37
100% Eilat NS	0.36	0.37	0.45	0.41	0.35	0.33	0.23	0.41	0.29	0.27	0.36	0.39
100% Eilat EW	0.51	0.64	0.69	0.53	0.53	0.53	0.37	0.58	0.45	0.46	0.30	0.52

Excitation	2 Nonlinear Dampers				4 Nonlinear Dampers				6 Nonlinear Dampers			
	RD			RBS	RD			RBS	RD			RBS
	1st*	2nd*	3rd*		1st*	2nd*	3rd*		1st*	2nd*	3rd*	
75% Taft N21E	0.31	0.22	0.35	0.46	0.32	0.18	0.13	0.46	0.19	0.12	0.11	0.36
50% Hachinohe NS	0.40	0.28	0.40	0.50	0.32	0.21	0.17	0.40	0.22	0.17	0.14	0.37
75% Miyagi-Ken-Oki EW	0.34	0.23	0.34	0.44	0.37	0.22	0.13	0.51	0.28	0.20	0.13	0.51
25% Pacoima Dam S74W	0.37	0.22	0.46	0.51	0.41	0.23	0.14	0.57	0.26	0.18	0.13	0.56
20% El Centro S00E	0.34	0.21	0.35	0.48	0.41	0.20	0.13	0.55	0.21	0.13	0.08	0.43
100% Eilat NS	0.40	0.26	0.54	0.50	0.46	0.26	0.14	0.68	0.28	0.20	0.11	0.58
100% Eilat EW	0.41	0.38	0.51	0.57	0.46	0.33	0.15	0.62	0.33	0.26	0.14	0.60

* Story No.

Table 5-XIV Range of Response Reduction Ratios for Tested Structures

	One Story	Three Story		
	2 Linear Dampers	2 Linear Dampers	4 Linear Dampers	6 Linear Dampers
RD	0.6 - 0.7	0.35 - 0.7	0.25 - 0.55	0.2 - 0.45
RBS	0.6 - 0.8	0.4 - 0.65	0.4 - 0.6	0.35 - 0.55

	One Story	Three Story		
	2 Nonlinear Dampers	2 Nonlinear Dampers	4 Nonlinear Dampers	6 Nonlinear Dampers
RD	0.4 - 0.6	0.2 - 0.55	0.15 - 0.45	0.1 - 0.35
RBS	0.55 - 0.7	0.4 - 0.6	0.4 - 0.7	0.35 - 0.6

RD = Reduction in Drift

RBS = Reduction in Base Shear

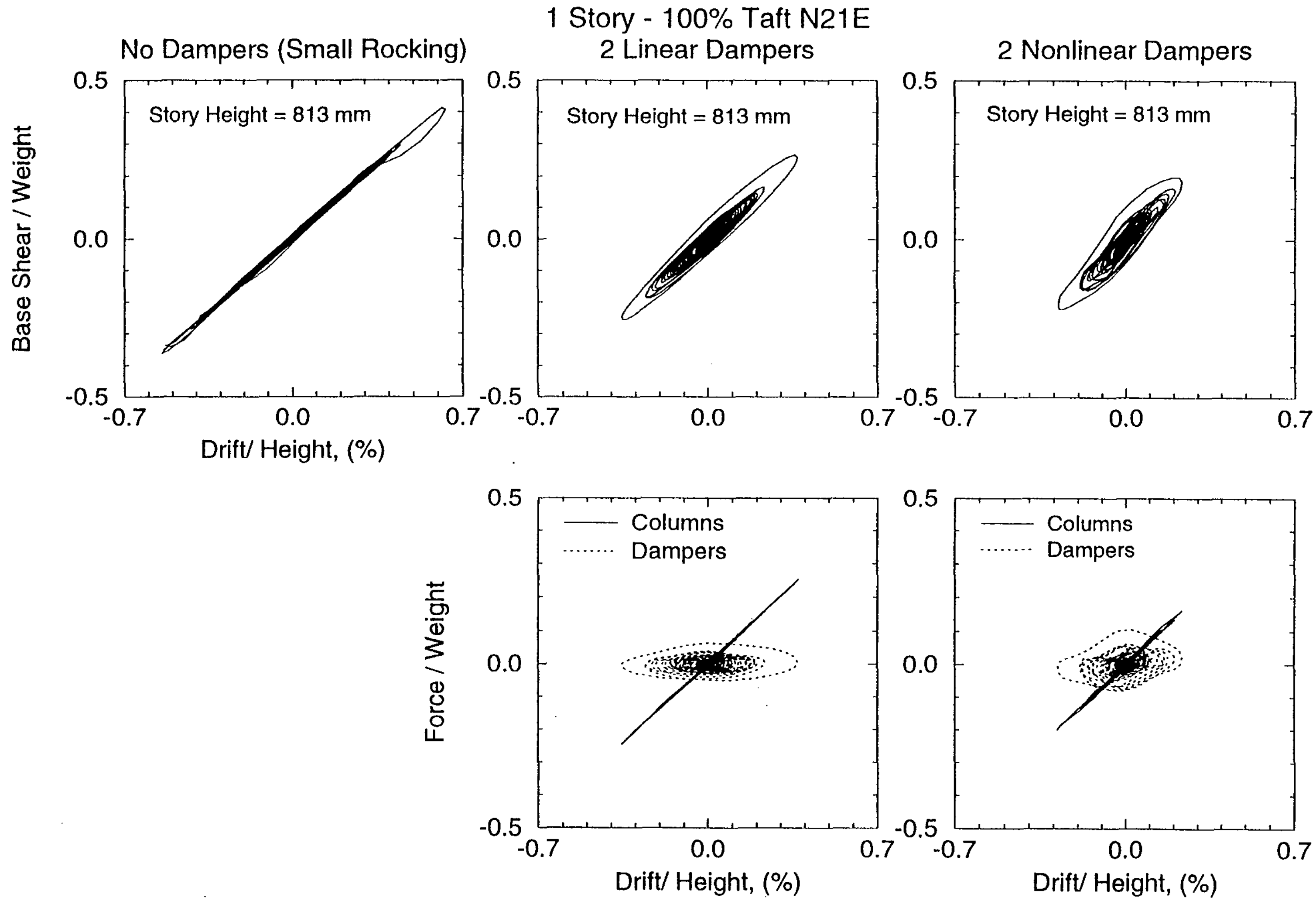

FIGURE 5-13 Comparison of Normalized Shear-Drift Loops of One-Story Structure without, with Two Linear and with Two Nonlinear Dampers Subjected to 100% Taft Earthquake

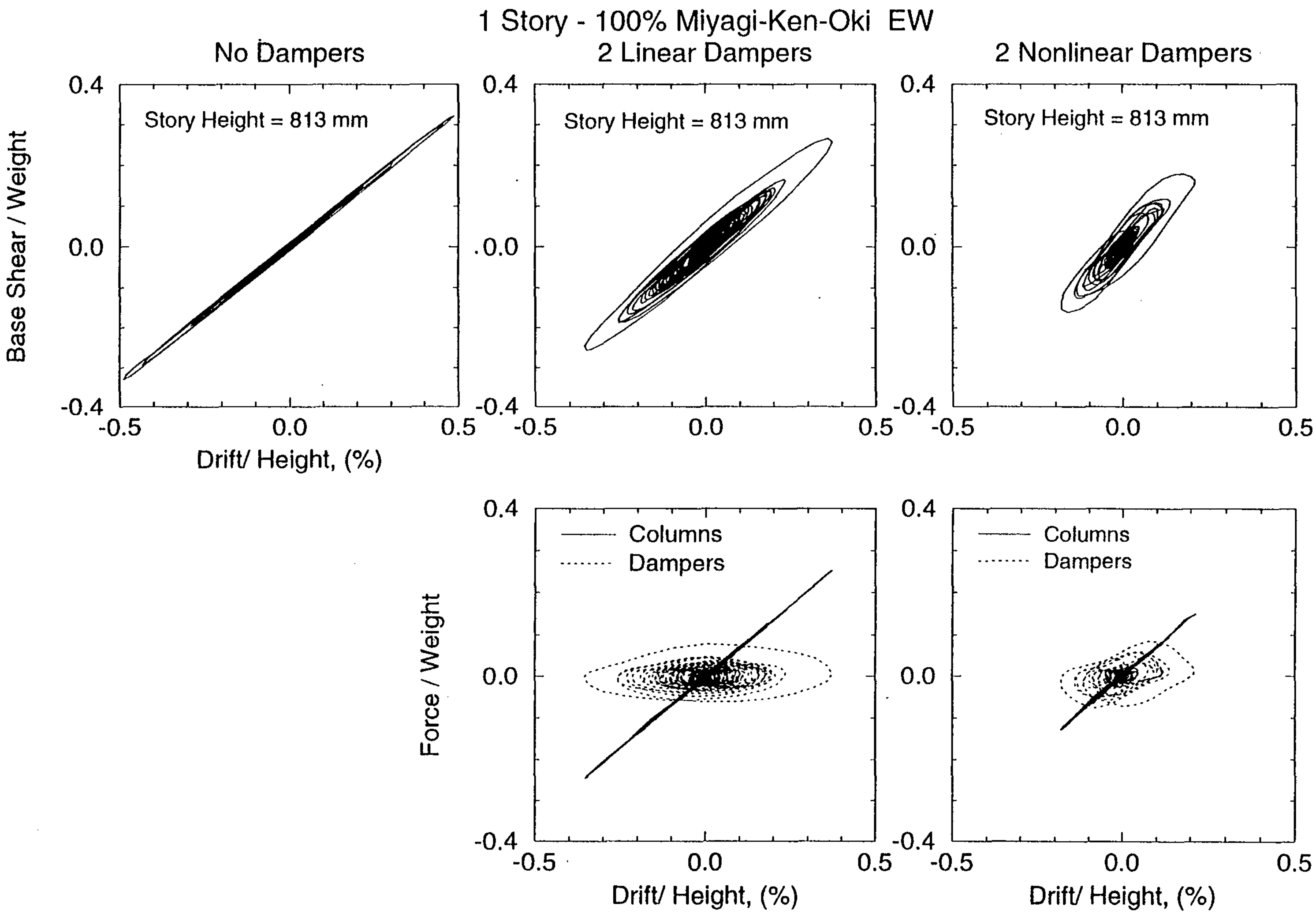

FIGURE 5-14 Comparison of Normalized Shear-Drift Loops of One-Story Structure without, with Two Linear and with Two Nonlinear Dampers Subjected to 100% Miyagi-Ken-Oki Earthquake

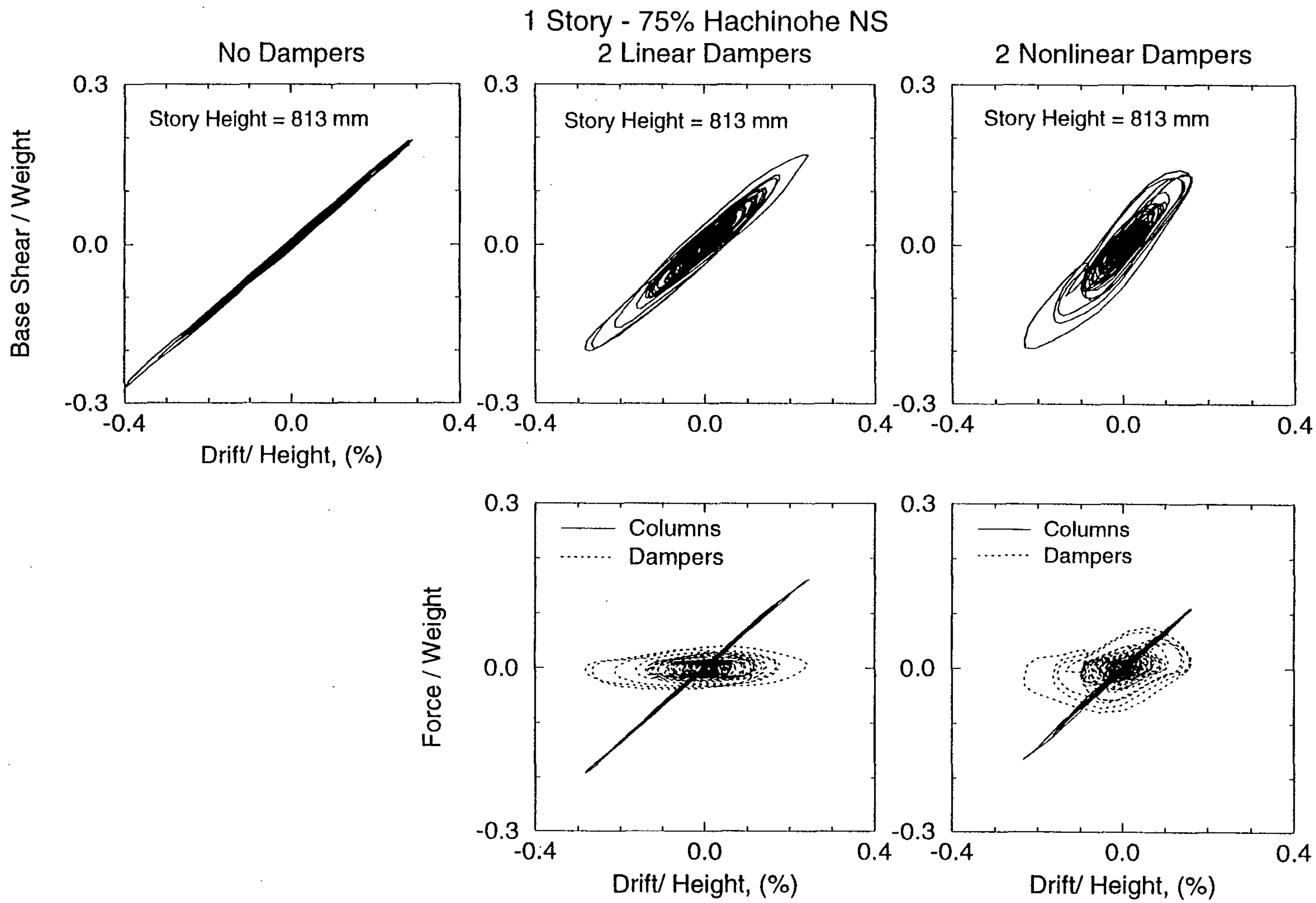

FIGURE 5-15 Comparison of Normalized Shear-Drift Loops of One-Story Structure without, with Two Linear and with Two Nonlinear Dampers Subjected to 75% Hachinohe Earthquake

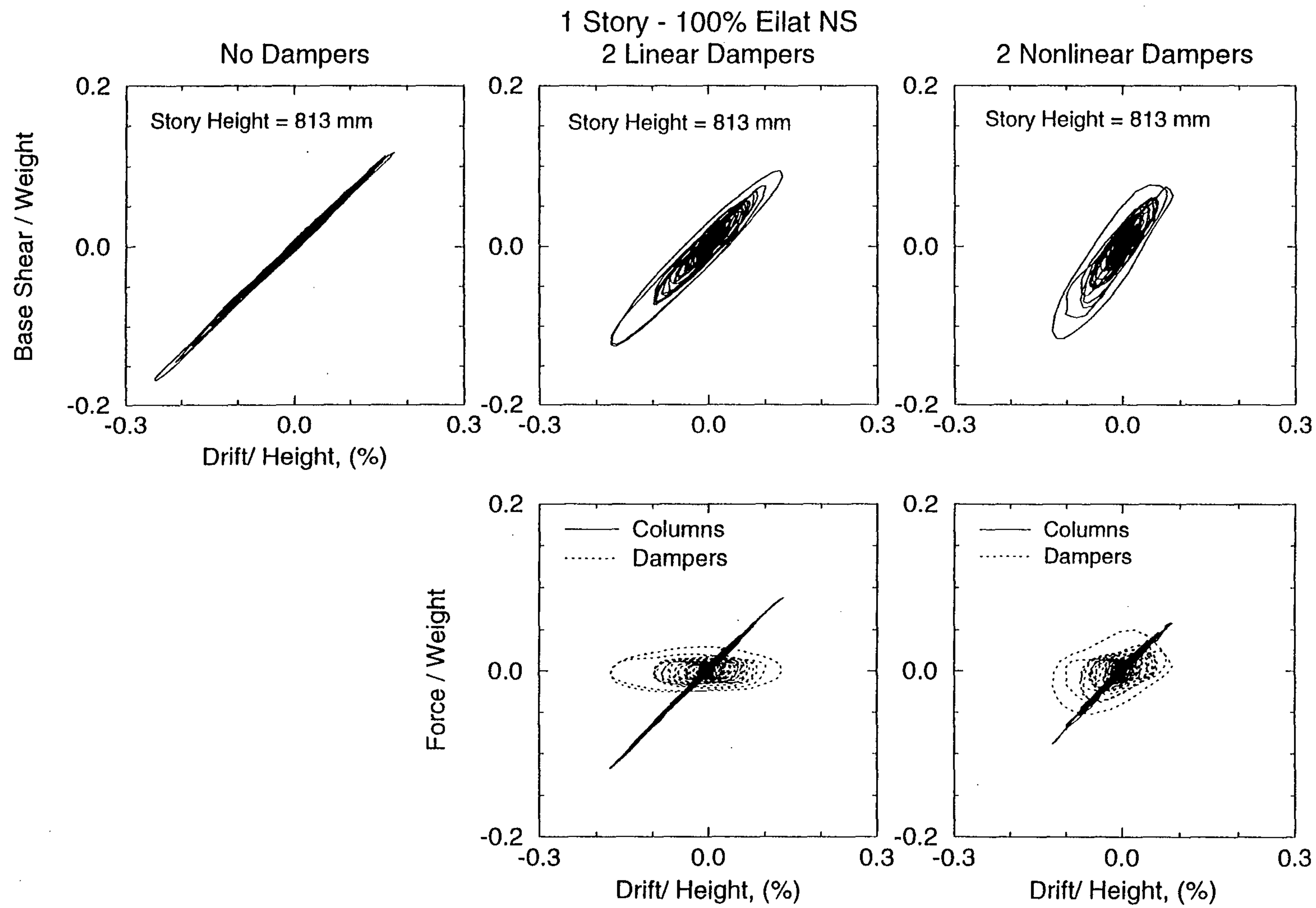

FIGURE 5-16 Comparison of Normalized Shear-Drift Loops of One-Story Structure without, with Two Linear and with Two Nonlinear Dampers Subjected to 100% Eilat NS Earthquake

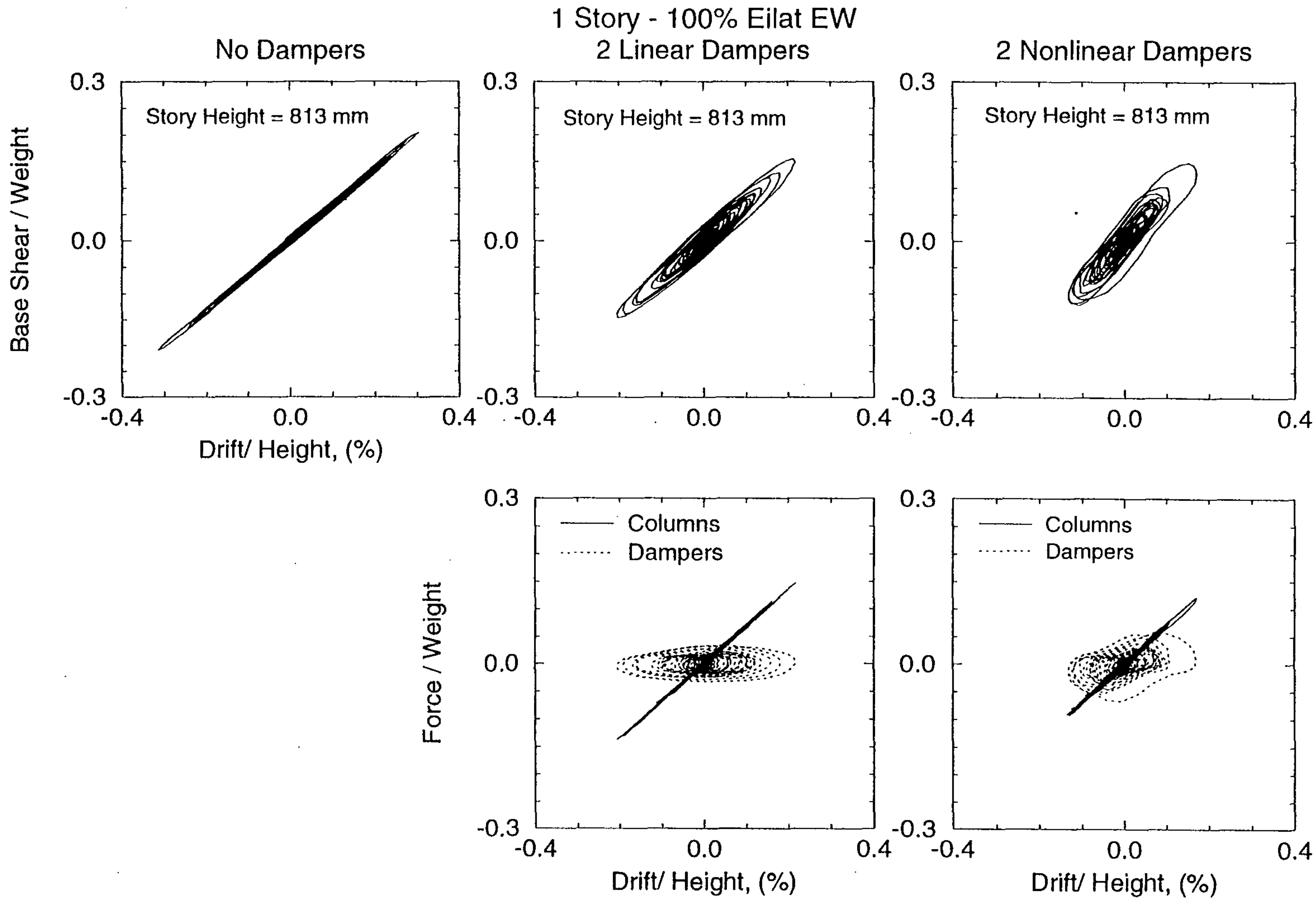

FIGURE 5-17 Comparison of Normalized Shear-Drift Loops of One-Story Structure without, with Two Linear and with Two Nonlinear Dampers Subjected to 100% Eilat EW Earthquake

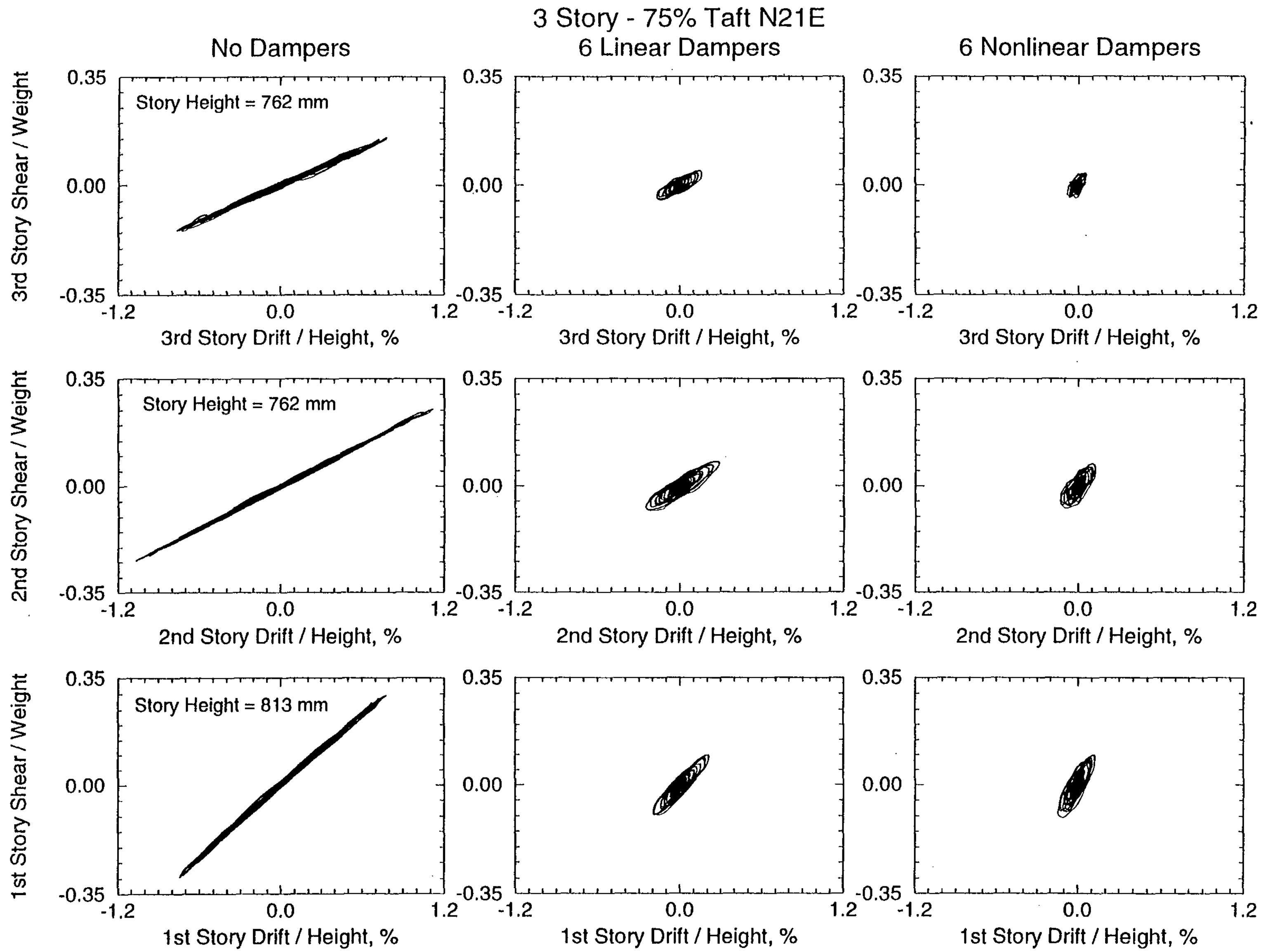

FIGURE 5-18 Comparison of Normalized Shear-Drift Loops of 3-Story Repaired Structure without, with Six Linear and with Six Nonlinear Dampers Subjected to 75% Taft Earthquake

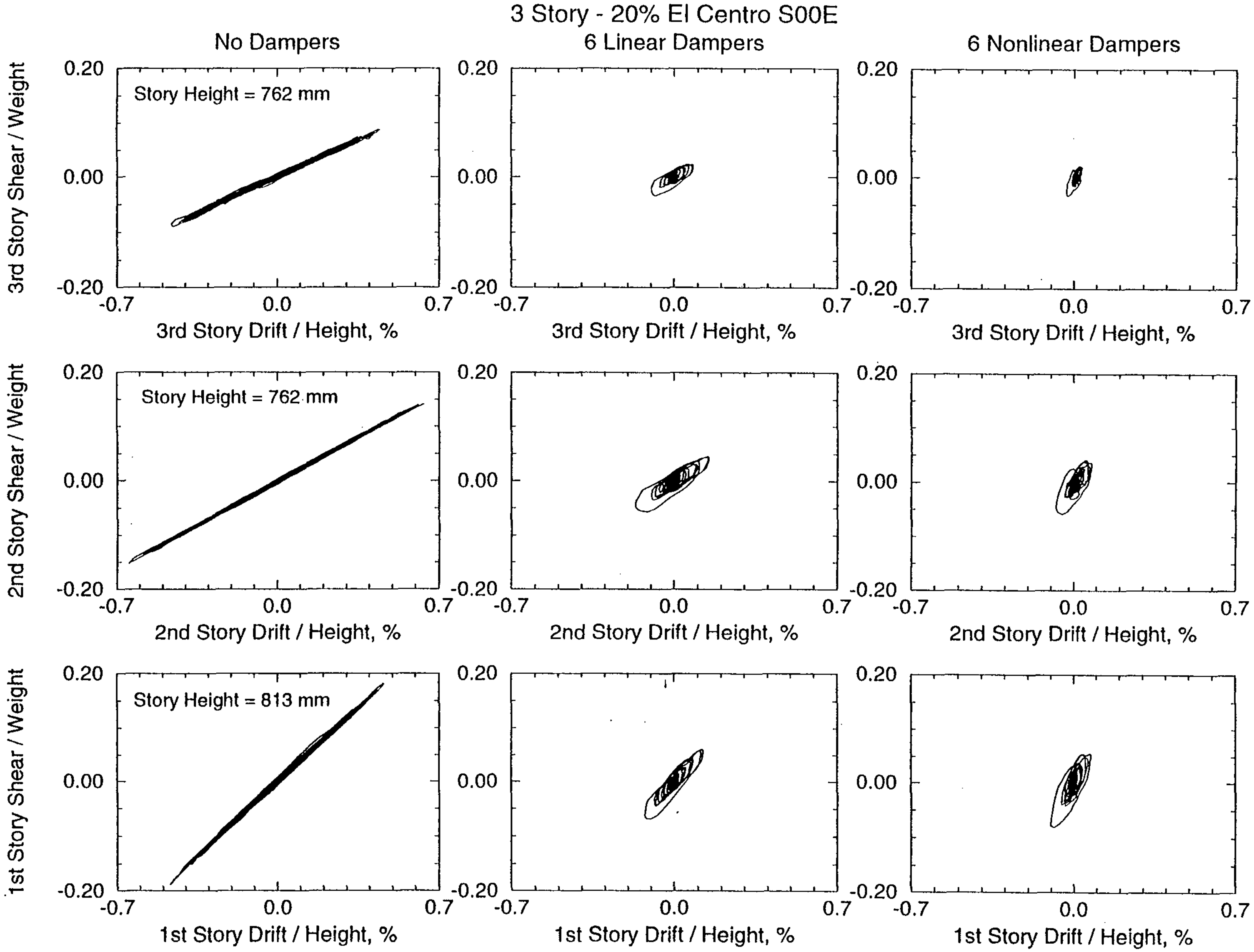

FIGURE 5-19 Comparison of Normalized Shear-Drift Loops of 3-Story Repaired Structure without, with Six Linear and with Six Nonlinear Dampers Subjected to 20% El Centro Earthquake

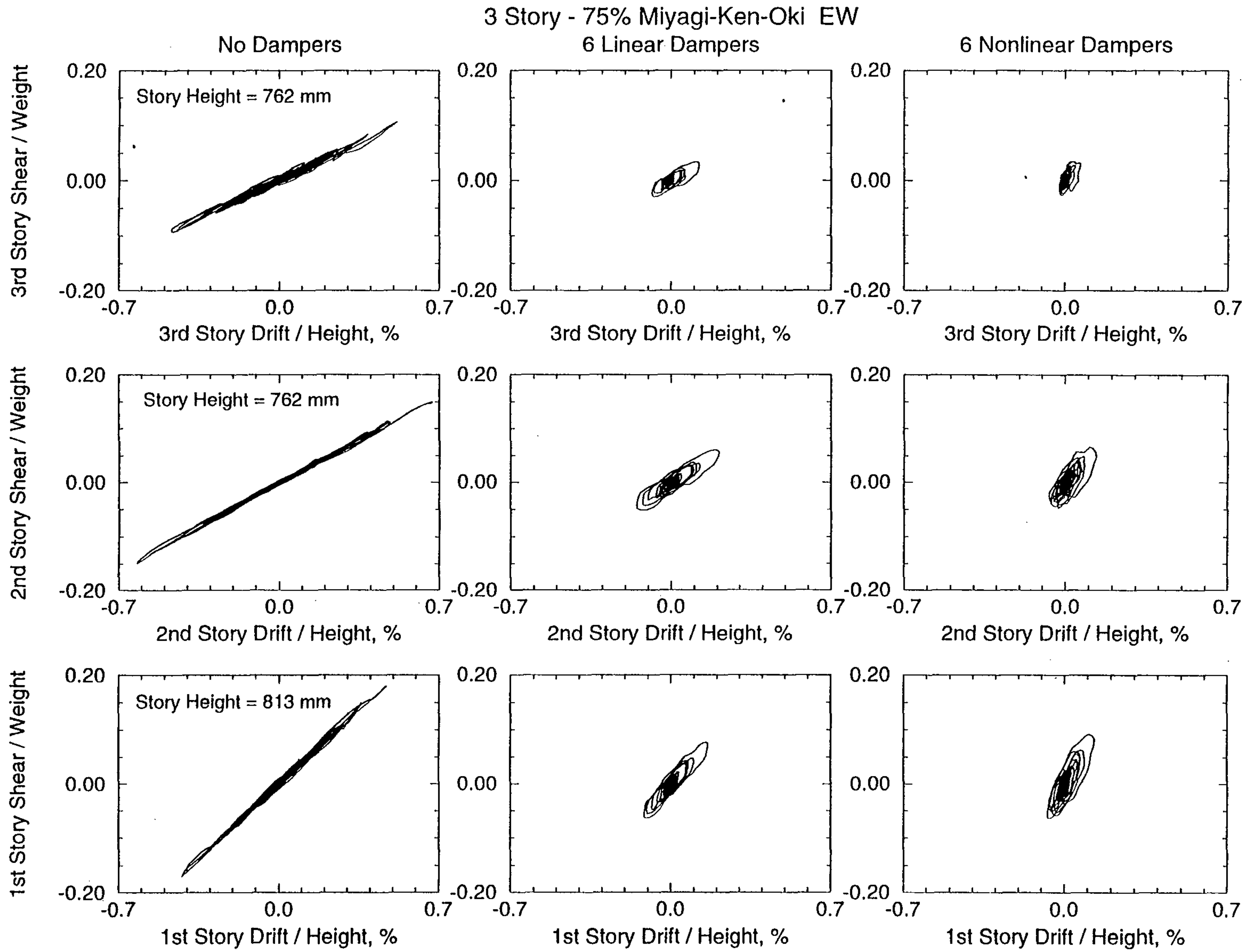

FIGURE 5-20 Comparison of Normalized Shear-Drift Loops of 3-Story Repaired Structure without, with Six Linear and with Six Nonlinear Dampers Subjected to 75% Miyagi-Ken-Oki Earthquake

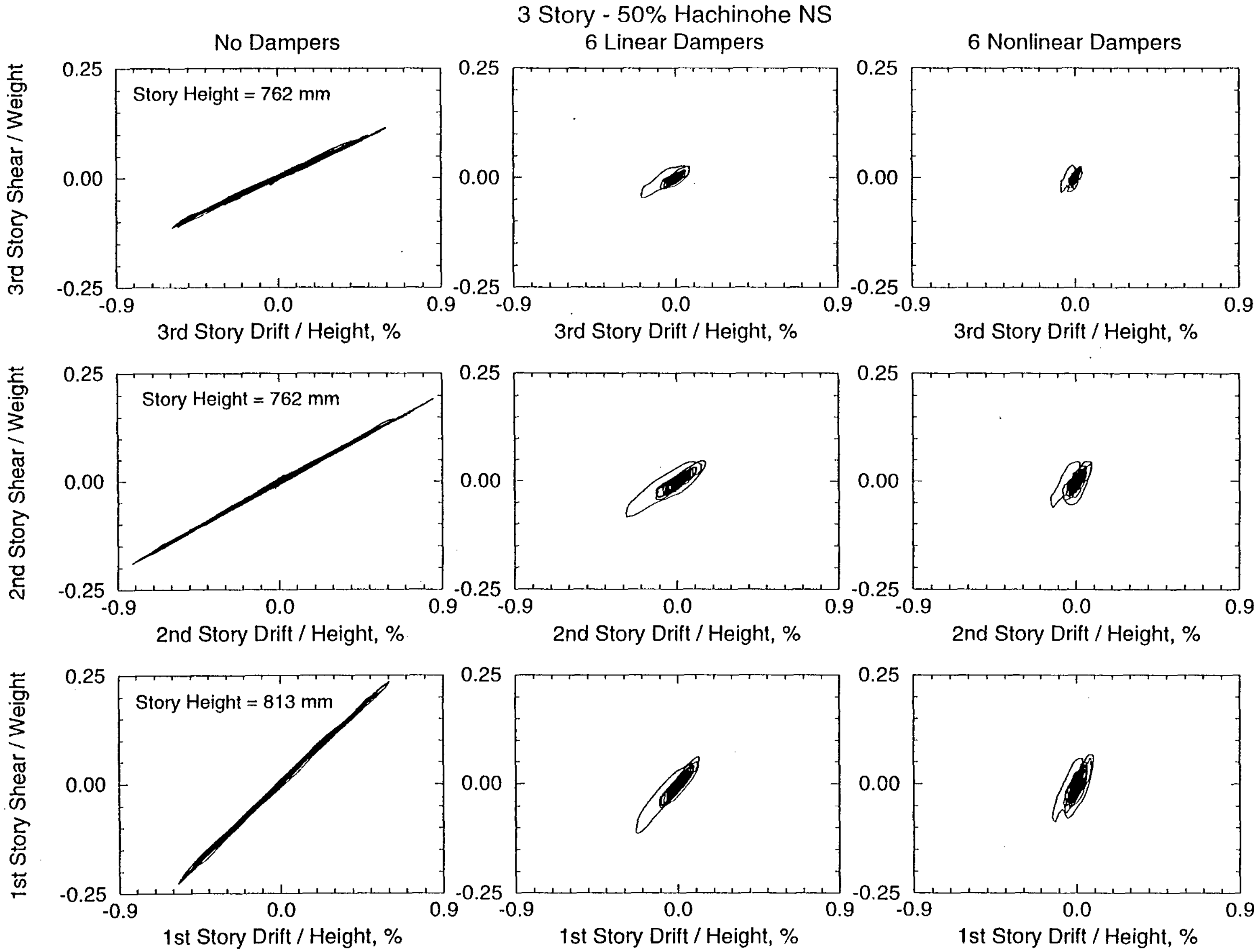

FIGURE 5-21 Comparison of Normalized Shear-Drift Loops of 3-Story Repaired Structure without, with Six Linear and with Six Nonlinear Dampers Subjected to 50% Hachinohe Earthquake

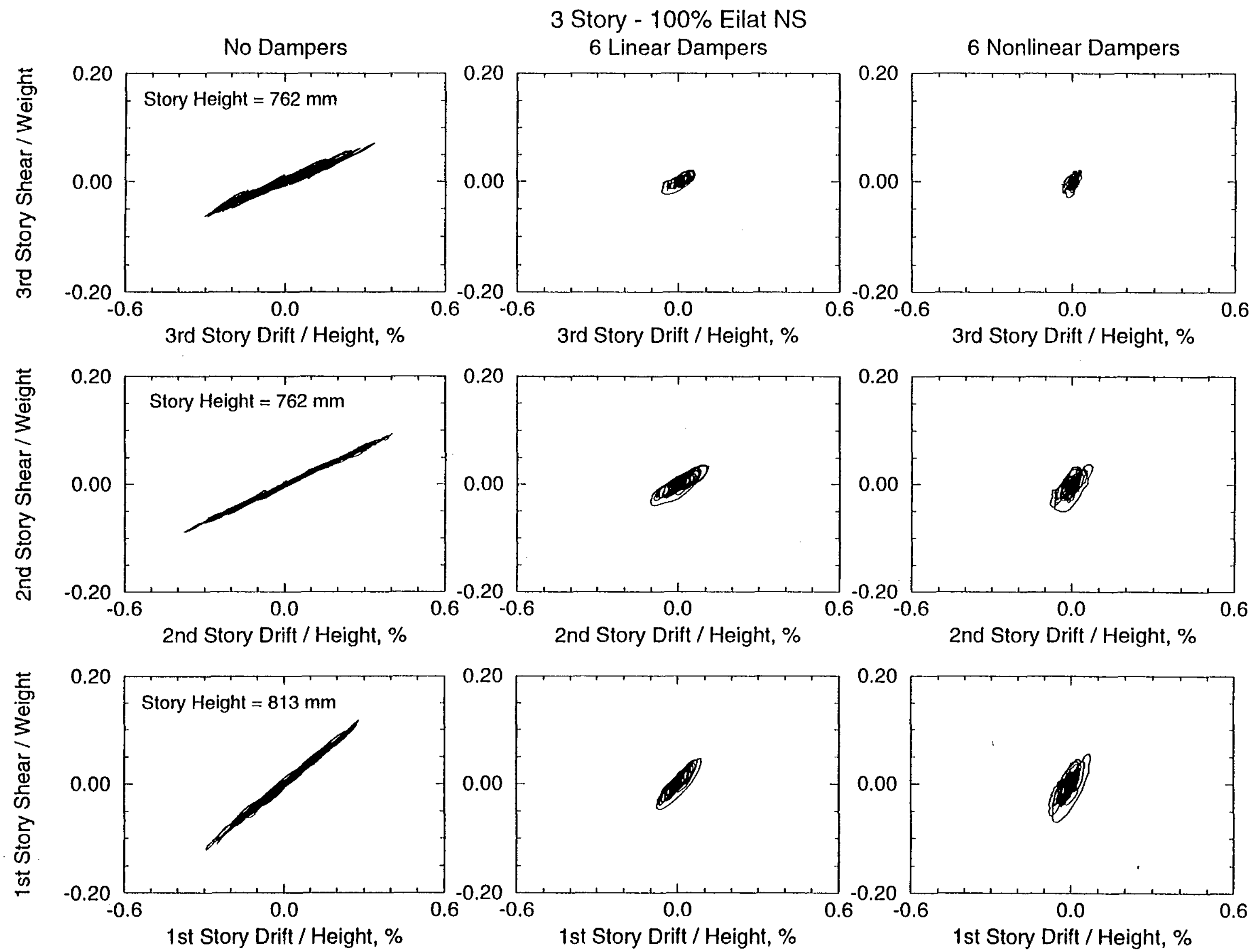

FIGURE 5-22 Comparison of Normalized Shear-Drift Loops of 3-Story Repaired Structure without, with Six Linear and with Six Nonlinear Dampers Subjected to 100% Eilat NS Earthquake

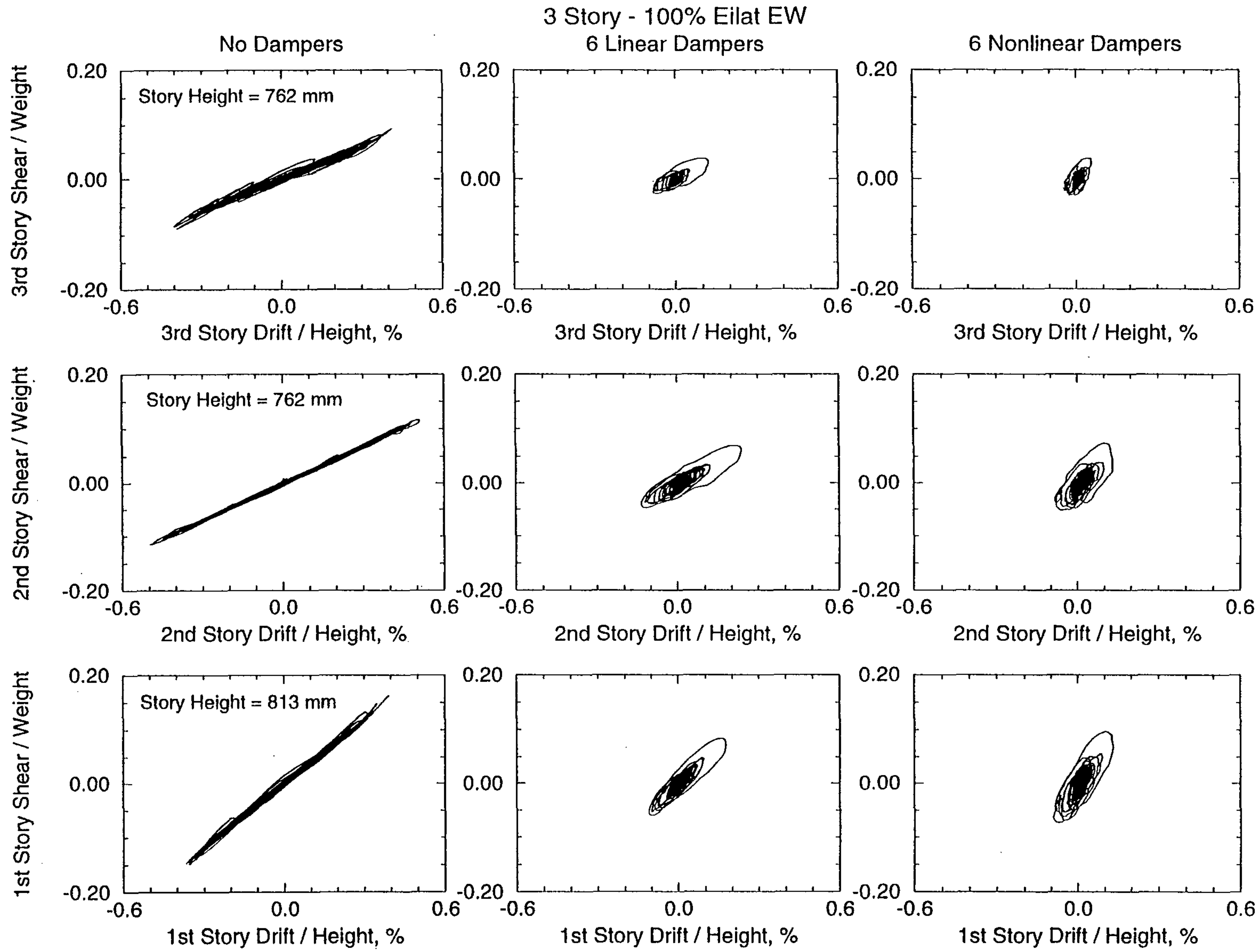

FIGURE 5-23 Comparison of Normalized Shear-Drift Loops of 3-Story Repaired Structure without, with Six Linear and with Six Nonlinear Dampers Subjected to 100% Eilat EW Earthquake

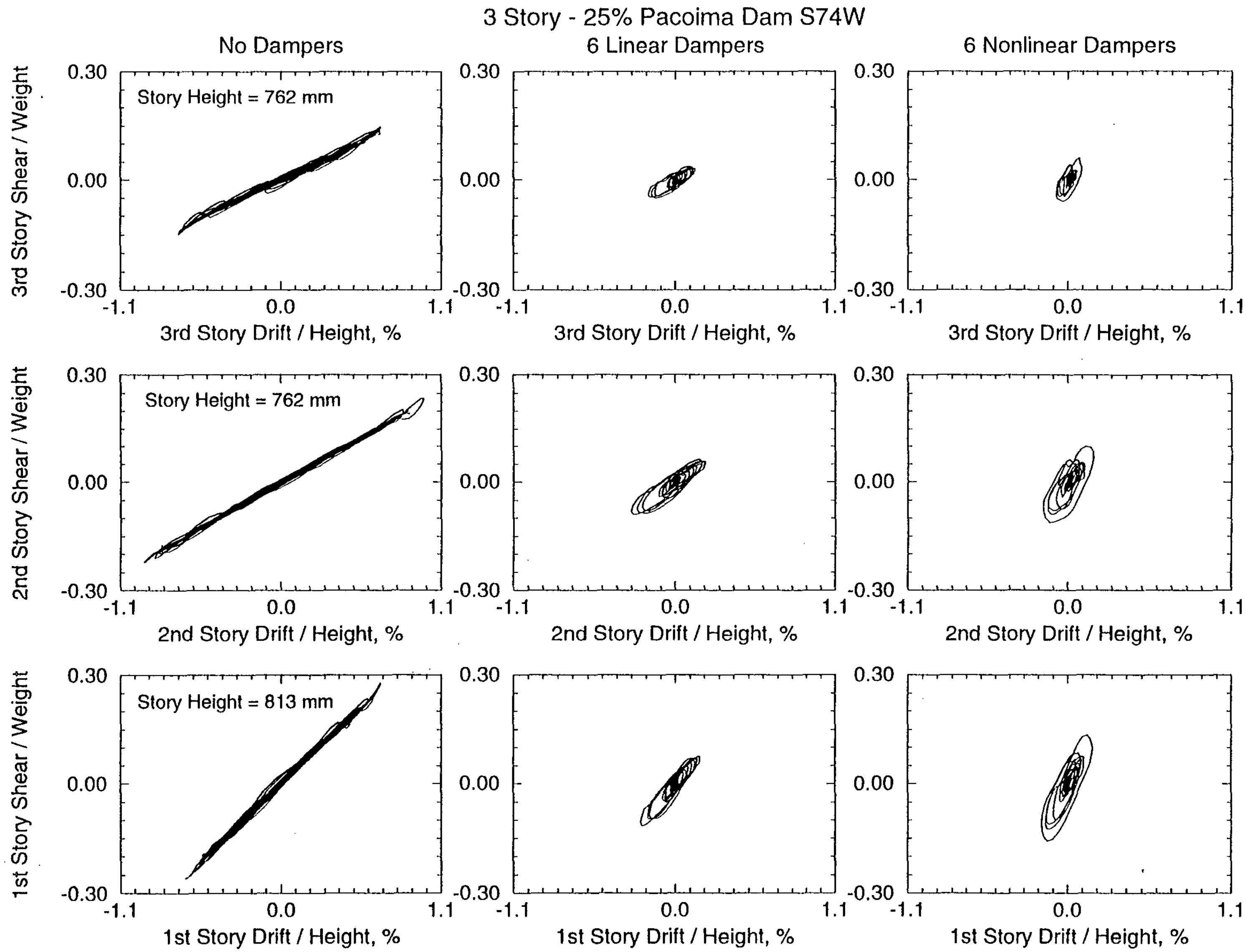

FIGURE 5-24 Comparison of Normalized Shear-Drift Loops of 3-Story Repaired Structure without, with Six Linear and with Six Nonlinear Dampers Subjected to 25% Pacoima Dam Earthquake

as those in Figures 5-13 to 5-24; note that the same input motions were used in testing of the structure without dampers) the resulting interstory velocities were below this limit and the forces mobilized in the nonlinear dampers were larger than those mobilized in the linear dampers.

A direct comparison of loops of story shear force versus drift for stronger input motions is provided in Figures 5-25 to 5-33 for the 3-story structure. There are some aspects of behavior seen in these figures that require discussion:

(a) In general, nonlinear dampers, as expected, produce larger drift response reduction than linear dampers.

(b) In some tests with small drift (thus, also low interstory velocity) the recorded loops exhibit a behavior that indicates higher effective stiffness (slope of loop) in the case of nonlinear dampers than in the case of linear dampers (e.g., see Figures 5-30 and 5-31). It would appear as if the nonlinear dampers exhibited stiffness, that is, they behaved as viscoelastic elements. While there may have been some stiffness contributed by the nonlinear dampers due to the generation of high frequency motion, the primary source of this phenomenon is the large damping force which in these tests was of the same order or larger than the restoring force. That is, the damping force is large enough and of such nature as to alter the appearance of the loop. Confirmation that the nonlinear dampers did not contribute to stiffness was made in the analytical prediction of response (see Section 6) in which the analytical model, without accounting for storage stiffness in the nonlinear dampers, provided results in good agreement with the experiments.

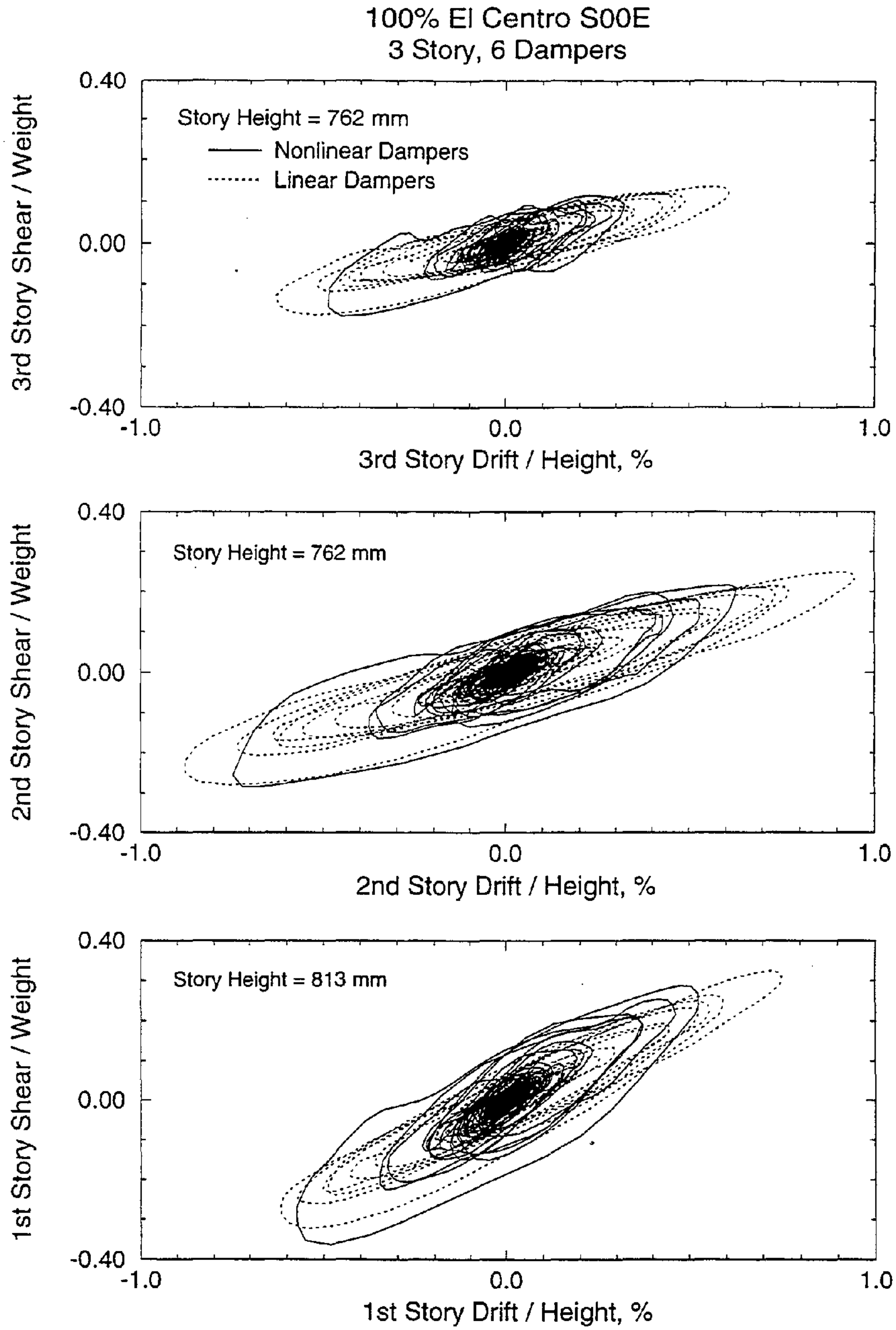

FIGURE 5-25 Comparison of Normalized Shear-Drift Loops of 3-Story Repaired Structure with Six Linear and Six Nonlinear Dampers Subjected to 100% El Centro Earthquake

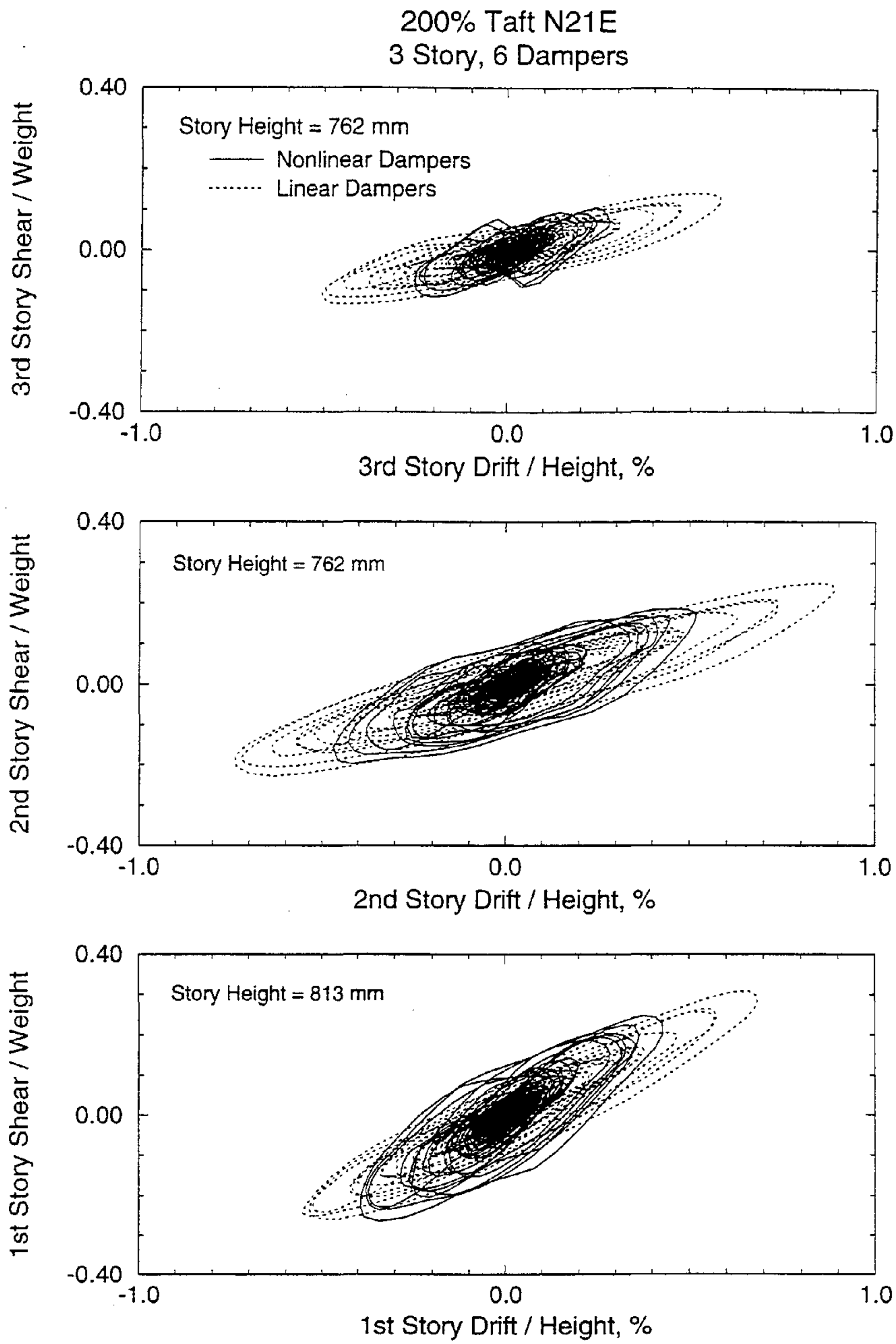

FIGURE 5-26 Comparison of Normalized Shear-Drift Loops of 3-Story Repaired Structure with Six Linear and Six Nonlinear Dampers Subjected to 200% Taft Earthquake

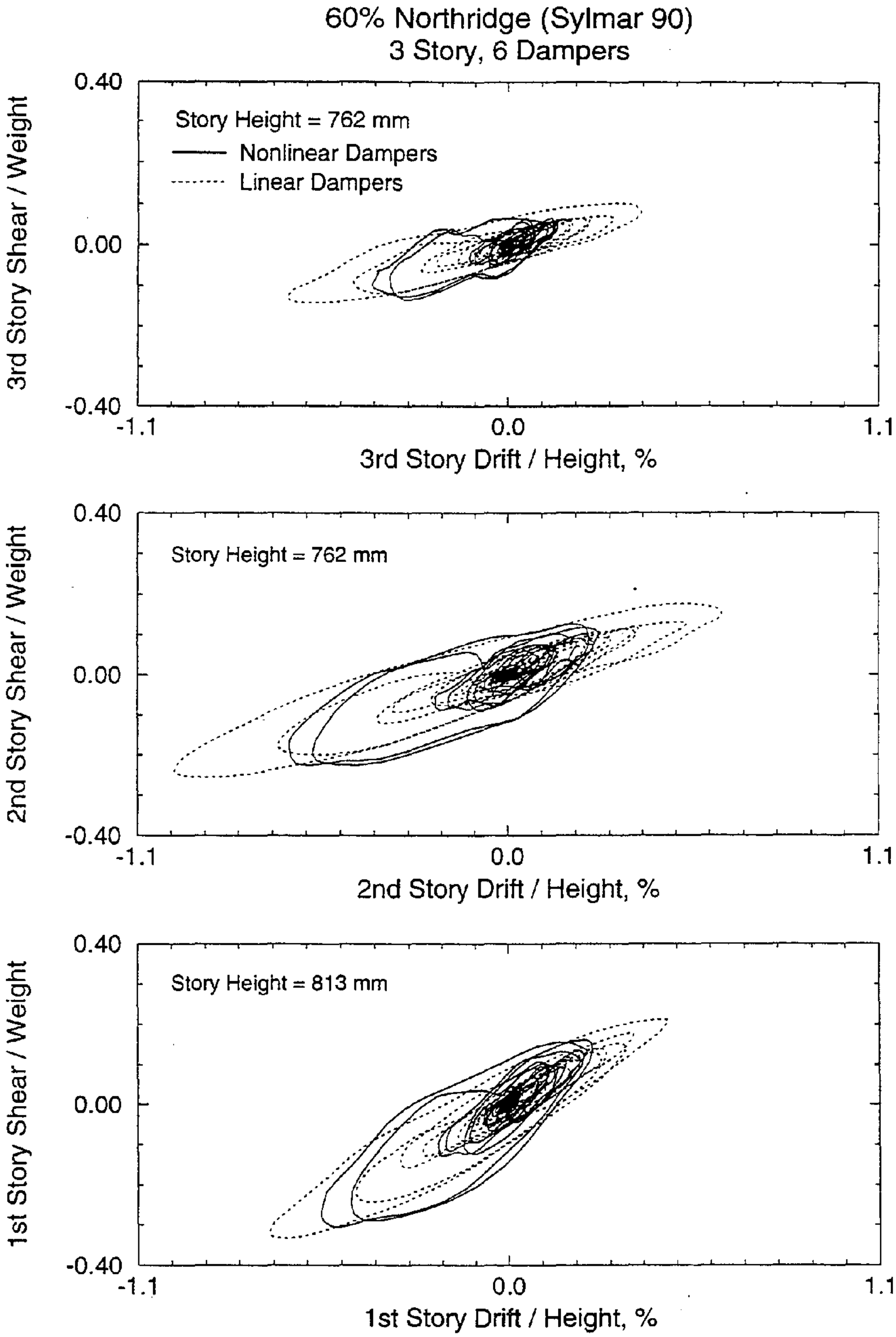

FIGURE 5-27 Comparison of Normalized Shear-Drift Loops of 3-Story Repaired Structure with Six Linear and Six Nonlinear Dampers Subjected to 60% Northridge (Sylmar 90) Earthquake

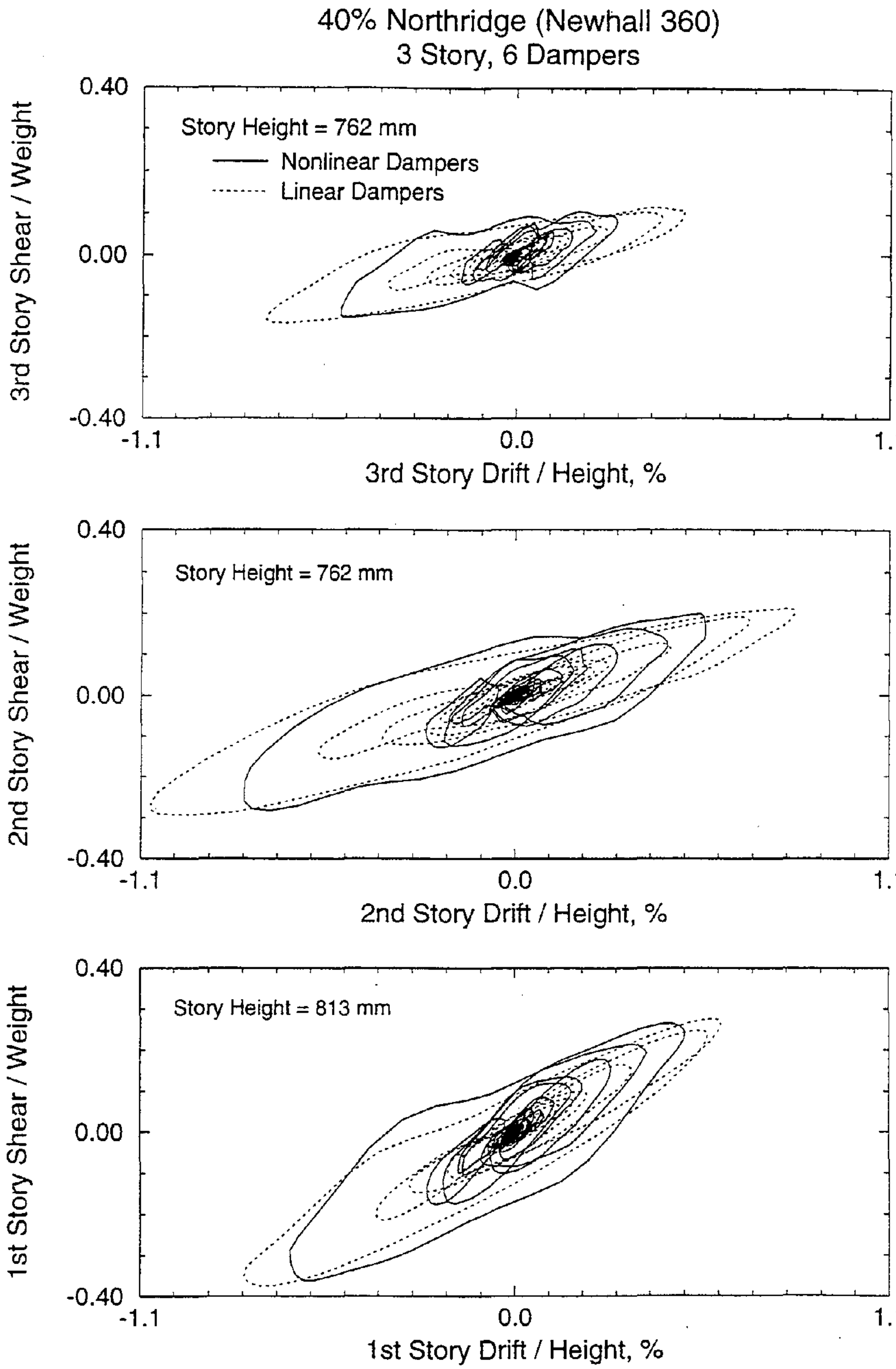

FIGURE 5-28 Comparison of Normalized Shear-Drift Loops of 3-Story Repaired Structure with Six Linear and Six Nonlinear Dampers Subjected to 40% Northridge (Newhall 360) Earthquake

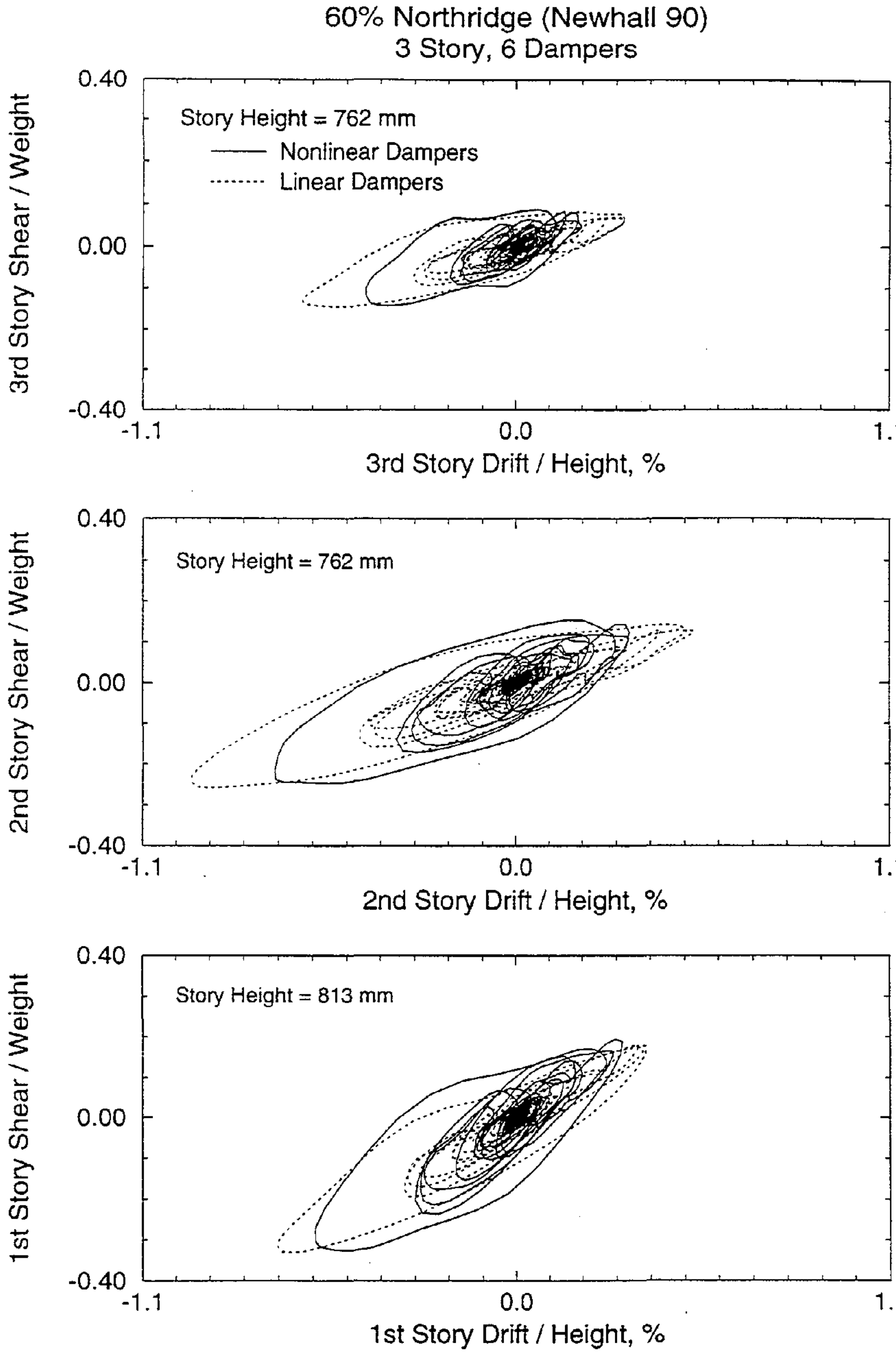

FIGURE 5-29 Comparison of Normalized Shear-Drift Loops of 3-Story Repaired Structure with Six Linear and Six Nonlinear Dampers Subjected to 60% Northridge (Newhall 90) Earthquake

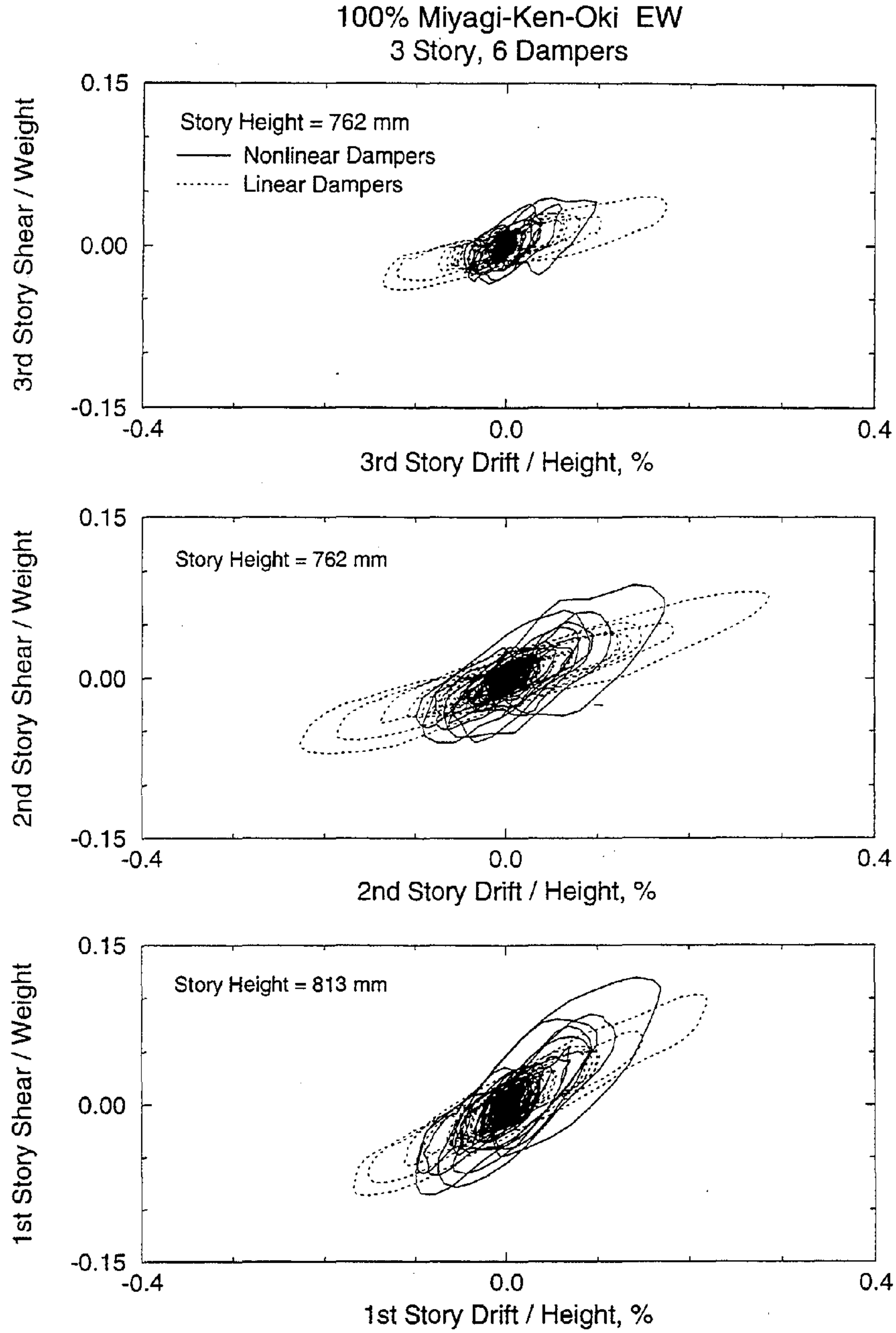

FIGURE 5-30 Comparison of Normalized Shear-Drift Loops of 3-Story Repaired Structure with Six Linear and Six Nonlinear Dampers Subjected to 100% Miyagi-Ken-Oki Earthquake

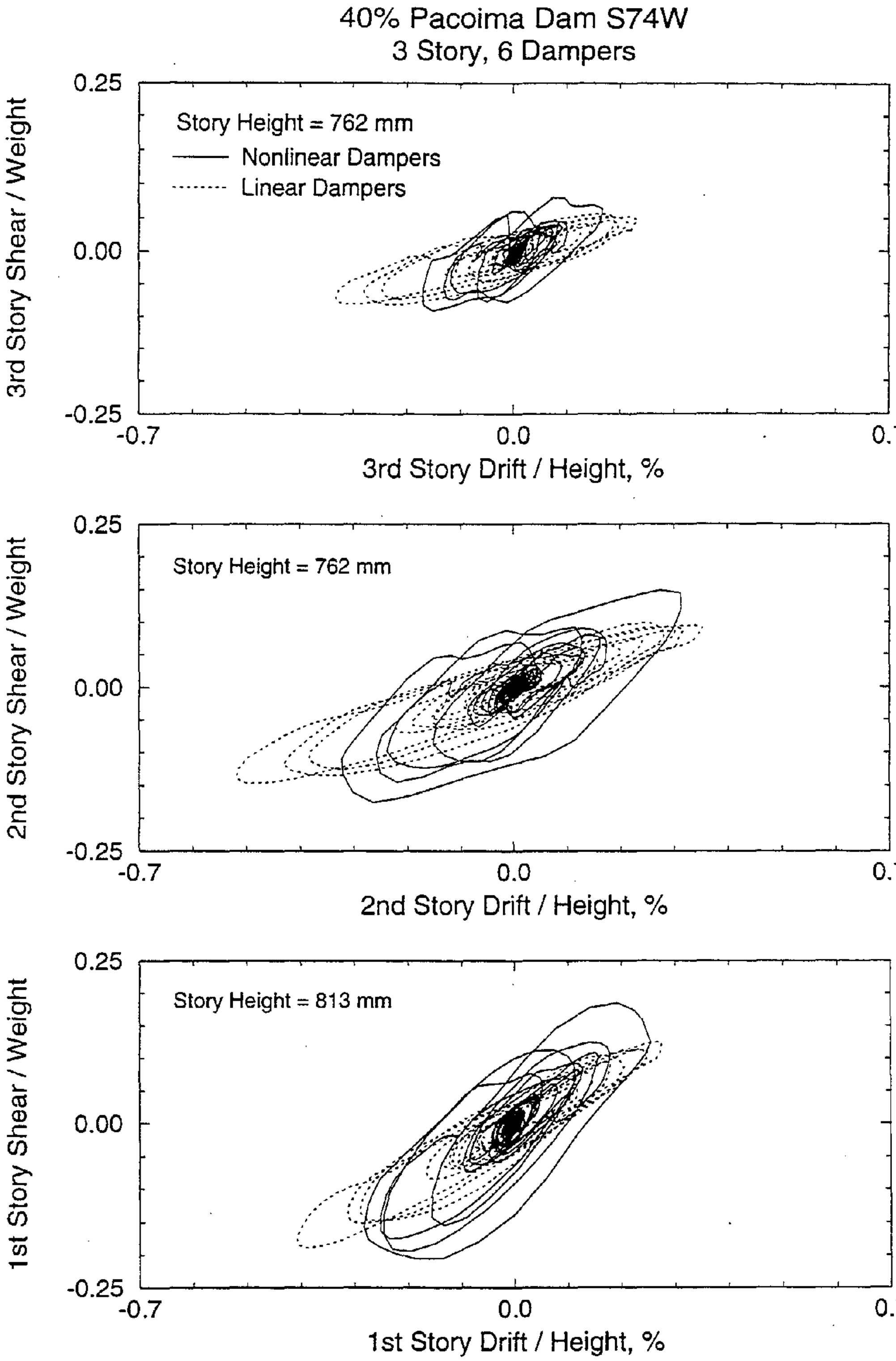

FIGURE 5-31 Comparison of Normalized Shear-Drift Loops of 3-Story Repaired Structure with Six Linear and Six Nonlinear Dampers Subjected to 40% Pacoima Dam Earthquake

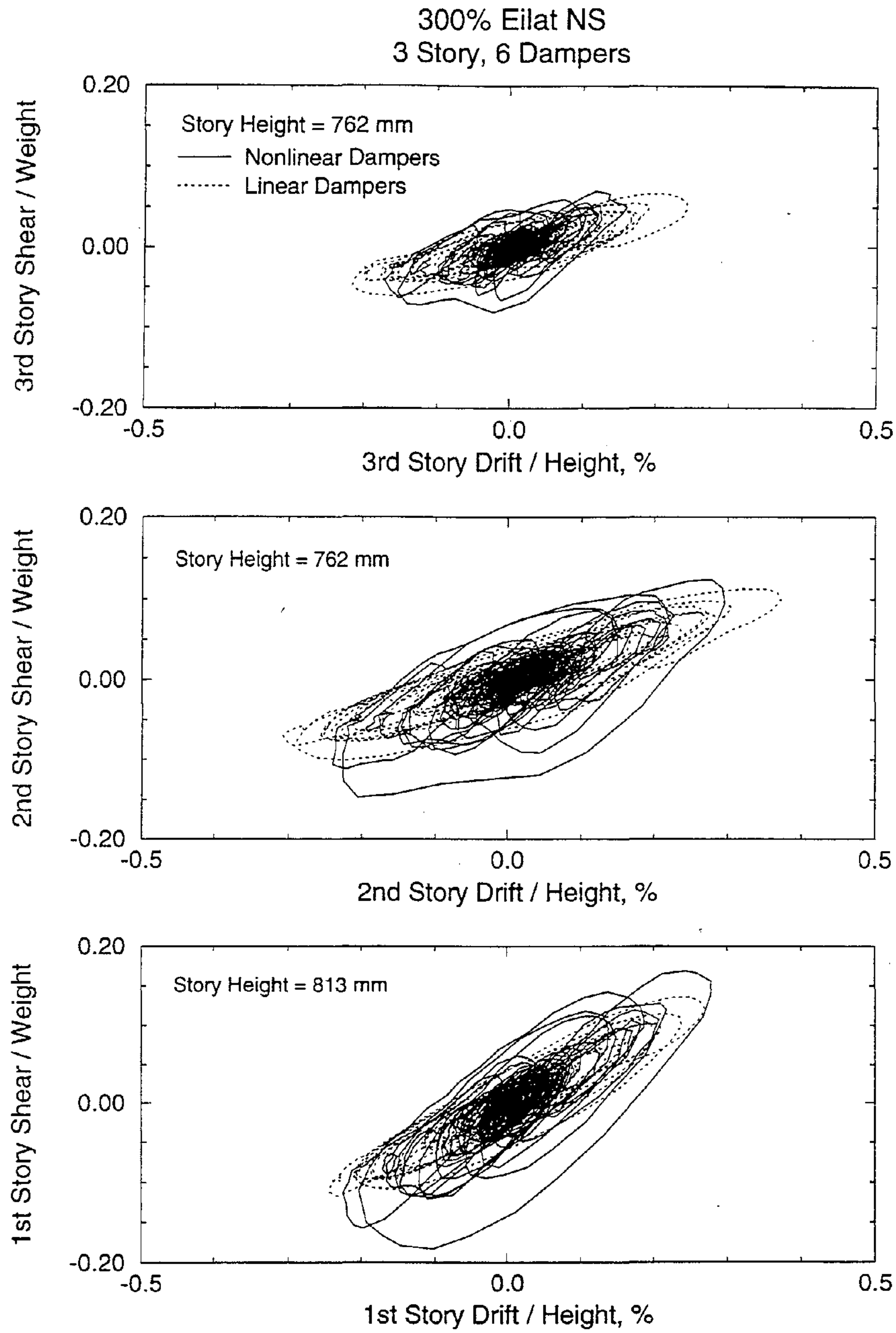

FIGURE 5-32 Comparison of Normalized Shear-Drift Loops of 3-Story Repaired Structure with Six Linear and Six Nonlinear Dampers Subjected to 300% Eilat NS Earthquake

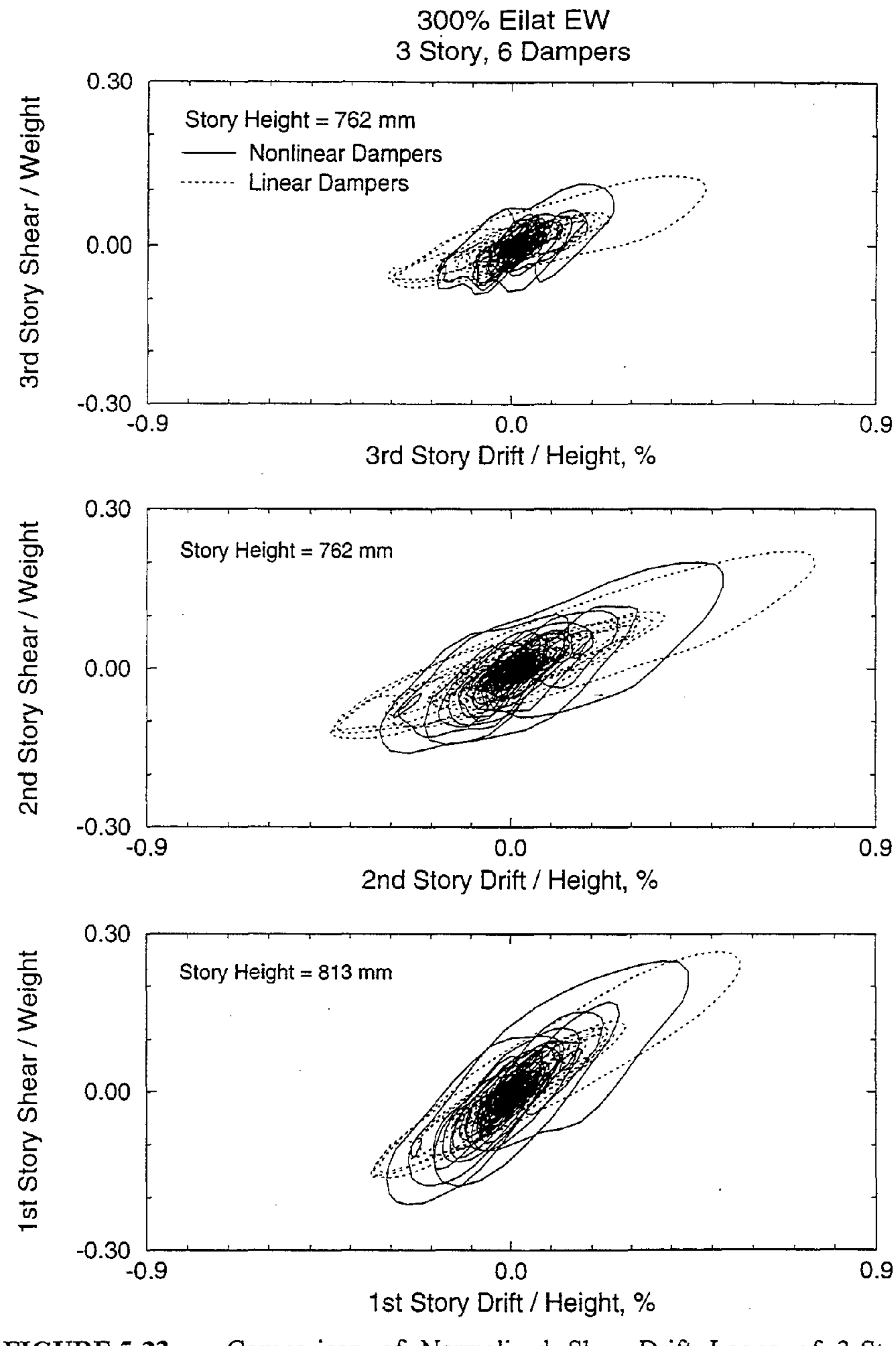

FIGURE 5-33 Comparison of Normalized Shear-Drift Loops of 3-Story Repaired Structure with Six Linear and Six Nonlinear Dampers Subjected to 300% Eilat EW Earthquake

(c) In some tests, particularly those with low interstory velocity, the story shear force in the case of nonlinear dampers exceeds that recorded in the case of linear dampers despite the lesser drift. This is due to the existence of a significant component of the peak damping force at the time of maximum drift. That is, due to the nonlinear nature of the damping force, a large portion of the peak damping force occur in-phase with the peak restoring force. Despite this, however, the shear force and moment actions in the columns are reduced (due to lesser drift) at the expense of higher axial column force (resulting from the damper force).

5.3.3 Floor Response Spectra

Figures 5-34 to 5-44 present floor response spectra for the tested 3-story structure without and with linear and nonlinear dampers. These spectra of acceleration were constructed using the recorded floor acceleration histories for a single degree of freedom system with natural frequency in the range 0.1 to 30 Hz and 2% damping ratio. They represent the response of light weight attachments (secondary systems) to the floor.

First, Figures 5-34 to 5-36 compare the floor response spectra of the structure without and with a complete vertical distribution of dampers for two weak earthquake components and one moderately strong earthquake. It is seen in these figures that the spectra for the structure without dampers exhibit distinct and large peaks around the natural frequencies of the structure. The spectra for the structure with dampers exhibit much lower ordinates over nearly the entire considered frequency range. Furthermore, for the case of weak excitation the spectra of the damped structure lack distinct peaks.

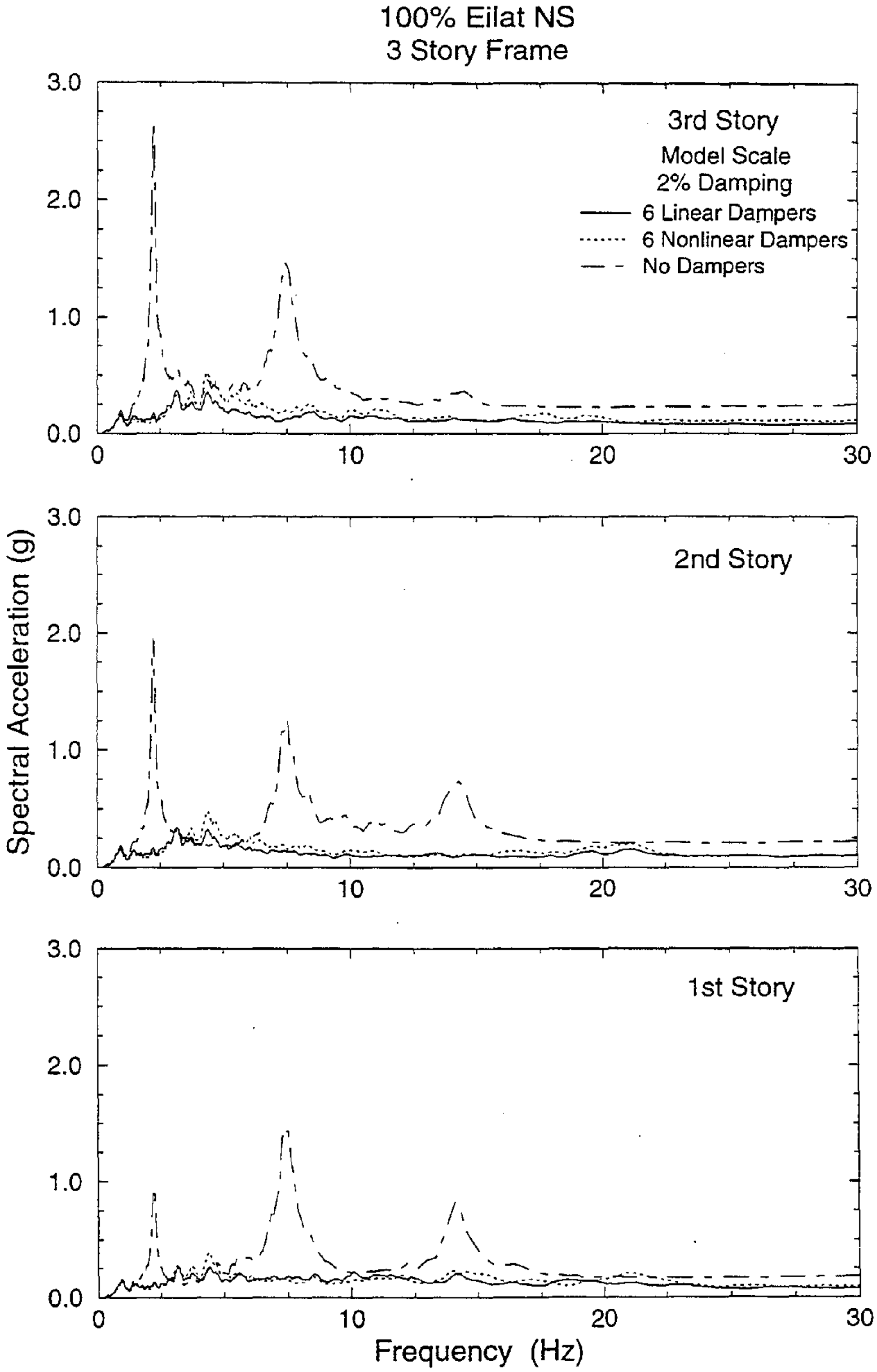

FIGURE 5-34 Comparison of Floor Response Spectra of 3-Story Repaired Structure without, with Six Linear and with Six Nonlinear Dampers Subjected to 100% Eilat NS Earthquake

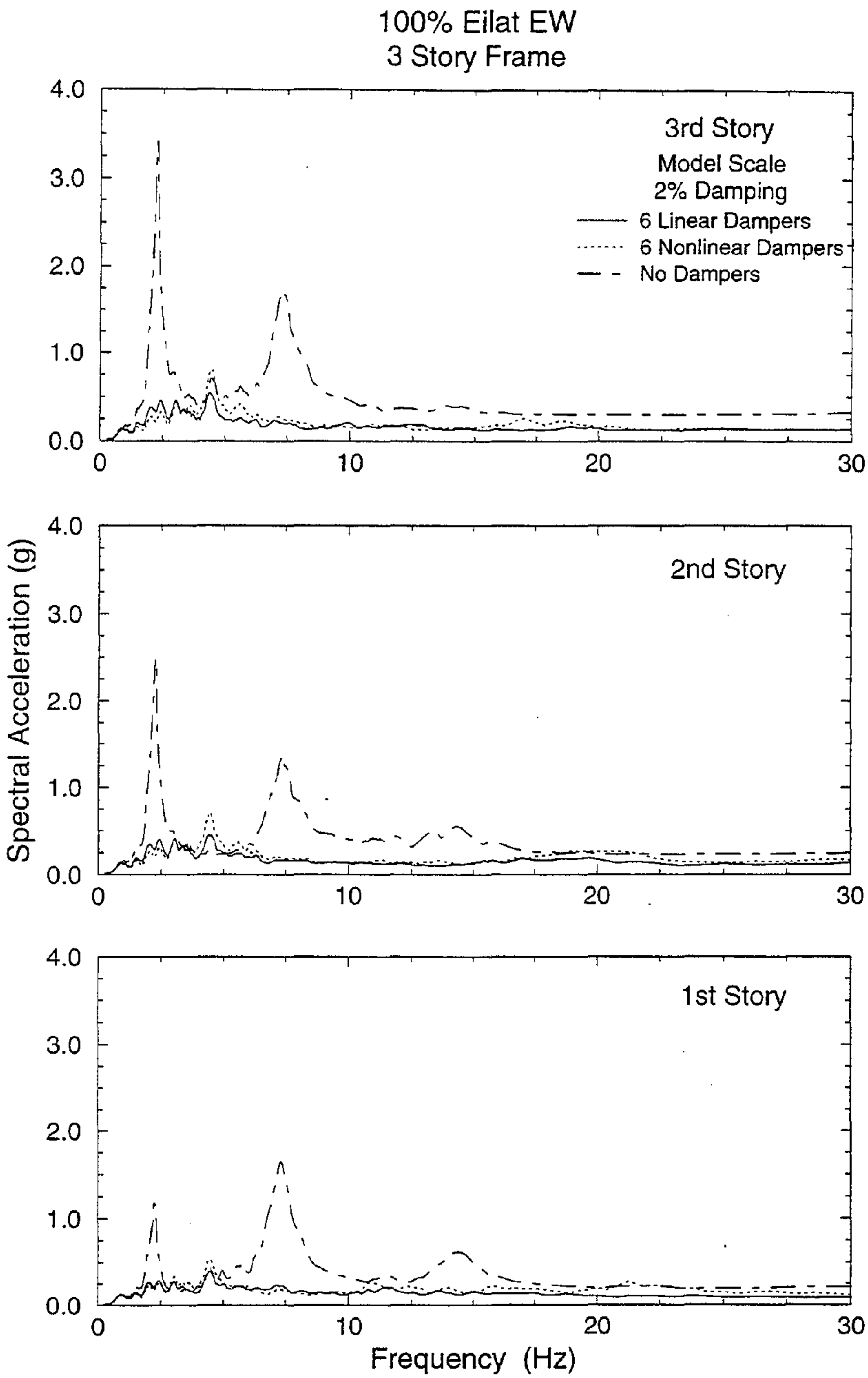

FIGURE 5-35 Comparison of Floor Response Spectra of 3-Story Repaired Structure without, with Six Linear and with Six Nonlinear Dampers Subjected to 100% Eilat EW Earthquake

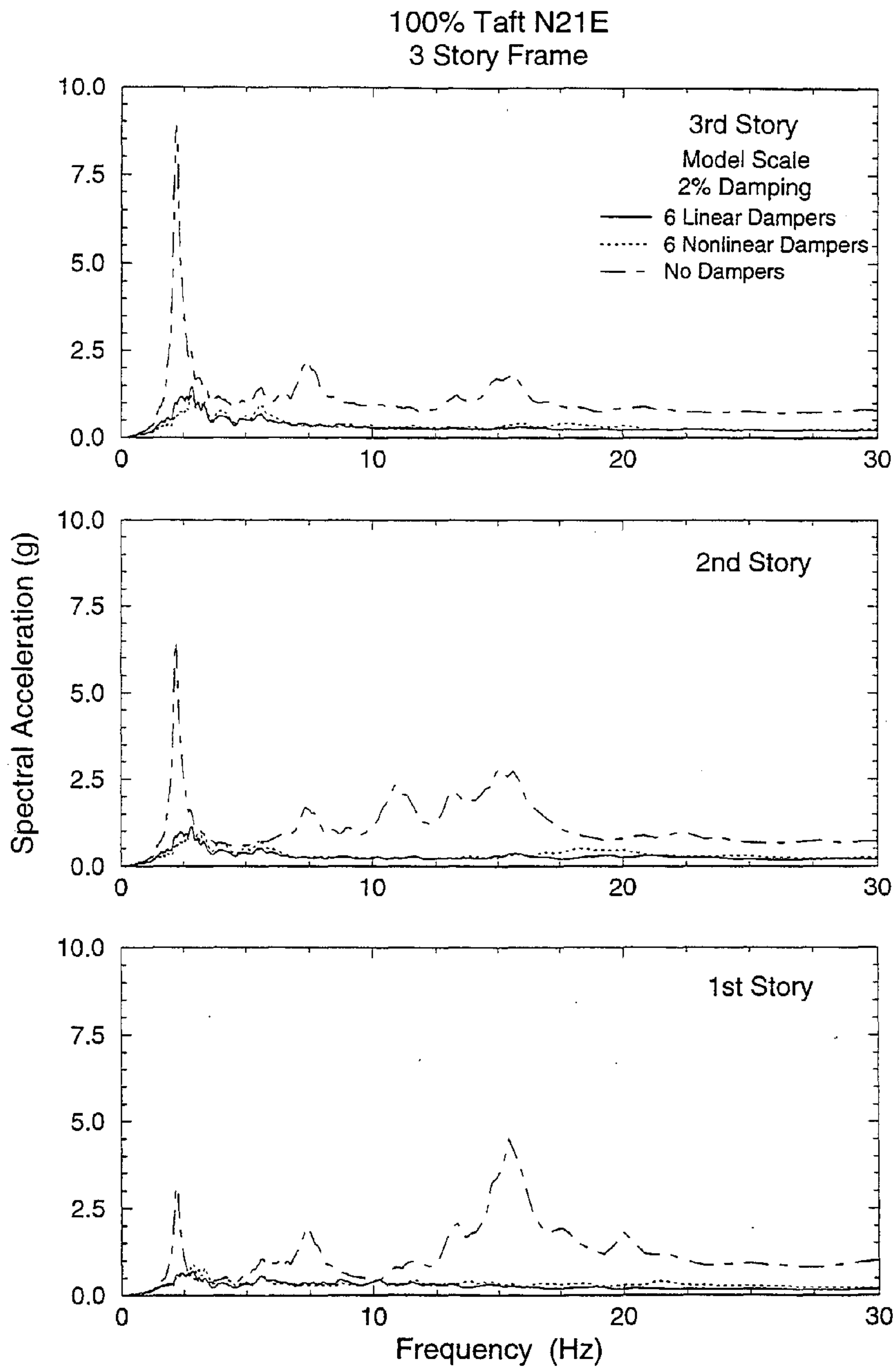

FIGURE 5-36 Comparison of Floor Response Spectra of 3-Story Repaired Structure without, with Six Linear and with Six Nonlinear Dampers Subjected to 100% Taft Earthquake

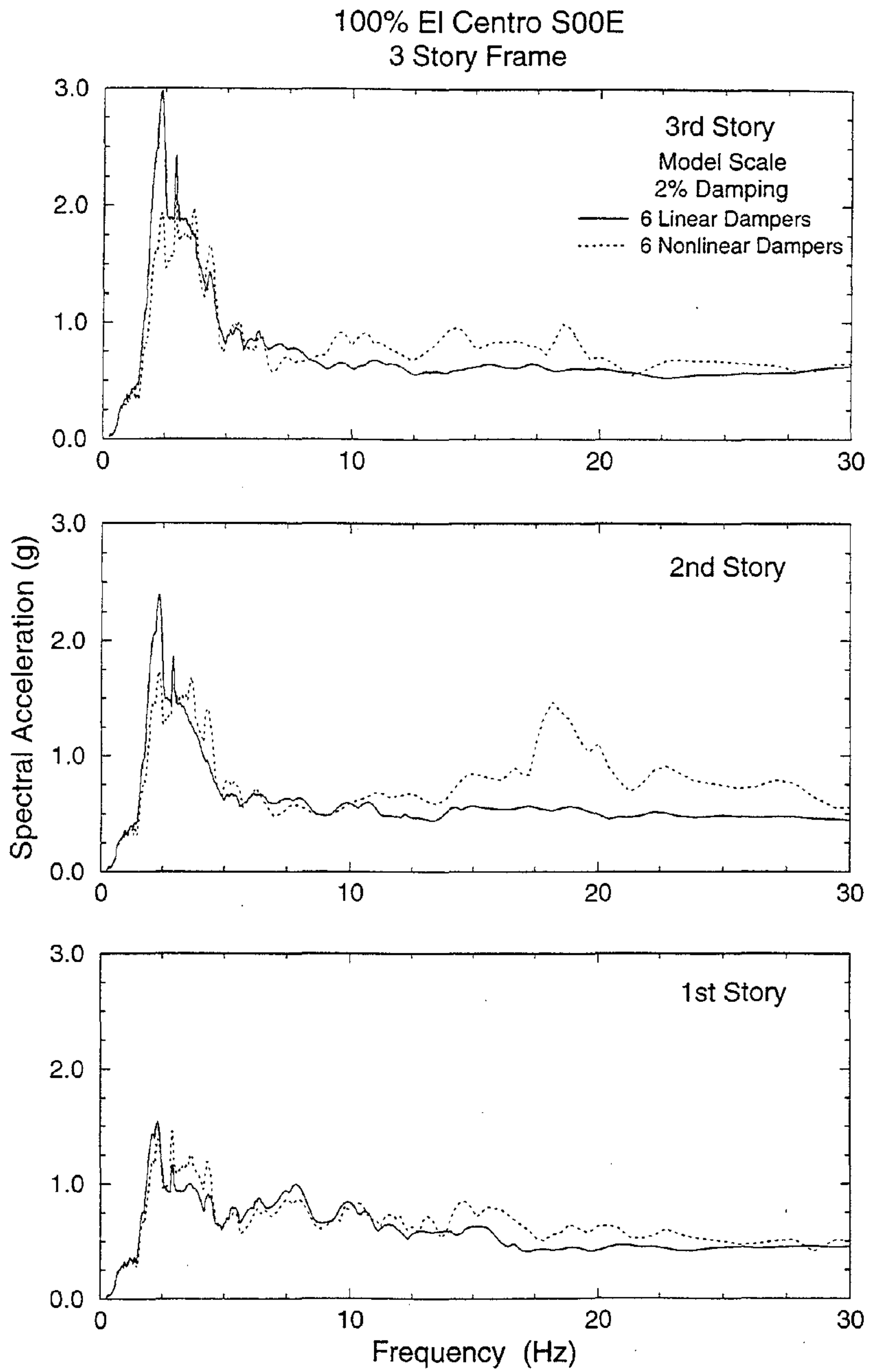

FIGURE 5-37 Comparison of Floor Response Spectra of 3-Story Repaired Structure with Six Linear and Six Nonlinear Dampers Subjected to 100% El Centro Earthquake

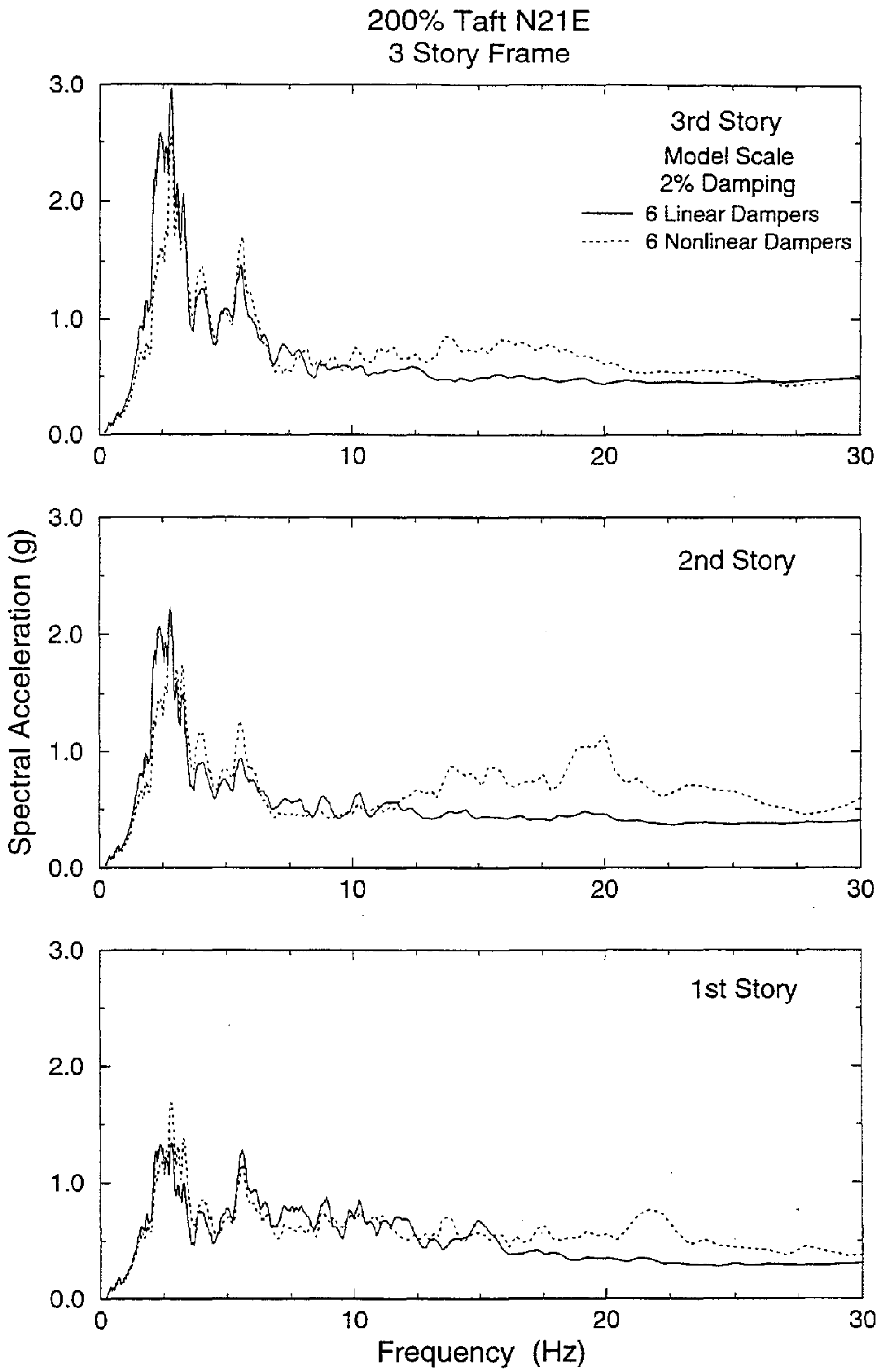

FIGURE 5-38 Comparison of Floor Response Spectra of 3-Story Repaired Structure with Six Linear and Six Nonlinear Dampers Subjected to 200% Taft Earthquake

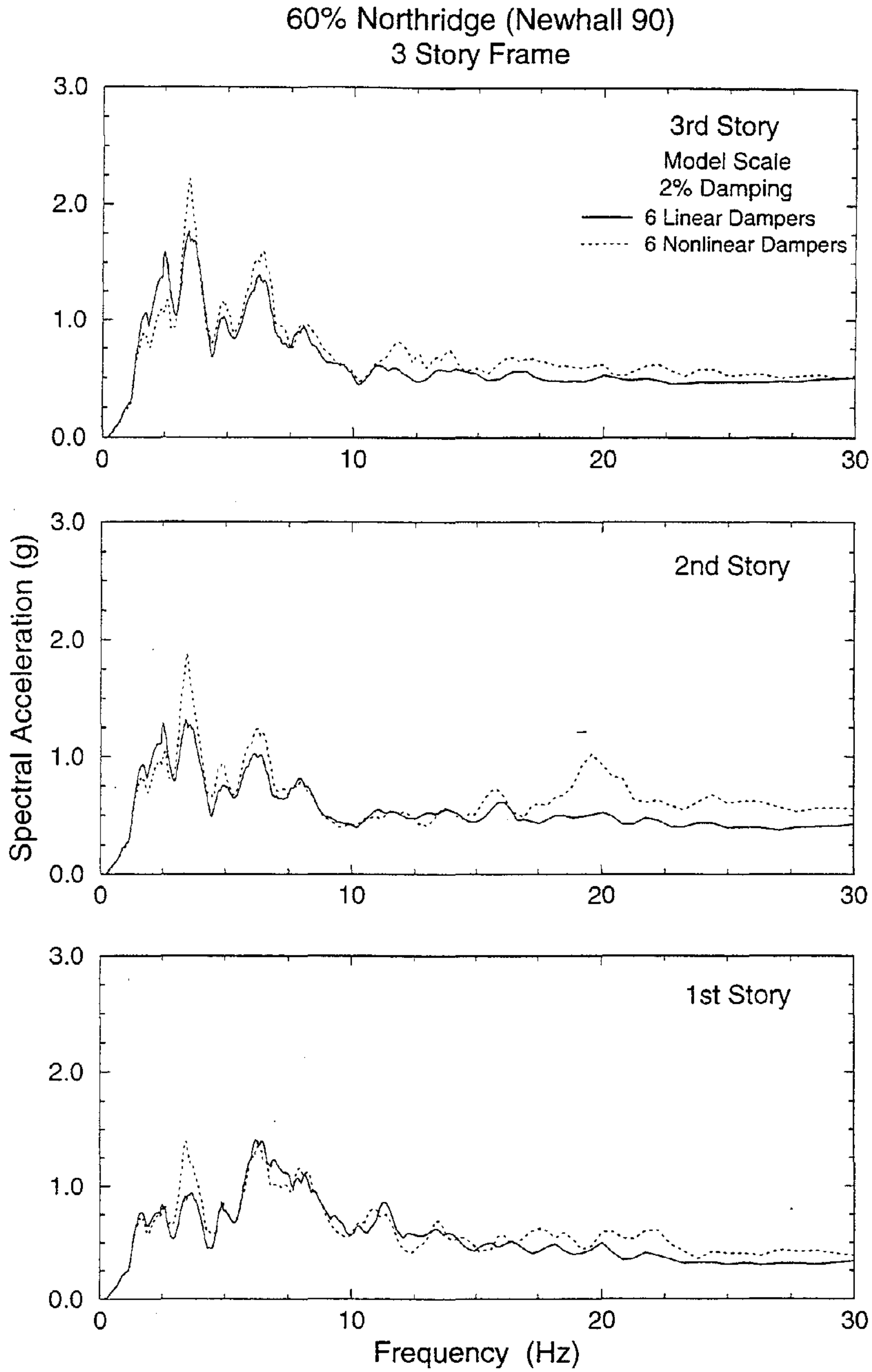

FIGURE 5-39 Comparison of Floor Response Spectra of 3-Story Repaired Structure with Six Linear and Six Nonlinear Dampers Subjected to 60% Northridge (Newhall 90) Earthquake

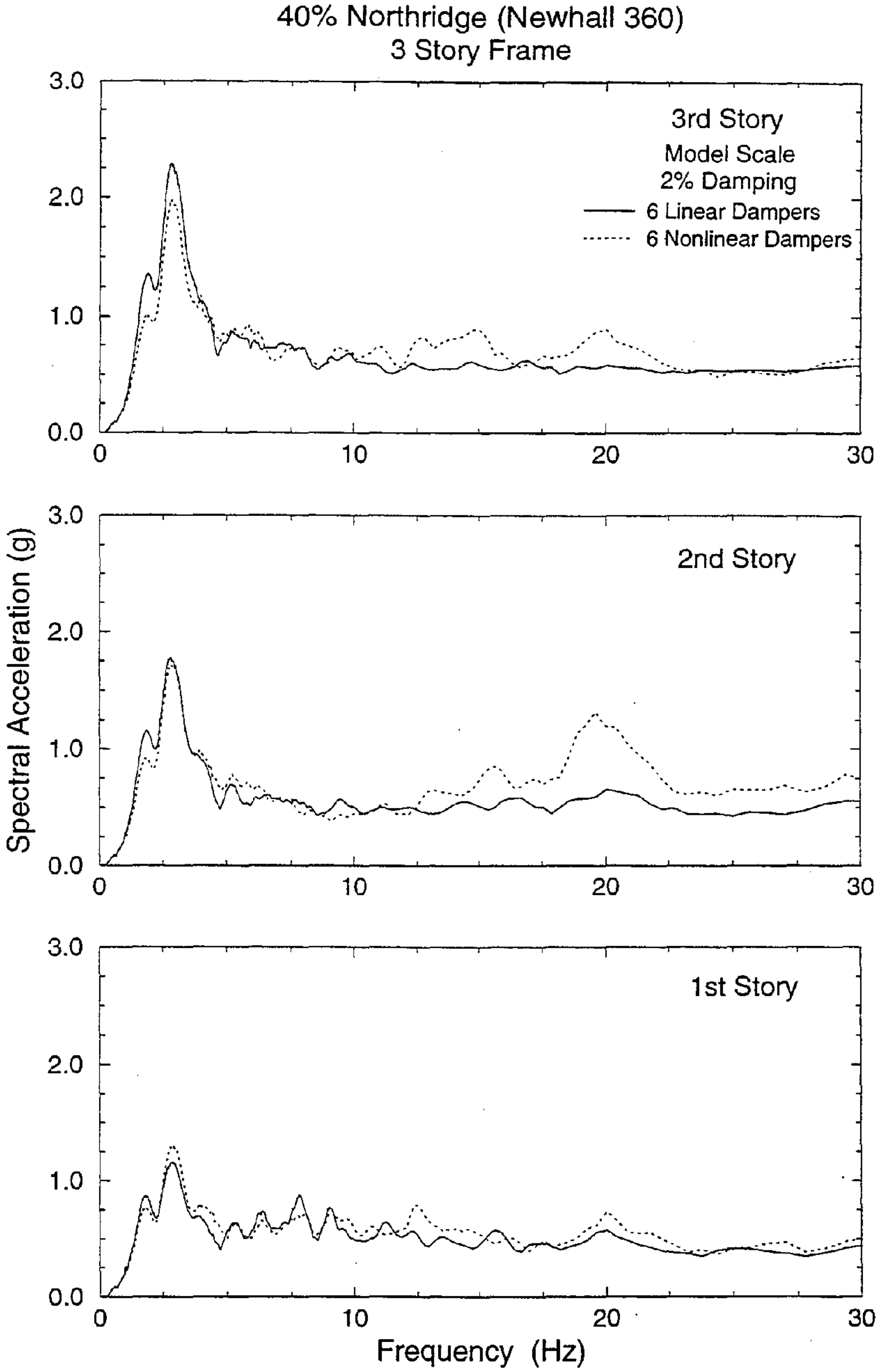

FIGURE 5-40 Comparison of Floor Response Spectra of 3-Story Repaired Structure with Six Linear and Six Nonlinear Dampers Subjected to 40% Northridge (Newhall 360) Earthquake

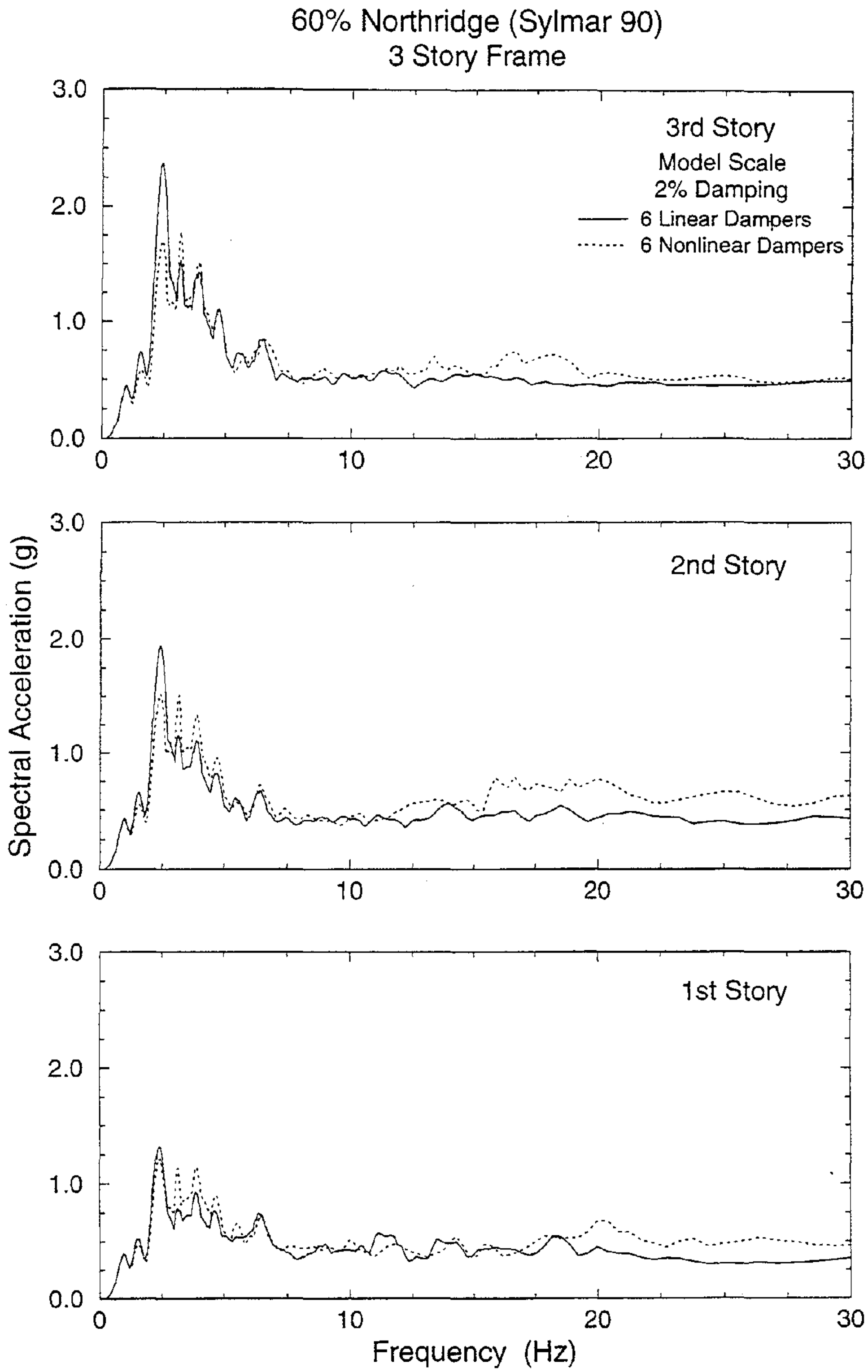

FIGURE 5-41 Comparison of Floor Response Spectra of 3-Story Repaired Structure with Six Linear and Six Nonlinear Dampers Subjected to 60% Northridge (Sylmar 90) Earthquake

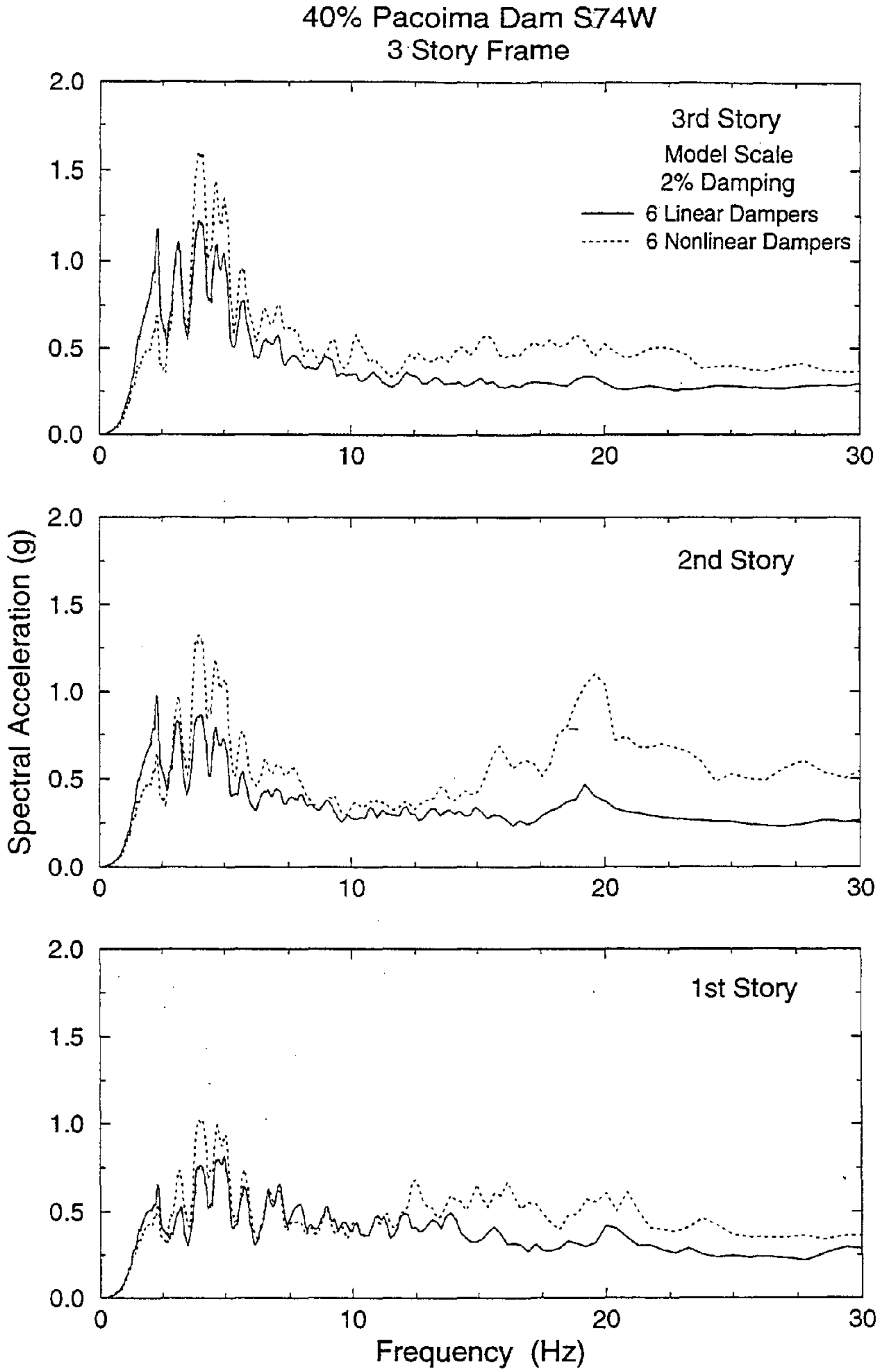

FIGURE 5-42 Comparison of Floor Response Spectra of 3-Story Repaired Structure with Six Linear and Six Nonlinear Dampers Subjected to 40% Pacoima Dam Earthquake

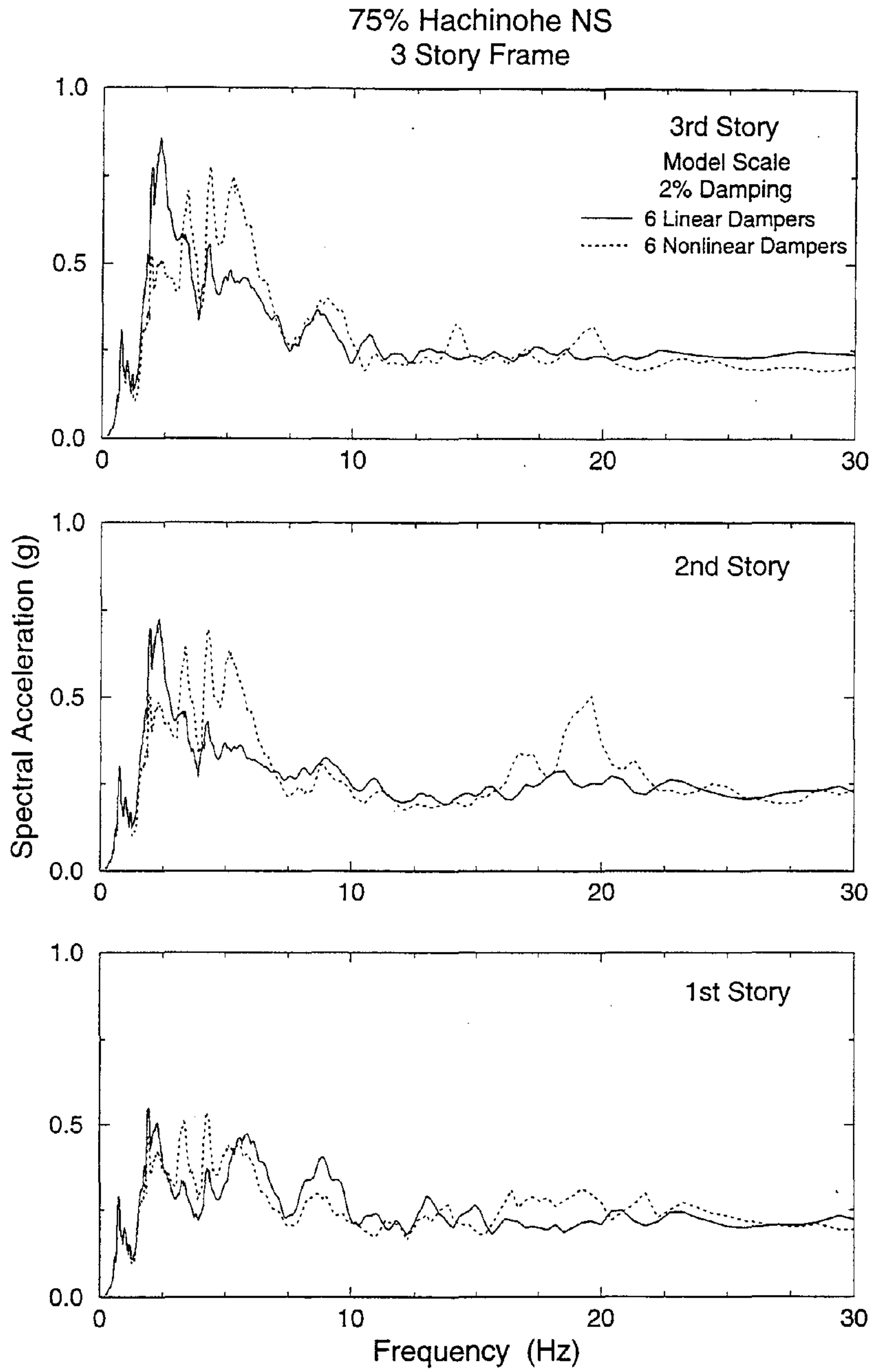

FIGURE 5-43 Comparison of Floor Response Spectra of 3-Story Repaired Structure with Six Linear and Six Nonlinear Dampers Subjected to 75% Hachinohe Earthquake

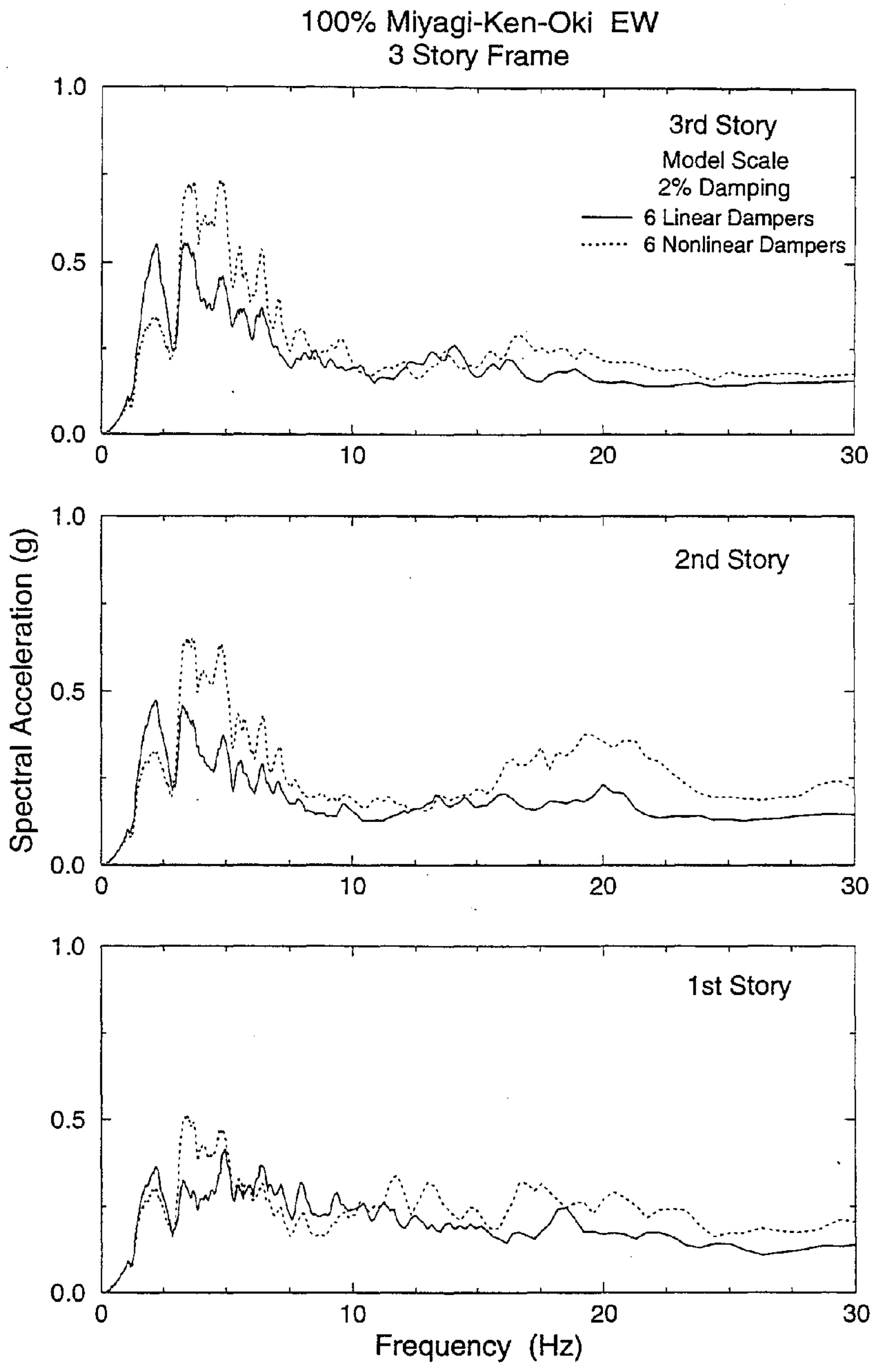

FIGURE 5-44 Comparison of Floor Response Spectra of 3-Story Repaired Structure with Six Linear and Six Nonlinear Dampers Subjected to 100% Miyagi-Ken-Oki Earthquake

Figures 5-37 to 5-41 compare floor spectra of the structure with linear and nonlinear dampers for stronger earthquake motions. In this case both sets of floor spectra exhibit peaks around the fundamental frequency of the structure. Peak spectral values in the two cases of dampers appear comparable in value, with the spectra of the structure with nonlinear dampers exhibiting moderately lower values than those of the structure with linear dampers. Moreover, the floor spectra of the structure with nonlinear dampers show in some cases moderately strong ordinates at high frequencies (around 20 Hz). This clearly indicates the existence of high frequency components in the response history of the structure, an expected phenomenon given the nonlinearity of the dampers.

Finally, Figures 5-42 to 5-44 compare floor spectra of the structure with linear and nonlinear dampers for weaker earthquake motions. The spectra resemble those of Figures 5-34 and 5-35 that lack distinct peaks at frequencies related to the natural frequencies of the structure. Rather, they exhibit moderately larger ordinates in the frequency range of 2 to 7 Hz. It is possible that this behavior is caused by the frictional behavior of the dampers (friction in seals) which tends to have some influence at low velocity motions when the damping force (due to fluid orificing) is low.

5.3.4 Energy Equation

The derivation of an energy equation and comparison of energy time histories for structures with and without dampers provide useful insight into the behavior of damped structures. The energy equation may be written in the form (Uang, 1988; Constantinou and Symans, 1992).

$$E = E_K + E_s + E_h + E_d \tag{5-1}$$

where E is the absolute input energy, E_k is the kinetic energy, E_s is the elastic (recoverable) strain energy, E_h is the energy dissipated in the structural system (inelastic action, friction in joints, etc.) and E_d is the energy dissipated by an added energy dissipation system.

For a single-degree-of-freedom system, such as the tested one-story structure, the equation of motion may be written in the form (see also Section 4.2)

$$m\ddot{u} + c_u\dot{u} + ku + \eta p_d = -m\ddot{u}_g \tag{5-2}$$

where ηp_d is the force from added viscous dampers, and the term $c_u\dot{u} + ku$ is used to model elastic behavior and inherent ability of the frame to dissipate energy (assumed here to be of viscous nature). The absolute input energy is the work done by the base shear on the ground displacement, that is,

$$E = \int_0^t m(\ddot{u} + \ddot{u}_g)du_g = \int_0^t m(\ddot{u} + \ddot{u}_g)\dot{u}_g dt \tag{5-3}$$

The kinetic energy is

$$E_k = \frac{1}{2}m(\dot{u} + \dot{u}_g)^2 \tag{5-4}$$

The strain energy is

$$E_s = \frac{1}{2} ku^2 \tag{5-5}$$

Finally, the energy dissipated by viscous dampers is

$$E_d = \int_0^t (\eta p_d \cos\theta) du = \int_0^t (\eta p_d \cos\theta) \dot{u} dt \tag{5-6}$$

Equations (5-3) to (5-6) allow the calculation of the basic energy components from measured dynamic response. That is, during testing the quantities $(\ddot{u} + \ddot{u}_g)$, $\dot{u}_g$, $\dot{u}$, u and ηp_d are either directly measured or calculated from measured response (e.g., velocities are obtained from numerical differentiation of displacement records). The remaining energy quantity, E_h , is then obtained from Equation (5-1).

An example of energy time histories is provided in Figure 5-45 for the tested one-story structure in the Taft earthquake. Each graph shows the history of the absolute input energy E, the history of energy $E - E_k - E_s$ and the history of energy E_d. For the structure without dampers, the quantity $E - E_k - E_s$ is equal to the energy dissipated by the structural frame, that is E_h. For the structure with dampers, the quantity $E - E_k - E_s - E_d$ is equal to the energy dissipated by the structural frame exclusive of dampers, that is, again E_h . These quantities are identified directly on each graph.

There are two important observations to be made in the results of Figure 5-45. The same observations can be made in the energy histories shown in Figure 5-46 for other earthquake inputs. The first observation is that the addition of dampers results in a substantial

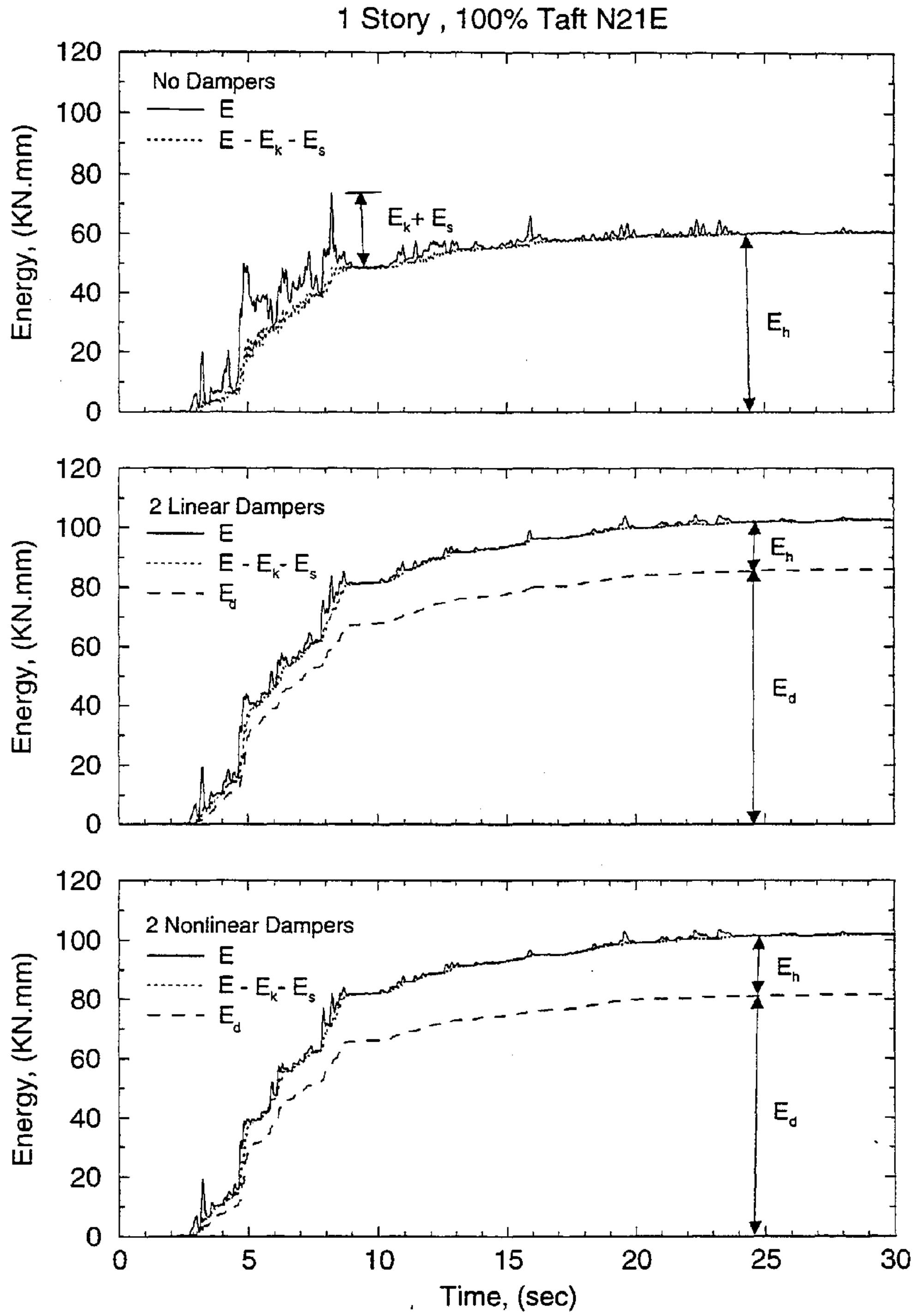

FIGURE 5-45 Energy Time Histories of One-Story Structure without, with Two Linear and with Two Nonlinear Dampers Subjected to 100% Taft Earthquake

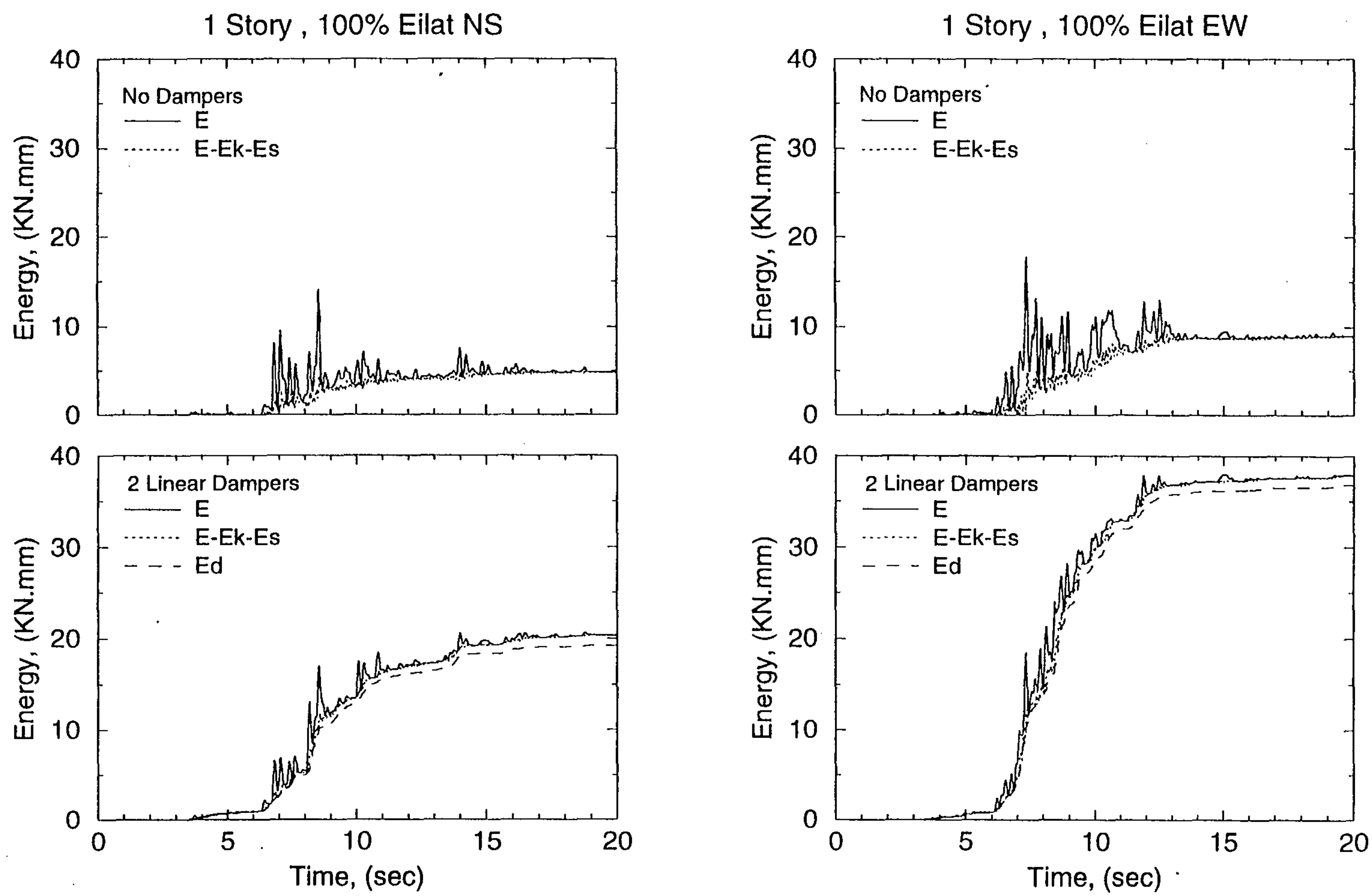

FIGURE 5-46 Energy Time Histories of One-Story Structure without and with Two Linear Dampers Subjected to 100% Eilat NS and 100% Eilat EW Earthquakes

reduction of kinetic and strain energy and of energy dissipated by the structural frame, E_h. The latter demonstrates reduction in damage or in the potential for damage of the structural frame. Rather, energy is dissipated in the added damping system.

The other observation is that the absolute input energy is more in the structure with dampers than in the structure without dampers. While this may not be always true, it is of significant interest to identify the reason for this increase in energy input and discuss its consequences. It should be noted that for some earthquakes this increase in energy input is substantial (about four times for the earthquake of Figure 5-46).

To gain some insight into the behavior of structures without and with dampers, Figure 5-47 is used to present recorded histories of base shear $m(\ddot{u}+\ddot{u}_g)$, ground velocity $\dot{u}_g$, power $m(\ddot{u}+\ddot{u}_g).\dot{u}_g$ and absolute energy input (Equation 5-3) in the tests with the Taft earthquake. It may be seen in these figures that the reason for increased energy input is not an increase in base shear or power but rather is the biasing of the power time history in the case of the structure with dampers. That is, despite the lesser instantaneous power in the case of the structure with dampers, its bias towards one direction leads to larger absolute input energy (which is the integral of power over time).

To further elucidate this difference, we consider power and energy requirements for imposing a harmonic displacement $u = u_o \sin\Omega t$ to a spring of constant k and a linear viscous damper of constant c. For the case of spring, the power P and energy E are

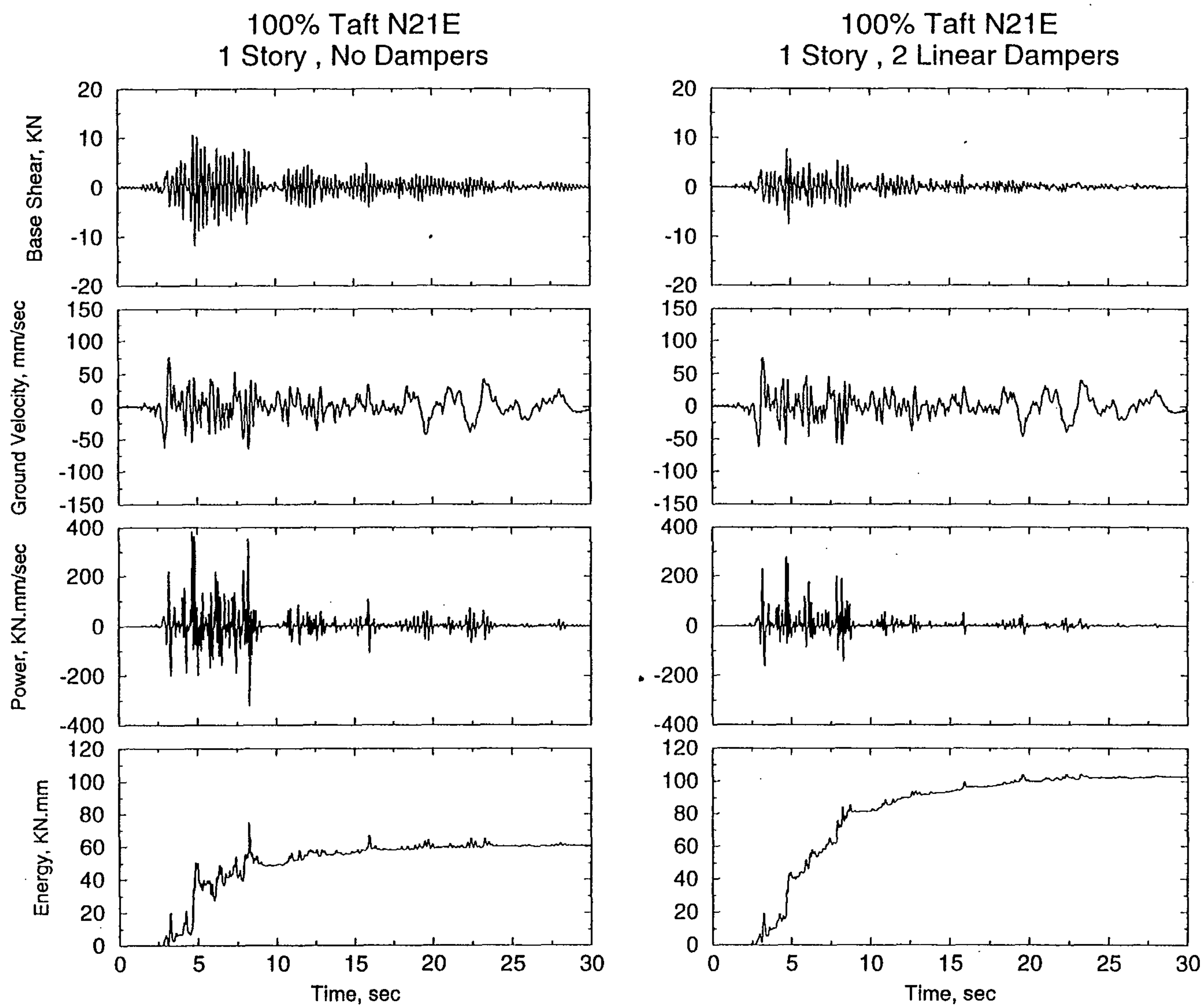

FIGURE 5-47 Base Shear, Power, and Energy Time Histories of One-Story Structure without and with Two Linear Dampers Subjected to 100% Taft Earthquake

$$P = ku\dot{u} = \frac{1}{2}ku_o^2\Omega\sin(2\Omega t) \tag{5-7}$$

$$E = \int_0^t kudu = \frac{1}{2}ku^2 \tag{5-8}$$

Graphs of power and energy input histories are shown in Figure 5-48. It may be seen that the power history is unbiased (zero mean), resulting in an energy input history that can not build up with time (recoverable energy).

For the case of linear viscous damper, the power and energy are

$$P = c\dot{u}^2 = cu_o^2\Omega^2\cos^2(\Omega t) \tag{5-9}$$

$$E = \int_0^t c\dot{u}^2 dt = \frac{1}{2}cu_o^2\Omega^2 t + \frac{1}{4}cu_o^2\Omega\sin(2\Omega t) \tag{5-10}$$

Figure 5-48 illustrates the histories of power and energy where it can be seen that the power is biased, leading to increased energy input with time.

It should be clear now that the final energy input (at the conclusion of excitation) is the energy dissipated in the structure (what anyway intuition suggests). For an undamped system, the final energy input is zero and the time history of energy input would exhibit large peaks of recoverable strain and kinetic energy. On the other hand, a highly damped structure would have large final input energy (this is dissipated energy) and small peaks of recoverable strain and kinetic energy. In the tested structure without dampers, the ability to dissipate energy was low resulting in low final input energy.

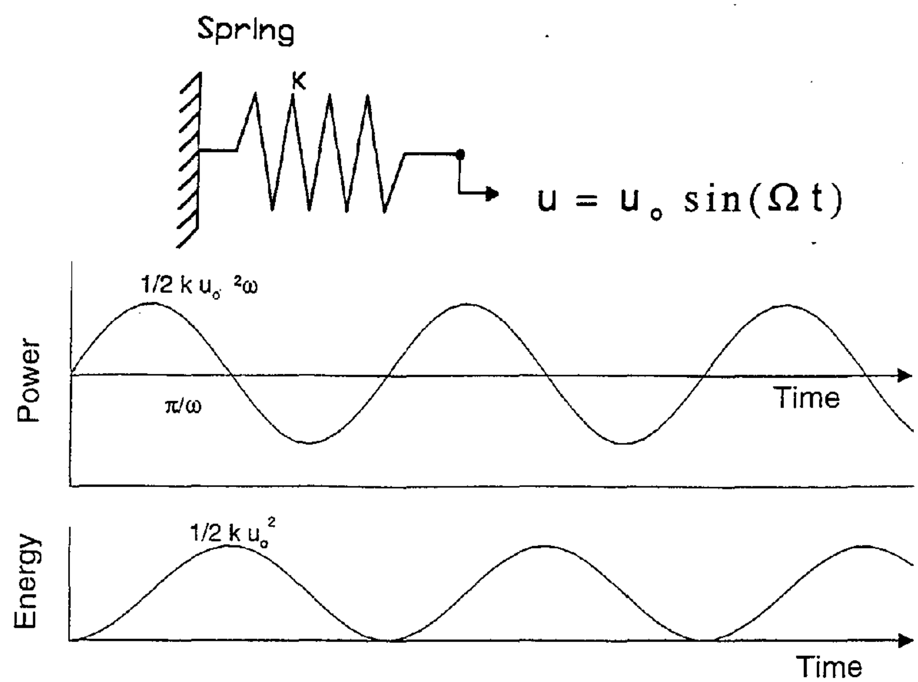

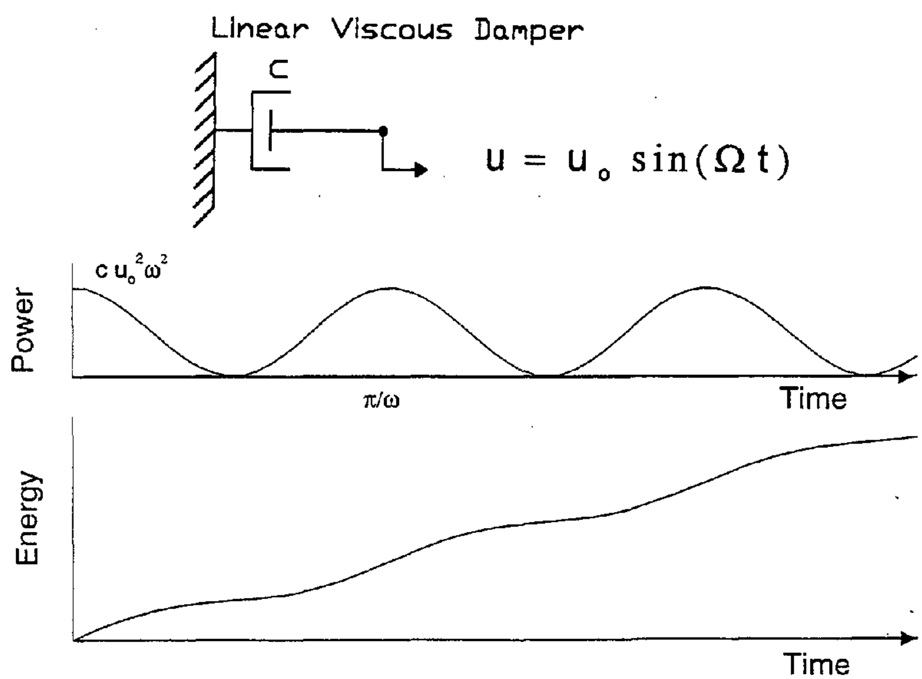

FIGURE 5-48 Comparison of Power, and Energy Time Histories of a Spring and a Linear Viscous Damper Subjected to Sinusoidal Motion

It should be noted that energy quantities of relevance to the seismic behavior of the structure are the sum of the kinetic and strain energies, which indicate the level of deformation in the structure, and the irrecoverable energy dissipated in the structural system exclusive of energy dissipating devices, E_h , which indicates the level of inelastic action (also related to damage) in the structure.

Clearly, the addition of energy dissipating devices results in reduction of both these energy quantities, resulting, thus, in improved performance.

SECTION 6

ANALYTICAL PREDICTION OF RESPONSE

6.1 Time History Analysis

The equations of motion of a structure with dampers was given previously in Section 4 (Equation 4-36), namely

$$[M]\{\ddot{U}\}+[C_u]\{\dot{U}\}+[K]\{U\}+\{PD\}=-[M]\{1\}\ddot{u}_g \tag{6-1}$$

The lumped mass matrix $[M]$ is diagonal, and the damping and stiffness matrices, $[C_u]$ and $[K]$, are constructed either analytically or from experimentally determined values for frequencies, damping ratios and mode shapes (see Equations 4-34 and 4-35).

The vector $\{PD\}$ is given by

$$\{PD\}=\begin{Bmatrix} \eta_k p_k \\ \vdots \\ \eta_j p_j - \eta_{j+1} p_{j+1} \\ \vdots \\ \eta_1 p_1 - \eta_2 p_2 \end{Bmatrix} \tag{6-2}$$

where η_j is the number of dampers at the j-th story and p_j is the horizontal component of force in a single damper at the j-th story. It is given for the case of linear dampers as

$$p_j = C_{oj}\cos^2\theta_j(\dot{u}_j - \dot{u}_{j-1}) \tag{6-3}$$

and for the case of nonlinear dampers as

$$p_j = C_{oj}(\cos\theta_j)^{1+\alpha_j}\left|(\dot{u}_j - \dot{u}_{j-1})\right|^{\alpha_j} \operatorname{sgn}(\dot{u}_j - \dot{u}_{j-1}) \tag{6-4}$$

where $j = 1,2$ and 3 ; and $\dot{u}_o = 0$.

It should be noted that Equation (6-3) can be simply obtained from Equation (6-4) by setting α equal to one.

The equations presented above can be written in first order form as follows :

$$\begin{bmatrix} [M] & [0] \\ [0] & [I] \end{bmatrix}\{\dot{Y}\} + \begin{bmatrix} [C_u] & [K] \\ -[I] & [0] \end{bmatrix}\{Y\} + \begin{Bmatrix} \{PD\} \\ \{0\} \end{Bmatrix} = \begin{Bmatrix} -[M]\{1\} \\ \{0\} \end{Bmatrix}\ddot{u}_g \tag{6-5}$$

where the vector $\{Y\}$ is defined as

$$\{Y\} = \begin{Bmatrix} \{\dot{U}\} \\ \{U\} \end{Bmatrix} \tag{6-6}$$

Equation (6-5) represents an initial value problem of a system of ordinary differential equations (note that $\{Y\}$ at zero time represents the initial conditions; which are zero for this problem). This equation can be solved numerically using any available subroutine (e.g., DIVPAG in IMSL 1987). Once the vector $\{Y\}$ at any time step is determined (that is, $\{U\}$ and $\{\dot{U}\}$ are known), the floor total accelerations are obtained by application of dynamic equilibrium as follows

$$\{\ddot{U}_T\} = \{\ddot{U}\} + \{1\}\ddot{u}_g = -[M]^{-1}\left([C_u]\{\dot{U}\} + [K]\{U\} + \{PD\}\right) \tag{6-7}$$

The vector of story shear forces is then obtained as follows

$$\{F\} = [M]\{\ddot{U}_T\} = -\left([C_u]\{\dot{U}\} + [K]\{U\} + \{PD\} \right) \tag{6-8}$$

The time history analysis of the single story structure is similar to the above development but with some simplifications.

6.2 Comparison between Experimental Results and Results of Response History Analysis

6.2.1 Single Story Structure with Linear Dampers

Figures 6-1 to 6-5 present comparisons between the experimental and analytical results for the single story structure with two linear dampers when subjected to different earthquake input motions. The viscous model of Equation (6-3) with $C_o = 16$ N.s/mm (that is, the average value - see Section 2) has been used. The base shear force and total axial damper force, both normalized by weight versus the story drift normalized by height are plotted for each test. The comparison shows very good agreement between analysis and experiment.

Figures 6-6 and 6-7 show comparison of time histories of analytical and experimental response for selected tests. It is evident that all response quantities are predicted well by analytical means.

A comparison of analytical response with the viscous model ($C_o = 16$ N.s/mm) and the Maxwell model (Equation (2-16) with $C_o = 16$ N.s/mm and λ = 0.008 s) is provided in Figure 6-8 for selected tests. The comparison shows insignificant differences between the predictions of the two models, leading to the conclusion that the dampers exhibited viscous behavior for practical purposes.

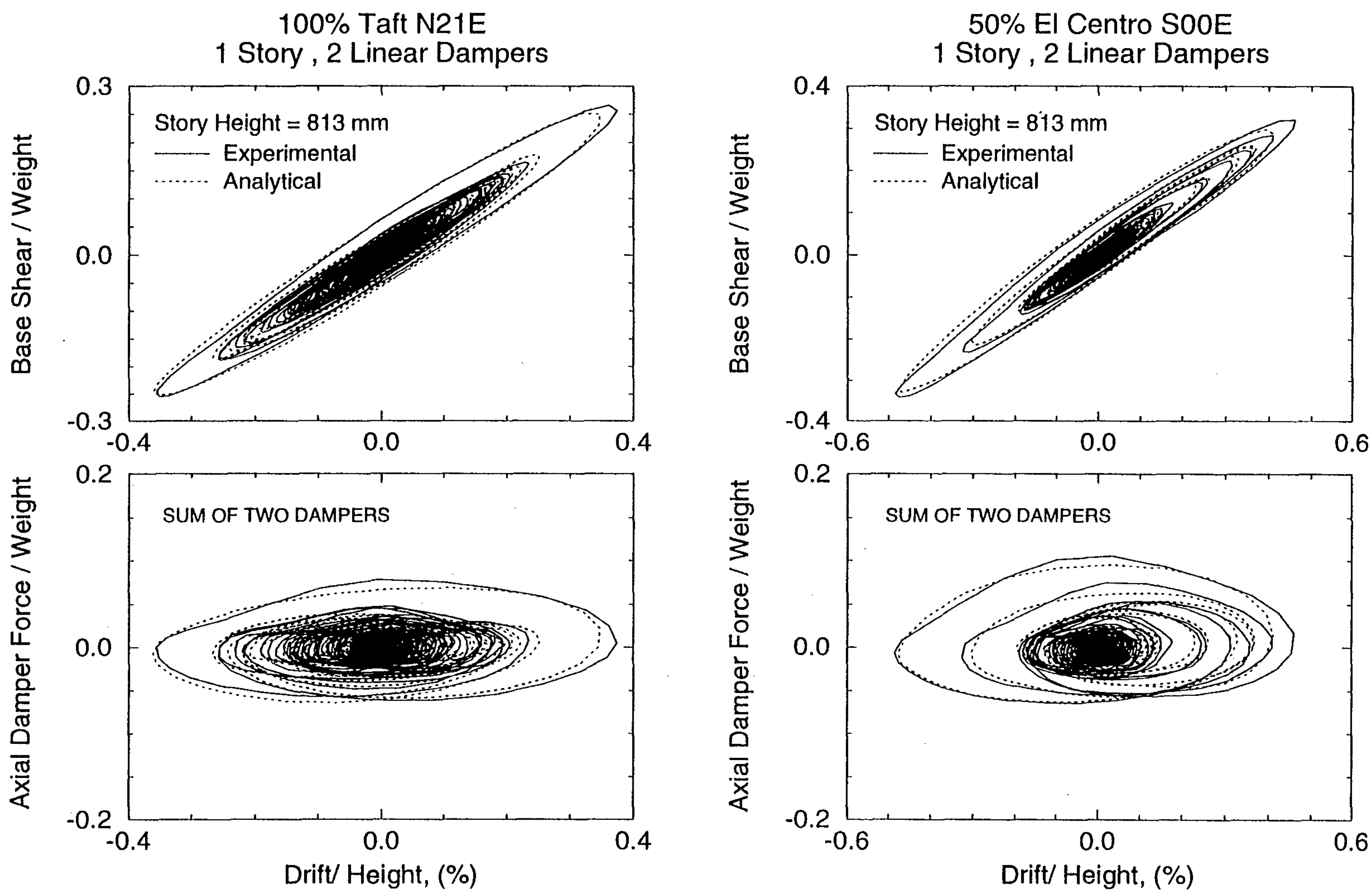

FIGURE 6-1 Comparison of Experimental and Analytical Results of One-Story Structure with Two Linear Dampers Subjected to 100% Taft and 50% El Centro Earthquakes

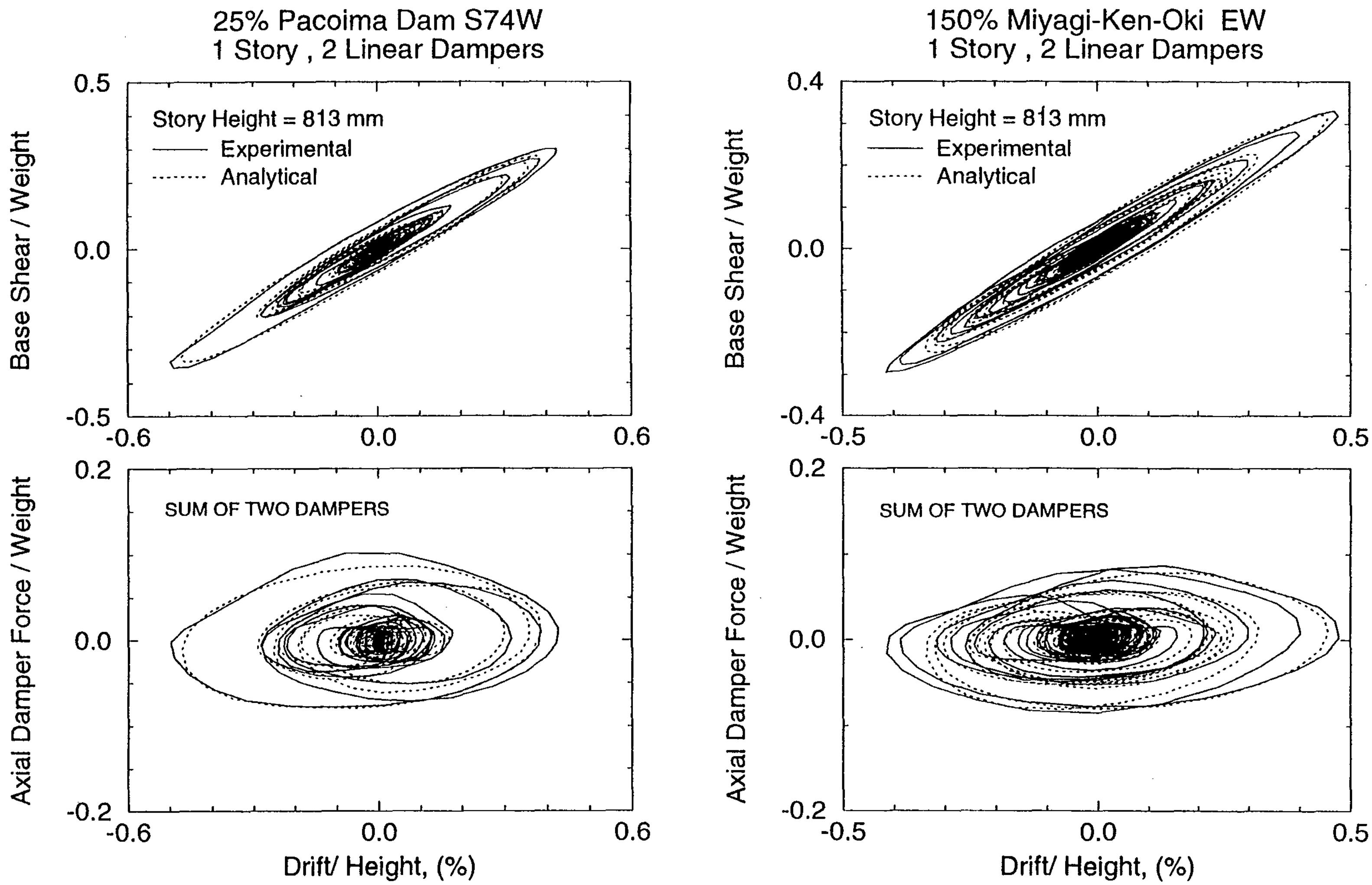

FIGURE 6-2 Comparison of Experimental and Analytical Results of One-Story Structure with Two Linear Dampers Subjected to 25% Pacoima Dam and 150% Miyagi-Ken-Oki Earthquakes

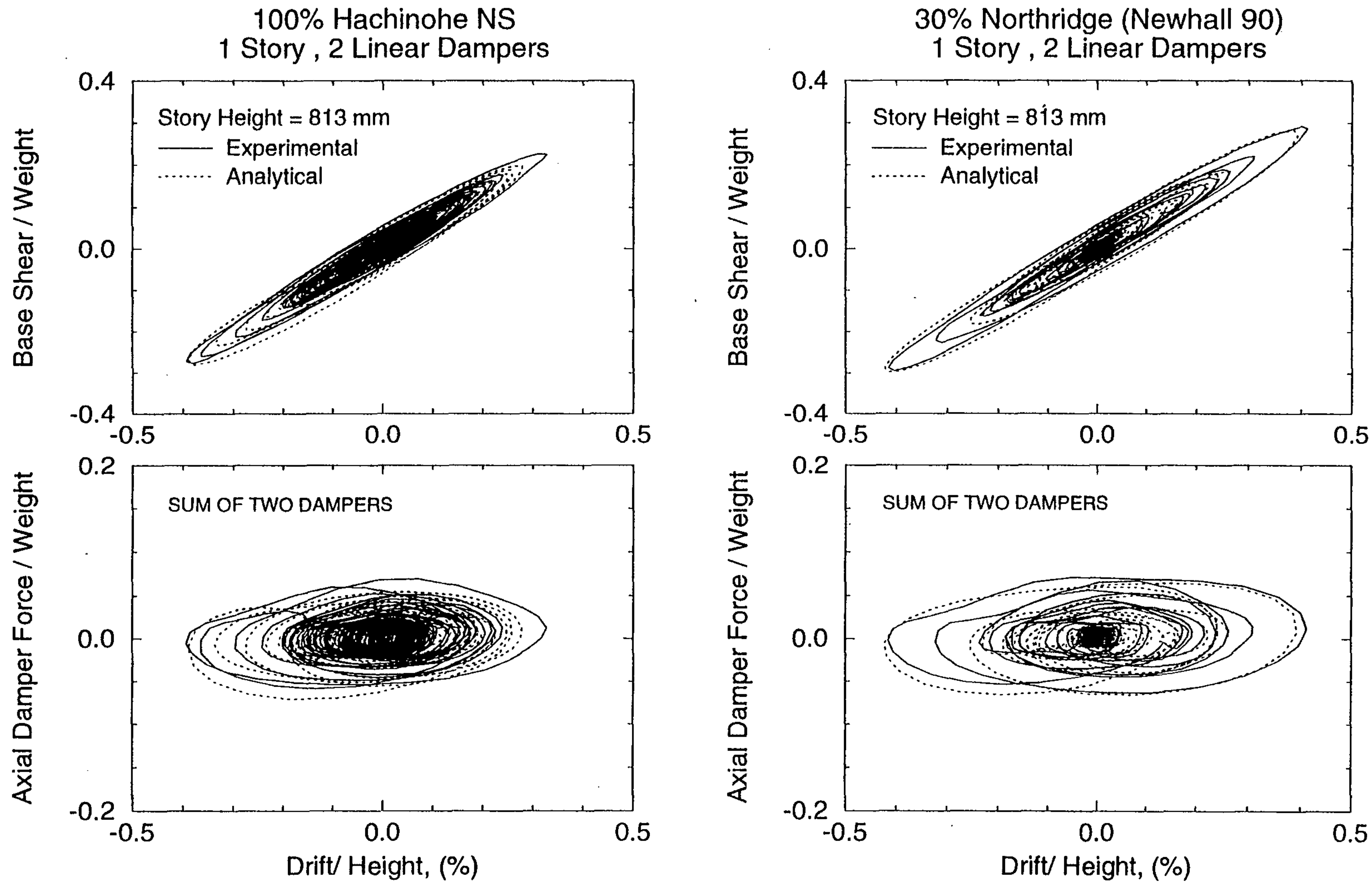

FIGURE 6-3 Comparison of Experimental and Analytical Results of One-Story Structure with Two Linear Dampers Subjected to 100% Hachinohe and 30% Northridge (Newhall 90) Earthquakes

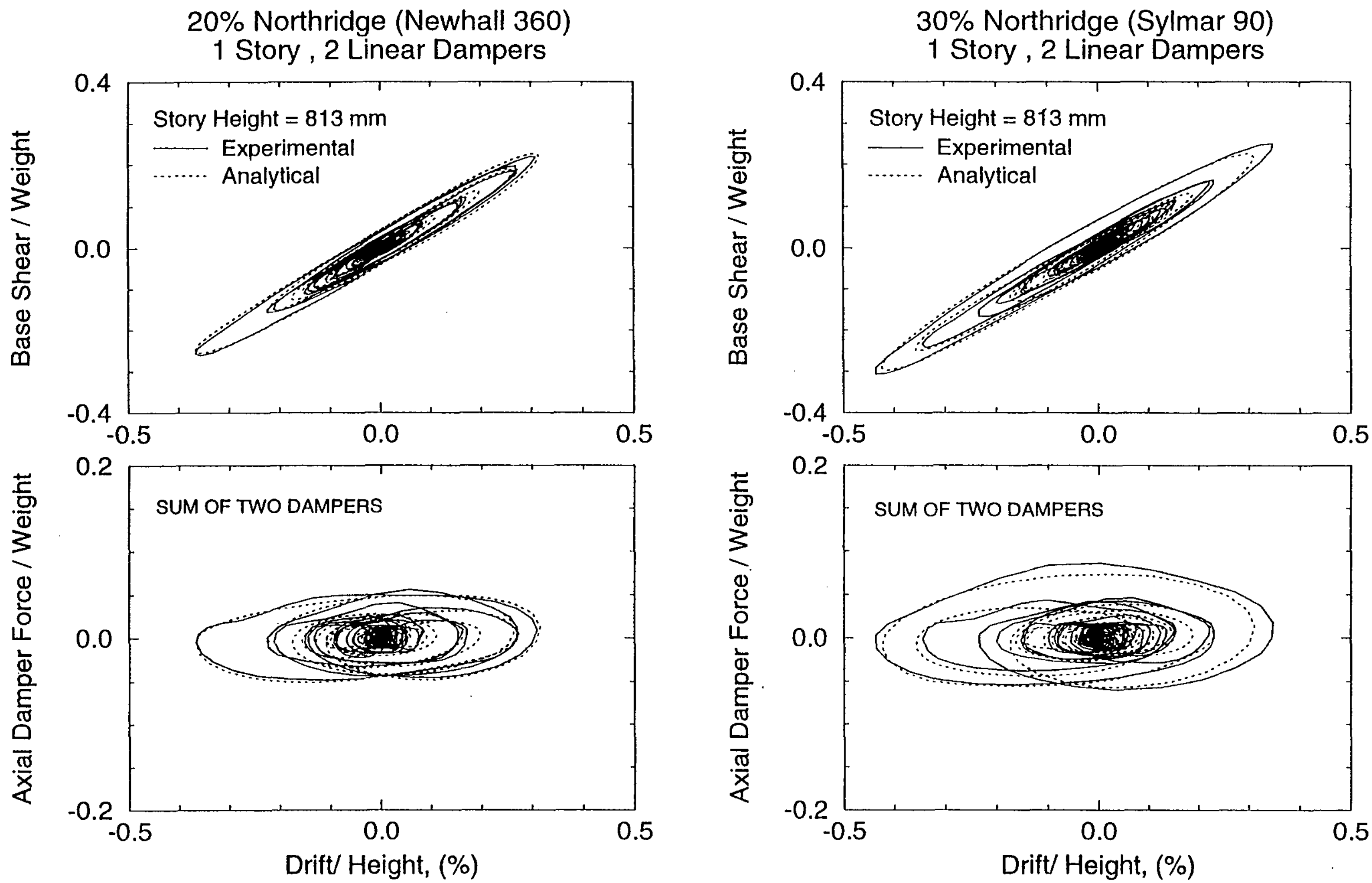

FIGURE 6-4 Comparison of Experimental and Analytical Results of One-Story Structure with Two Linear Dampers Subjected to 20% Northridge (Newhall 360) and 30% Northridge (Sylmar 90) Earthquakes

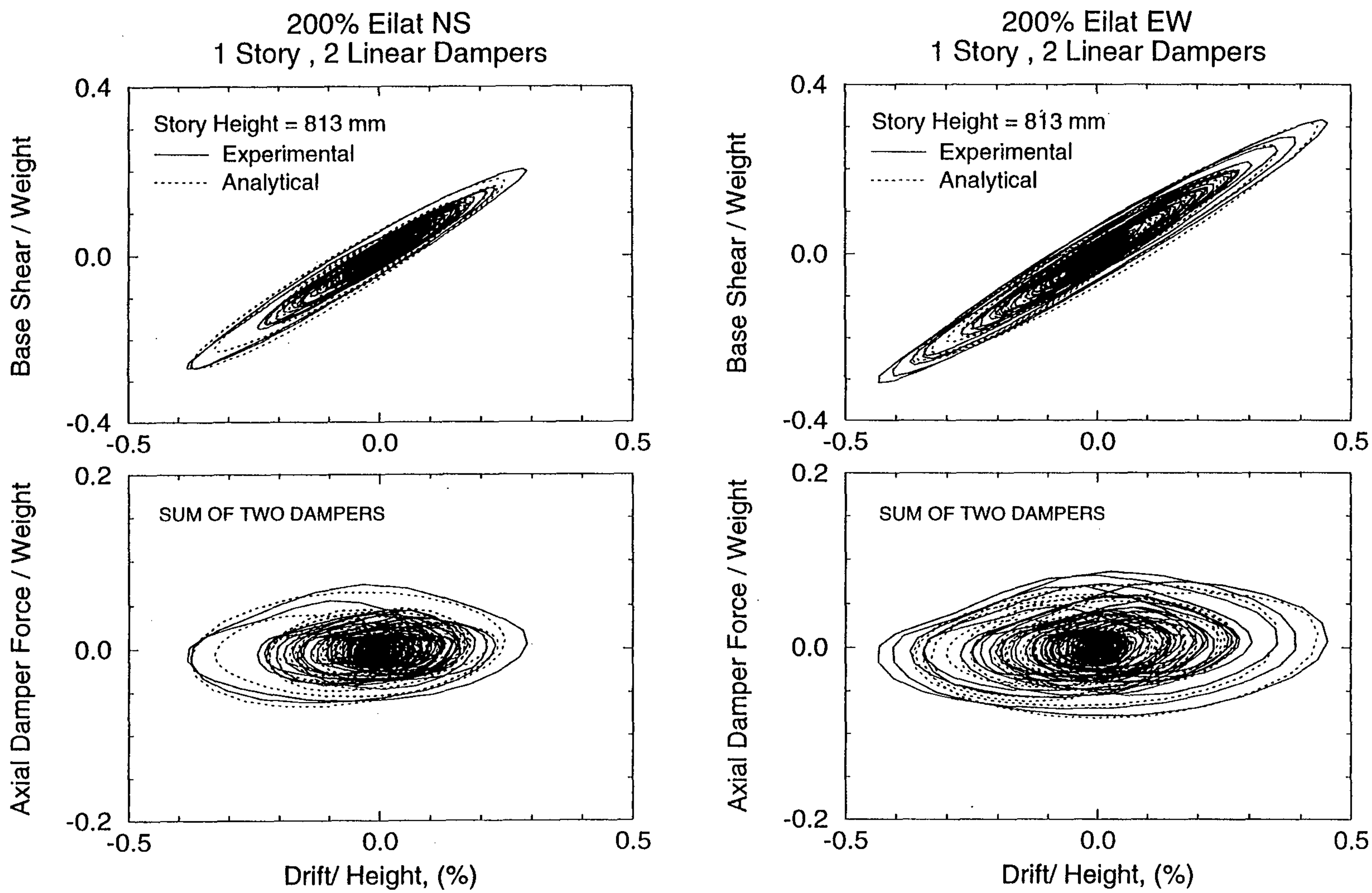

FIGURE 6-5 Comparison of Experimental and Analytical Results of One-Story Structure with Two Linear Dampers Subjected to 200% Eilat NS and 200% Eilat EW Earthquakes

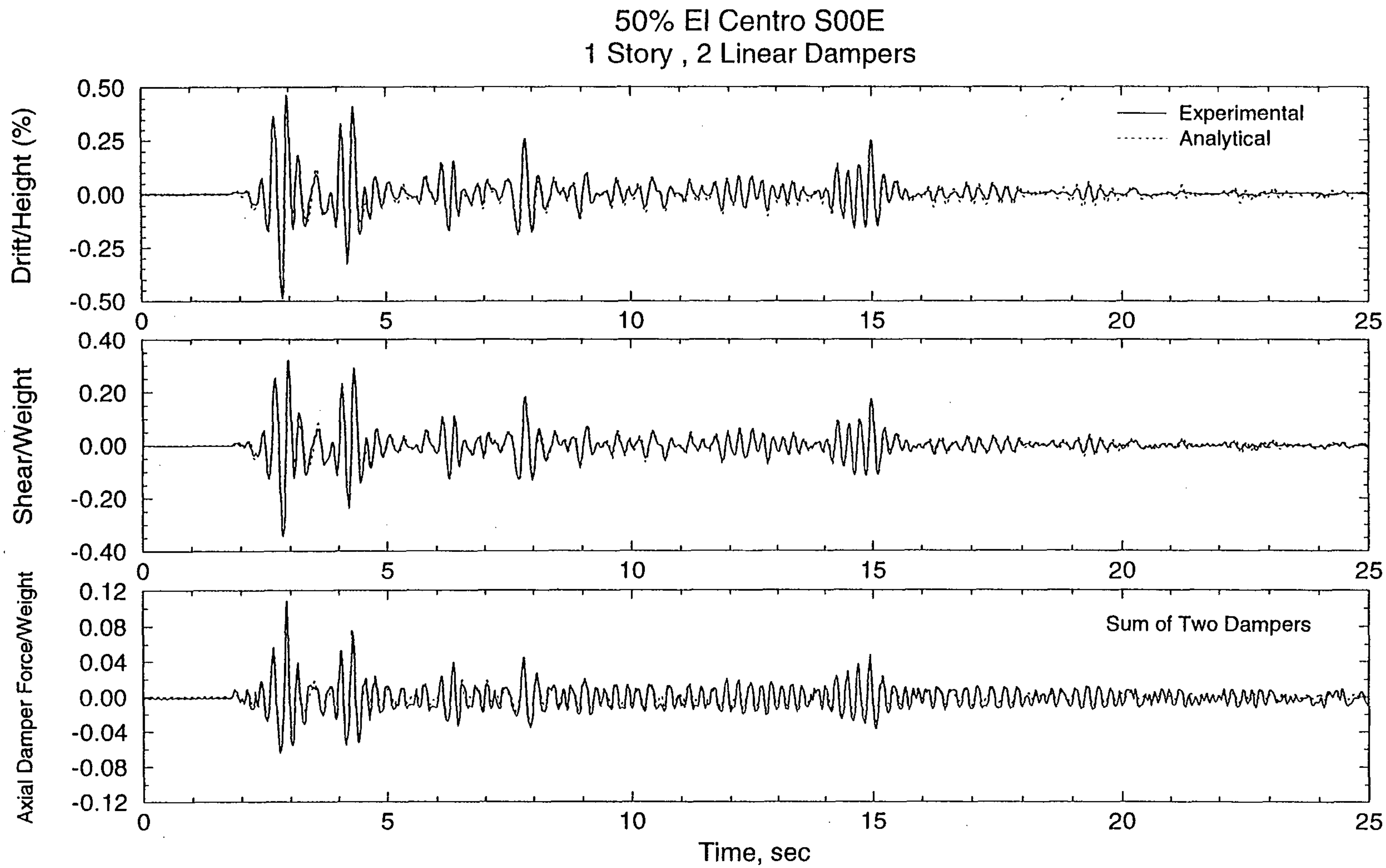

FIGURE 6-6 Comparison of Experimental and Analytical Time Histories of Response of One-Story Structure with Two Linear Dampers Subjected to 50% El Centro Earthquake

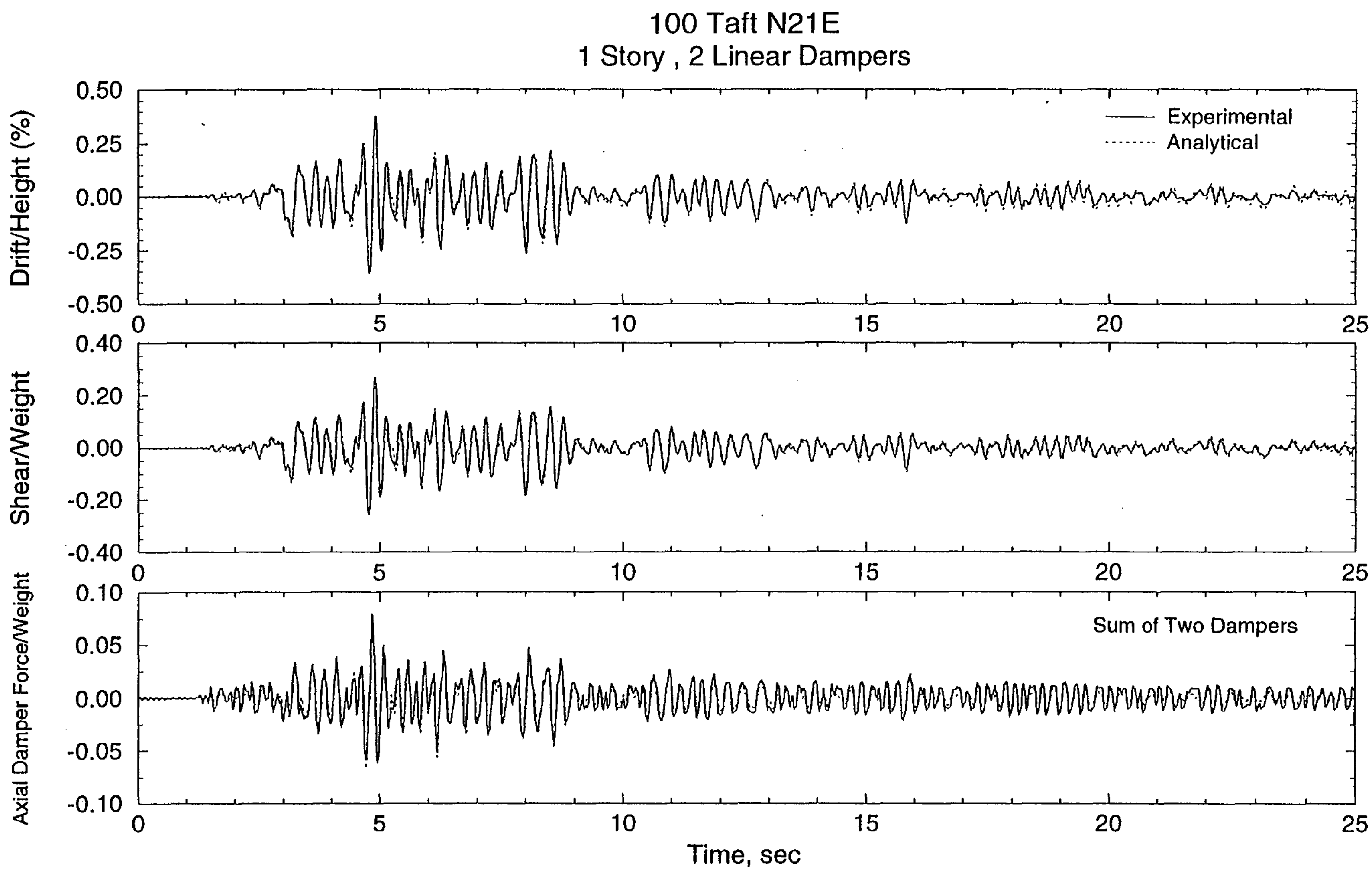

FIGURE 6-7 Comparison of Experimental and Analytical Time Histories of Response of One-Story Structure with Two Linear Dampers Subjected to 100% Taft Earthquake

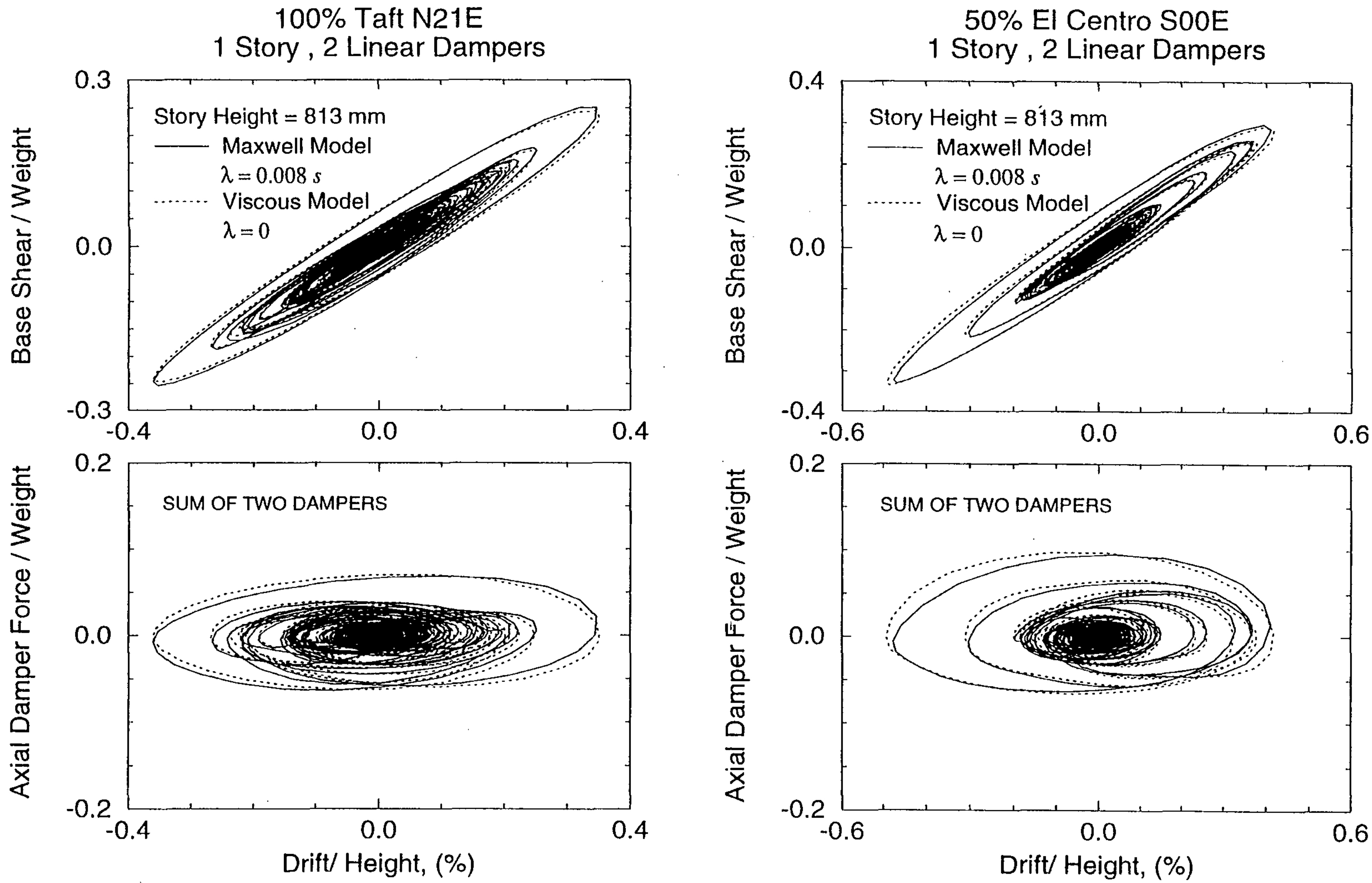

FIGURE 6-8 Comparison of Analytical Results Obtained with the Viscous ($\lambda = 0$) and with the Maxwell ($\lambda = 0.008$) Models for the One-Story Structure with Two Linear Dampers Subjected to 100% Taft and 50% El Centro Earthquakes

6.2.2 Three Story Structure with Linear Dampers

Comparisons of experimental and analytical results for the 3-story structure are presented in Figures 6-9 to 6-18. In these figures, story shear forces normalized to the total weight versus story drifts normalized to story heights are plotted for the case of six linear dampers (two at each story). The analytical results were produced by the analysis procedure described in Section 6.1, that is, solution of Equations (6-1) to (6-3). A value of $C_o = 16$ N.s/mm was used for all six dampers.

The agreement between the analytical and experimental results is generally good. It should be noted that the analytical results are based on an average value for constant C_o, whereas the dampers exhibited a variation of properties about this value. Unfortunately, not all linear dampers were tested (see Section 2), nor a record of placement of each damper was kept. Had the properties of each damper were known, it would have been possible to obtain a better agreement between analytical and experimental results.

6.2.3 Three Story Structure with Nonlinear Dampers

Comparisons of the experimental and analytical shear force-drift loops of the 3-story structure with six nonlinear dampers are presented in Figures 6-19 to 6-24 for selected tests. For the analytical prediction, the model described by Equations (6-1), (6-2) and (6-4) has been used. Since each nonlinear damper was tested, it was possible to incorporate in the analytical model the calibrated model of each damper (see Section 2). That is parameter α was specified as 0.5 for

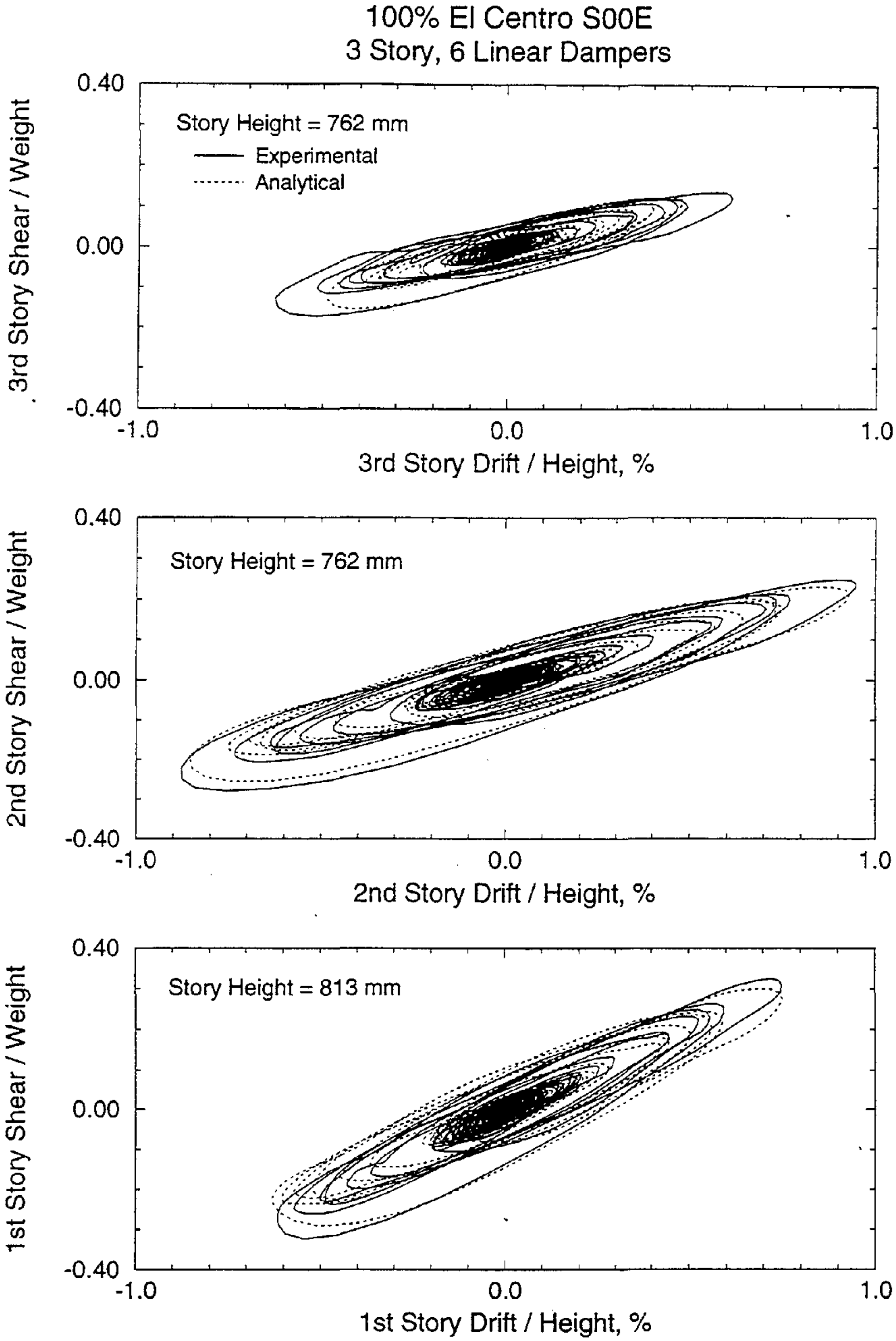

FIGURE 6-9 Comparison of Experimental and Analytical Results of 3-Story Repaired Structure with Six Linear Dampers Subjected to 100% El Centro Earthquake

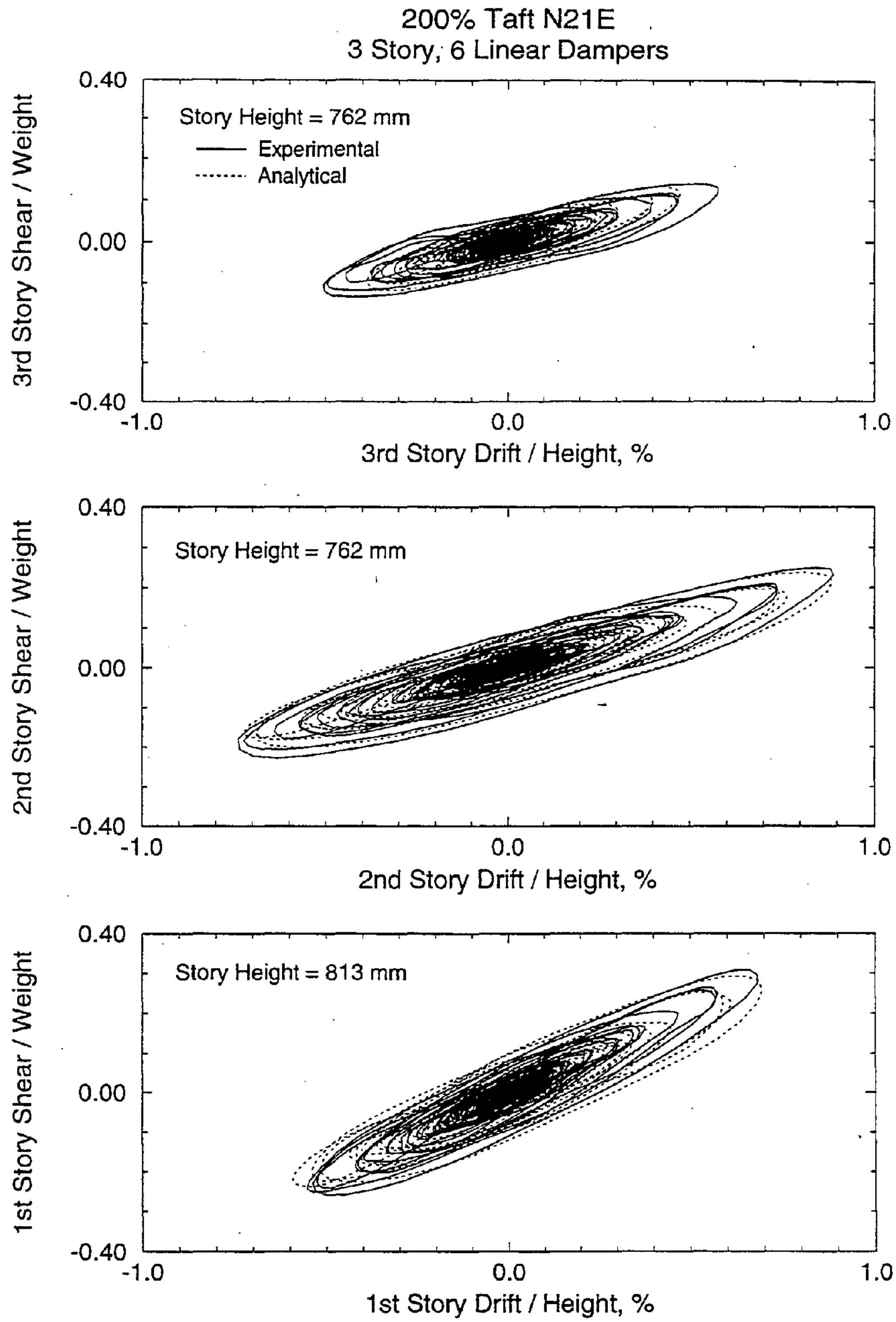

FIGURE 6-10 Comparison of Experimental and Analytical Results of 3-Story Repaired Structure with Six Linear Dampers Subjected to 200% Taft Earthquake

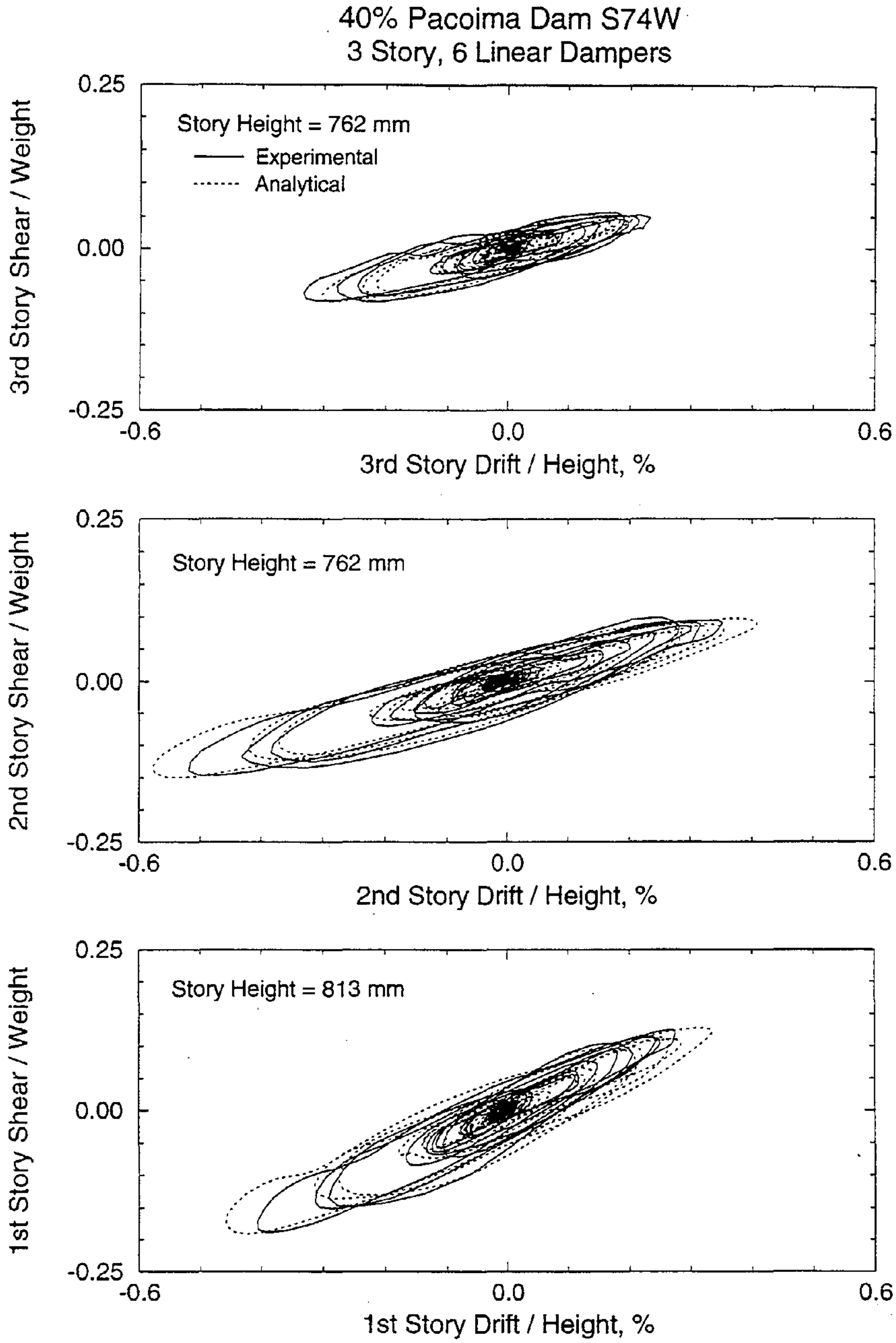

FIGURE 6-11 Comparison of Experimental and Analytical Results of 3-Story Repaired Structure with Six Linear Dampers Subjected to 40% Pacoima Dam Earthquake

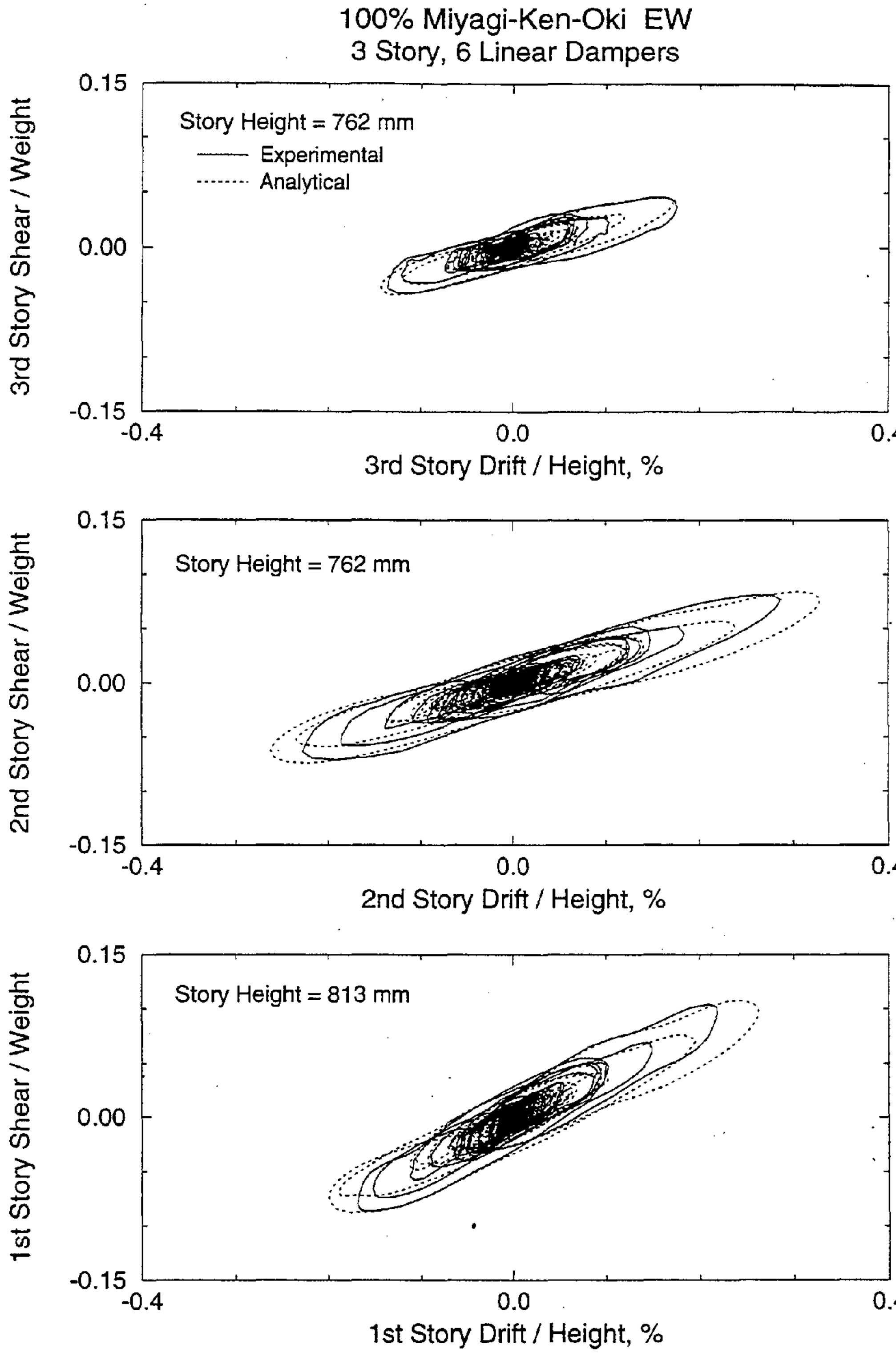

FIGURE 6-12 Comparison of Experimental and Analytical Results of 3-Story Repaired Structure with Six Linear Dampers Subjected to 100% Miyagi-Ken-Oki Earthquake

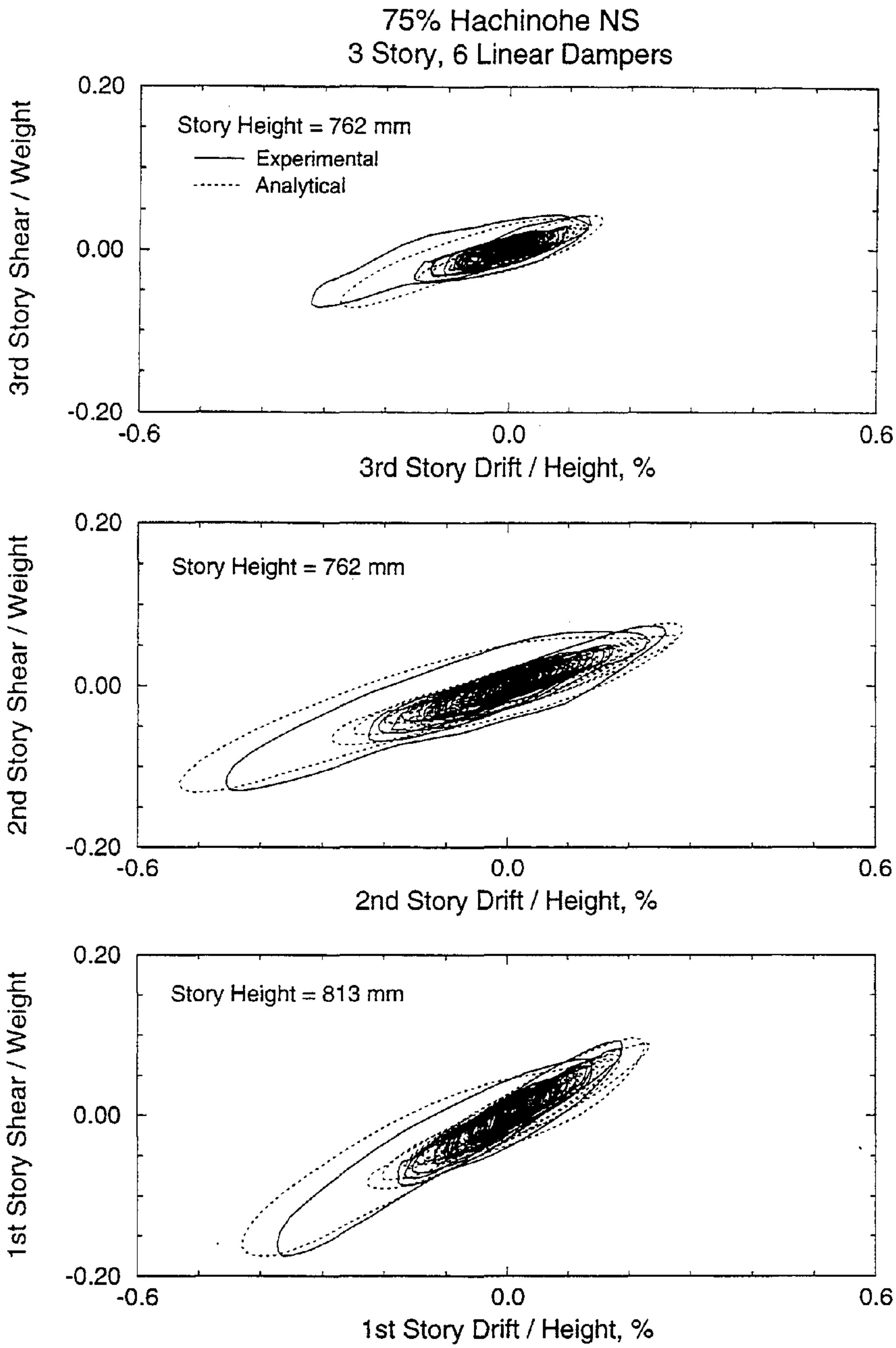

FIGURE 6-13 Comparison of Experimental and Analytical Results of 3-Story Repaired Structure with Six Linear Dampers Subjected to 75% Hachinohe Earthquake

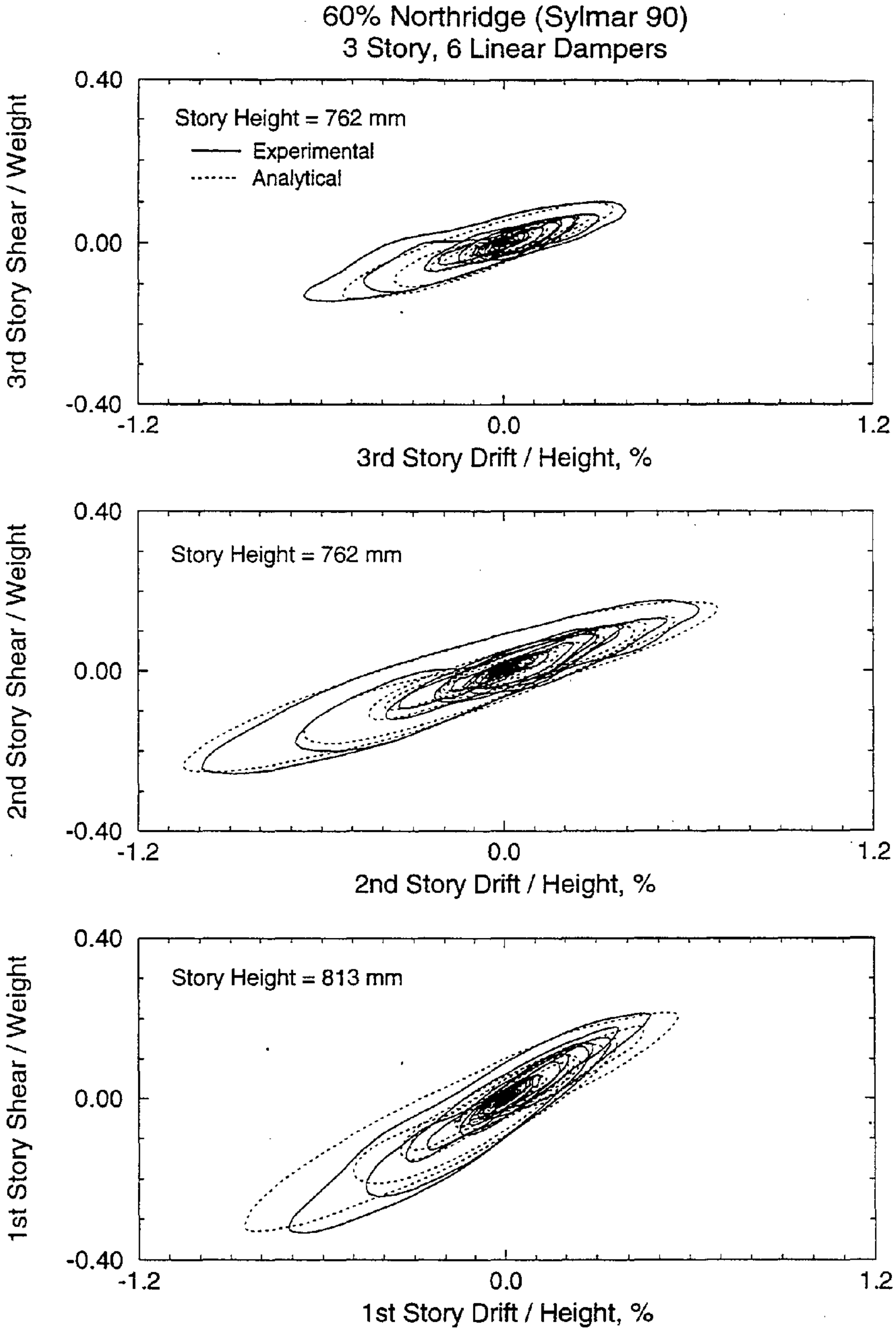

FIGURE 6-14 Comparison of Experimental and Analytical Results of 3-Story Repaired Structure with Six Linear Dampers Subjected to 60% Northridge (Sylmar 90) Earthquake

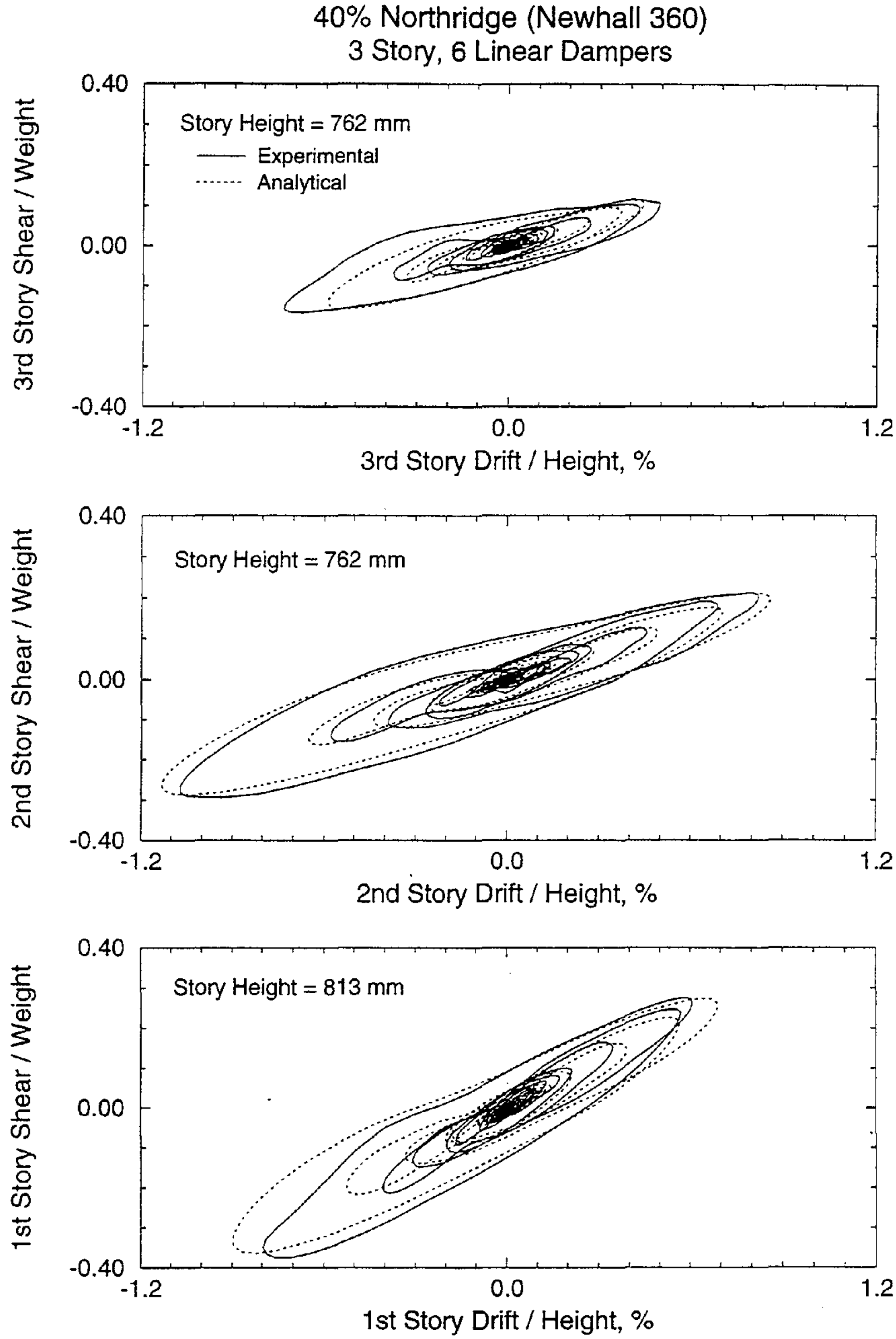

FIGURE 6-15 Comparison of Experimental and Analytical Results of 3-Story Repaired Structure with Six Linear Dampers Subjected to 40% Northridge (Newhall 360) Earthquake

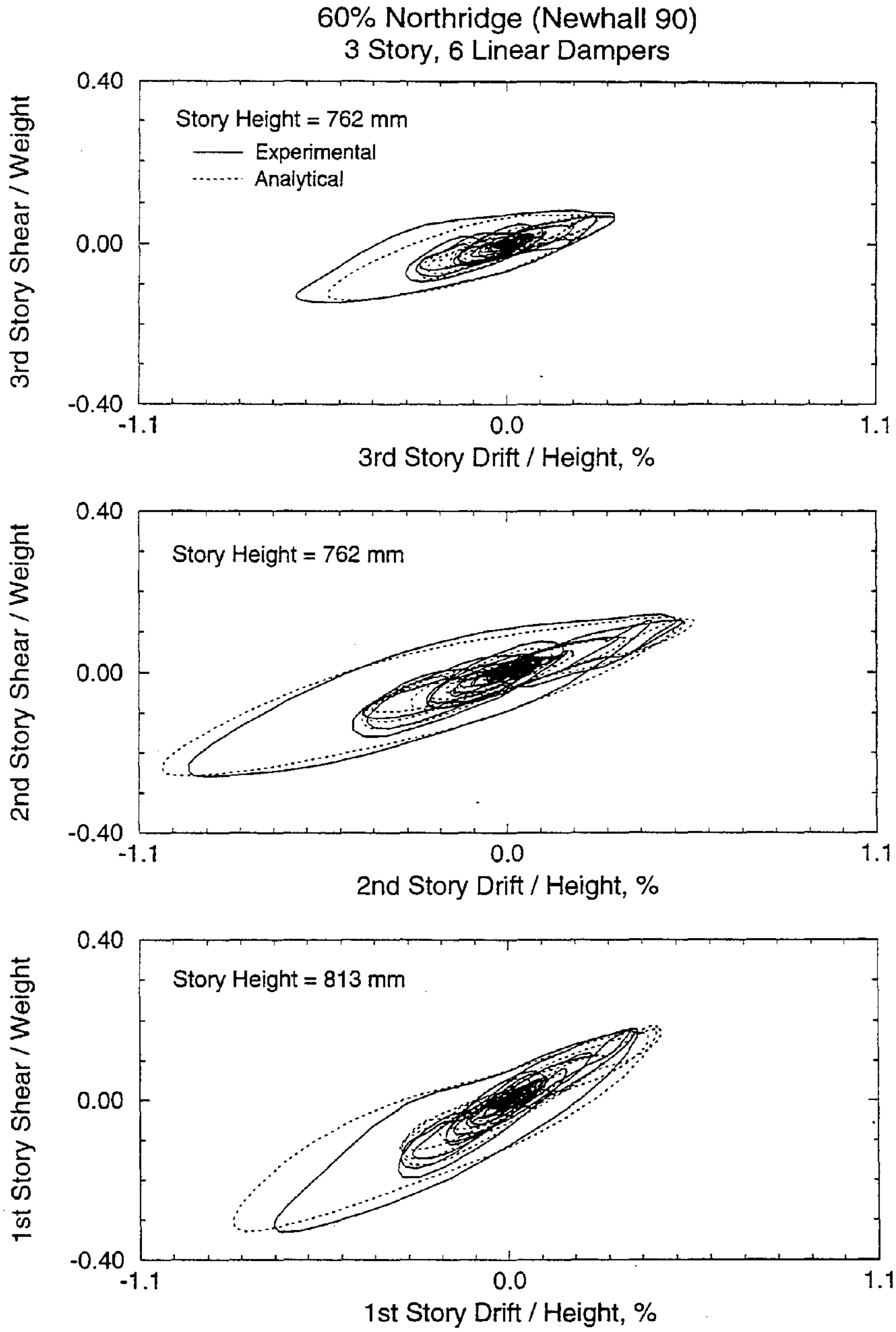

FIGURE 6-16 Comparison of Experimental and Analytical Results of 3-Story Repaired Structure with Six Linear Dampers Subjected to 60% Northridge (Newhall 90) Earthquake

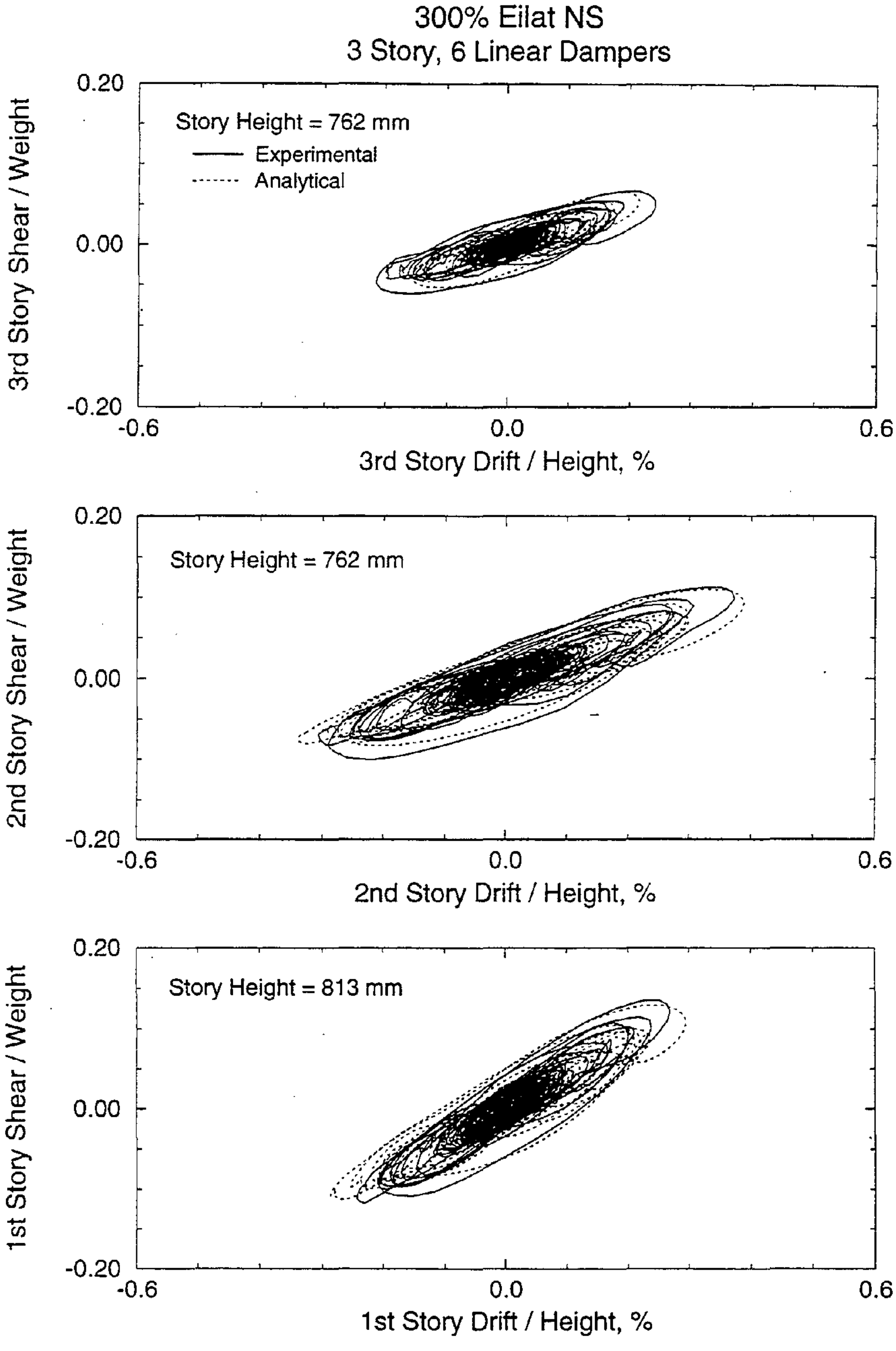

FIGURE 6-17 Comparison of Experimental and Analytical Results of 3-Story Repaired Structure with Six Linear Dampers Subjected to 300% Eilat NS Earthquake

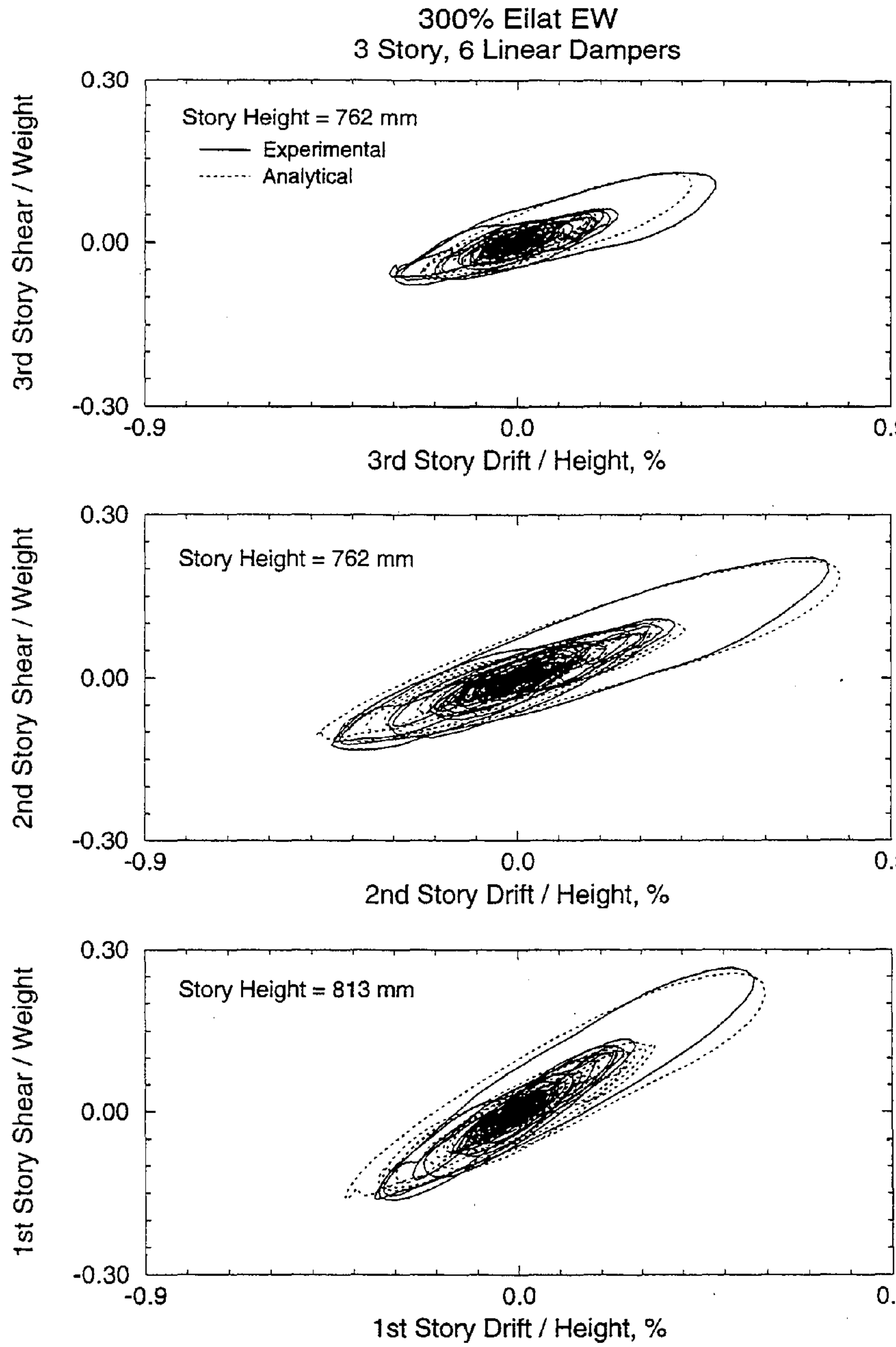

FIGURE 6-18 Comparison of Experimental and Analytical Results of 3-Story Repaired Structure with Six Linear Dampers Subjected to 300% Eilat EW Earthquake

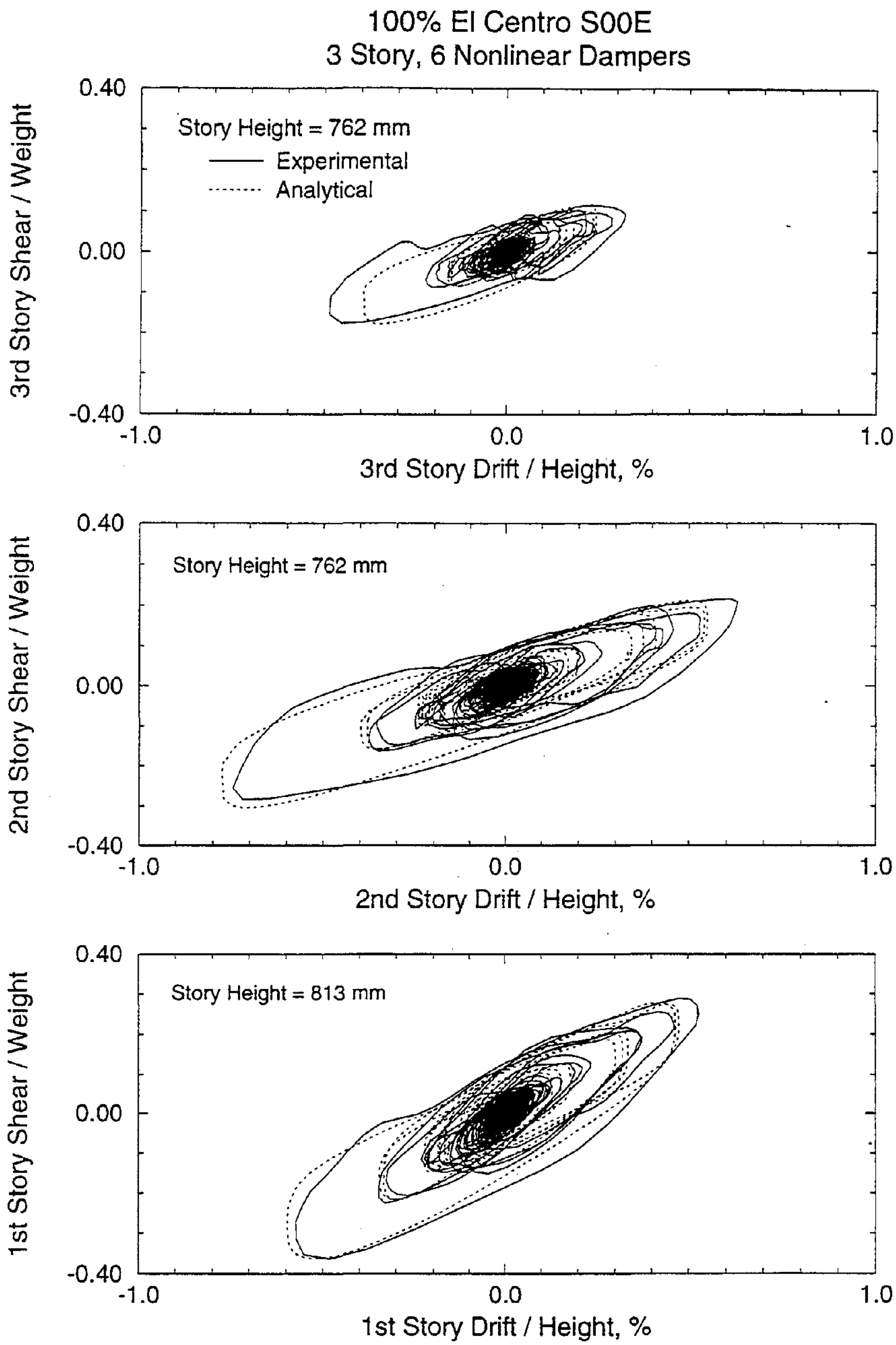

FIGURE 6-19 Comparison of Experimental and Analytical Results of 3-Story Repaired Structure with Six Nonlinear Dampers Subjected to 100% El Centro Earthquake

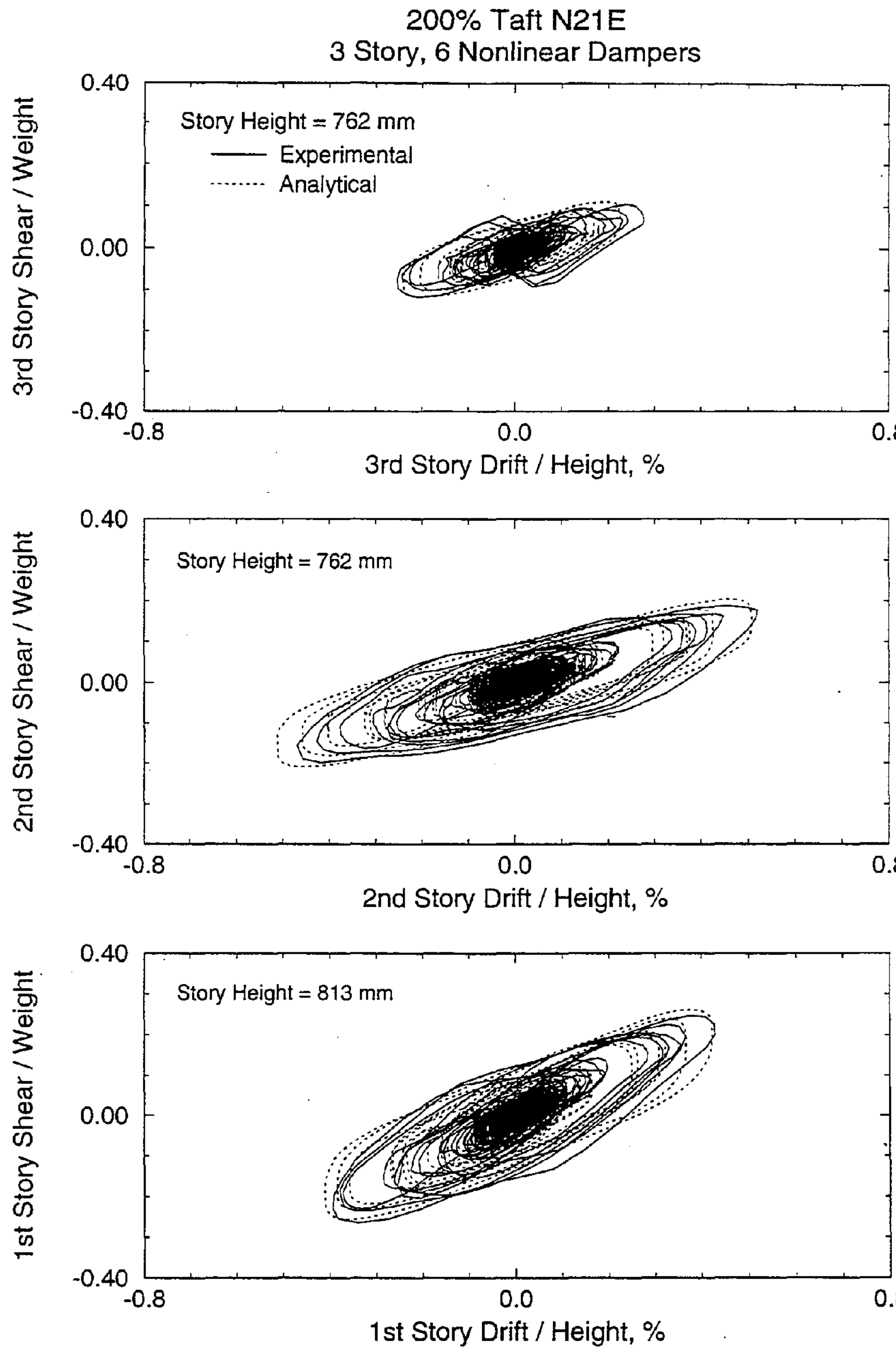

FIGURE 6-20 Comparison of Experimental and Analytical Results of 3-Story Repaired Structure with Six Nonlinear Dampers Subjected to 200% Taft Earthquake

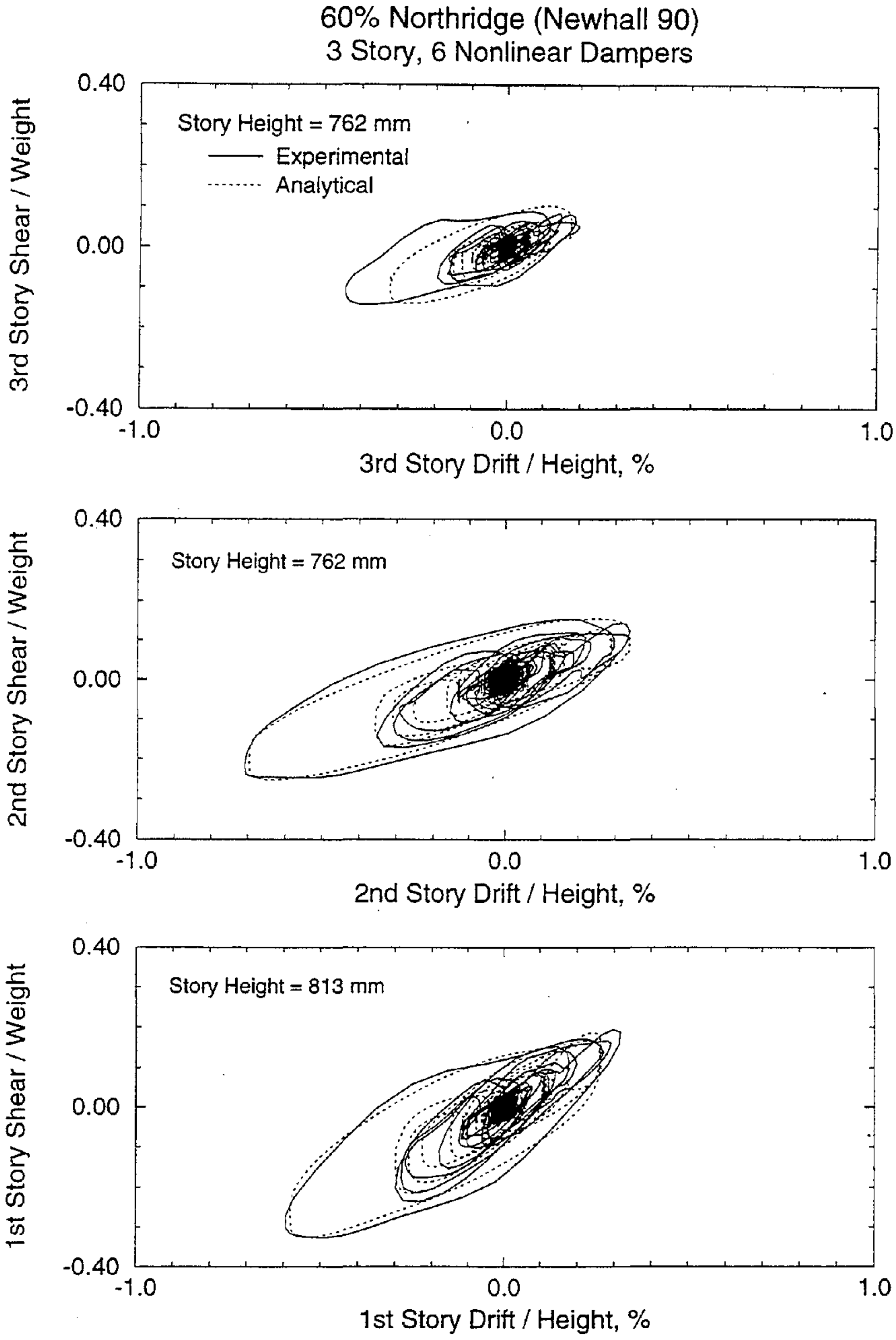

FIGURE 6-21 Comparison of Experimental and Analytical Results of 3-Story Repaired Structure with Six Nonlinear Dampers Subjected to 60% Northridge (Newhall 90) Earthquake

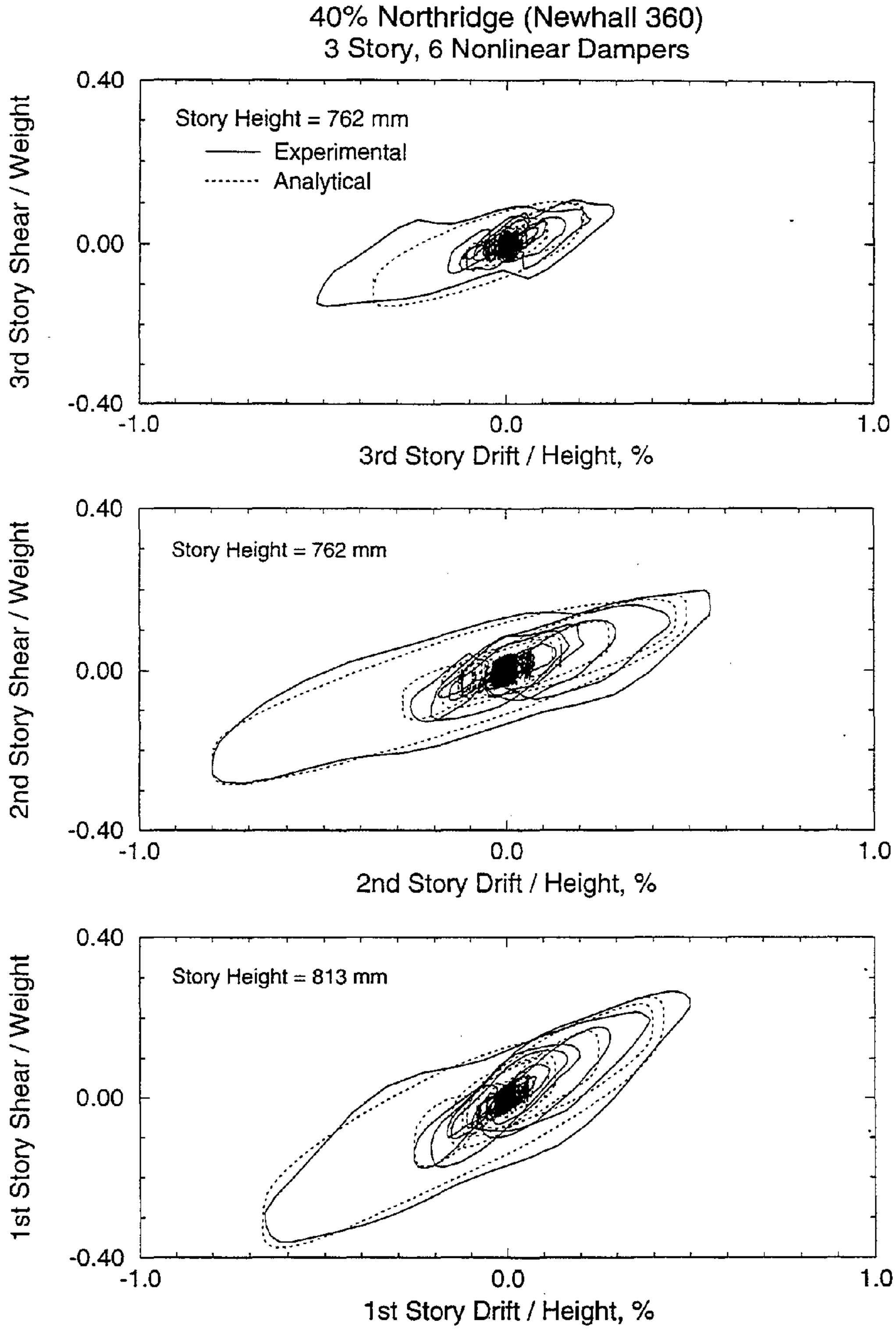

FIGURE 6-22 Comparison of Experimental and Analytical Results of 3-Story Repaired Structure with Six Nonlinear Dampers Subjected to 40% Northridge (Newhall 360) Earthquake

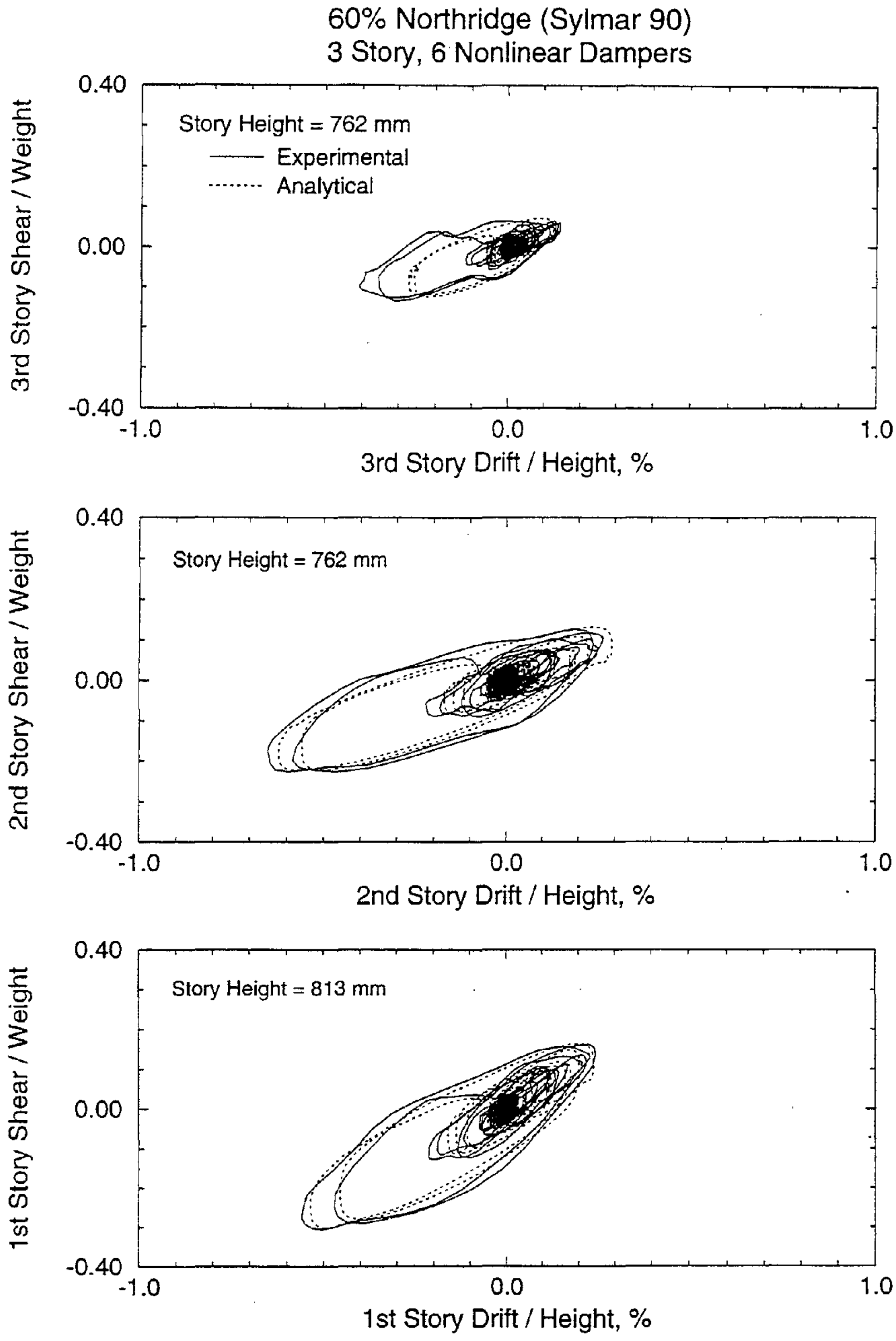

FIGURE 6-23 Comparison of Experimental and Analytical Results of 3-Story Repaired Structure with Six Nonlinear Dampers Subjected to 60% Northridge (Sylmar 90) Earthquake

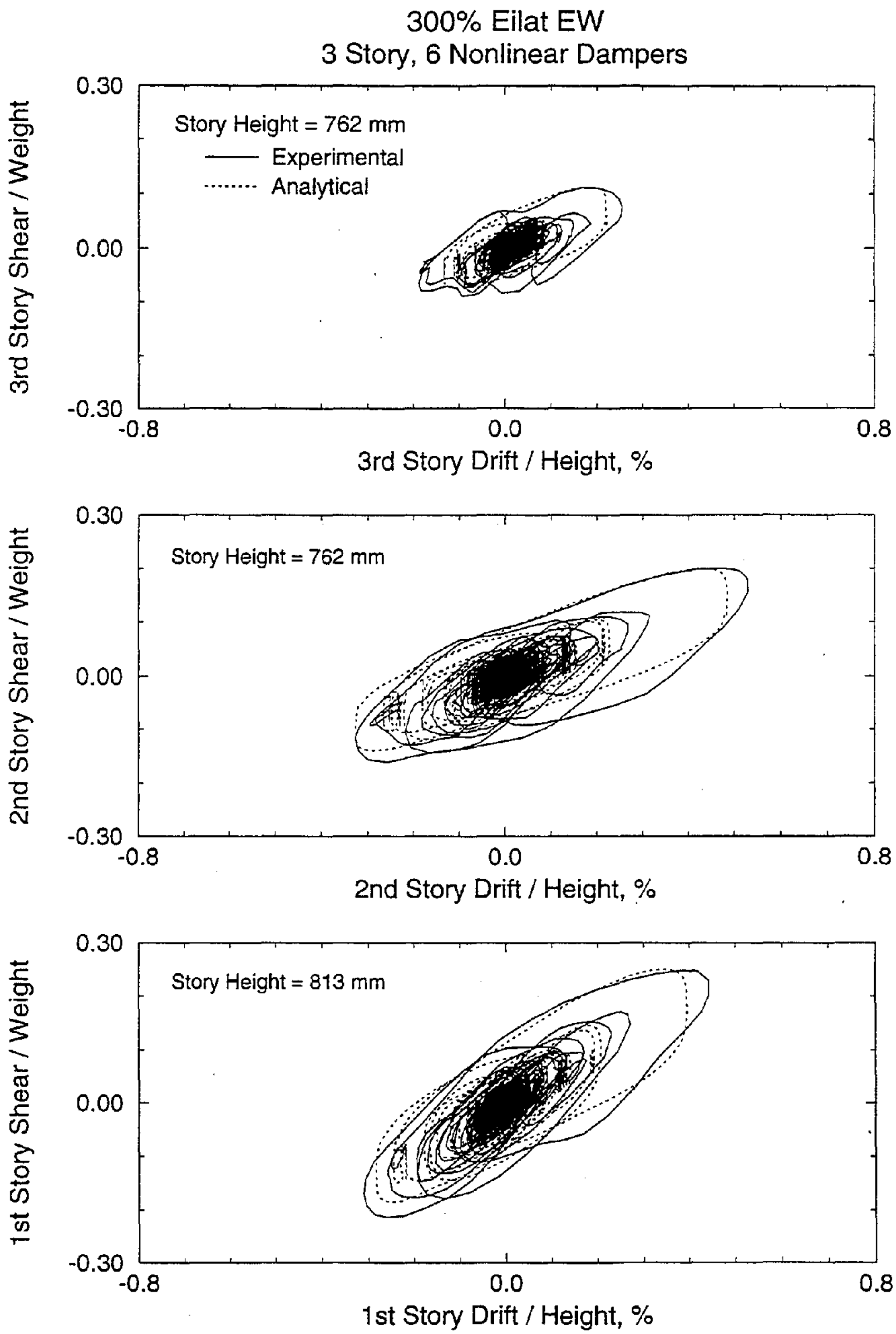

FIGURE 6-24 Comparison of Experimental and Analytical Results of 3-Story Repaired Structure with Six Nonlinear Dampers Subjected to 300% Eilat EW Earthquake

all dampers and damping constants were specified as $C_{o1} = 300 \ N(s/mm)^{1/2}$, $C_{o2} = 235 \ N(s/mm)^{1/2}$ and $C_{o3} = 220 \ N(s/mm)^{1/2}$ (see Figure 2-10).

It may be observed that the analytical prediction is generally good. However it should be noted that the analytical model under-predicts displacements when they are small (e.g., third story drift). This has been the result of the inability of the calibrated model of the nonlinear dampers to capture their behavior in the very low velocity range. Analyses were repeated with a more refined model for the dampers (see Section 2), in which the low velocity behavior of the dampers was approximated by a linear viscous model. Figures 6-25 to 6-30 presents a comparison of results for the same tests as these in Figures 6-19 to 6-25. Indeed, the analytical prediction is improved.

6.3 Simplified Analysis Procedure

The simplified analysis procedure presented herein is based on the Linear Static Procedure of the NEHRP Guidelines for the Seismic Rehabilitation of Buildings (FEMA 1996) as it is applied to structures with viscous energy dissipation systems. This procedure applies to structures that remain essentially elastic for the design basis earthquake. It is based on application of modal analysis procedures using the undamped frequencies and mode shapes of the structure, and the use of damped response spectra for the effective damping provided by the energy dissipation system. These damped response spectra are constructed from the 5%-damped response spectrum using appropriate de-amplification factors for higher damping.

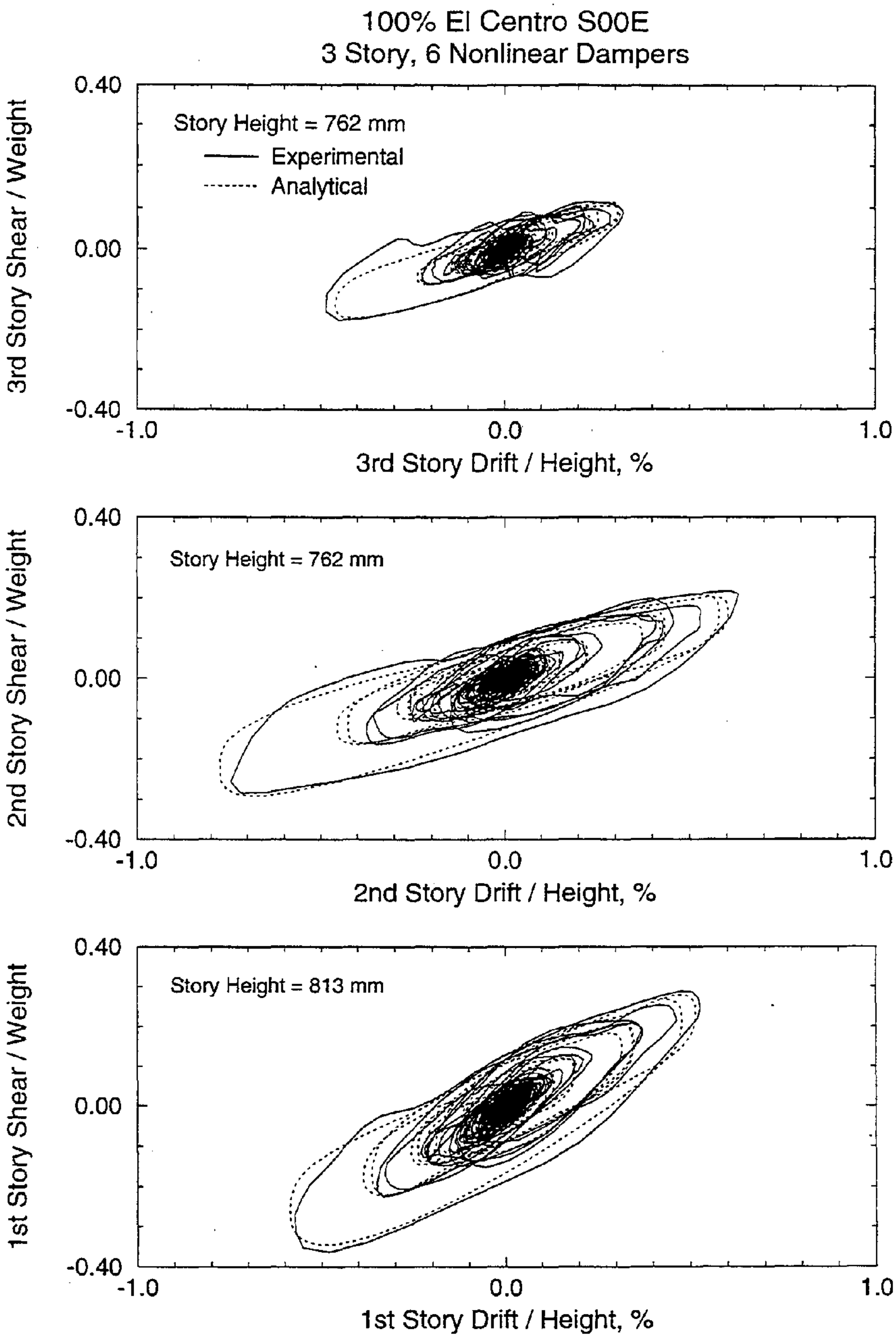

FIGURE 6-25 Comparison of Experimental and Analytical Results of 3-Story Repaired Structure with Six Nonlinear Dampers Subjected to 100% El Centro Earthquake (Refined Model of Nonlinear Dampers)

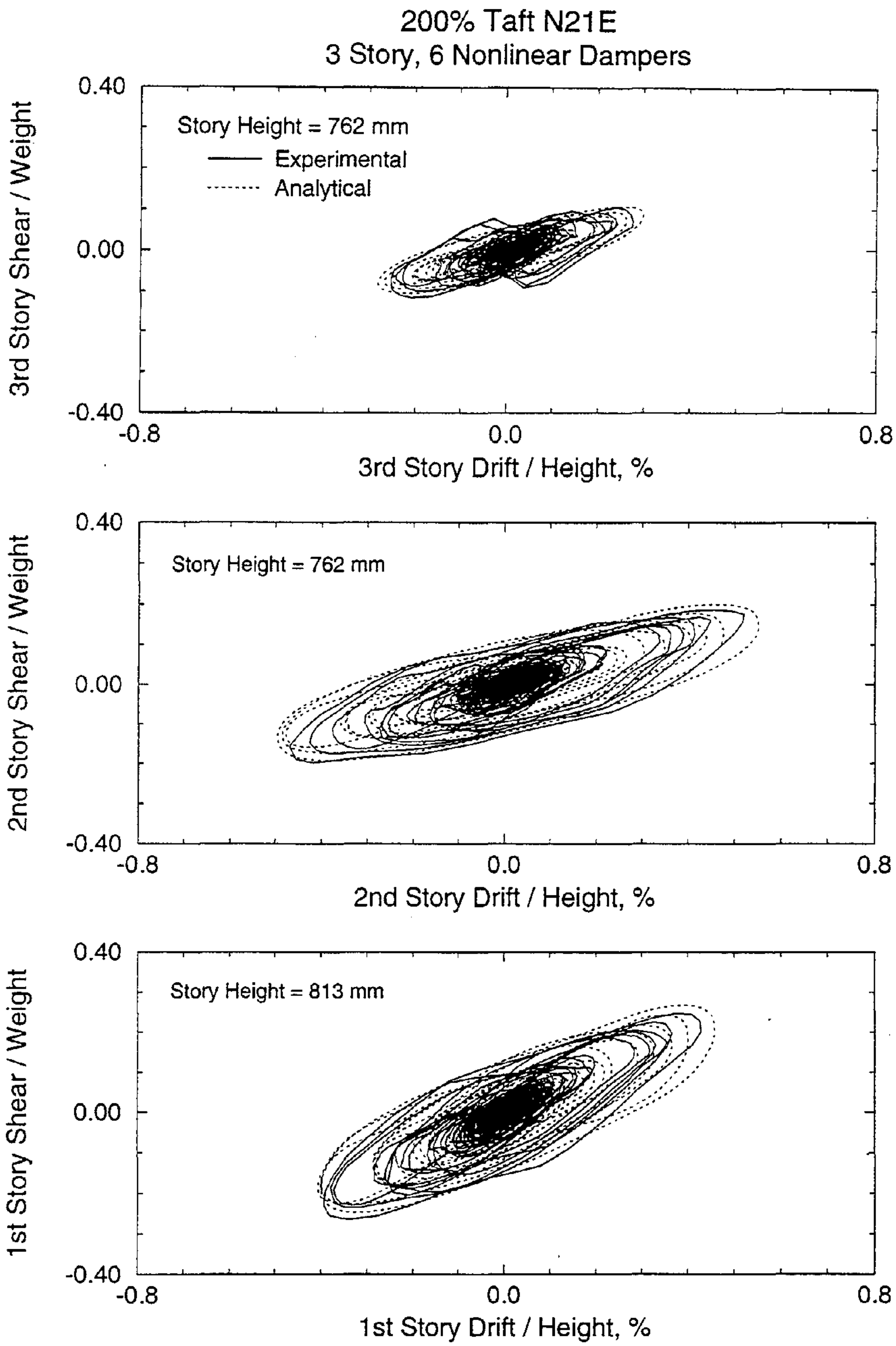

FIGURE 6-26 Comparison of Experimental and Analytical Results of 3-Story Repaired Structure with Six Nonlinear Dampers Subjected to 200% Taft Earthquake (Refined Model of Nonlinear Dampers)

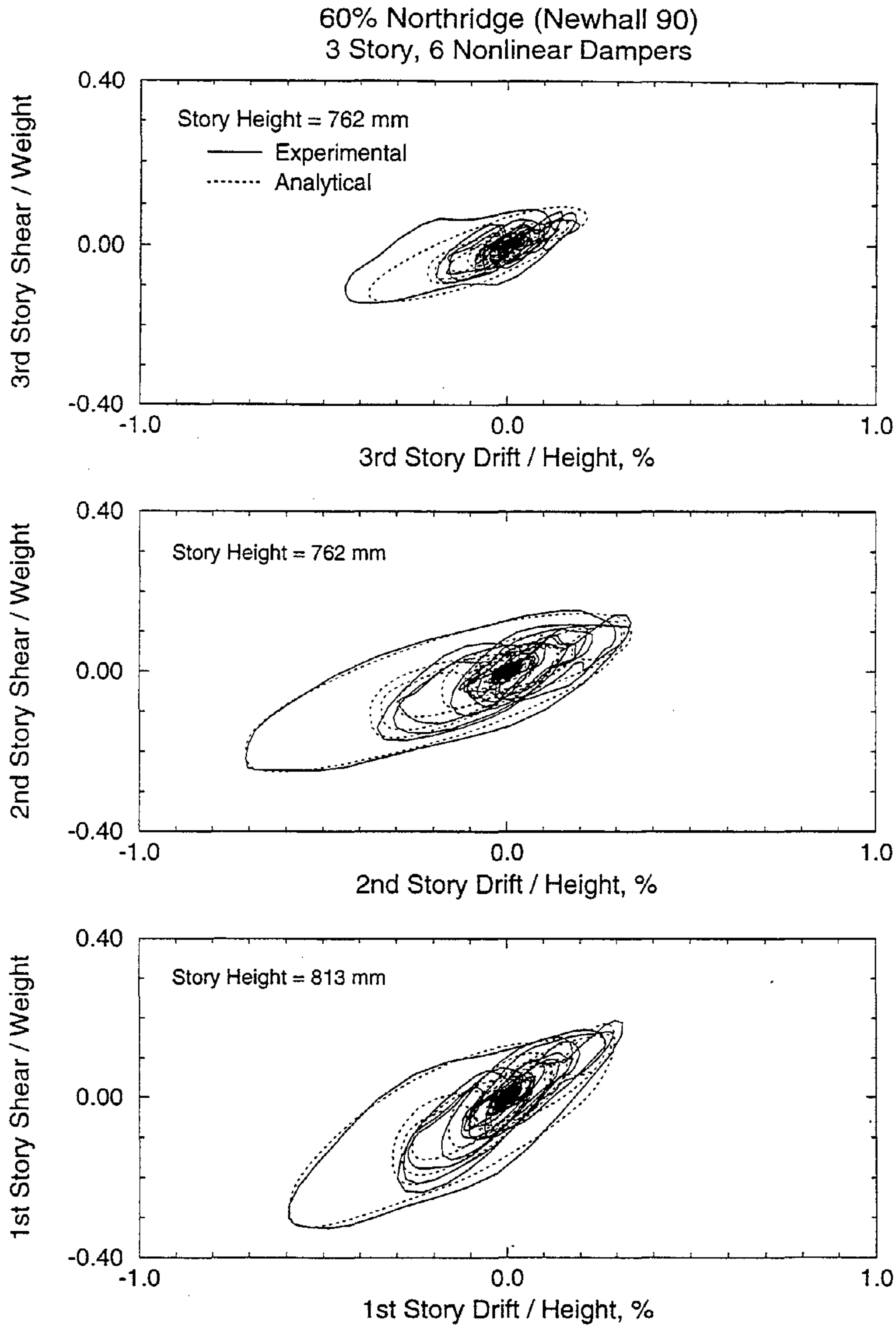

FIGURE 6-27 Comparison of Experimental and Analytical Results of 3-Story Repaired Structure with Six Nonlinear Dampers Subjected to 60% Northridge (Newhall 90) Earthquake (Refined Model of Nonlinear Dampers)

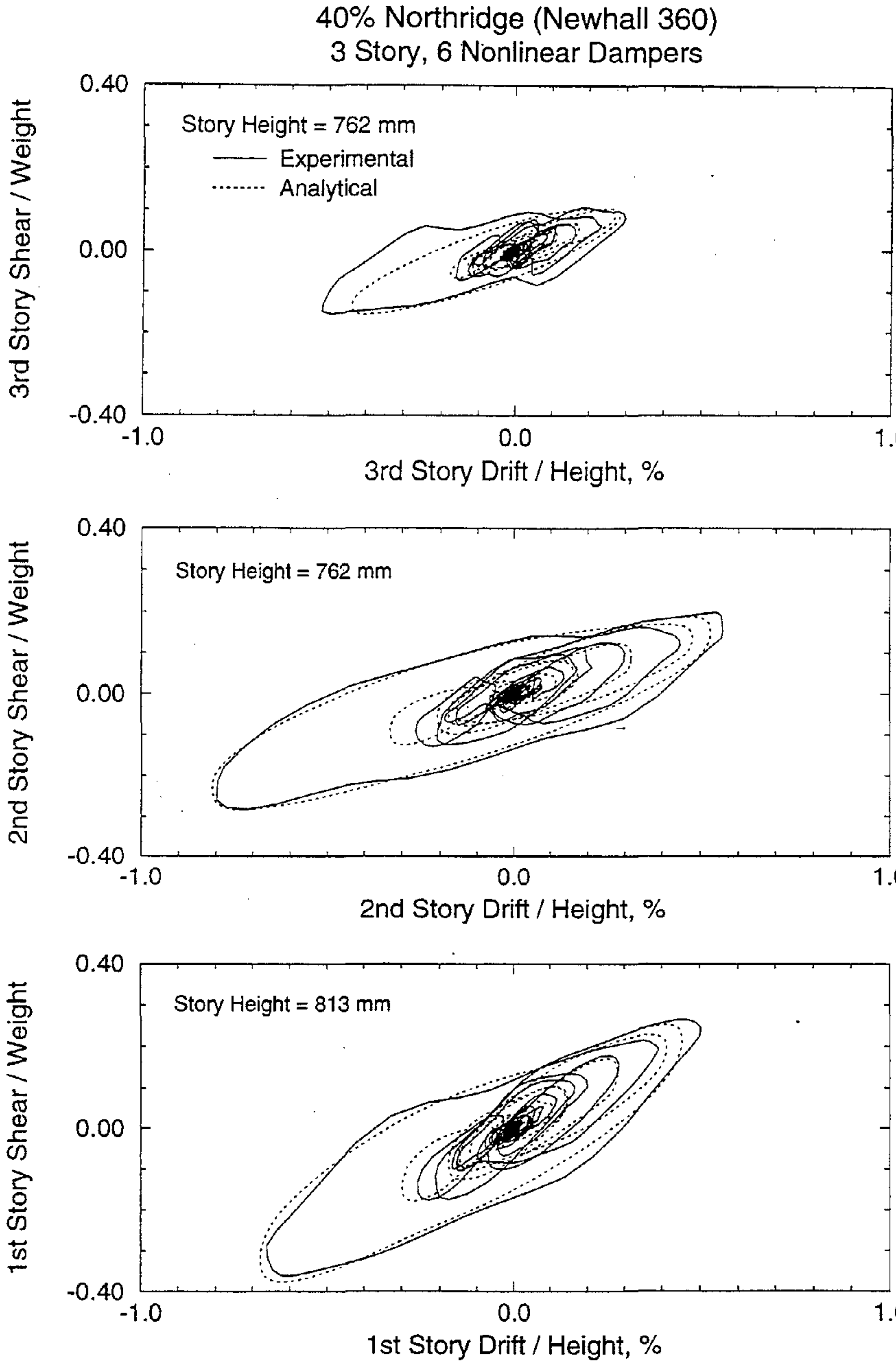

FIGURE 6-28 Comparison of Experimental and Analytical Results of 3-Story Repaired Structure with Six Nonlinear Dampers Subjected to 40% Northridge (Newhall 360) Earthquake (Refined Model of Nonlinear Dampers)

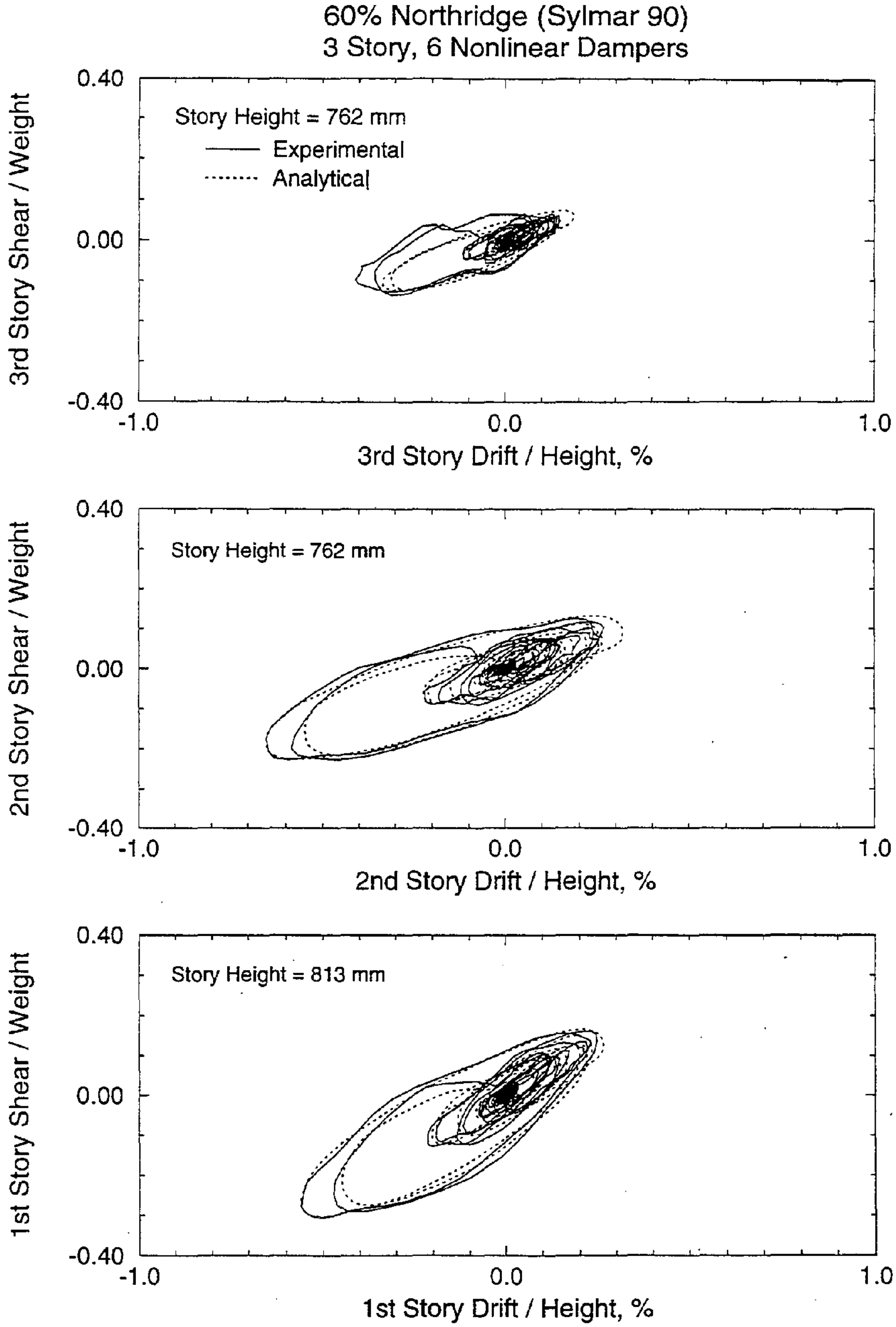

FIGURE 6-29 Comparison of Experimental and Analytical Results of 3-Story Repaired Structure with Six Nonlinear Dampers Subjected to 60% Northridge (Sylmar 90) Earthquake (Refined Model of Nonlinear Dampers)

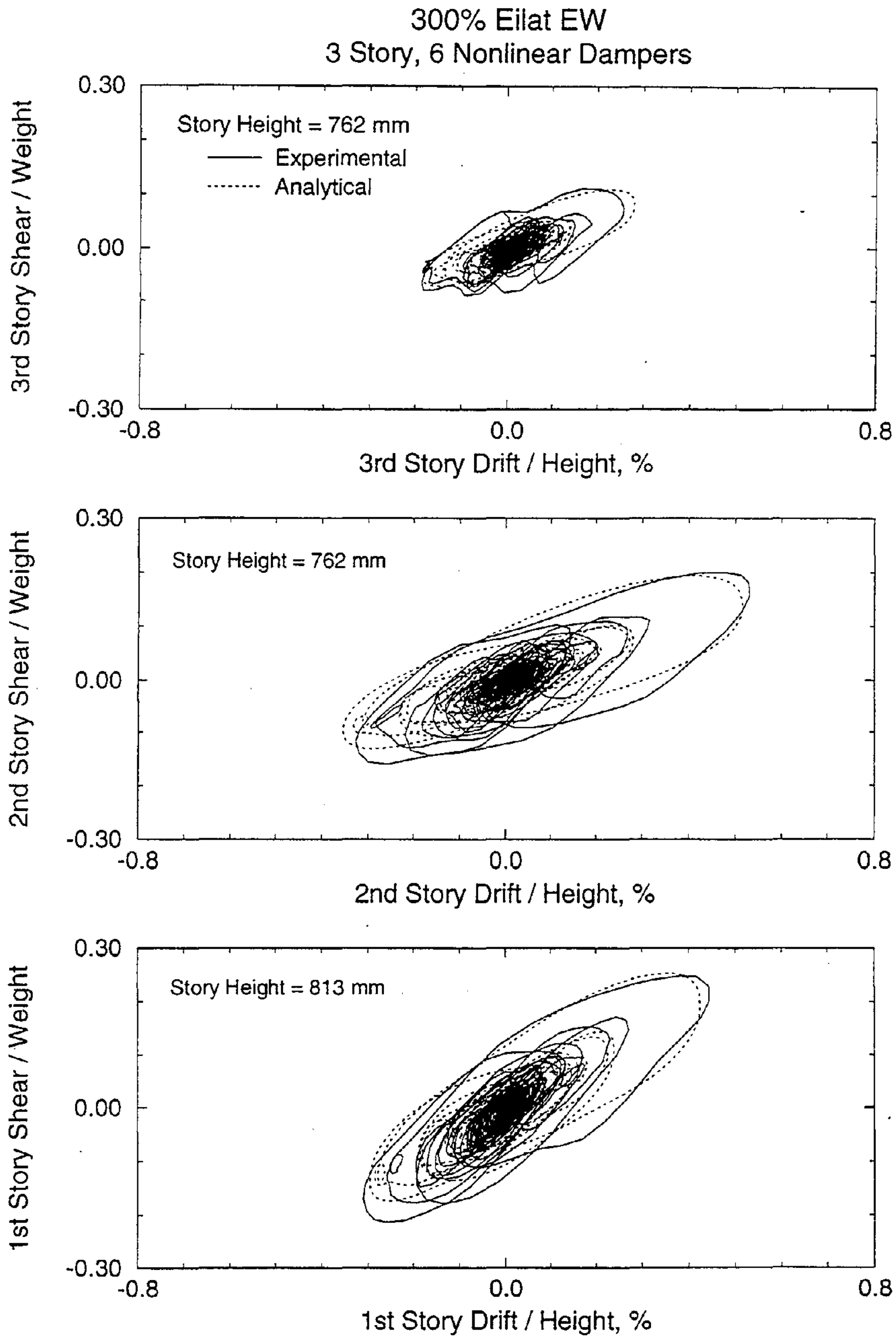

FIGURE 6-30 Comparison of Experimental and Analytical Results of 3-Story Repaired Structure with Six Nonlinear Dampers Subjected to 300% Eilat EW Earthquake (Refined Model of Nonlinear Dampers)

The procedure followed herein is essentially the same as the Linear Static Procedure, except that the actual damped response spectra are used. This, of course, is possible since the actual ground motions are available.

6.3.1 Description of Simplified Analysis Procedure

The simplified procedure is based on estimation of the damping effect by calculating the effective damping ratio as

$$\beta_{eff} = \beta + \frac{\sum_j W_j}{4\pi . W_s} \tag{6-9}$$

where β is the damping ratio in the structural frame exclusive of dampers, W_j is the energy dissipated in damper j and W_s is the maximum strain energy in the frame. Energies W_j and W_s are evaluated for the actual damper and frame displacements. Moreover, summation $\sum$ extends over all devices j.

In the case of linear viscous damping devices, Equation (6-9) assumes a simple form that was presented in Constantinou and Symans (1992). Herein, we specialize Equation (6-9) in the case of nonlinear dampers. The energy dissipated by a nonlinear damper (described by Equation (6-4)) during harmonic motion at frequency ω_k has been determined by Soong and Constantinou (1994) to be

$$W_j = C_{o_j} \lambda_j \omega_k^{\alpha_j} \cos^{1+\alpha_j} \theta_j (u_j - u_{j-1})^{1+\alpha_j} \tag{6-10}$$

where

$$\lambda_j = 4\frac{\Gamma^2(1+\frac{\alpha_j}{2})}{\Gamma(2+\alpha_j)}(2^{\alpha_j}) \tag{6-11}$$

in which Γ is the gamma function. Values of quantity λ can be found tabulated in FEMA (1996). Specific values of λ that are of interest herein are $\lambda = \pi$ for $\alpha = 1$ and $\lambda = 3.496$ for $\alpha = 0.5$.

The maximum strain energy may more conveniently be evaluated as maximum kinetic energy. Again considering harmonic motion at frequency ω_k, energy W_s is given by

$$W_s = \frac{1}{2}\omega_k^2 \sum_i m_i u_i^2 \tag{6-12}$$

where the summation extends over all lumped masses m_i. It follows that the contribution to the effective damping from dampers is

$$\xi_k = \frac{\sum_j \eta_j C_{oj} \lambda \cos^{1+\alpha}\theta_j (u_j - u_{j-1})^{1+\alpha}}{2\pi\omega_k^{2-\alpha}\sum_i m_i u_i^2} \tag{6-13}$$

where now summation j extends over all stories (assumed that each story has η_j identical dampers with constant C_{oj}) and summation i extends over all floors. Moreover, it has been assumed that all dampers have identical parameter $\alpha_j = \alpha$.

In an attempt to derive the contribution to damping in each mode of vibration, we assume that

$$u_j = A\phi_j \tag{6-14}$$

where ϕ_j is the model displacement corresponding to displacement u_j (ϕ_j is assumed dimensionless) and A is the amplitude (with dimension of length). It follows that

$$\xi_k = \frac{\sum_j \eta_j C_{oj} \lambda \cos^{1+\alpha}\theta_j (\phi_j - \phi_{j-1})^{1+\alpha}}{2\pi A^{1-\alpha}\omega_k^{2-\alpha}\sum_i m_i \phi_i^2} \tag{6-15}$$

For the case of linear dampers ($\alpha = 1$), Equation (6-15) simplifies to

$$\xi_k = \frac{\sum_j \eta_j C_{oj} \cos^2\theta_j (\phi_j - \phi_{j-1})^2}{2\omega_k \sum_i m_i \phi_i^2} \tag{6-16}$$

which is identical to the results presented in Constantinou and Symans (1992). In Equations (6-15) and (6-16), ω_k is the frequency and ϕ_j is the modal displacement of the *k*-th mode.

Important in the application of Equation (6-15) and (6-16) is the assumption that the frequencies and mode shapes of the damped structure are identical to those of the structure exclusive of the viscous dampers. This, of course, is an approximation since the damped structure is non-classically damped. Another important assumption made is that modal analysis procedures are applicable to nonlinear structures (in this case, linear frame with nonlinear dampers).

Particularly, the application of Equation (6-15) for the calculation of the damping ratio depends on the interpretation of quantity A. Since the seismic response is primarily in the first mode, Equation (6-15) may be applied for the prediction of the first mode damping ratio. However, it would be incorrect to apply this equation to the prediction of the damping ratio in the higher modes because of ambiguity of quantity A (it cannot be interpreted as the amplitude of the higher mode contribution to the displacements). This issue is further discussed in Section 6.3.4.

The simplified analysis of the damped structure is performed by application of modal analysis theory. Briefly describing this theory, a building is represented by a series of single-degree-of-freedom systems, each one of which is characterized by frequency ω_k, damping ratio ξ_k and weight w_k^* (k denotes the k-th mode).

$$w_k^* = \sum_i w_i \phi_i \tag{6-17}$$

where w_i is the reactive weight lumped at floor i and ϕ_i is the modal displacement of degree-of-freedom i of the k-th mode (herein, the model of the structural system has one degree-of-freedom per floor). Each one of these single-degree-of-freedom systems is excited at the base by excitation $\Gamma_k \ddot{u}_g$, where Γ_k is the modal participation factor:

$$\Gamma_k = \frac{\sum_i w_i \phi_i}{\sum_i w_i \phi_i^2} \tag{6-18}$$

For each mode of vibration the peak spectral response is obtained directly from response spectra of motion $\ddot{u}_g$. This response consists of the spectral displacement Sd_k, the spectral acceleration (or pseudo-acceleration, that is, acceleration at the instant of maximum displacement)

$Sa_k = \omega_k^2 Sd_k$ and the maximum acceleration Sm_k (if spectra of maximum acceleration are available). Typically, only the 5%-damped spectral acceleration spectrum is available (the usual analysis specification). The NEHRP Guidelines (FEMA 1996) describe a procedure for constructing spectra of pseudo-acceleration through the use of de-amplification factors for the effective damping in the system and the use of the 5%-damped spectrum. Moreover, the same guidelines prescribe that the maximum acceleration is related to the pseudo-acceleration through

$$Sm_k = Sa_k (f_1 + 2\beta_{eff} f_2) \tag{6-19}$$

where

$$f_1 = \cos\left[\tan^{-1}(2\beta_{eff})\right] \tag{6-20}$$

$$f_2 = \sin\left[\tan^{-1}(2\beta_{eff})\right] \tag{6-21}$$

Equations (6-19) to (6-21) are based on the assumption of harmonic response. Under these conditions, it may be shown that any response quantity at the stage of maximum acceleration may be determined as f_1 times the response at the stage of maximum drift plus f_2 times the response at the stage of maximum velocity (see Constantinou et. al., 1996). Equations (6-19) to (6-21) are strictly applicable to the case of linear viscous behavior. When the viscous behavior is highly nonlinear (say $\alpha < 0.5$), the damper force-displacement loops resemble hysteretic loops and the peak damper force occurs nearly instantaneously with the peak restoring force (that is, the instance of maximum acceleration is nearly the same as the instance of maximum drift).

With the peak spectral response determined either directly from response spectra or approximately by the procedure of the NEHRP Guidelines, the contribution of the k-th mode to the peak response of the building is:

Displacement at floor i

$$u_i = \phi_i \Gamma_k Sd_k \tag{6-22}$$

Acceleration of floor i at instant of maximum displacement

$$a_i = \phi_i \Gamma_k Sa_k \tag{6-23}$$

Base shear at instant of maximum displacement

$$V_k = w_k^* \Gamma_k Sa_k / g \tag{6-24}$$

It should be noted that quantity $w_k^* \Gamma_k$ represents the modal weight. Equations (6-22) to (6-24) describe the response at the stage of maximum displacement.

This information is, typically, sufficient for the design of buildings without energy dissipation devices. However, for buildings with viscous or viscoelastic energy dissipation devices, it is important to calculate the response at the stages of maximum velocity and of maximum acceleration (Constantinou et al 1996, FEMA 1996). The maximum velocity is typically determined in a simplified analysis as pseudo-velocity, that is, $\omega_k Sd_k$.

6.3.2 Prediction of Dynamic Properties of Tested 3-Story Structure

The damping ratio of the tested 3-story structure with linear dampers is predicted by the simplified procedure (Equations 6-9 and 6-16) and compared to results of rigorous analysis. Since the tested dampers exhibited stiffness at high frequencies, the analysis method described in Section 4.3.4 and based on the Maxwell model for the dampers produces what we will call "exact" results. They are presented in table 6-I. The same method of analysis, however based on the viscous model for the dampers, produces nearly exact results on the damping ratio for the first mode and over-estimates the damping ratio for the higher modes. This is due to the fact that the viscous model is incapable of predicting the increases in higher modes frequencies that results from the stiffening effect of the dampers.

The predictions of the simplified procedure (that is, Equations (6-9) and (6-16), with β being 0.027 for the first mode and 0.01 for the higher modes) are nearly identical to the results of the rigorous analysis with the viscous model in the case of a complete vertical distribution of dampers. This is due to the fact that the structure with a complete vertical distribution of dampers has mild non-proportional damping (that is, the damping matrix is some-how close to being proportional to the stiffness matrix). The structure with incomplete vertical distribution of dampers has strong non-proportional damping. Nevertheless, the simplified procedure predicts good estimates of the damping ratio, which can lead to conservative estimation of response (as seen in Table 6-I, the first mode damping ratio is under-predicted).

Table 6-I Damping Ratio (in % of Critical) as Predicted by Different Analytical Methods for 3-Story Structure

Number of Dampers	Rigorous Method Maxwell Model			Rigorous Method Viscous Model			Simplified Procedure (Equation 6-16)		
	Mode 1	Mode 2	Mode 3	Mode 1	Mode 2	Mode 3	Mode 1	Mode 2	Mode 3
2	12.57	1.34	23.57	12.70	1.42	29.83	10.49	1.33	29.47
4	15.44	33.14	32.85	15.63	36.21	42.37	14.65	36.82	40.81
6	21.79	47.10	33.50	21.61	46.56	48.67	21.32	46.64	48.30
Remarks on Model of Dampers	$C_o = 17.7 N.s/mm$ $\lambda = 0.008\,\text{sec}$			$C_o = 16 N.s/mm$ $\lambda = 0$			$C_o = 16 N.s/mm$		

6.3.3 Prediction of Response of 3-Story Structure with Linear Dampers

A simplified analysis of the 3-story structure with a complete vertical distribution of linear dampers is presented in detail for the case of the El Centro 100% motion. Table 6-II presents the modal properties and the spectral response of the structure. It should be noted that the spectral displacement, Sd_k, has been obtained directly from the high damping response spectra of Figure 3-13, whereas the spectral acceleration has been determined as $Sa_k = \omega_k^2 Sd_k$. Moreover, the average value of damping constant of the damper, that is $C_o = 16.0$ N.s/mm, has been used.

Table 6-III presents a summary of peak modal responses and of combined responses by use of the SRSS rule. It should be noted that the damper axial displacement has been calculated as story drift times $\cos\theta_j$ and that the damper axial velocity has been calculated as displacement times ω_k (that is, as pseudo-velocity). The damper axial force is given by damper axial velocity times C_o. Moreover, the maximum floor inertia force has been calculated as floor mass times acceleration at instant of maximum displacement (Equation (6-23)) times factor $(f_1 + 2\beta_{eff} f_2)$. The maximum story shear forces were then calculated from equilibrium.

Table 6-III contains also the peak recorded (experimental) response. It may be observed that displacements are predicted well and that story shear forces are under-predicted by approximately 15%. The reason for this under-prediction is the approximate nature of factor $(f_1 + 2\beta_{eff} f_2)$ used to estimate the maximum acceleration from spectral acceleration.

Furthermore, the damper forces are predicted well given that the damping constants (C_o) were not exactly known and an average value was used in the calculation. It should be noted that the

Table 6-II Modal Properties of 3-Story Structure with Six Linear Dampers and Spectral Response for El Centro 100% Motion

	Mode 1	Mode 2	Mode 3
Period (sec)	0.439	0.133	0.070
Frequency (Hz)	2.28	7.52	14.26
Frequency $\omega_k (rad/\sec)$	14.33	47.25	89.60
	Mode Shapes		
Floor 3	1	1	1
Floor 2	0.736	-0.843	-2.727
Floor 1	0.360	-1.016	3.174
Modal Weight (N)	24652	2523	960
Participation Factor Γ_k	1.2541	-0.3132	0.0782
Effective Damping β_{eff}	0.22	0.48	0.50
Spectral Displacement $Sd_k(mm)$	14.0	2.0	0.6
Spectral Acceleration $Sa_k(g)$	0.293	0.455	0.491
Factor f_1	0.912	0.720	0.707
Factor f_2	0.403	0.695	0.707
Factor $(f_1 + 2\beta_{eff} f_2)$	1.092	1.391	1.414

Table 6-III Summary of Results of Simplified Analysis Procedure of 3-Story Structure with Six Linear Dampers for El Centro 100% Motion

Peak Response Quantity	Floor or Story	Mode 1	Mode 2	Mode 3	SRSS	Experimental
Floor Displacement (mm)	3	17.984	-0.626	0.047	17.995	17.8
	2	13.237	0.528	-0.128	13.248	13.3
	1	6.474	0.636	0.149	6.507	6.1
Story Drift (mm)	3	4 .747	1.154	0.175	4.888	4.8
	2	6.736	0.108	0.277	6.770	7.2
	1	6.474	0.636	0.149	6.507	6.1
Damper Axial Displacement (mm)	3	4.026	0.979	0.148	4.146	4.1
	2	5.735	0.092	0.126	5.737	6.1
	1	5.238	0.515	0.121	5.265	4.9
Damper Axial Velocity (mm/sec)	3	57.675	46.257	13.261	75.113	64.5
	2	82.158	4.347	11.289	83.044	97.0
	1	75.035	24.334	10.841	79.624	82.0
Damper Axial Force (N)	3	922.8	740.1	212.2	1201.8	968.0*
	2	1314.5	69.6	180.6	1328.7	1589.0*
	1	1200.6	389.3	173.5	1274.0	1521.0*
Maximum Floor Inertia Force (N)	3	3936	-1945	533		
	2	2897	1639	-1425		N/A
	1	1417	1975	1690		
Maximum Story Shear Force (N)	3	3936	1945	533	4423	4895
	2	6833	306	919	6901	7878
	1	8250	1669	771	8452	9116

* : Average Value (measured directly from shear force - drift loops and corrected for angle of dampers)

actual values of damping constant (for the three tested devices ; for the other three the constant is not known) were within ± 15% of the utilized value (see Section 2).

Figure 6-31 presents a comparison of important response quantities of the 3-story structure with six linear dampers in three selected earthquakes. These quantities were either measured or analytically predicted by the time history and simplified analysis procedures. Evidently, the simplified analysis procedure provides good estimates of dynamic response.

6.3.4 Prediction of Response of 3-Story Structure with Nonlinear Dampers

The simplified analysis procedure is applied to the case of the 3-story structure with a complete vertical distribution of nonlinear dampers for the El Centro 100% motion.

Utilizing Equation (6-15) for the first mode of the structure (modal properties are those reported in Table 6-II) and using $\alpha = 0.5$, $C_{o1} = 300 \quad N(s/mm)^{1/2}$, $C_{o2} = 235 \quad N(s/mm)^{1/2}$ and $C_{o3} = 220 \quad N(s/mm)^{1/2}$, we obtain

$$\xi_1 = 1.4718/\sqrt{A} \tag{6-25}$$

where A is in units of mm. Noting that the mode shape has been normalized to a unit value for the top floor displacement, A represents the peak displacement of the top floor. Moreover, utilizing the average value of $C_o = 252 \quad N(s/mm)^{1/2}$ (see Figure 2-8) we calculate

$$\xi_1 = 1.4477/\sqrt{A} \tag{6-26}$$

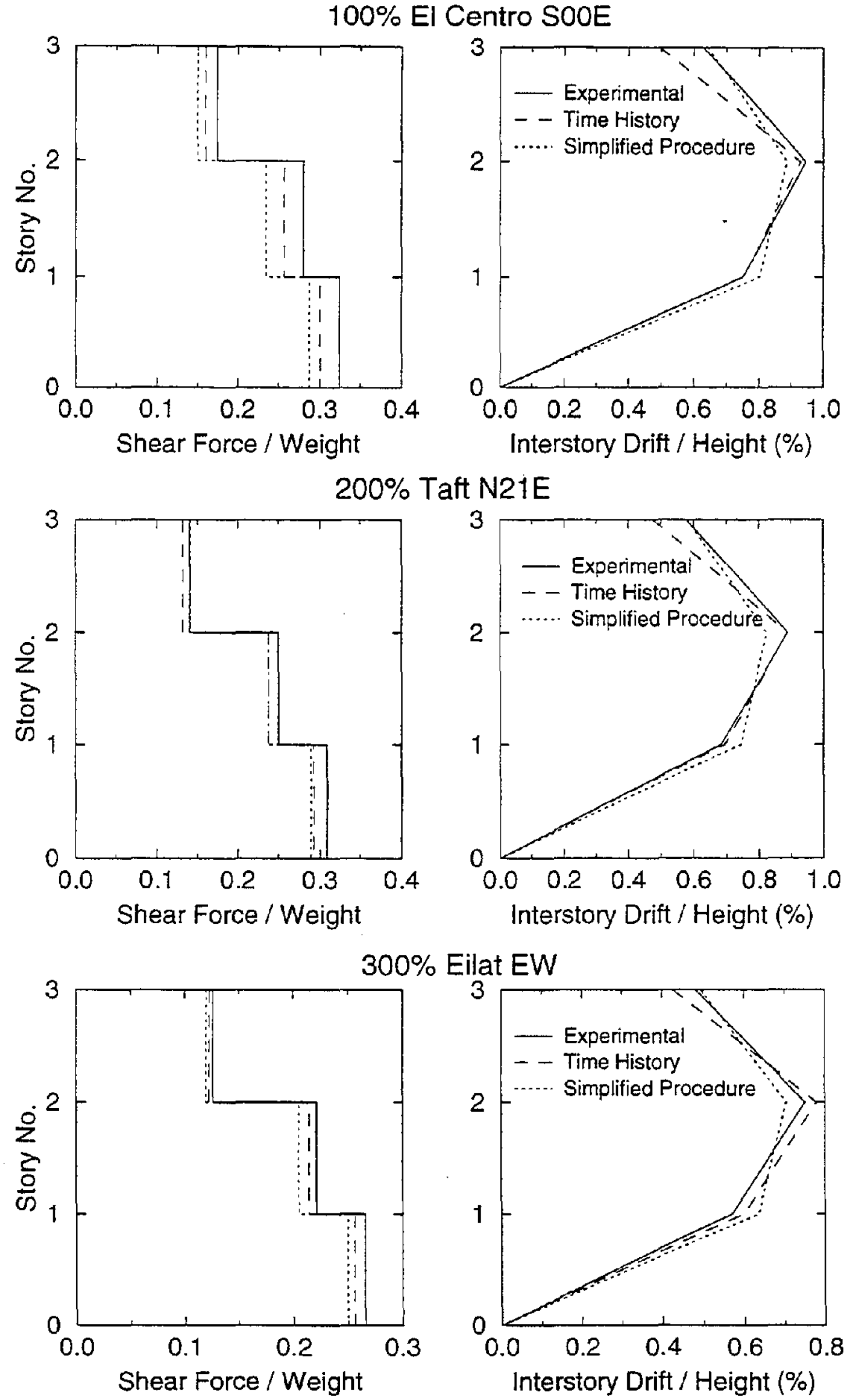

FIGURE 6-31 Comparison of Story Shear and Interstory Drift Profiles obtained Experimentally and Analytically (using Time History and Simplified Analysis Procedure) of 3-Story Repaired Structure with Six Linear Dampers Subjected to 100% El Centro, 200% Taft, and 300% Eilat EW Earthquakes

which differs from Equation (6-25) by less than 2%. This indicates that the actual distribution of damping constant is not important in the calculation of the damping ratio. It is, however, important in the calculation of forces in individual dampers.

Table 6-IV lists values of the first mode damping ratio for various values of the top floor displacement A.

Table 6-IV Values of First Mode Damping Ratio as Function of Top Floor Displacement

Top Floor *Displacement A* (*mm*)	6	8	10	12	14	16	18
ξ_1	0.60	0.52	0.46	0.42	0.39	0.37	0.35

Since the damping ratio is amplitude-dependent, the analysis requires an iterative process. However, due to the weak dependency of the damping ratio on amplitude and the insensitivity of response to changes in the damping ratio (when it is large), it is possible to obtain the response in a single iteration. That is, assuming that the top floor displacement will be in the range of 10 to 16 mm, the effective damping will be of the order of 0.40. Accordingly, the first mode spectral response is $Sd_1 = 10$ mm and $Sa_1 = \omega_1^2 Sd_1 = 0.21$ g (from Figure 3-13 for period of 0.44 sec and damping of 0.4). The calculated response in the first mode is presented in Table 6-V. Since the calculated top floor displacement is 12.5 mm, the assumed value $\xi_1 = 0.40$ is valid. It should be noted that the analysis procedure is identical to that followed for the case of linear dampers. Exception is the calculation of the story shear forces, which were calculated as superposition of peak restoring force and of peak horizontal component of damper force. The former has been

Table 6-V Summary of Results of Simplified Analysis Procedure of 3-Story Structure with Six Nonlinear Dampers for El Centro 100% Motion

Peak Response Quantity	Floor or Story	Mode 1	Mode 2	Mode 3	SRSS	Experimental
Floor Displacement (mm)	3	12.541	-0.626	0.047	12.557	13.6
	2	9.230	0.528	-0.128	9.246	10.2
	1	4.515	0.636	0.149	4.562	4.6
Story Drift (mm)	3	3.311	1.154	0.175	3.511	3.7
	2	4.715	0.108	0.277	4.724	5.7
	1	4.515	0.636	0.149	4.562	4.6
Damper Axial Displacement (mm)	3	2.679	0.979	0.148	2.856	3.2
	2	3.999	0.092	0.126	4.002	4.8
	1	3.829	0.515	0.121	3.865	3.8
Damper Axial Velocity (mm/sec)	3	38.385	46.257	13.261	61.555	49.5
	2	57.229	4.347	11.289	58.562	82.0
	1	54.869	24.334	10.841	60.994	65.0
Damper Axial Force (N)	3	1363.0	823.4	236.0	1609.8	1327.0*
	2	1778.8	67.4	175.0	1788.7	2004.0*
	1	2222.2	491.5	219.0	2286.4	2318.0*
Maximum Floor Inertia Force (N)	3		-1859	484		
	2	N/A	1567	-1321		N/A
	1		1889	1537		
Maximum Story Shear Force (N)	3	4782	1859	484	5153	4980
	2	7305	292	837	7359	8015
	1	8773	1597	700	8945	10213

* : Average Value (measured directly from shear force - drift loops and corrected for angle of dampers)

calculated from fictitious floor inertia forces that were based on the spectral acceleration, that is $F_i = m_i \Gamma_1 \phi_i Sa_1$.

The calculation of response in the higher modes is complicated by the fact that Equation (6-15) is not directly applicable. To obtain estimates of the damping ratio in the higher modes, we resort to a physical interpretation of the higher mode response. The higher mode response may be viewed as a small amplitude, higher frequency motion centered around the first mode response. Accordingly, we may define an effective damping constant for each damper based on the slope of the force-velocity curve of the damper at the calculated velocity in the first mode. That is, the effective (linearized) damping constant C_{ol} is given by

$$C_{ol} = \alpha C_o \dot{u}_1^{\alpha - 1} \tag{6-27}$$

where $\dot{u}_1$ is the calculated damper velocity in the first mode. This concept is illustrated in Figure 6-32, whereas Table 6-VI presents calculations of the effective damping constant (for $\alpha = 0.5$). Utilizing these values of linearized damping constant and Equation (6-16), the damping ratios in the second and third modes have been determined to be 0.48 and 0.45, respectively. That is, they are essentially the same as those of the structure with linear dampers (see Table 6-II). This should be expected since, on the average, the effective damping constant is about equal to the damping constant of the linear dampers (=16.0 N.s/mm).

Calculations of response in the higher modes are presented in Table 6-V. These calculations are based on the following quantities. For the second mode: $Sd_2 = 2$ mm, $Sa_2 = 0.455$ g, $(f_1 + 2\beta_{eff} f_2) = 1.391$. For the third mode: $Sd_3 = 0.6$ mm, $Sa_3 = 0.491$ g, $(f_1 + 2\beta_{eff} f_2) = 1.345$.

Table 6-VI **Effective Damping Constant for Calculation of Higher Mode Response**

Story	Damping Constant $C_o(N.(s/mm)^{1/2})$	First Mode Velocity $\dot{u}_1(mm/s)$	Effective Damping Constant $C_{ol}(N.s/mm)$
3	220	38.4	17.8
2	235	57.3	15.5
1	300	54.9	20.2

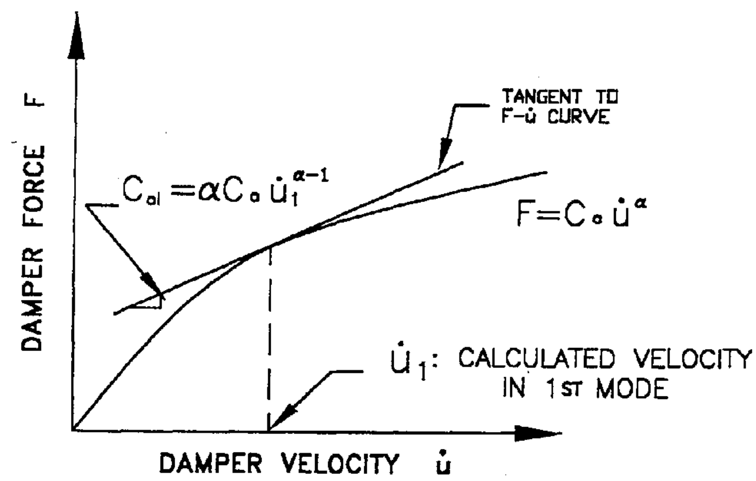

FIGURE 6-32 Effective (Linearized) Damping Constant for Higher Mode Response Calculation

Note that Equation (6-19) is used since effective linear damper behavior has been assumed. Moreover, for the calculation of damper forces, the effective damping constants in Table 6-VI have been used.

A comparison of the results of the simplified analysis to experimental results in Table 6-V reveals overall good agreement between the two sets of results. Particularly, the analytical prediction is within about 15% of the experimental response. It is worthy of noting that had the simplified analysis been entirely based on the Linear Static Procedure of FEMA (1996), the analytical prediction would, probably, have been overall conservative due to the use of conservative response de-amplification factors for high damping. Further systematic comparisons of "exact" and simplified results along the lines established in Constantinou et al (1996) are needed.

SECTION 7

SUMMARY AND CONCLUSIONS

A combined experimental and analytical study has been conducted in order to assess the impact of increasing the seismic energy dissipation capacity of structures by using supplemental linear and nonlinear viscous damping devices. The experimental part of the program consisted of component testing of devices and of shake table testing of one-story and 3-story model structures. The analytical study consisted of calculations of response by time history and by simplified methods of analysis, and of comparisons to experimental results.

The component testing of the dampers revealed their mechanical properties, which were then used for the development and calibration of mathematical models for these devices. These models were utilized in the identification of structural properties and the analytical prediction of the seismic response of the tested structure.

The shaking table testing of the model 3-story structure was conducted with various configurations of dampers which included complete and incomplete vertical distributions. Testing was also conducted on the model one-story and three-story structures without dampers in a configuration resembling moment resisting frames. Testing was conducted with ten different earthquake records, white noise excitations and a number of sinusoidal motions of specified amplitudes and frequencies.

The conclusions of this study are summarized below:

a) The addition of fluid viscous dampers to the tested structures resulted in significant reductions in both drift and total shear force response (total force includes the restoring and damping force components). In a comparison to the response of the same structures without dampers, the addition of dampers resulted in drift reduction by 30% to 90% and shear force reduction by 20% to 65%.

b) Reduction of the total shear force response was possible because the tested structure remained in the elastic range. Such reductions in the total shear force cannot be realized when the structure undergoes significant inelastic action. However, whether the action in the structural frame is elastic or inelastic, the addition of dampers results in significant drift reduction, which in turn results in a comparable reduction of shear force and bending moment in the columns.

c) The reduction in drift response was significant in all conducted tests, which included some near-fault earthquake motions with high velocity, single pulse characteristics.

d) Nonlinear dampers generally produced more drift response reduction than linear dampers. This was achieved with either a modest reduction or a modest increase in the total shear force response.

e) Floor response spectra of the damped structure had, in general, significant lower ordinates than those of the structure without dampers. Typically, the addition of nonlinear dampers resulted in the appearance of high frequency components in the floor response spectra. It is believed that this phenomenon has been induced by the nonlinearity of the dampers.

f) Time history analysis of the tested structures with linear and nonlinear dampers produced results in good agreement with the results of the experiments.

g) Calculations of peak seismic response by a simplified method produced results that were within about 15% of the experimental results. This simplified analysis procedure has been largely based on the Linear Static Procedure of the NEHRP Guidelines for the Seismic Rehabilitation of Buildings. The applicability of this procedure to the case of nonlinear dampers has not been previously confirmed. This study produced a modification of the Linear Static Procedure that is applicable to the case of nonlinear dampers and is sufficiently accurate for design purposes.

SECTION 8

REFERENCES

Chung, L.L., Lin, R.C., Soong, T.T. and Reinhorn, A.M., (1988), "Experimental Study of Active Control of MDOF Structures Under Seismic Excitations," Report No. NCEER-88-0025, National Center for Earthquake Engineering Research, Buffalo, New York.

Clough, R.W. and Penzien, J., (1993), "Dynamics of Structures," McGraw-Hill, New York.

Constantinou, M.C. and Symans, M.D., (1992), "Experimental and Analytical Investigation of Seismic Response of Structures with Supplemental Fluid Viscous Dampers," Report No. NCEER-92-0032, National Center for Earthquake Engineering Research, Buffalo, New York.

Constantinou, M.C., Soong, T.T. and Dargush G.F., (1996), "Passive Energy Dissipation Systems for Structural Design and Retrofit," Monograph of National Center for Earthquake Engineering Research, Buffalo, New York.

Federal Emergency Management Agency - FEMA, (1996), "NEHRP Guidelines and Commentary for the Seismic Rehabilitation of Buildings," Reports No. 273 and 274, September, Ballot Version.

International Mathematical Statistical Library - IMSL, (1987), Subroutine DIVPAG, Houston, Texas.

Kelly, J.M., (1993), "Earthquake Resistant Design with Rubber," Springer - Verlag, London.

Reinhorn, A.M., Li, C. and Constantinou M.C., (1995), "Experimental and Analytical Investigation of Seismic Retrofit of Structures with Supplemental Damping: Part I - Fluid

Viscous Damping Devices," Report No. NCEER-95-0001, National Center for Earthquake Engineering Research, Buffalo, New York.

Rodriguez, S., Seim, C. And Ingham, T., (1994), "Earthquake Protective Systems for the Seismic Upgrade of the Golden Gate Bridge," Proc. 3rd U.S.-Japan Workshop on Protective Systems for Bridges, Berkeley, CA, January.

Skinner, R.I, Tyler, Robinson, W.H., Mc Verry, G.H., (1993), "An Introduction to Seismic Isolation," John Wiley and Sons, New York.

Soong, T.T. and Constantinou, M.C., (1994), "Passive and Active Structural Vibration Control in Civil Engineering," Springer - Verlag, New York.

Soong, T.T. and Dargush G.F., (1996), "Passive Energy Dissipation Systems in Structural Engineering," Wiley and Sons, London.

Symans, M.D. and Constantinou, M.C., (1995), "Development and Experimental Study of Semi-Active Fluid Damping Devices for Seismic Protection of Structures," Report No. NCEER-95-0011, National Center for Earthquake Engineering Research, Buffalo, New York.

Tsopelas, P., Okamoto, S., Constantinou, M.C., Ozaki, D. And Fujii, S., (1994), "NCEER-Taisei Corporation Research Program on Sliding Seismic Isolation Systems for Bridges: Experimental and Analytical Study of Systems Consisting of Sliding Bearings, Rubber Restoring Force Devices and Fluid Dampers," Volumes I and II, Report No. NCEER-94-0002, National Center for Earthquake Engineering Research, Buffalo, New York.

Uang, C-M. and Bertero, V.V., (1988), "Use of Energy as a Design Criterion in Earthquake-Resistant Design," Report No. UCB/EERC-88/18, University of California, Berkeley.

NATIONAL CENTER FOR EARTHQUAKE ENGINEERING RESEARCH
LIST OF TECHNICAL REPORTS

The National Center for Earthquake Engineering Research (NCEER) publishes technical reports on a variety of subjects related to earthquake engineering written by authors funded through NCEER. These reports are available from both NCEER Publications and the National Technical Information Service (NTIS). Requests for reports should be directed to NCEER Publications, National Center for Earthquake Engineering Research, State University of New York at Buffalo, Red Jacket Quadrangle, Buffalo, New York 14261. Reports can also be requested through NTIS, 5285 Port Royal Road, Springfield, Virginia 22161. NTIS accession numbers are shown in parenthesis, if available.

NCEER-87-0001 "First-Year Program in Research, Education and Technology Transfer," 3/5/87, (PB88-134275, A04, MF-A01).

NCEER-87-0002 "Experimental Evaluation of Instantaneous Optimal Algorithms for Structural Control," by R.C. Lin, T.T. Soong and A.M. Reinhorn, 4/20/87, (PB88-134341, A04, MF-A01).

NCEER-87-0003 "Experimentation Using the Earthquake Simulation Facilities at University at Buffalo," by A.M. Reinhorn and R.L. Ketter, to be published.

NCEER-87-0004 "The System Characteristics and Performance of a Shaking Table," by J.S. Hwang, K.C. Chang and G.C. Lee, 6/1/87, (PB88-134259, A03, MF-A01). This report is available only through NTIS (see address given above).

NCEER-87-0005 "A Finite Element Formulation for Nonlinear Viscoplastic Material Using a Q Model," by O. Gyebi and G. Dasgupta, 11/2/87, (PB88-213764, A08, MF-A01).

NCEER-87-0006 "Symbolic Manipulation Program (SMP) - Algebraic Codes for Two and Three Dimensional Finite Element Formulations," by X. Lee and G. Dasgupta, 11/9/87, (PB88-218522, A05, MF-A01).

NCEER-87-0007 "Instantaneous Optimal Control Laws for Tall Buildings Under Seismic Excitations," by J.N. Yang, A. Akbarpour and P. Ghaemmaghami, 6/10/87, (PB88-134333, A06, MF-A01). This report is only available through NTIS (see address given above).

NCEER-87-0008 "IDARC: Inelastic Damage Analysis of Reinforced Concrete Frame - Shear-Wall Structures," by Y.J. Park, A.M. Reinhorn and S.K. Kunnath, 7/20/87, (PB88-134325, A09, MF-A01). This report is only available through NTIS (see address given above).

NCEER-87-0009 "Liquefaction Potential for New York State: A Preliminary Report on Sites in Manhattan and Buffalo," by M. Budhu, V. Vijayakumar, R.F. Giese and L. Baumgras, 8/31/87, (PB88-163704, A03, MF-A01). This report is available only through NTIS (see address given above).

NCEER-87-0010 "Vertical and Torsional Vibration of Foundations in Inhomogeneous Media," by A.S. Veletsos and K.W. Dotson, 6/1/87, (PB88-134291, A03, MF-A01). This report is only available through NTIS (see address given above).

NCEER-87-0011 "Seismic Probabilistic Risk Assessment and Seismic Margins Studies for Nuclear Power Plants," by Howard H.M. Hwang, 6/15/87, (PB88-134267, A03, MF-A01). This report is only available through NTIS (see address given above).

NCEER-87-0012 "Parametric Studies of Frequency Response of Secondary Systems Under Ground-Acceleration Excitations," by Y. Yong and Y.K. Lin, 6/10/87, (PB88-134309, A03, MF-A01). This report is only available through NTIS (see address given above).

NCEER-87-0013 "Frequency Response of Secondary Systems Under Seismic Excitation," by J.A. HoLung, J. Cai and Y.K. Lin, 7/31/87, (PB88-134317, A05, MF-A01). This report is only available through NTIS (see address given above).

NCEER-87-0014 "Modelling Earthquake Ground Motions in Seismically Active Regions Using Parametric Time Series Methods," by G.W. Ellis and A.S. Cakmak, 8/25/87, (PB88-134283, A08, MF-A01). This report is only available through NTIS (see address given above).

NCEER-87-0015 "Detection and Assessment of Seismic Structural Damage," by E. DiPasquale and A.S. Cakmak, 8/25/87, (PB88-163712, A05, MF-A01). This report is only available through NTIS (see address given above).

NCEER-87-0016 "Pipeline Experiment at Parkfield, California," by J. Isenberg and E. Richardson, 9/15/87, (PB88-163720, A03, MF-A01). This report is available only through NTIS (see address given above).

NCEER-87-0017 "Digital Simulation of Seismic Ground Motion," by M. Shinozuka, G. Deodatis and T. Harada, 8/31/87, (PB88-155197, A04, MF-A01). This report is available only through NTIS (see address given above).

NCEER-87-0018 "Practical Considerations for Structural Control: System Uncertainty, System Time Delay and Truncation of Small Control Forces," J.N. Yang and A. Akbarpour, 8/10/87, (PB88-163738, A08, MF-A01). This report is only available through NTIS (see address given above).

NCEER-87-0019 "Modal Analysis of Nonclassically Damped Structural Systems Using Canonical Transformation," by J.N. Yang, S. Sarkani and F.X. Long, 9/27/87, (PB88-187851, A04, MF-A01).

NCEER-87-0020 "A Nonstationary Solution in Random Vibration Theory," by J.R. Red-Horse and P.D. Spanos, 11/3/87, (PB88-163746, A03, MF-A01).

NCEER-87-0021 "Horizontal Impedances for Radially Inhomogeneous Viscoelastic Soil Layers," by A.S. Veletsos and K.W. Dotson, 10/15/87, (PB88-150859, A04, MF-A01).

NCEER-87-0022 "Seismic Damage Assessment of Reinforced Concrete Members," by Y.S. Chung, C. Meyer and M. Shinozuka, 10/9/87, (PB88-150867, A05, MF-A01). This report is available only through NTIS (see address given above).

NCEER-87-0023 "Active Structural Control in Civil Engineering," by T.T. Soong, 11/11/87, (PB88-187778, A03, MF-A01).

NCEER-87-0024 "Vertical and Torsional Impedances for Radially Inhomogeneous Viscoelastic Soil Layers," by K.W. Dotson and A.S. Veletsos, 12/87, (PB88-187786, A03, MF-A01).

NCEER-87-0025 "Proceedings from the Symposium on Seismic Hazards, Ground Motions, Soil-Liquefaction and Engineering Practice in Eastern North America," October 20-22, 1987, edited by K.H. Jacob, 12/87, (PB88-188115, A23, MF-A01).

NCEER-87-0026 "Report on the Whittier-Narrows, California, Earthquake of October 1, 1987," by J. Pantelic and A. Reinhorn, 11/87, (PB88-187752, A03, MF-A01). This report is available only through NTIS (see address given above).

NCEER-87-0027 "Design of a Modular Program for Transient Nonlinear Analysis of Large 3-D Building Structures," by S. Srivastav and J.F. Abel, 12/30/87, (PB88-187950, A05, MF-A01). This report is only available through NTIS (see address given above).

NCEER-87-0028 "Second-Year Program in Research, Education and Technology Transfer," 3/8/88, (PB88-219480, A04, MF-A01).

NCEER-88-0001 "Workshop on Seismic Computer Analysis and Design of Buildings With Interactive Graphics," by W. McGuire, J.F. Abel and C.H. Conley, 1/18/88, (PB88-187760, A03, MF-A01). This report is only available through NTIS (see address given above).

NCEER-88-0002 "Optimal Control of Nonlinear Flexible Structures," by J.N. Yang, F.X. Long and D. Wong, 1/22/88, (PB88-213772, A06, MF-A01).

NCEER-88-0003 "Substructuring Techniques in the Time Domain for Primary-Secondary Structural Systems," by G.D. Manolis and G. Juhn, 2/10/88, (PB88-213780, A04, MF-A01).

NCEER-88-0004 "Iterative Seismic Analysis of Primary-Secondary Systems," by A. Singhal, L.D. Lutes and P.D. Spanos, 2/23/88, (PB88-213798, A04, MF-A01).

NCEER-88-0005 "Stochastic Finite Element Expansion for Random Media," by P.D. Spanos and R. Ghanem, 3/14/88, (PB88-213806, A03, MF-A01).

NCEER-88-0006 "Combining Structural Optimization and Structural Control," by F.Y. Cheng and C.P. Pantelides, 1/10/88, (PB88-213814, A05, MF-A01).

NCEER-88-0007 "Seismic Performance Assessment of Code-Designed Structures," by H.H-M. Hwang, J-W. Jaw and H-J. Shau, 3/20/88, (PB88-219423, A04, MF-A01). This report is only available through NTIS (see address given above).

NCEER-88-0008 "Reliability Analysis of Code-Designed Structures Under Natural Hazards," by H.H-M. Hwang, H. Ushiba and M. Shinozuka, 2/29/88, (PB88-229471, A07, MF-A01). This report is only available through NTIS (see address given above).

NCEER-88-0009 "Seismic Fragility Analysis of Shear Wall Structures," by J-W Jaw and H.H-M. Hwang, 4/30/88, (PB89-102867, A04, MF-A01).

NCEER-88-0010 "Base Isolation of a Multi-Story Building Under a Harmonic Ground Motion - A Comparison of Performances of Various Systems," by F-G Fan, G. Ahmadi and I.G. Tadjbakhsh, 5/18/88, (PB89-122238, A06, MF-A01). This report is only available through NTIS (see address given above).

NCEER-88-0011 "Seismic Floor Response Spectra for a Combined System by Green's Functions," by F.M. Lavelle, L.A. Bergman and P.D. Spanos, 5/1/88, (PB89-102875, A03, MF-A01).

NCEER-88-0012 "A New Solution Technique for Randomly Excited Hysteretic Structures," by G.Q. Cai and Y.K. Lin, 5/16/88, (PB89-102883, A03, MF-A01).

NCEER-88-0013 "A Study of Radiation Damping and Soil-Structure Interaction Effects in the Centrifuge," by K. Weissman, supervised by J.H. Prevost, 5/24/88, (PB89-144703, A06, MF-A01).

NCEER-88-0014 "Parameter Identification and Implementation of a Kinematic Plasticity Model for Frictional Soils," by J.H. Prevost and D.V. Griffiths, to be published.

NCEER-88-0015 "Two- and Three- Dimensional Dynamic Finite Element Analyses of the Long Valley Dam," by D.V. Griffiths and J.H. Prevost, 6/17/88, (PB89-144711, A04, MF-A01).

NCEER-88-0016 "Damage Assessment of Reinforced Concrete Structures in Eastern United States," by A.M. Reinhorn, M.J. Seidel, S.K. Kunnath and Y.J. Park, 6/15/88, (PB89-122220, A04, MF-A01). This report is only available through NTIS (see address given above).

NCEER-88-0017 "Dynamic Compliance of Vertically Loaded Strip Foundations in Multilayered Viscoelastic Soils," by S. Ahmad and A.S.M. Israil, 6/17/88, (PB89-102891, A04, MF-A01).

NCEER-88-0018 "An Experimental Study of Seismic Structural Response With Added Viscoelastic Dampers," by R.C. Lin, Z. Liang, T.T. Soong and R.H. Zhang, 6/30/88, (PB89-122212, A05, MF-A01). This report is available only through NTIS (see address given above).

NCEER-88-0019 "Experimental Investigation of Primary - Secondary System Interaction," by G.D. Manolis, G. Juhn and A.M. Reinhorn, 5/27/88, (PB89-122204, A04, MF-A01).

NCEER-88-0020 "A Response Spectrum Approach For Analysis of Nonclassically Damped Structures," by J.N. Yang, S. Sarkani and F.X. Long, 4/22/88, (PB89-102909, A04, MF-A01).

NCEER-88-0021 "Seismic Interaction of Structures and Soils: Stochastic Approach," by A.S. Veletsos and A.M. Prasad, 7/21/88, (PB89-122196, A04, MF-A01). This report is only available through NTIS (see address given above).

NCEER-88-0022 "Identification of the Serviceability Limit State and Detection of Seismic Structural Damage," by E. DiPasquale and A.S. Cakmak, 6/15/88, (PB89-122188, A05, MF-A01). This report is available only through NTIS (see address given above).

NCEER-88-0023 "Multi-Hazard Risk Analysis: Case of a Simple Offshore Structure," by B.K. Bhartia and E.H. Vanmarcke, 7/21/88, (PB89-145213, A05, MF-A01).

NCEER-88-0024 "Automated Seismic Design of Reinforced Concrete Buildings," by Y.S. Chung, C. Meyer and M. Shinozuka, 7/5/88, (PB89-122170, A06, MF-A01). This report is available only through NTIS (see address given above).

NCEER-88-0025 "Experimental Study of Active Control of MDOF Structures Under Seismic Excitations," by L.L. Chung, R.C. Lin, T.T. Soong and A.M. Reinhorn, 7/10/88, (PB89-122600, A04, MF-A01).

NCEER-88-0026 "Earthquake Simulation Tests of a Low-Rise Metal Structure," by J.S. Hwang, K.C. Chang, G.C. Lee and R.L. Ketter, 8/1/88, (PB89-102917, A04, MF-A01).

NCEER-88-0027 "Systems Study of Urban Response and Reconstruction Due to Catastrophic Earthquakes," by F. Kozin and H.K. Zhou, 9/22/88, (PB90-162348, A04, MF-A01).

NCEER-88-0028 "Seismic Fragility Analysis of Plane Frame Structures," by H.H-M. Hwang and Y.K. Low, 7/31/88, (PB89-131445, A06, MF-A01).

NCEER-88-0029 "Response Analysis of Stochastic Structures," by A. Kardara, C. Bucher and M. Shinozuka, 9/22/88, (PB89-174429, A04, MF-A01).

NCEER-88-0030 "Nonnormal Accelerations Due to Yielding in a Primary Structure," by D.C.K. Chen and L.D. Lutes, 9/19/88, (PB89-131437, A04, MF-A01).

NCEER-88-0031 "Design Approaches for Soil-Structure Interaction," by A.S. Veletsos, A.M. Prasad and Y. Tang, 12/30/88, (PB89-174437, A03, MF-A01). This report is available only through NTIS (see address given above).

NCEER-88-0032 "A Re-evaluation of Design Spectra for Seismic Damage Control," by C.J. Turkstra and A.G. Tallin, 11/7/88, (PB89-145221, A05, MF-A01).

NCEER-88-0033 "The Behavior and Design of Noncontact Lap Splices Subjected to Repeated Inelastic Tensile Loading," by V.E. Sagan, P. Gergely and R.N. White, 12/8/88, (PB89-163737, A08, MF-A01).

NCEER-88-0034 "Seismic Response of Pile Foundations," by S.M. Mamoon, P.K. Banerjee and S. Ahmad, 11/1/88, (PB89-145239, A04, MF-A01).

NCEER-88-0035 "Modeling of R/C Building Structures With Flexible Floor Diaphragms (IDARC2)," by A.M. Reinhorn, S.K. Kunnath and N. Panahshahi, 9/7/88, (PB89-207153, A07, MF-A01).

NCEER-88-0036 "Solution of the Dam-Reservoir Interaction Problem Using a Combination of FEM, BEM with Particular Integrals, Modal Analysis, and Substructuring," by C-S. Tsai, G.C. Lee and R.L. Ketter, 12/31/88, (PB89-207146, A04, MF-A01).

NCEER-88-0037 "Optimal Placement of Actuators for Structural Control," by F.Y. Cheng and C.P. Pantelides, 8/15/88, (PB89-162846, A05, MF-A01).

NCEER-88-0038 "Teflon Bearings in Aseismic Base Isolation: Experimental Studies and Mathematical Modeling," by A. Mokha, M.C. Constantinou and A.M. Reinhorn, 12/5/88, (PB89-218457, A10, MF-A01). This report is available only through NTIS (see address given above).

NCEER-88-0039 "Seismic Behavior of Flat Slab High-Rise Buildings in the New York City Area," by P. Weidlinger and M. Ettouney, 10/15/88, (PB90-145681, A04, MF-A01).

NCEER-88-0040 "Evaluation of the Earthquake Resistance of Existing Buildings in New York City," by P. Weidlinger and M. Ettouney, 10/15/88, to be published.

NCEER-88-0041 "Small-Scale Modeling Techniques for Reinforced Concrete Structures Subjected to Seismic Loads," by W. Kim, A. El-Attar and R.N. White, 11/22/88, (PB89-189625, A05, MF-A01).

NCEER-88-0042 "Modeling Strong Ground Motion from Multiple Event Earthquakes," by G.W. Ellis and A.S. Cakmak, 10/15/88, (PB89-174445, A03, MF-A01).

NCEER-88-0043 "Nonstationary Models of Seismic Ground Acceleration," by M. Grigoriu, S.E. Ruiz and E. Rosenblueth, 7/15/88, (PB89-189617, A04, MF-A01).

NCEER-88-0044 "SARCF User's Guide: Seismic Analysis of Reinforced Concrete Frames," by Y.S. Chung, C. Meyer and M. Shinozuka, 11/9/88, (PB89-174452, A08, MF-A01).

NCEER-88-0045 "First Expert Panel Meeting on Disaster Research and Planning," edited by J. Pantelic and J. Stoyle, 9/15/88, (PB89-174460, A05, MF-A01). This report is only available through NTIS (see address given above).

NCEER-88-0046 "Preliminary Studies of the Effect of Degrading Infill Walls on the Nonlinear Seismic Response of Steel Frames," by C.Z. Chrysostomou, P. Gergely and J.F. Abel, 12/19/88, (PB89-208383, A05, MF-A01).

NCEER-88-0047 "Reinforced Concrete Frame Component Testing Facility - Design, Construction, Instrumentation and Operation," by S.P. Pessiki, C. Conley, T. Bond, P. Gergely and R.N. White, 12/16/88, (PB89-174478, A04, MF-A01).

NCEER-89-0001 "Effects of Protective Cushion and Soil Compliancy on the Response of Equipment Within a Seismically Excited Building," by J.A. HoLung, 2/16/89, (PB89-207179, A04, MF-A01).

NCEER-89-0002 "Statistical Evaluation of Response Modification Factors for Reinforced Concrete Structures," by H.H-M. Hwang and J-W. Jaw, 2/17/89, (PB89-207187, A05, MF-A01).

NCEER-89-0003 "Hysteretic Columns Under Random Excitation," by G-Q. Cai and Y.K. Lin, 1/9/89, (PB89-196513, A03, MF-A01).

NCEER-89-0004 "Experimental Study of 'Elephant Foot Bulge' Instability of Thin-Walled Metal Tanks," by Z-H. Jia and R.L. Ketter, 2/22/89, (PB89-207195, A03, MF-A01).

NCEER-89-0005 "Experiment on Performance of Buried Pipelines Across San Andreas Fault," by J. Isenberg, E. Richardson and T.D. O'Rourke, 3/10/89, (PB89-218440, A04, MF-A01). This report is available only through NTIS (see address given above).

NCEER-89-0006 "A Knowledge-Based Approach to Structural Design of Earthquake-Resistant Buildings," by M. Subramani, P. Gergely, C.H. Conley, J.F. Abel and A.H. Zaghw, 1/15/89, (PB89-218465, A06, MF-A01).

NCEER-89-0007 "Liquefaction Hazards and Their Effects on Buried Pipelines," by T.D. O'Rourke and P.A. Lane, 2/1/89, (PB89-218481, A09, MF-A01).

NCEER-89-0008 "Fundamentals of System Identification in Structural Dynamics," by H. Imai, C-B. Yun, O. Maruyama and M. Shinozuka, 1/26/89, (PB89-207211, A04, MF-A01).

NCEER-89-0009 "Effects of the 1985 Michoacan Earthquake on Water Systems and Other Buried Lifelines in Mexico," by A.G. Ayala and M.J. O'Rourke, 3/8/89, (PB89-207229, A06, MF-A01).

NCEER-89-R010 "NCEER Bibliography of Earthquake Education Materials," by K.E.K. Ross, Second Revision, 9/1/89, (PB90-125352, A05, MF-A01). This report is replaced by NCEER-92-0018.

NCEER-89-0011 "Inelastic Three-Dimensional Response Analysis of Reinforced Concrete Building Structures (IDARC-3D), Part I - Modeling," by S.K. Kunnath and A.M. Reinhorn, 4/17/89, (PB90-114612, A07, MF-A01).

NCEER-89-0012 "Recommended Modifications to ATC-14," by C.D. Poland and J.O. Malley, 4/12/89, (PB90-108648, A15, MF-A01).

NCEER-89-0013 "Repair and Strengthening of Beam-to-Column Connections Subjected to Earthquake Loading," by M. Corazao and A.J. Durrani, 2/28/89, (PB90-109885, A06, MF-A01).

NCEER-89-0014 "Program EXKAL2 for Identification of Structural Dynamic Systems," by O. Maruyama, C-B. Yun, M. Hoshiya and M. Shinozuka, 5/19/89, (PB90-109877, A09, MF-A01).

NCEER-89-0015 "Response of Frames With Bolted Semi-Rigid Connections, Part I - Experimental Study and Analytical Predictions," by P.J. DiCorso, A.M. Reinhorn, J.R. Dickerson, J.B. Radziminski and W.L. Harper, 6/1/89, to be published.

NCEER-89-0016 "ARMA Monte Carlo Simulation in Probabilistic Structural Analysis," by P.D. Spanos and M.P. Mignolet, 7/10/89, (PB90-109893, A03, MF-A01).

NCEER-89-P017 "Preliminary Proceedings from the Conference on Disaster Preparedness - The Place of Earthquake Education in Our Schools," Edited by K.E.K. Ross, 6/23/89, (PB90-108606, A03, MF-A01).

NCEER-89-0017 "Proceedings from the Conference on Disaster Preparedness - The Place of Earthquake Education in Our Schools," Edited by K.E.K. Ross, 12/31/89, (PB90-207895, A012, MF-A02). This report is available only through NTIS (see address given above).

NCEER-89-0018 "Multidimensional Models of Hysteretic Material Behavior for Vibration Analysis of Shape Memory Energy Absorbing Devices, by E.J. Graesser and F.A. Cozzarelli, 6/7/89, (PB90-164146, A04, MF-A01).

NCEER-89-0019 "Nonlinear Dynamic Analysis of Three-Dimensional Base Isolated Structures (3D-BASIS)," by S. Nagarajaiah, A.M. Reinhorn and M.C. Constantinou, 8/3/89, (PB90-161936, A06, MF-A01). This report has been replaced by NCEER-93-0011.

NCEER-89-0020 "Structural Control Considering Time-Rate of Control Forces and Control Rate Constraints," by F.Y. Cheng and C.P. Pantelides, 8/3/89, (PB90-120445, A04, MF-A01).

NCEER-89-0021 "Subsurface Conditions of Memphis and Shelby County," by K.W. Ng, T-S. Chang and H-H.M. Hwang, 7/26/89, (PB90-120437, A03, MF-A01).

NCEER-89-0022 "Seismic Wave Propagation Effects on Straight Jointed Buried Pipelines," by K. Elhmadi and M.J. O'Rourke, 8/24/89, (PB90-162322, A10, MF-A02).

NCEER-89-0023 "Workshop on Serviceability Analysis of Water Delivery Systems," edited by M. Grigoriu, 3/6/89, (PB90-127424, A03, MF-A01).

NCEER-89-0024 "Shaking Table Study of a 1/5 Scale Steel Frame Composed of Tapered Members," by K.C. Chang, J.S. Hwang and G.C. Lee, 9/18/89, (PB90-160169, A04, MF-A01).

NCEER-89-0025 "DYNA1D: A Computer Program for Nonlinear Seismic Site Response Analysis - Technical Documentation," by Jean H. Prevost, 9/14/89, (PB90-161944, A07, MF-A01). This report is available only through NTIS (see address given above).

NCEER-89-0026 "1:4 Scale Model Studies of Active Tendon Systems and Active Mass Dampers for Aseismic Protection," by A.M. Reinhorn, T.T. Soong, R.C. Lin, Y.P. Yang, Y. Fukao, H. Abe and M. Nakai, 9/15/89, (PB90-173246, A10, MF-A02).

NCEER-89-0027 "Scattering of Waves by Inclusions in a Nonhomogeneous Elastic Half Space Solved by Boundary Element Methods," by P.K. Hadley, A. Askar and A.S. Cakmak, 6/15/89, (PB90-145699, A07, MF-A01).

NCEER-89-0028 "Statistical Evaluation of Deflection Amplification Factors for Reinforced Concrete Structures," by H.H.M. Hwang, J-W. Jaw and A.L. Ch'ng, 8/31/89, (PB90-164633, A05, MF-A01).

NCEER-89-0029 "Bedrock Accelerations in Memphis Area Due to Large New Madrid Earthquakes," by H.H.M. Hwang, C.H.S. Chen and G. Yu, 11/7/89, (PB90-162330, A04, MF-A01).

NCEER-89-0030 "Seismic Behavior and Response Sensitivity of Secondary Structural Systems," by Y.Q. Chen and T.T. Soong, 10/23/89, (PB90-164658, A08, MF-A01).

NCEER-89-0031 "Random Vibration and Reliability Analysis of Primary-Secondary Structural Systems," by Y. Ibrahim, M. Grigoriu and T.T. Soong, 11/10/89, (PB90-161951, A04, MF-A01).

NCEER-89-0032 "Proceedings from the Second U.S. - Japan Workshop on Liquefaction, Large Ground Deformation and Their Effects on Lifelines, September 26-29, 1989," Edited by T.D. O'Rourke and M. Hamada, 12/1/89, (PB90-209388, A22, MF-A03).

NCEER-89-0033 "Deterministic Model for Seismic Damage Evaluation of Reinforced Concrete Structures," by J.M. Bracci, A.M. Reinhorn, J.B. Mander and S.K. Kunnath, 9/27/89, (PB91-108803, A06, MF-A01).

NCEER-89-0034 "On the Relation Between Local and Global Damage Indices," by E. DiPasquale and A.S. Cakmak, 8/15/89, (PB90-173865, A05, MF-A01).

NCEER-89-0035 "Cyclic Undrained Behavior of Nonplastic and Low Plasticity Silts," by A.J. Walker and H.E. Stewart, 7/26/89, (PB90-183518, A10, MF-A01).

NCEER-89-0036 "Liquefaction Potential of Surficial Deposits in the City of Buffalo, New York," by M. Budhu, R. Giese and L. Baumgrass, 1/17/89, (PB90-208455, A04, MF-A01).

NCEER-89-0037 "A Deterministic Assessment of Effects of Ground Motion Incoherence," by A.S. Veletsos and Y. Tang, 7/15/89, (PB90-164294, A03, MF-A01).

NCEER-89-0038 "Workshop on Ground Motion Parameters for Seismic Hazard Mapping," July 17-18, 1989, edited by R.V. Whitman, 12/1/89, (PB90-173923, A04, MF-A01).

NCEER-89-0039 "Seismic Effects on Elevated Transit Lines of the New York City Transit Authority," by C.J. Costantino, C.A. Miller and E. Heymsfield, 12/26/89, (PB90-207887, A06, MF-A01).

NCEER-89-0040 "Centrifugal Modeling of Dynamic Soil-Structure Interaction," by K. Weissman, Supervised by J.H. Prevost, 5/10/89, (PB90-207879, A07, MF-A01).

NCEER-89-0041 "Linearized Identification of Buildings With Cores for Seismic Vulnerability Assessment," by I-K. Ho and A.E. Aktan, 11/1/89, (PB90-251943, A07, MF-A01).

NCEER-90-0001 "Geotechnical and Lifeline Aspects of the October 17, 1989 Loma Prieta Earthquake in San Francisco," by T.D. O'Rourke, H.E. Stewart, F.T. Blackburn and T.S. Dickerman, 1/90, (PB90-208596, A05, MF-A01).

NCEER-90-0002 "Nonnormal Secondary Response Due to Yielding in a Primary Structure," by D.C.K. Chen and L.D. Lutes, 2/28/90, (PB90-251976, A07, MF-A01).

NCEER-90-0003 "Earthquake Education Materials for Grades K-12," by K.E.K. Ross, 4/16/90, (PB91-251984, A05, MF-A05). This report has been replaced by NCEER-92-0018.

NCEER-90-0004 "Catalog of Strong Motion Stations in Eastern North America," by R.W. Busby, 4/3/90, (PB90-251984, A05, MF-A01).

NCEER-90-0005 "NCEER Strong-Motion Data Base: A User Manual for the GeoBase Release (Version 1.0 for the Sun3)," by P. Friberg and K. Jacob, 3/31/90 (PB90-258062, A04, MF-A01).

NCEER-90-0006 "Seismic Hazard Along a Crude Oil Pipeline in the Event of an 1811-1812 Type New Madrid Earthquake," by H.H.M. Hwang and C-H.S. Chen, 4/16/90, (PB90-258054, A04, MF-A01).

NCEER-90-0007 "Site-Specific Response Spectra for Memphis Sheahan Pumping Station," by H.H.M. Hwang and C.S. Lee, 5/15/90, (PB91-108811, A05, MF-A01).

NCEER-90-0008 "Pilot Study on Seismic Vulnerability of Crude Oil Transmission Systems," by T. Ariman, R. Dobry, M. Grigoriu, F. Kozin, M. O'Rourke, T. O'Rourke and M. Shinozuka, 5/25/90, (PB91-108837, A06, MF-A01).

NCEER-90-0009 "A Program to Generate Site Dependent Time Histories: EQGEN," by G.W. Ellis, M. Srinivasan and A.S. Cakmak, 1/30/90, (PB91-108829, A04, MF-A01).

NCEER-90-0010 "Active Isolation for Seismic Protection of Operating Rooms," by M.E. Talbott, Supervised by M. Shinozuka, 6/8/9, (PB91-110205, A05, MF-A01).

NCEER-90-0011 "Program LINEARID for Identification of Linear Structural Dynamic Systems," by C-B. Yun and M. Shinozuka, 6/25/90, (PB91-110312, A08, MF-A01).

NCEER-90-0012 "Two-Dimensional Two-Phase Elasto-Plastic Seismic Response of Earth Dams," by A.N. Yiagos, Supervised by J.H. Prevost, 6/20/90, (PB91-110197, A13, MF-A02).

NCEER-90-0013 "Secondary Systems in Base-Isolated Structures: Experimental Investigation, Stochastic Response and Stochastic Sensitivity," by G.D. Manolis, G. Juhn, M.C. Constantinou and A.M. Reinhorn, 7/1/90, (PB91-110320, A08, MF-A01).

NCEER-90-0014 "Seismic Behavior of Lightly-Reinforced Concrete Column and Beam-Column Joint Details," by S.P. Pessiki, C.H. Conley, P. Gergely and R.N. White, 8/22/90, (PB91-108795, A11, MF-A02).

NCEER-90-0015 "Two Hybrid Control Systems for Building Structures Under Strong Earthquakes," by J.N. Yang and A. Danielians, 6/29/90, (PB91-125393, A04, MF-A01).

NCEER-90-0016 "Instantaneous Optimal Control with Acceleration and Velocity Feedback," by J.N. Yang and Z. Li, 6/29/90, (PB91-125401, A03, MF-A01).

NCEER-90-0017 "Reconnaissance Report on the Northern Iran Earthquake of June 21, 1990," by M. Mehrain, 10/4/90, (PB91-125377, A03, MF-A01).

NCEER-90-0018 "Evaluation of Liquefaction Potential in Memphis and Shelby County," by T.S. Chang, P.S. Tang, C.S. Lee and H. Hwang, 8/10/90, (PB91-125427, A09, MF-A01).

NCEER-90-0019 "Experimental and Analytical Study of a Combined Sliding Disc Bearing and Helical Steel Spring Isolation System," by M.C. Constantinou, A.S. Mokha and A.M. Reinhorn, 10/4/90, (PB91-125385, A06, MF-A01). This report is available only through NTIS (see address given above).

NCEER-90-0020 "Experimental Study and Analytical Prediction of Earthquake Response of a Sliding Isolation System with a Spherical Surface," by A.S. Mokha, M.C. Constantinou and A.M. Reinhorn, 10/11/90, (PB91-125419, A05, MF-A01).

NCEER-90-0021 "Dynamic Interaction Factors for Floating Pile Groups," by G. Gazetas, K. Fan, A. Kaynia and E. Kausel, 9/10/90, (PB91-170381, A05, MF-A01).

NCEER-90-0022 "Evaluation of Seismic Damage Indices for Reinforced Concrete Structures," by S. Rodriguez-Gomez and A.S. Cakmak, 9/30/90, PB91-171322, A06, MF-A01).

NCEER-90-0023 "Study of Site Response at a Selected Memphis Site," by H. Desai, S. Ahmad, E.S. Gazetas and M.R. Oh, 10/11/90, (PB91-196857, A03, MF-A01).

NCEER-90-0024 "A User's Guide to Strongmo: Version 1.0 of NCEER's Strong-Motion Data Access Tool for PCs and Terminals," by P.A. Friberg and C.A.T. Susch, 11/15/90, (PB91-171272, A03, MF-A01).

NCEER-90-0025 "A Three-Dimensional Analytical Study of Spatial Variability of Seismic Ground Motions," by L-L. Hong and A.H.-S. Ang, 10/30/90, (PB91-170399, A09, MF-A01).

NCEER-90-0026 "MUMOID User's Guide - A Program for the Identification of Modal Parameters," by S. Rodriguez-Gomez and E. DiPasquale, 9/30/90, (PB91-171298, A04, MF-A01).

NCEER-90-0027 "SARCF-II User's Guide - Seismic Analysis of Reinforced Concrete Frames," by S. Rodriguez-Gomez, Y.S. Chung and C. Meyer, 9/30/90, (PB91-171280, A05, MF-A01).

NCEER-90-0028 "Viscous Dampers: Testing, Modeling and Application in Vibration and Seismic Isolation," by N. Makris and M.C. Constantinou, 12/20/90 (PB91-190561, A06, MF-A01).

NCEER-90-0029 "Soil Effects on Earthquake Ground Motions in the Memphis Area," by H. Hwang, C.S. Lee, K.W. Ng and T.S. Chang, 8/2/90, (PB91-190751, A05, MF-A01).

NCEER-91-0001 "Proceedings from the Third Japan-U.S. Workshop on Earthquake Resistant Design of Lifeline Facilities and Countermeasures for Soil Liquefaction, December 17-19, 1990," edited by T.D. O'Rourke and M. Hamada, 2/1/91, (PB91-179259, A99, MF-A04).

NCEER-91-0002 "Physical Space Solutions of Non-Proportionally Damped Systems," by M. Tong, Z. Liang and G.C. Lee, 1/15/91, (PB91-179242, A04, MF-A01).

NCEER-91-0003 "Seismic Response of Single Piles and Pile Groups," by K. Fan and G. Gazetas, 1/10/91, (PB92-174994, A04, MF-A01).

NCEER-91-0004 "Damping of Structures: Part 1 - Theory of Complex Damping," by Z. Liang and G. Lee, 10/10/91, (PB92-197235, A12, MF-A03).

NCEER-91-0005 "3D-BASIS - Nonlinear Dynamic Analysis of Three Dimensional Base Isolated Structures: Part II," by S. Nagarajaiah, A.M. Reinhorn and M.C. Constantinou, 2/28/91, (PB91-190553, A07, MF-A01). This report has been replaced by NCEER-93-0011.

NCEER-91-0006 "A Multidimensional Hysteretic Model for Plasticity Deforming Metals in Energy Absorbing Devices," by E.J. Graesser and F.A. Cozzarelli, 4/9/91, (PB92-108364, A04, MF-A01).

NCEER-91-0007 "A Framework for Customizable Knowledge-Based Expert Systems with an Application to a KBES for Evaluating the Seismic Resistance of Existing Buildings," by E.G. Ibarra-Anaya and S.J. Fenves, 4/9/91, (PB91-210930, A08, MF-A01).

NCEER-91-0008 "Nonlinear Analysis of Steel Frames with Semi-Rigid Connections Using the Capacity Spectrum Method," by G.G. Deierlein, S-H. Hsieh, Y-J. Shen and J.F. Abel, 7/2/91, (PB92-113828, A05, MF-A01).

NCEER-91-0009 "Earthquake Education Materials for Grades K-12," by K.E.K. Ross, 4/30/91, (PB91-212142, A06, MF-A01). This report has been replaced by NCEER-92-0018.

NCEER-91-0010 "Phase Wave Velocities and Displacement Phase Differences in a Harmonically Oscillating Pile," by N. Makris and G. Gazetas, 7/8/91, (PB92-108356, A04, MF-A01).

NCEER-91-0011 "Dynamic Characteristics of a Full-Size Five-Story Steel Structure and a 2/5 Scale Model," by K.C. Chang, G.C. Yao, G.C. Lee, D.S. Hao and Y.C. Yeh," 7/2/91, (PB93-116648, A06, MF-A02).

NCEER-91-0012 "Seismic Response of a 2/5 Scale Steel Structure with Added Viscoelastic Dampers," by K.C. Chang, T.T. Soong, S-T. Oh and M.L. Lai, 5/17/91, (PB92-110816, A05, MF-A01).

NCEER-91-0013 "Earthquake Response of Retaining Walls; Full-Scale Testing and Computational Modeling," by S. Alampalli and A-W.M. Elgamal, 6/20/91, to be published.

NCEER-91-0014 "3D-BASIS-M: Nonlinear Dynamic Analysis of Multiple Building Base Isolated Structures," by P.C. Tsopelas, S. Nagarajaiah, M.C. Constantinou and A.M. Reinhorn, 5/28/91, (PB92-113885, A09, MF-A02).

NCEER-91-0015 "Evaluation of SEAOC Design Requirements for Sliding Isolated Structures," by D. Theodossiou and M.C. Constantinou, 6/10/91, (PB92-114602, A11, MF-A03).

NCEER-91-0016 "Closed-Loop Modal Testing of a 27-Story Reinforced Concrete Flat Plate-Core Building," by H.R. Somaprasad, T. Toksoy, H. Yoshiyuki and A.E. Aktan, 7/15/91, (PB92-129980, A07, MF-A02).

NCEER-91-0017 "Shake Table Test of a 1/6 Scale Two-Story Lightly Reinforced Concrete Building," by A.G. El-Attar, R.N. White and P. Gergely, 2/28/91, (PB92-222447, A06, MF-A02).

NCEER-91-0018 "Shake Table Test of a 1/8 Scale Three-Story Lightly Reinforced Concrete Building," by A.G. El-Attar, R.N. White and P. Gergely, 2/28/91, (PB93-116630, A08, MF-A02).

NCEER-91-0019 "Transfer Functions for Rigid Rectangular Foundations," by A.S. Veletsos, A.M. Prasad and W.H. Wu, 7/31/91, to be published.

NCEER-91-0020 "Hybrid Control of Seismic-Excited Nonlinear and Inelastic Structural Systems," by J.N. Yang, Z. Li and A. Danielians, 8/1/91, (PB92-143171, A06, MF-A02).

NCEER-91-0021 "The NCEER-91 Earthquake Catalog: Improved Intensity-Based Magnitudes and Recurrence Relations for U.S. Earthquakes East of New Madrid," by L. Seeber and J.G. Armbruster, 8/28/91, (PB92-176742, A06, MF-A02).

NCEER-91-0022 "Proceedings from the Implementation of Earthquake Planning and Education in Schools: The Need for Change - The Roles of the Changemakers," by K.E.K. Ross and F. Winslow, 7/23/91, (PB92-129998, A12, MF-A03).

NCEER-91-0023 "A Study of Reliability-Based Criteria for Seismic Design of Reinforced Concrete Frame Buildings," by H.H.M. Hwang and H-M. Hsu, 8/10/91, (PB92-140235, A09, MF-A02).

NCEER-91-0024 "Experimental Verification of a Number of Structural System Identification Algorithms," by R.G. Ghanem, H. Gavin and M. Shinozuka, 9/18/91, (PB92-176577, A18, MF-A04).

NCEER-91-0025 "Probabilistic Evaluation of Liquefaction Potential," by H.H.M. Hwang and C.S. Lee," 11/25/91, (PB92-143429, A05, MF-A01).

NCEER-91-0026 "Instantaneous Optimal Control for Linear, Nonlinear and Hysteretic Structures - Stable Controllers," by J.N. Yang and Z. Li, 11/15/91, (PB92-163807, A04, MF-A01).

NCEER-91-0027 "Experimental and Theoretical Study of a Sliding Isolation System for Bridges," by M.C. Constantinou, A. Kartoum, A.M. Reinhorn and P. Bradford, 11/15/91, (PB92-176973, A10, MF-A03).

NCEER-92-0001 "Case Studies of Liquefaction and Lifeline Performance During Past Earthquakes, Volume 1: Japanese Case Studies," Edited by M. Hamada and T. O'Rourke, 2/17/92, (PB92-197243, A18, MF-A04).

NCEER-92-0002 "Case Studies of Liquefaction and Lifeline Performance During Past Earthquakes, Volume 2: United States Case Studies," Edited by T. O'Rourke and M. Hamada, 2/17/92, (PB92-197250, A20, MF-A04).

NCEER-92-0003 "Issues in Earthquake Education," Edited by K. Ross, 2/3/92, (PB92-222389, A07, MF-A02).

NCEER-92-0004 "Proceedings from the First U.S. - Japan Workshop on Earthquake Protective Systems for Bridges," Edited by I.G. Buckle, 2/4/92, (PB94-142239, A99, MF-A06).

NCEER-92-0005 "Seismic Ground Motion from a Haskell-Type Source in a Multiple-Layered Half-Space," A.P. Theoharis, G. Deodatis and M. Shinozuka, 1/2/92, to be published.

NCEER-92-0006 "Proceedings from the Site Effects Workshop," Edited by R. Whitman, 2/29/92, (PB92-197201, A04, MF-A01).

NCEER-92-0007 "Engineering Evaluation of Permanent Ground Deformations Due to Seismically-Induced Liquefaction," by M.H. Baziar, R. Dobry and A-W.M. Elgamal, 3/24/92, (PB92-222421, A13, MF-A03).

NCEER-92-0008 "A Procedure for the Seismic Evaluation of Buildings in the Central and Eastern United States," by C.D. Poland and J.O. Malley, 4/2/92, (PB92-222439, A20, MF-A04).

NCEER-92-0009 "Experimental and Analytical Study of a Hybrid Isolation System Using Friction Controllable Sliding Bearings," by M.Q. Feng, S. Fujii and M. Shinozuka, 5/15/92, (PB93-150282, A06, MF-A02).

NCEER-92-0010 "Seismic Resistance of Slab-Column Connections in Existing Non-Ductile Flat-Plate Buildings," by A.J. Durrani and Y. Du, 5/18/92, (PB93-116812, A06, MF-A02).

NCEER-92-0011 "The Hysteretic and Dynamic Behavior of Brick Masonry Walls Upgraded by Ferrocement Coatings Under Cyclic Loading and Strong Simulated Ground Motion," by H. Lee and S.P. Prawel, 5/11/92, to be published.

NCEER-92-0012 "Study of Wire Rope Systems for Seismic Protection of Equipment in Buildings," by G.F. Demetriades, M.C. Constantinou and A.M. Reinhorn, 5/20/92, (PB93-116655, A08, MF-A02).

NCEER-92-0013 "Shape Memory Structural Dampers: Material Properties, Design and Seismic Testing," by P.R. Witting and F.A. Cozzarelli, 5/26/92, (PB93-116663, A05, MF-A01).

NCEER-92-0014 "Longitudinal Permanent Ground Deformation Effects on Buried Continuous Pipelines," by M.J. O'Rourke, and C. Nordberg, 6/15/92, (PB93-116671, A08, MF-A02).

NCEER-92-0015 "A Simulation Method for Stationary Gaussian Random Functions Based on the Sampling Theorem," by M. Grigoriu and S. Balopoulou, 6/11/92, (PB93-127496, A05, MF-A01).

NCEER-92-0016 "Gravity-Load-Designed Reinforced Concrete Buildings: Seismic Evaluation of Existing Construction and Detailing Strategies for Improved Seismic Resistance," by G.W. Hoffmann, S.K. Kunnath, A.M. Reinhorn and J.B. Mander, 7/15/92, (PB94-142007, A08, MF-A02).

NCEER-92-0017 "Observations on Water System and Pipeline Performance in the Limón Area of Costa Rica Due to the April 22, 1991 Earthquake," by M. O'Rourke and D. Ballantyne, 6/30/92, (PB93-126811, A06, MF-A02).

NCEER-92-0018 "Fourth Edition of Earthquake Education Materials for Grades K-12," Edited by K.E.K. Ross, 8/10/92, (PB93-114023, A07, MF-A02).

NCEER-92-0019 "Proceedings from the Fourth Japan-U.S. Workshop on Earthquake Resistant Design of Lifeline Facilities and Countermeasures for Soil Liquefaction," Edited by M. Hamada and T.D. O'Rourke, 8/12/92, (PB93-163939, A99, MF-E11).

NCEER-92-0020 "Active Bracing System: A Full Scale Implementation of Active Control," by A.M. Reinhorn, T.T. Soong, R.C. Lin, M.A. Riley, Y.P. Wang, S. Aizawa and M. Higashino, 8/14/92, (PB93-127512, A06, MF-A02).

NCEER-92-0021 "Empirical Analysis of Horizontal Ground Displacement Generated by Liquefaction-Induced Lateral Spreads," by S.F. Bartlett and T.L. Youd, 8/17/92, (PB93-188241, A06, MF-A02).

NCEER-92-0022 "IDARC Version 3.0: Inelastic Damage Analysis of Reinforced Concrete Structures," by S.K. Kunnath, A.M. Reinhorn and R.F. Lobo, 8/31/92, (PB93-227502, A07, MF-A02).

NCEER-92-0023 "A Semi-Empirical Analysis of Strong-Motion Peaks in Terms of Seismic Source, Propagation Path and Local Site Conditions, by M. Kamiyama, M.J. O'Rourke and R. Flores-Berrones, 9/9/92, (PB93-150266, A08, MF-A02).

NCEER-92-0024 "Seismic Behavior of Reinforced Concrete Frame Structures with Nonductile Details, Part I: Summary of Experimental Findings of Full Scale Beam-Column Joint Tests," by A. Beres, R.N. White and P. Gergely, 9/30/92, (PB93-227783, A05, MF-A01).

NCEER-92-0025 "Experimental Results of Repaired and Retrofitted Beam-Column Joint Tests in Lightly Reinforced Concrete Frame Buildings," by A. Beres, S. El-Borgi, R.N. White and P. Gergely, 10/29/92, (PB93-227791, A05, MF-A01).

NCEER-92-0026 "A Generalization of Optimal Control Theory: Linear and Nonlinear Structures," by J.N. Yang, Z. Li and S. Vongchavalitkul, 11/2/92, (PB93-188621, A05, MF-A01).

NCEER-92-0027 "Seismic Resistance of Reinforced Concrete Frame Structures Designed Only for Gravity Loads: Part I - Design and Properties of a One-Third Scale Model Structure," by J.M. Bracci, A.M. Reinhorn and J.B. Mander, 12/1/92, (PB94-104502, A08, MF-A02).

NCEER-92-0028 "Seismic Resistance of Reinforced Concrete Frame Structures Designed Only for Gravity Loads: Part II - Experimental Performance of Subassemblages," by L.E. Aycardi, J.B. Mander and A.M. Reinhorn, 12/1/92, (PB94-104510, A08, MF-A02).

NCEER-92-0029 "Seismic Resistance of Reinforced Concrete Frame Structures Designed Only for Gravity Loads: Part III - Experimental Performance and Analytical Study of a Structural Model," by J.M. Bracci, A.M. Reinhorn and J.B. Mander, 12/1/92, (PB93-227528, A09, MF-A01).

NCEER-92-0030 "Evaluation of Seismic Retrofit of Reinforced Concrete Frame Structures: Part I - Experimental Performance of Retrofitted Subassemblages," by D. Choudhuri, J.B. Mander and A.M. Reinhorn, 12/8/92, (PB93-198307, A07, MF-A02).

NCEER-92-0031 "Evaluation of Seismic Retrofit of Reinforced Concrete Frame Structures: Part II - Experimental Performance and Analytical Study of a Retrofitted Structural Model," by J.M. Bracci, A.M. Reinhorn and J.B. Mander, 12/8/92, (PB93-198315, A09, MF-A03).

NCEER-92-0032 "Experimental and Analytical Investigation of Seismic Response of Structures with Supplemental Fluid Viscous Dampers," by M.C. Constantinou and M.D. Symans, 12/21/92, (PB93-191435, A10, MF-A03).

NCEER-92-0033 "Reconnaissance Report on the Cairo, Egypt Earthquake of October 12, 1992," by M. Khater, 12/23/92, (PB93-188621, A03, MF-A01).

NCEER-92-0034 "Low-Level Dynamic Characteristics of Four Tall Flat-Plate Buildings in New York City," by H. Gavin, S. Yuan, J. Grossman, E. Pekelis and K. Jacob, 12/28/92, (PB93-188217, A07, MF-A02).

NCEER-93-0001 "An Experimental Study on the Seismic Performance of Brick-Infilled Steel Frames With and Without Retrofit," by J.B. Mander, B. Nair, K. Wojtkowski and J. Ma, 1/29/93, (PB93-227510, A07, MF-A02).

NCEER-93-0002 "Social Accounting for Disaster Preparedness and Recovery Planning," by S. Cole, E. Pantoja and V. Razak, 2/22/93, (PB94-142114, A12, MF-A03).

NCEER-93-0003 "Assessment of 1991 NEHRP Provisions for Nonstructural Components and Recommended Revisions," by T.T. Soong, G. Chen, Z. Wu, R-H. Zhang and M. Grigoriu, 3/1/93, (PB93-188639, A06, MF-A02).

NCEER-93-0004 "Evaluation of Static and Response Spectrum Analysis Procedures of SEAOC/UBC for Seismic Isolated Structures," by C.W. Winters and M.C. Constantinou, 3/23/93, (PB93-198299, A10, MF-A03).

NCEER-93-0005 "Earthquakes in the Northeast - Are We Ignoring the Hazard? A Workshop on Earthquake Science and Safety for Educators," edited by K.E.K. Ross, 4/2/93, (PB94-103066, A09, MF-A02).

NCEER-93-0006 "Inelastic Response of Reinforced Concrete Structures with Viscoelastic Braces," by R.F. Lobo, J.M. Bracci, K.L. Shen, A.M. Reinhorn and T.T. Soong, 4/5/93, (PB93-227486, A05, MF-A02).

NCEER-93-0007 "Seismic Testing of Installation Methods for Computers and Data Processing Equipment," by K. Kosar, T.T. Soong, K.L. Shen, J.A. HoLung and Y.K. Lin, 4/12/93, (PB93-198299, A07, MF-A02).

NCEER-93-0008 "Retrofit of Reinforced Concrete Frames Using Added Dampers," by A. Reinhorn, M. Constantinou and C. Li, to be published.

NCEER-93-0009 "Seismic Behavior and Design Guidelines for Steel Frame Structures with Added Viscoelastic Dampers," by K.C. Chang, M.L. Lai, T.T. Soong, D.S. Hao and Y.C. Yeh, 5/1/93, (PB94-141959, A07, MF-A02).

NCEER-93-0010 "Seismic Performance of Shear-Critical Reinforced Concrete Bridge Piers," by J.B. Mander, S.M. Waheed, M.T.A. Chaudhary and S.S. Chen, 5/12/93, (PB93-227494, A08, MF-A02).

NCEER-93-0011 "3D-BASIS-TABS: Computer Program for Nonlinear Dynamic Analysis of Three Dimensional Base Isolated Structures," by S. Nagarajaiah, C. Li, A.M. Reinhorn and M.C. Constantinou, 8/2/93, (PB94-141819, A09, MF-A02).

NCEER-93-0012 "Effects of Hydrocarbon Spills from an Oil Pipeline Break on Ground Water," by O.J. Helweg and H.H.M. Hwang, 8/3/93, (PB94-141942, A06, MF-A02).

NCEER-93-0013 "Simplified Procedures for Seismic Design of Nonstructural Components and Assessment of Current Code Provisions," by M.P. Singh, L.E. Suarez, E.E. Matheu and G.O. Maldonado, 8/4/93, (PB94-141827, A09, MF-A02).

NCEER-93-0014 "An Energy Approach to Seismic Analysis and Design of Secondary Systems," by G. Chen and T.T. Soong, 8/6/93, (PB94-142767, A11, MF-A03).

NCEER-93-0015 "Proceedings from School Sites: Becoming Prepared for Earthquakes - Commemorating the Third Anniversary of the Loma Prieta Earthquake," Edited by F.E. Winslow and K.E.K. Ross, 8/16/93, (PB94-154275, A16, MF-A02).

NCEER-93-0016 "Reconnaissance Report of Damage to Historic Monuments in Cairo, Egypt Following the October 12, 1992 Dahshur Earthquake," by D. Sykora, D. Look, G. Croci, E. Karaesmen and E. Karaesmen, 8/19/93, (PB94-142221, A08, MF-A02).

NCEER-93-0017 "The Island of Guam Earthquake of August 8, 1993," by S.W. Swan and S.K. Harris, 9/30/93, (PB94-141843, A04, MF-A01).

NCEER-93-0018 "Engineering Aspects of the October 12, 1992 Egyptian Earthquake," by A.W. Elgamal, M. Amer, K. Adalier and A. Abul-Fadl, 10/7/93, (PB94-141983, A05, MF-A01).

NCEER-93-0019 "Development of an Earthquake Motion Simulator and its Application in Dynamic Centrifuge Testing," by I. Krstelj, Supervised by J.H. Prevost, 10/23/93, (PB94-181773, A-10, MF-A03).

NCEER-93-0020 "NCEER-Taisei Corporation Research Program on Sliding Seismic Isolation Systems for Bridges: Experimental and Analytical Study of a Friction Pendulum System (FPS)," by M.C. Constantinou, P. Tsopelas, Y-S. Kim and S. Okamoto, 11/1/93, (PB94-142775, A08, MF-A02).

NCEER-93-0021 "Finite Element Modeling of Elastomeric Seismic Isolation Bearings," by L.J. Billings, Supervised by R. Shepherd, 11/8/93, to be published.

NCEER-93-0022 "Seismic Vulnerability of Equipment in Critical Facilities: Life-Safety and Operational Consequences," by K. Porter, G.S. Johnson, M.M. Zadeh, C. Scawthorn and S. Eder, 11/24/93, (PB94-181765, A16, MF-A03).

NCEER-93-0023 "Hokkaido Nansei-oki, Japan Earthquake of July 12, 1993, by P.I. Yanev and C.R. Scawthorn, 12/23/93, (PB94-181500, A07, MF-A01).

NCEER-94-0001 "An Evaluation of Seismic Serviceability of Water Supply Networks with Application to the San Francisco Auxiliary Water Supply System," by I. Markov, Supervised by M. Grigoriu and T. O'Rourke, 1/21/94, (PB94-204013, A07, MF-A02).

NCEER-94-0002 "NCEER-Taisei Corporation Research Program on Sliding Seismic Isolation Systems for Bridges: Experimental and Analytical Study of Systems Consisting of Sliding Bearings, Rubber Restoring Force Devices and Fluid Dampers," Volumes I and II, by P. Tsopelas, S. Okamoto, M.C. Constantinou, D. Ozaki and S. Fujii, 2/4/94, (PB94-181740, A09, MF-A02 and PB94-181757, A12, MF-A03).

NCEER-94-0003 "A Markov Model for Local and Global Damage Indices in Seismic Analysis," by S. Rahman and M. Grigoriu, 2/18/94, (PB94-206000, A12, MF-A03).

NCEER-94-0004 "Proceedings from the NCEER Workshop on Seismic Response of Masonry Infills," edited by D.P. Abrams, 3/1/94, (PB94-180783, A07, MF-A02).

NCEER-94-0005 "The Northridge, California Earthquake of January 17, 1994: General Reconnaissance Report," edited by J.D. Goltz, 3/11/94, (PB193943, A10, MF-A03).

NCEER-94-0006 "Seismic Energy Based Fatigue Damage Analysis of Bridge Columns: Part I - Evaluation of Seismic Capacity," by G.A. Chang and J.B. Mander, 3/14/94, (PB94-219185, A11, MF-A03).

NCEER-94-0007 "Seismic Isolation of Multi-Story Frame Structures Using Spherical Sliding Isolation Systems," by T.M. Al-Hussaini, V.A. Zayas and M.C. Constantinou, 3/17/94, (PB193745, A09, MF-A02).

NCEER-94-0008 "The Northridge, California Earthquake of January 17, 1994: Performance of Highway Bridges," edited by I.G. Buckle, 3/24/94, (PB94-193851, A06, MF-A02).

NCEER-94-0009 "Proceedings of the Third U.S.-Japan Workshop on Earthquake Protective Systems for Bridges," edited by I.G. Buckle and I. Friedland, 3/31/94, (PB94-195815, A99, MF-A06).

NCEER-94-0010 "3D-BASIS-ME: Computer Program for Nonlinear Dynamic Analysis of Seismically Isolated Single and Multiple Structures and Liquid Storage Tanks," by P.C. Tsopelas, M.C. Constantinou and A.M. Reinhorn, 4/12/94, (PB94-204922, A09, MF-A02).

NCEER-94-0011 "The Northridge, California Earthquake of January 17, 1994: Performance of Gas Transmission Pipelines," by T.D. O'Rourke and M.C. Palmer, 5/16/94, (PB94-204989, A05, MF-A01).

NCEER-94-0012 "Feasibility Study of Replacement Procedures and Earthquake Performance Related to Gas Transmission Pipelines," by T.D. O'Rourke and M.C. Palmer, 5/25/94, (PB94-206638, A09, MF-A02).

NCEER-94-0013 "Seismic Energy Based Fatigue Damage Analysis of Bridge Columns: Part II - Evaluation of Seismic Demand," by G.A. Chang and J.B. Mander, 6/1/94, (PB95-18106, A08, MF-A02).

NCEER-94-0014 "NCEER-Taisei Corporation Research Program on Sliding Seismic Isolation Systems for Bridges: Experimental and Analytical Study of a System Consisting of Sliding Bearings and Fluid Restoring Force/Damping Devices," by P. Tsopelas and M.C. Constantinou, 6/13/94, (PB94-219144, A10, MF-A03).

NCEER-94-0015 "Generation of Hazard-Consistent Fragility Curves for Seismic Loss Estimation Studies," by H. Hwang and J-R. Huo, 6/14/94, (PB95-181996, A09, MF-A02).

NCEER-94-0016 "Seismic Study of Building Frames with Added Energy-Absorbing Devices," by W.S. Pong, C.S. Tsai and G.C. Lee, 6/20/94, (PB94-219136, A10, A03).

NCEER-94-0017 "Sliding Mode Control for Seismic-Excited Linear and Nonlinear Civil Engineering Structures," by J. Yang, J. Wu, A. Agrawal and Z. Li, 6/21/94, (PB95-138483, A06, MF-A02).

NCEER-94-0018 "3D-BASIS-TABS Version 2.0: Computer Program for Nonlinear Dynamic Analysis of Three Dimensional Base Isolated Structures," by A.M. Reinhorn, S. Nagarajaiah, M.C. Constantinou, P. Tsopelas and R. Li, 6/22/94, (PB95-182176, A08, MF-A02).

NCEER-94-0019 "Proceedings of the International Workshop on Civil Infrastructure Systems: Application of Intelligent Systems and Advanced Materials on Bridge Systems," Edited by G.C. Lee and K.C. Chang, 7/18/94, (PB95-252474, A20, MF-A04).

NCEER-94-0020 "Study of Seismic Isolation Systems for Computer Floors," by V. Lambrou and M.C. Constantinou, 7/19/94, (PB95-138533, A10, MF-A03).

NCEER-94-0021 "Proceedings of the U.S.-Italian Workshop on Guidelines for Seismic Evaluation and Rehabilitation of Unreinforced Masonry Buildings," Edited by D.P. Abrams and G.M. Calvi, 7/20/94, (PB95-138749, A13, MF-A03).

NCEER-94-0022 "NCEER-Taisei Corporation Research Program on Sliding Seismic Isolation Systems for Bridges: Experimental and Analytical Study of a System Consisting of Lubricated PTFE Sliding Bearings and Mild Steel Dampers," by P. Tsopelas and M.C. Constantinou, 7/22/94, (PB95-182184, A08, MF-A02).

NCEER-94-0023 "Development of Reliability-Based Design Criteria for Buildings Under Seismic Load," by Y.K. Wen, H. Hwang and M. Shinozuka, 8/1/94, (PB95-211934, A08, MF-A02).

NCEER-94-0024 "Experimental Verification of Acceleration Feedback Control Strategies for an Active Tendon System," by S.J. Dyke, B.F. Spencer, Jr., P. Quast, M.K. Sain, D.C. Kaspari, Jr. and T.T. Soong, 8/29/94, (PB95-212320, A05, MF-A01).

NCEER-94-0025 "Seismic Retrofitting Manual for Highway Bridges," Edited by I.G. Buckle and I.F. Friedland, published by the Federal Highway Administration (PB95-212676, A15, MF-A03).

NCEER-94-0026 "Proceedings from the Fifth U.S.-Japan Workshop on Earthquake Resistant Design of Lifeline Facilities and Countermeasures Against Soil Liquefaction," Edited by T.D. O'Rourke and M. Hamada, 11/7/94, (PB95-220802, A99, MF-E08).

NCEER-95-0001 "Experimental and Analytical Investigation of Seismic Retrofit of Structures with Supplemental Damping: Part 1 - Fluid Viscous Damping Devices," by A.M. Reinhorn, C. Li and M.C. Constantinou, 1/3/95, (PB95-266599, A09, MF-A02).

NCEER-95-0002 "Experimental and Analytical Study of Low-Cycle Fatigue Behavior of Semi-Rigid Top-And-Seat Angle Connections," by G. Pekcan, J.B. Mander and S.S. Chen, 1/5/95, (PB95-220042, A07, MF-A02).

NCEER-95-0003 "NCEER-ATC Joint Study on Fragility of Buildings," by T. Anagnos, C. Rojahn and A.S. Kiremidjian, 1/20/95, (PB95-220026, A06, MF-A02).

NCEER-95-0004 "Nonlinear Control Algorithms for Peak Response Reduction," by Z. Wu, T.T. Soong, V. Gattulli and R.C. Lin, 2/16/95, (PB95-220349, A05, MF-A01).

NCEER-95-0005 "Pipeline Replacement Feasibility Study: A Methodology for Minimizing Seismic and Corrosion Risks to Underground Natural Gas Pipelines," by R.T. Eguchi, H.A. Seligson and D.G. Honegger, 3/2/95, (PB95-252326, A06, MF-A02).

NCEER-95-0006 "Evaluation of Seismic Performance of an 11-Story Frame Building During the 1994 Northridge Earthquake," by F. Naeim, R. DiSulio, K. Benuska, A. Reinhorn and C. Li, to be published.

NCEER-95-0007 "Prioritization of Bridges for Seismic Retrofitting," by N. Basöz and A.S. Kiremidjian, 4/24/95, (PB95-252300, A08, MF-A02).

NCEER-95-0008 "Method for Developing Motion Damage Relationships for Reinforced Concrete Frames," by A. Singhal and A.S. Kiremidjian, 5/11/95, (PB95-266607, A06, MF-A02).

NCEER-95-0009 "Experimental and Analytical Investigation of Seismic Retrofit of Structures with Supplemental Damping: Part II - Friction Devices," by C. Li and A.M. Reinhorn, 7/6/95, (PB96-128087, A11, MF-A03).

NCEER-95-0010 "Experimental Performance and Analytical Study of a Non-Ductile Reinforced Concrete Frame Structure Retrofitted with Elastomeric Spring Dampers," by G. Pekcan, J.B. Mander and S.S. Chen, 7/14/95, (PB96-137161, A08, MF-A02).

NCEER-95-0011 "Development and Experimental Study of Semi-Active Fluid Damping Devices for Seismic Protection of Structures," by M.D. Symans and M.C. Constantinou, 8/3/95, (PB96-136940, A23, MF-A04).

NCEER-95-0012 "Real-Time Structural Parameter Modification (RSPM): Development of Innervated Structures," by Z. Liang, M. Tong and G.C. Lee, 4/11/95, (PB96-137153, A06, MF-A01).

NCEER-95-0013 "Experimental and Analytical Investigation of Seismic Retrofit of Structures with Supplemental Damping: Part III - Viscous Damping Walls," by A.M. Reinhorn and C. Li, 10/1/95, (PB96-176409, A11, MF-A03).

NCEER-95-0014 "Seismic Fragility Analysis of Equipment and Structures in a Memphis Electric Substation," by J-R. Huo and H.H.M. Hwang, (PB96-128087, A09, MF-A02), 8/10/95.

NCEER-95-0015 "The Hanshin-Awaji Earthquake of January 17, 1995: Performance of Lifelines," Edited by M. Shinozuka, 11/3/95, (PB96-176383, A15, MF-A03).

NCEER-95-0016 "Highway Culvert Performance During Earthquakes," by T.L. Youd and C.J. Beckman, available as NCEER-96-0015.

NCEER-95-0017 "The Hanshin-Awaji Earthquake of January 17, 1995: Performance of Highway Bridges," Edited by I.G. Buckle, 12/1/95, to be published.

NCEER-95-0018 "Modeling of Masonry Infill Panels for Structural Analysis," by A.M. Reinhorn, A. Madan, R.E. Valles, Y. Reichmann and J.B. Mander, 12/8/95.

NCEER-95-0019 "Optimal Polynomial Control for Linear and Nonlinear Structures," by A.K. Agrawal and J.N. Yang, 12/11/95, (PB96-168737, A07, MF-A02).

NCEER-95-0020 "Retrofit of Non-Ductile Reinforced Concrete Frames Using Friction Dampers," by R.S. Rao, P. Gergely and R.N. White, 12/22/95, (PB97-133508, A10, MF-A02).

NCEER-95-0021 "Parametric Results for Seismic Response of Pile-Supported Bridge Bents," by G. Mylonakis, A. Nikolaou and G. Gazetas, 12/22/95, (PB97-100242, A12, MF-A03).

NCEER-95-0022 "Kinematic Bending Moments in Seismically Stressed Piles," by A. Nikolaou, G. Mylonakis and G. Gazetas, 12/23/95.

NCEER-96-0001 "Dynamic Response of Unreinforced Masonry Buildings with Flexible Diaphragms," by A.C. Costley and D.P. Abrams," 10/10/96.

NCEER-96-0002 "State of the Art Review: Foundations and Retaining Structures," by I. Po Lam, to be published.

NCEER-96-0003 "Ductility of Rectangular Reinforced Concrete Bridge Columns with Moderate Confinement," by N. Wehbe, M. Saiidi, D. Sanders and B. Douglas, 11/7/96, (PB97-133557, A06, MF-A02).

NCEER-96-0004 "Proceedings of the Long-Span Bridge Seismic Research Workshop," edited by I.G. Buckle and I.M. Friedland, to be published.

NCEER-96-0005 "Establish Representative Pier Types for Comprehensive Study: Eastern United States," by J. Kulicki and Z. Prucz, 5/28/96.

NCEER-96-0006 "Establish Representative Pier Types for Comprehensive Study: Western United States," by R. Imbsen, R.A. Schamber and T.A. Osterkamp, 5/28/96.

NCEER-96-0007 "Nonlinear Control Techniques for Dynamical Systems with Uncertain Parameters," by R.G. Ghanem and M.I. Bujakov, 5/27/96, (PB97-100259, A17, MF-A03).

NCEER-96-0008 "Seismic Evaluation of a 30-Year Old Non-Ductile Highway Bridge Pier and Its Retrofit," by J.B. Mander, B. Mahmoodzadegan, S. Bhadra and S.S. Chen, 5/31/96.

NCEER-96-0009 "Seismic Performance of a Model Reinforced Concrete Bridge Pier Before and After Retrofit," by J.B. Mander, J.H. Kim and C.A. Ligozio, 5/31/96.

NCEER-96-0010 "IDARC2D Version 4.0: A Computer Program for the Inelastic Damage Analysis of Buildings," by R.E. Valles, A.M. Reinhorn, S.K. Kunnath, C. Li and A. Madan, 6/3/96, (PB97-100234, A17, MF-A03).

NCEER-96-0011 "Estimation of the Economic Impact of Multiple Lifeline Disruption: Memphis Light, Gas and Water Division Case Study," by S.E. Chang, H.A. Seligson and R.T. Eguchi, 8/16/96, (PB97-133490, A11, MF-A03).

NCEER-96-0012 "Proceedings from the Sixth Japan-U.S. Workshop on Earthquake Resistant Design of Lifeline Facilities and Countermeasures Against Soil Liquefaction, Edited by M. Hamada and T. O'Rourke, 9/11/96, (PB97-133581, A99, MF-A06).

NCEER-96-0013 "Chemical Hazards, Mitigation and Preparedness in Areas of High Seismic Risk: A Methodology for Estimating the Risk of Post-Earthquake Hazardous Materials Release," by H.A. Seligson, R.T. Eguchi, K.J. Tierney and K. Richmond, 11/7/96.

NCEER-96-0014 "Response of Steel Bridge Bearings to Reversed Cyclic Loading," by J.B. Mander, D-K. Kim, S.S. Chen and G.J. Premus, 11/13/96, (PB97-140735, A12, MF-A03).

NCEER-96-0015 "Highway Culvert Performance During Past Earthquakes," by T.L. Youd and C.J. Beckman, 11/25/96, (PB97-133532, A06, MF-A01).

NCEER-97-0001 "Evaluation, Prevention and Mitigation of Pounding Effects in Building Structures," by R.E. Valles and A.M. Reinhorn, 2/20/97.

NCEER-97-0002 "Seismic Design Criteria for Bridges and Other Highway Structures," by C. Rojahn, R. Mayes, D.G. Anderson, J. Clark, J.H. Hom, R.V. Nutt and M.J. O'Rourke, 4/30/97.

NCEER-97-0003 "Proceedings of the U.S.-Italian Workshop on Seismic Evaluation and Retrofit," Edited by D.P. Abrams and G.M. Calvi, 3/19/97.

NCEER-97-0004 "Investigation of Seismic Response of Buildings with Linear and Nonlinear Fluid Viscous Dampers," by A.A. Seleemah and M.C. Constantinou, 5/21/97.

NATIONAL CENTER FOR EARTHQUAKE ENGINEERING RESEARCH

Headquartered at the State University of New York at Buffalo

State University of New York at Buffalo
Red Jacket Quadrangle
Buffalo, New York 14261
Telephone: 716/645-3391
FAX: 716/645-3399

ISSN 1088-3800

U.S. DEPARTMENT OF COMMERCE
Technology Administration
National Technical Information Service
Springfield, VA 22161   (703) 487-4650